

Development of Self-Adhesive, Low Shrinkage, Re-mineralising and High Strength Dental Composites

Thesis submitted by

Hesham Ben Nuba

A thesis submitted in the fulfilment of the requirement for the Degree
of Doctor of Philosophy

Eastman Dental Institute

Division of Biomaterials and Tissue Engineering

University College London

256 Gray's Inn Road

London

WC1X 8LD

2015

DECLARATION

I confirm that the work presented in this thesis is my own. Where information has been derived from other sources, I confirm that this has been indicated in the thesis.

SIGNED.....

DATE / / 2016

ACKNOWLEDGEMENTS

First of all I thank almighty Allah who gave me the endurance during the course of my PhD. I would like to express my deep gratitude to my primary supervisor Dr Anne Young, for her guidance in directing my research. Her unique encouragement throughout, constructive criticism and support have made this study possible. I am grateful to my second and third supervisors Dr Laurent Bozec and Dr Paul Ashly for their guidance, help and advice throughout the project.

Added to this, my appreciation goes to Dr. Graham Palmer, Dr. Wendy Xia and Dr. Nicky Mordan for their kind cooperation, generous assistance and sharing of information. Recognition is also given to my fellow PhD students and staff of BTE department for academic support and friendship over the past four years.

Finally, deep appreciation is felt for my wife Runwa for her dedication, kindness and support when most needed. Finally, my greatest personal indebtedness goes to my parents for their unending and support

Abstract

Resin based restorative composite materials are widely used for restoring both anterior and posterior teeth. Their major drawbacks, however, include complex bonding procedures, polymerisation shrinkage and potential for bond failure ultimately resulting in bacterial microleakage, recurrent caries and pulpal inflammation.

This project's aim was to characterise self-adhesive, antibacterial releasing, remineralising and high strength dental composites. The new composites contain UDMA as a bulk dimethacrylate monomer and PPGDMA as a high molecular weight diluent monomer instead of conventional Bis-GMA and TEGDMA respectively. NTGGMA adhesive co-initiator was added instead of DMPT. Adhesion promoting monomers 4-META or HEMA (5 wt %) were also included to enhance bonding to dentine (ivory). The monomers were combined with silane treated glass filler. This glass was mixed with total calcium phosphate levels (MCPM and TCP of equal mass) of 0, 10, 20 or 40 wt %. Furthermore, CHX and glass fibre were each included at 5 wt %. The powder liquid ratio was 3:1 by weight. Commercial dental composites Z250, Ecusphere and Gradia and experimental formulations with 4-META or HEMA and solely 100 wt % glass particles were used as controls.

The degree of conversion after 20 s light cure was determined by FTIR. Cure data was used with the composite compositions to calculate the polymerisation shrinkage. The depth of cure was measured using ISO 4049. Subsequently, the mass and volume change and CHX release upon water immersion were determined over 5 and 4 months respectively. The mechanical properties biaxial flexural strength and modulus were determined dry and after 24 h, 7 days and 28 days immersion in water. The adhesion properties were assessed using a push out and shear test. Dry and hydrated ivory dentine with and without phosphoric acid etching for 20 s were investigated. The experiential formulations had ~ 77 % conversion as compared to ~ 50 – 60 % for commercial composites. The polymerisation shrinkage was ~ 3.4 – 3.7 % and the depth of cure decreased linearly with CaP increase after cured for 20 and 40 s. The mass and volume change and CHX release increased linearly with CaP increase and formulations with HEMA had higher water sorption and CHX releases compared to 4-META formulations.

Control experimental composites achieved a flexural strength of ~170 MPa with no CHX or CaP. This decreased with CHX addition or increased CaP. Provided the CaP level was less than 20 %, however, strength was greater or comparable to Gradia and above 70 MPa even after immersion in water for 28 days.

The commercial composite exhibited the lowest push out and shear bond strengths to dentine. Replacement of HEMA with 4-META, increasing CaP, acid-etching or hydration of dentine and addition of Ibond adhesive, all significantly increased bond strengths between the composite and dentine.

The new material, with adhesive monomer 4-META and reactive calcium phosphate, shows potential as a high conversion, antibacterial releasing, high strength and self-adhering composite, which should reduce restoration failure resulting from shrinkage and secondary caries. The use of ivory made it possible to determine the differences in bonding capability of multiple commercial and experimental formulations under wide ranging conditions.

TABLE OF CONTENTS

1. Introduction.....	22
2. Literature review	24
2.1. Dental caries.....	24
2.2. Prevalence of dental caries	24
2.3. Pathogenesis.....	25
2.4. Factors involved in caries development.....	25
2.4.1. Dental biofilm	25
2.4.2. Dietary factors.....	26
2.4.3. Saliva.....	26
2.5. Tooth Structure.....	27
2.5.1. Enamel	27
2.5.2. Dentine.....	28
2.6. Demineralisation and remineralisation of tooth structure	29
2.7. Concept of adhesion	29
2.7.1. Enamel bonding	30
2.7.2. Dentine bonding.....	30
2.8. Current restorative materials	31
2.8.1. Amalgam restoration.....	31
2.8.2. Glass ionomer cements	32
2.8.3. Resin modified glass ionomer cements and compomers	33
2.8.4. Dental composite	34
2.9. Properties of dental composites.....	44
2.9.1. Handling properties.....	44
2.9.2. Degree of conversion	44
2.9.3. Polymerisation shrinkage.....	45
2.9.4. Depth of cure.....	46
2.9.5. Water sorption.....	47
2.9.6. Wear resistance	48
2.9.7. Mechanical properties	49
2.9.8. Bond strength	49
2.10. Dental adhesives.....	50

2.10.1.	Etch- and rinse application	51
2.10.2.	Self-etch adhesive	51
2.11.	Antibacterial and dental composites	52
2.11.1.	Soluble antibacterial agents.....	53
2.11.2.	Other antibacterial agents used previously in dental composites.....	54
2.12.	Remineralising dental composites.....	54
2.12.1.	Amorphous calcium phosphate	55
2.12.2.	Other calcium phosphates used previously in dental composites	55
2.13.	Self- adhesive dental composites	56
2.14.	Outline for experimental composites	56
3.	Null hypothesis	58
4.	Aims and objectives	59
4.1.	Aims	59
4.2.	Objectives.....	60
5.	Materials and methods	62
5.1.	Materials.....	63
5.1.1.	Commercial dental materials	63
5.1.2.	Experimental composites	63
5.1.3.	Formulation of experimental dental compositions	65
5.1.4.	Preparation of experimental formulations	66
5.1.5.	Paste preparations	67
5.2.	Methods.....	69
5.2.1.	Degree of monomer conversion.....	69
5.2.2.	Polymerisation shrinkage.....	73
5.2.3.	Depth of cure.....	74
5.2.4.	Mass and volume change	76
5.2.5.	Ultraviolet-visible Spectroscopy.....	77
5.2.6.	Biaxial flexural strength test and modulus.....	81
5.2.7.	Adhesion test.....	85
5.2.8.	Statistical analysis	90
6.	Control and commercial dental composites	93
6.1.	Introduction	93
6.2.	FTIR spectra for individual dental monomers	94

6.3.	FTIR spectra for commercial composites	95
6.3.1.	Z250	95
6.3.2.	Gradia.....	96
6.3.3.	Ecusphere.....	97
6.3.4.	FTIR spectra for control experimental.....	98
6.4.	Degree of conversion of control formulations and commercial composites.....	99
6.5.	Depth of cure.....	101
6.6.	Mass and volume change	102
6.7.	Biaxial flexural strength and Young's modulus.....	104
6.7.1.	Biaxial flexural strength.....	104
6.7.2.	Young's modulus	105
6.8.	Push out adhesion test	107
6.8.1.	Dry ivory dentine	107
6.8.2.	Wet (control hydration) ivory dentine	108
6.8.3.	Push out stress with self-adhesive Ibond	111
6.9.	Shear test	113
6.9.1.	Shear bond strength with self-adhesive Ibond	114
6.10.	Discussion	116
6.10.1.	Degree of monomer conversion	116
6.10.2.	Depth of cure.....	118
6.10.3.	Mass and volume change	119
6.10.4.	Biaxial flexural strength and modulus	121
6.10.5.	Push out test	123
6.10.6.	Shear bond strength.....	126
7.	Experimental formulations with 4-META or HEMA, CHX, glass fibre and different levels of CaP.	129
7.1.	Introduction	129
7.2.	FTIR spectra for experimental formulations.....	130
7.3.	Degree of monomer conversion	132
7.3.1.	Experimental formulations with 4-META.....	132
7.3.2.	Experimental formulations with HEMA.....	133
7.4.	Polymerisation shrinkage	135
7.4.1.	Experimental formulations with 4-META.....	135
7.4.2.	Experimental formulations with HEMA.....	136

7.5.	Depth of cure	137
7.5.1.	Experimental formulations with 4-META.....	137
7.5.2.	Experimental formulations with HEMA.....	139
7.6.	Mass and volume change	141
7.6.1.	Experimental formulations 4-META.....	141
7.6.2.	Experimental formulations with HEMA.....	144
7.7.	Chlorhexidine release	147
7.7.1.	Experimental formulations with 4-META.....	147
7.7.2.	Experimental formulations with HEMA.....	149
7.8.	Biaxial flexural strength and modulus	152
7.8.1.	BFS for experimental formulation with 4-META	152
7.8.2.	BFS for experimental formulations with HEMA.....	157
7.9.	Push out adhesion test	162
7.9.1.	Experimental formulations with 4-META.....	162
7.9.2.	Experimental formulations with HEMA.....	169
7.10.	Shear test	176
7.10.1.	Experimental formulations with 4-META	176
7.10.2.	Experimental formulations with HEMA	181
7.11.	Discussion	185
7.11.1.	Degree of conversion	186
7.11.2.	Polymerisation shrinkage	186
7.11.3.	Depth of cure.....	188
7.11.4.	Mass and volume change	189
7.11.5.	Chlorhexidine release.....	192
7.11.6.	Biaxial flexure strength and modulus	194
7.11.7.	Push out test	196
7.11.8.	Shear bond strength.....	199
8.	Conclusion	200
8.1.	Commercial and control composites	200
8.2.	Experimental formulations with CaP and CHX.....	201
9.	Future work.....	203
10.	List of presentations and publication	205
11.	Appendices.....	206

11.1. Appendix 1 (Preliminary work)	206
11.1.1. Biaxial flexural strength test	206
11.1.2. Formulations for push out adhesion test	207
11.2. Factorial analysis	208
11.3. Results.....	210
11.2. Appendix 2	215
Effect of PLR (3:1or 4:1) on push out test for control formulation with 4-META.....	215
11.3. Appendix 3	216
Effect of different diluent and co-initiators on push out test	216
11.4. Appendix 4.....	218
12. References.....	220

LIST OF TABLES

Table 5-1: Details of commercial dental composite investigated in this project. Description, chemical component and shade are provided by the manufacturer.	63
Table 5-2: Details of monomers, initiator and activator used throughout this project. Molecular weight information was provided by the manufacturer.....	64
Table 5-3: Summaries of filler phase materials used throughout this project as provided from the manufacturer.	65
Table 5-4: Chemical composition of the powder phases of experimental composites.....	66
Table 5-5: Chemical composition of the monomer phases.....	66
Table 5-6: Shows the X and Y axis for Linest equation for experimental formulations with 4-META and HEMA.....	91
Table 7-1 : Depth of cure for 4-META formulations with CaP (0, 10, 20 and 40 wt %) and CHX after curing time of 20 and 40 s from the up surface. The lower section gives linear regression analysis with gradient, intercept and R^2 values for average depth of cure versus Cap wt %.....	138
Table 7-2: Depth of cure for HEMA formulations with CaP (0, 10, 20 and 40 wt %) and CHX after curing time of 20 and 40 s from the up surface. The lower section gives linear regression analysis with gradient, intercept and R^2 values for average depth of cure versus CaP wt %.....	1400
Table 7-3: Initial gradient of mass and volume change vs SQRT time and maximum mass & volume increase and linear regression analysis of the results versus CaP wt % for 4-META formulations with CaP (0, 10, 20 and 40 wt %) and CHX.	143
Table 7-4: Initial gradient mass and volume change vs SQRT time and maximum mass and volume increase and linear regression analysis of the results versus CaP wt % for HEMA formulations with CaP (0, 10, 20 and 40 wt %) and CHX.	146
Table 7-5: Initial gradient of CHX release versus SQRT time and total CHX release for 4-META formulations with different level of CaP (0, 10, 20 and 40 wt %) and 5 wt % CHX with linear regression results versus Ca P wt %.	148
Table 7-6: Initial gradient of CHX release and total CHX release versus SQRT time for HEMA formulations with CaP (0, 10, 20 and 40 wt %) and 5 wt % CHX with linear regression analysis versus CaP wt%.	150

Table 7-7: Biaxial flexural strength for 4-META formulations with CaP (0, 10, 20 and 40 wt %) before and after 24 h, 7 and 28 days immersion in deionised water. Additionally gradient, intercept and R^2 from linear regression analysis versus CaP level is provided in lower section. 153

Table 7-8: Young's modulus and gradient, intercept and R^2 from linear regression analysis versus CaP for experimental formulations with 4-META and CaP (0, 10, 20 and 40 wt %) before and after 24 h, 7 and 28 days immersion in deionised water. 156

Table 7-9: Biaxial flexural strength of HEMA formulations with CaP (0, 10, 20 and 40 wt %) before and after 24 h, 7 and 28 days immersion in water and linear regression analysis with gradient, intercept and R^2 values from average BFS versus CaP. 158

Table 7-10: Young's modulus, gradient, intercept and R^2 from linear regression of formulations with HEMA and CaP (0, 10, 20 and 40 wt %) before and after 24 h, 7 and 28 day immersed in deionised water. 160

Table 7-11: Push out stress for dry ivory dentine, using etching with phosphoric acid for 20s or non-etching for 4-META formulations with Cap (0, 10, 20 and 40 wt %). Additionally, gradient, intercept and R^2 from linear regression analysis values CaP level is provided. 163

Table 7-12: Push out stress for wet ivory (control hydration) gradient, intercept and R^2 from linear regression for 4-META formulations with and Cap (0, 10, 20 and 40 wt %) and etching with phosphoric acid for 20s or no-etching. 166

Table 7-13: push out stress gradient, intercept and R^2 from linear regression analysis versus CaP for 4-META formulations with Cap (0, 10, 20 and 40% wt) and self-adhesive agent Ibond. 168

Table 7-14: Push out stress for wet ivory (controlled hydration) gradient, intercept and R^2 from linear regression analysis of formulation with HEMA, Cap (0, 10, 20 and 40 wt %), etching with phosphoric acid for 20s or no-etching. 170

Table 7-15: Push out stress using wet ivory (control hydration) for HEMA formulations with CaP (0, 10, 20 and 40 wt %) after etching the dentine with phosphoric acid for 20 s or no-etching. Lower section gives linear regression analysis with gradient, intercept and R^2 for average data versus CaP wt %. 173

Table 7-16: Push out stress for experimental formulation with HEMA, Cap (40, 20, 10 and 0% wt) and self-adhesive agent Ibond. Lower section gives linear regression analysis with gradient, intercept and R^2 for average data versus CaP wt %. 175

Table 7-17: shear bond strength gradient, intercept and R^2 from linear regression analysis versus CaP for 4-META formulation with Cap (0, 10, 20 and 40 wt %) after etching with phosphoric acid for 20s or no-etching.	177
Table 7-18: shear bond strength gradient, intercept and R^2 from linear regression of formulation with 4-META, Cap (0, 10, 20 and 40 wt %) and self-adhesive Ibond.	180
Table 7-19: Linear regression analysis of shear bond strength versus CaP for HEMA formulations with CaP (0, 10, 20 and 40 wt %) upon dentine etching with phosphoric acid for 20s and no etching.	182
Table 11-1: Variables for series two formulations.....	207
Table 11-2: Variables factors for series three formulations (etching with 37 % phosphoric acid or no etching).	207
Table 11-3: Variables factors of series four push out test (etching of ivory dentine for 20s or 120 s with 37% phosphoric acid).....	208

LIST OF FIGURE

Figure 2-1: (a) Primary dental caries of posterior molar teeth (b) Secondary caries in premolar teeth under amalgam restoration (14, 15).....	24
Figure 2-2: SEM images of human dentine tubules (39).....	28
Figure 2-3: Dental composites based on filler particles size (87).....	35
Figure 2-4: Chemical structure of Bis-GMA.....	37
Figure 2-5: Chemical structure of UDMA.....	37
Figure 2-6: Chemical structure of TEGDMA.....	38
Figure 2-7: Chemical structure of PPGDMA.....	39
Figure 2-8: Chemical structure of HEMA.....	40
Figure 2-9: Chemical structure of 4-META.....	40
Figure 2-10: Chemical structure of Camphorquinone CQ.....	41
Figure 2-11: Chemical structure of DMPT.....	41
Figure 2-12: Chemical structure of NTGGMA.....	42
Figure 5-1: Filler powder and monomer mix on a rubber mixing pad prior to mixing.....	67
Figure 5-2: Light cured dental composite disc (10 × 1mm thickness) after removed from metal ring.....	68
Figure 5-3: Schematic diagram of FTIR.....	72
Figure 5-4: Diagram showing UV spectrum of chlorhexidine in water.....	78
Figure 5-5: Diagram of UV spectrometer.....	79
Figure 5-6: Calibration curve of the absorbance of 5 wt % CHX concentrations (absorption at 255 nm).....	81
Figure 5-7: BFS jig with ‘ball on ring’ jig.....	83
Figure 5-8: Schematic of Biaxial test.....	84
Figure 5-9: Load vs. central deflection plot generated by the computer connected to the load of the cell.....	84
Figure 5-10: Schematic photographs ivory tusk rectangular block and cylindrical holes.....	86
Figure 5-11: Push out test using Instron instrument and ivory dentine filled with composite.....	87
Figure 5-12: Ivory dentine fixed in self-cured acrylic resin.....	88
Figure 5-13: a) Ivory sample secured in flat edge shear fixture jig, b) Instron machine with “flat-edge” shear bond testing jig.....	89
Figure 6-1: FTIR spectra for monomers used in commercial dental composites.....	94

Figure 6-2: FTIR spectra for Z250 dental composite before and after light cure for 40 s	95
Figure 6-3: FTIR spectra for Gradia dental composite before and after light cure for 40 s .	96
Figure 6-4: FTIR spectra for Ecusphere dental composite before and after light cure for 40 s	97
Figure 6-5: FTIR spectra for control experimental formulations with 4-META (a) and HEMA (b) before and after curing for 40 s	98
Figure 6-6: Degree of conversion for control experimental and commercial composites after curing for 40 s. The error bars indicate 95 % C.I of the mean (n=5).....	99
Figure 6-7: Depth of cure for control formulations with 4-META / HEMA and commercial dental composites after curing for 20 and 40 s. The error bars represent the 95 % C.I . (n=3)	101
Figure 6-8: Mass and volume change (a and b) in deionised water for control experimental formulations with 4-META/ HEMA and the commercial composites. The error bars represent 95% C.I of the mean (n=3).	103
Figure 6-9: BFS for control experimental and commercial dental composites dry and wet (after immersion in water for 24 h, 7 day and 28 days). The error bars represent 95% C.I of the mean. (n=6).	104
Figure 6-10: Young's modulus for control experimental and commercial dental composites dry and wet (after immersion in deionised water for 24 h, 7 day and 28 days). The error bars indicate 95 % C.I of the mean. (n=6).....	106
Figure 6-11: Push out stress with dry ivory dentine for control experimental formulation and commercial composites with acid etched dentine for 20 s and no-etched. The errors represent 95 % C.I of the mean. (n=6).	107
Figure 6-12: Push out stress with wet ivory dentine for control experimental and commercial composites with acid etched dentine for 20 s or no-etched. The error bars represent 95% C.I of the mean. (n=6).....	109
Figure 6-13: Push out stress with wet ivory dentine for control formulations and commercial composites with self-adhesive Ibond. The error bars represent 95 % C.I of the mean. (n=6).	111
Figure 6-14: Shear bond strength with ivory dentine for control formulations and commercial composites with acid etching dentine for 20 s or no etching. The error bars represent 95% C.I of the mean. (n=6).....	113
Figure 6-15: Shear bond strength with ivory dentine for control formulations and commercial composites with Ibond. The error bars indicate 95% C.I of the mean. (n=6).....	115

Figure 7-1: Representative FTIR spectra of experimental formulations containing adhesive monomer a) 4-META and b) HEMA before and after curing for 40 s. The specific examples have PLR 3:1, 20 wt % CaP and 5 wt % CHX and fibre..... 131

Figure 7-2: Degree of conversion for 4-META formulations with CaP (0, 10, 20 and 40 wt %), 5 wt % CHX and fibre, in addition of control formulation after curing for 40 s. The error bars represent 95% C.I of the mean (n=5). 132

Figure 7-3: Degree of conversion for HEMA formulations with CaP (0, 10, 20 and 40 wt %), 5 wt % CHX and fibre in addition of control formulation after curing for 40 s. The error bars indicate 95 % C.I of the mean (n=5). 133

Figure 7-4: Polymerisation shrinkage for 4-META formulations with CaP (0, 10, 20 and 40 wt %), 5 wt % CHX and fibre in addition of control formulation after curing for 40 s. The error bars represent 95 % C.I of the mean (n=5). 135

Figure 7-5: Polymerisation shrinkage for HEMA formulations with CaP (0, 10, 20 and 40 wt %), 5 wt % CHX and glass fibre in addition of control formulation after curing for 40 s. The error bars represent 95 % C.I of the mean (n=5). 136

Figure 7-6: Depth of cure for 4-META formulations with CaP (0, 10, 20 and 40 wt %), 5 wt % CHX and fibre in addition of control formulation after curing for 20 and 40 s. The errors indicate 95% C.I of the mean (n=3). 137

Figure 7-7: Depth of cure for HEMA formulations with CaP (0, 10, 20 and 40 % wt) and CHX and fibre at 5 wt % and control formulation after cured for 20 or 40 s. The error bars indicate 95% C.I of the mean (n=3). 139

Figure 7-8: (a) and (b): Mass and volume change in deionised water for 4-META formulations with different CaP level (0, 10, 20, and 40 % wt), 5 wt % CHX and control experimental formulation. Error bars give 95 % C.I of the mean (n=3). 142

Figure 7-9: (a) and (b): Mass and volume change in deionised water for HEMA formulations with 5 wt % CHX and fibre, CaP (0, 10, 20, and 40 wt %) in addition of control experimental formulation. Error bars indicate 95 % C.I of the mean (n=3). 145

Figure 7-10: Chlorhexidine release into deionised water as a function of square root (SQRT) of time for 4-META formulations with CaP (0, 10, 20 and 40 wt %) and 5 wt % CHX. The error bars indicate 95% C.I of the mean (n=3). 147

Figure 7-11: Chlorhexidine release into deionised waster as a function of square root (SQRT) of time for HEMA formulations with CaP (0, 10, 20 and 40 wt %) and 5 wt % CHX. Error bars indicate 95% C.I of the mean (n=3). 149

Figure 7-12: Biaxial flexural strength for 4-META formulations with added CHX, Fibres (5 wt %) in addition to CaP (0, 10, 20 and 40 wt %) and control experimental formulation. The error bars give 95% C.I of the mean (n=6)	152
Figure 7-13: Young's modulus for 4-META experimental composites with added CHX, Fibres (5 wt %) in addition to CaP (0, 10, 20 and 40 wt %) and control formulation. The error bars indicate 95% C.I of the mean (n=6).....	155
Figure 7-14: Biaxial flexural strength of HEMA experimental composites with added CaP (0, 10, 20 and 40 wt %) in addition to CHX, Fibres (5 wt %) and control formulation. The errors bars give 95% C.I of the mean (n=6).....	157
Figure 7-15: Young's modulus of experimental composites containing HEMA with added CHX, Fibres (5 wt %) in addition to CaP (0, 10, 20 and 40 wt %) and control formulation. Error bars indicate 95% C.I of the mean (n=6).....	159
Figure 7-16: Push out stress for dry ivory dentine with 4-META formulations with added CHX and fibre at 5 wt %, Cap (0, 10, 20 and 40 wt %) in addition of control formulation. Dentine etching with phosphoric acid was for 20s or no-etching. The error bars represent 95 % C.I of the mean. (n=6).	162
Figure 7-17: Push out stress for wet ivory dentine (control hydration) sample with 4-META formulation with added CHX and fibre at 5 wt % and Cap (0, 10, 20 and 40 wt %), in addition of control formulation. Dentine was etching with phosphoric acid for 20s or no-etching. The errors bars indicate 95% C.I of the mean (n=6).....	165
Figure 7-18: Push out stress for 4-META formulation with Cap (0, 10, 20 and 40 wt %) and 5 wt % CHX and fibre in addition of control formulation with self-adhesive Ibond. The errors bars give 95% C.I of the mean. (n=6).....	167
Figure 7-19: Push out stress for dry ivory sample with HEMA formulation with Cap (0, 10, 20 and 40 wt %), 5 wt % CHX and fibre and control formulation after etching with phosphoric acid for 20 s or 0 s of dentine. The error bars give 95 % C.I of the mean (n= 6).	169
Figure 7-20: Push out stress for wet ivory dentine for formulations with HEMA, CaP (0, 10, 20 and 40 wt %) and etching with phosphoric acid for 20s or no-etching. Errors bars indicate 95% C.I of the mean. (n=6).	172
Figure 7-21: Push out stress for wet ivory dentine (control hydration) sample with HEMA formulations with Cap (0, 10, 20 and 40 wt %) after etching of dentine with phosphoric acid for 20s or no-etching. The errors bars represent 95% C.I of the mean. (n=6).....	174

Figure 7-22: Shear bond strength for wet ivory dentine for 4-META formulation with Cap (0, 10, 20 and 40 wt %), 5 wt % CHX and fibre in addition of control formulation after etching with phosphoric acid for 20 s or 0 s. The error bars represent 95% C.I of the mean (n=6).....176

Figure 7-23: Shear bond strength for 4-META formulation with Cap (40, 20, 10 and 0% wt), CHX and glass fibre at (5 wt %) in addition of control formulation and self-adhesive Ibond. The error bars indicate 95% C.I of the mean..... 179

Figure 7-24: Shear bond strength for wet ivory dentine for HEMA formulations with Cap (0, 10, 20 and 40 wt %), CHX and glass fibre at 5 wt % in addition of control formulation after etching with phosphoric acid for 20 s or 0 s. The error bars represent 95% C.I of the mean (n=6).181

Figure 7-25: Shear bond strength for wet ivory dentine for HEMA formulation with Cap (0, 10, 20 and 40 wt %), 5 wt % CHX and glass fibre in addition of control formulation and Ibond. The error bars represent 95% C.I of the mean (n=3). 183

Figure 11-1: Variables for series one formulations.206

Figure 11-2: Variable combinations for a two level factorial experimental design involving three variables. +1 and -1 refer to high and low values of the variable respectively.....209

Figure 11-4: a) Biaxial flexure strength of series one formulation with variables 4-META/ PMDM, TCP/MCPM and PLR. The errors represent 95% C.I of the mean (n=6). b) Factorial analysis of series one formulations. a1 is 4-META / PMDM, a2 CaP (MCPM / TCP,40 or 10 wt %) and a3 is PLR.211

Figure 11-5: a) Biaxial flexure strength of series two formulation with variables 4META/ HEMA, CaP (TCP/MCPM) and TCP particles size. b) Factorial analysis of series two formulations. a1 is CaP (MCPM / TCP,40 or 10 wt %), a2 TCP size and a3 4-META / HEMA is PLR. The errors represent 95% C.I of the mean (n=6).212

Figure 11-6: a) Push out stress for series three formulations with variables 4-META/ HEMA, CaP (40 and 10 wt %) and etching and non-etchingfor 20 s. b) factorial analysis for series three formulations a1 is 4-META / HEMA, a2 is CaP MCPM / TCP (40 or 10 wt %) and a3 is etching / non-etching phosphoric acid . The error bars showing 95 % confidence interval (n=3).213

Figure 11-7: Push out stress for four formulations with 4META/ PMDM, CaP (40 or 10 wt %) and etching with 37 % phosphoric acid for 20 s and 120s. b) Factorial analysis of series four formulations a1 4-META/PMDM, a2 CaP wt % and a3 etching with 37 % phosphoric acid for 20 s and 120s. The errors represent 95% C.I of the mean (n=3).214

Figure 11-8: push out stress for control formulation with 4-META, PLR 3:1or4:1 and etching with phosphoric acid for 20s or no-etching. The errors represent 95 % C.I of the mean. (n=3).....215

Figure 11-9: push out stress for control formulation with 4-META, PPGDMA or TEGDMA, NTGGMA or DMPT and etching with phosphoric acid for 20s or no-etching. The errors represent 95 % C.I of the mean. (n=3).....217

ABBREVIATION

4-META	4-methacryloyloxyethyl trimellitic acid anhydride
ACP	Amorphous calcium phosphate
BAC	Benzalkonium chloride
BFS	Biaxial flexure strength
Bis-GMA	Bis glycidyl ether dimethacrylate
Ca	Calcium
CaP	Calcium phosphate
C.I	Confident interval
CHX	Chlorhexidine diacetate,
CQ	Camphorquinone
DSC	Differential scanning calorimetry
DCPA	Dicalcium phosphate anhydrite
DMAEMA	Dimethylaminoethyl methacrylate
DMFT	Decayed, Missing, and Filled Teeth
DMPT	N, N-dimethyl-p-toluidine
FTIR	Fourier transforms infrared spectroscopy
GIC	Glass ionomer cement,
H	Hours
HA	Hydroxyapatite
HEMA	2-Hydroxyethylmethacrylate
IR	Infrared spectroscopy
LED	Light emitting diodes
MCPM	Monocalcium phosphate monohydrate
MDP	10-Methacryloyloxydecyl dihydrogen phosphate
MDPB	Methacryloyloxydodecylpyridinium bromide
Min	Minute
MPa	Mega Pascal
MPS	Methacryloxypropyltrimethoxysilane
NMR	Nuclear magnetic resonance
NTGGMA	N-tolylglycine Glycidyl Methacrylate
nm	Nanometre

PAA	Polyalkenoic acid/Poly acrylic acid
PLR	Powder liquid ratio
PO	Phosphate
PPGDMA	Poly (propylene Glycol 425Dimethacrylate)
QADM	Quaternary ammonium dimethacrylate
μm	Micro meter
R•	Free radical
RMGICs	Resin modified glass ionomer cements
S	Seconds
TCP	β-Tricalcium phosphate
TEGDMA	Triethylene glycol dimethacrylate
T _g	Glass transition temperature
Wt %	weight percent
UDMA	Urethane dimethacrylate
UV	Ultraviolet spectroscopy
Vol %	Volume percent

1. Introduction

Dental caries is a highly common disease which affects adults and children worldwide. Presently, dental composites are widely used for restoring caries affected teeth and are the material of choice for dentists and patients. This is primarily due to their excellent aesthetics (1). Good aesthetics is particularly important for anterior teeth. Amalgam restorations, however, have better longevity than dental composites particularly for posterior teeth where strength is more of an issue (2). One study showed the survival level in permanent teeth after 7 years was 67 % for dental composites and 95 % for amalgam restorations (3). Composite restorations therefore require more frequent replacement and repair at a much higher rate than amalgam causing further loss of the sound tooth structure. Currently, replacement of tooth restorations dominates about 60 % of dentist's clinical time (4).

Dental composites in the past have failed due to low mechanical properties. In the 1990 's composite flexure strength was ~ 80 to 120 MPa while amalgam restorations have a flexural strength above 400 MPa (5, 6). Nowadays, recurrent caries is however a more serious issue as composite strengths have improved. Upon placement dental composites shrink. This polymerisation shrinkage affects integrity of bonding between the restoration and tooth structure and result in gaps at the tooth interface (7). This gap allows bacteria and oral fluid to accumulate between the restoration and dentine, leading to sensitivity, discoloration of the restoration and secondary caries with continuing tooth demineralisation. In addition composite restorative materials, exhibit a tendency to accumulate bacteria biofilms more than other restoration materials (8). This has been attributed to lack of or limited antibacterial properties and presence of uncured monomer (9). Furthermore, the need to use complex bonding procedures make composite placement difficult.

There have been many attempts to develop dental composites that are antibacterial, remineralising and self-adhesive but no formulations are as yet ideal largely due to reductions

in strength. The project aim was therefore to develop unique bioactive dental composites with better degree of conversion, water sorption induced expansion to compensate for shrinkage, antibacterial and remineralising agent release, high strength, and the ability to self-adhere to the tooth structure without a bonding agent as compared to current dental composite.

The proposed composites will contain monomers with potential for higher conversion and hydrophilic components (e.g. monomers with amine or carboxylic acid groups) that will encourage swelling as result of water sorption. This process will counteract polymerisation shrinkage. Moreover, acidic and basic groups at the material surface could enable bonding to dentine through ionic interaction which may lead to improved composite adhesion. Calcium phosphate fillers, with the potential to re-mineralise minor defects in the tooth structure, will also be added. The calcium phosphate has to be more soluble than hydroxyapatite in order to be released from the set composite. Finally, chlorhexidine will be included to provide antibacterial action. Combined calcium phosphate and chlorhexidine penetration into the surrounding carious dentine will provide a mechanism to improve tissue resistance to on-going enzymatic and bacterial damage. This should help prevent further tooth decay.

2. Literature review

2.1. Dental caries

Dental caries occurs as a result of bacteria on the tooth surface and subsurface, causing acid production and localised destruction (10). Dental caries is also related to the high consumption of dietary foods containing sugar, low saliva flow and low exposure to fluoride (11). It can be classified as primary or secondary caries. White spot caries (initial caries) is the first attack of caries on a sound tooth surface (enamel) (Figure 2.1a), whereas secondary caries is a carious lesion that develops adjacent to or beneath a restorative filling in an old cavity (Figure 2-1 b) (12, 13).

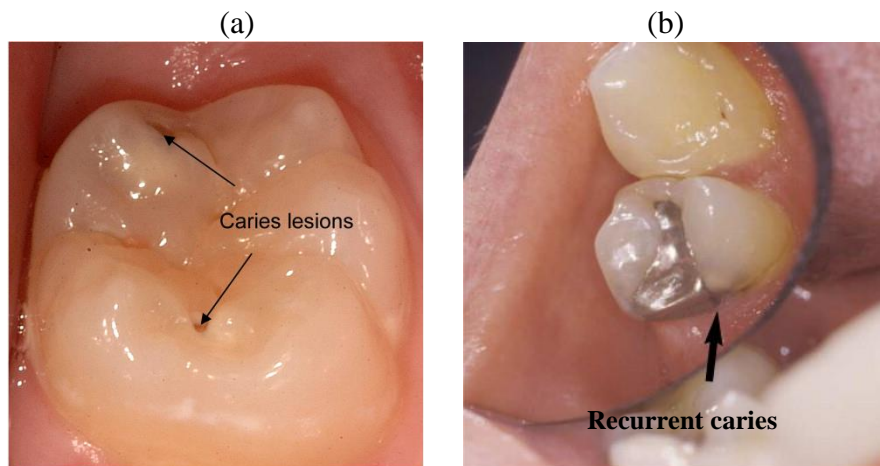


Figure 2-1: (a) Primary dental caries of posterior molar teeth (b) Secondary caries in premolar teeth under amalgam restoration (14, 15).

2.2. Prevalence of dental caries

Dental caries is one of the most common chronic diseases affecting both children and adults globally (16). It affects about 36 % of the entire population (17). The US department of health has reported a 46 % prevalence of dental caries in children aged between 4 and 11 year old. With people above 15 years old this rose to 80 % prevalence (18). A UK report indicated a 31 % prevalence of dental caries in children aged 5 and 91 % in those above 20 years old (19).

Toothache and difficulties with eating due to missing or broken teeth have a major impact on people's daily life. In 2009, WHO claimed that poor oral health might have an effect on general health as well as quality of life. Many dental diseases are now also related to various chronic diseases (16).

2.3. Pathogenesis

Tooth caries occur upon fluctuation in the pH (demineralisation and remineralisation) of the tooth surface (20). Caries lesion occurs initially within dental plaque. The plaque covers the tooth area and protects the bacteria from mastication and wear (12). The plaque must be properly removed to prevent the caries lesion developing (21, 22).

Many types of bacteria responsible for oral diseases have been identified (e.g. *Streptococcus mutans* and *Lactobacilli*) (23). Below a pH of 5.5, demineralisation (the dissolution of the hydroxyapatite) occurs (24, 25). If the demineralisation is not reversed by remineralisation the issue can progress to the pulp (24). Once tooth structure has been damaged by caries it may require restoration (13).

2.4. Factors involved in caries development

Dental caries is a multifactorial disease; the main determining factors of caries activity are the agent (cariogenic micro-organism), fluoride exposure, diet and saliva. The complex interactions between saliva structure and secretion, diet, pH fluctuations at different sites of the tooth determine the rate of initiation and progression of dental caries.

2.4.1. Dental biofilm

A dental biofilm (plaque) is a complex microbial community; it is the aetiological agent for major dental caries. "*Streptococcus mutans* and "*Lactobacilli*" have generally been found at higher concentrations on caries lesions (26). These bacteria produce acid and are categorised

as acidogenic. Moreover, “*Streptococcus mutans*” produces extracellular polysaccharides which help in bacteria attachment to and colonization of the tooth surface. Other bacteria that are aciduric can survive and grow under acidic conditions. These bacteria, however, make up less than 1 % of dental plaque (26, 27).

The biofilms can also develop on the surface of different filling restorations. These biofilms are responsible for secondary caries formation. The cariogenicity of the dental biofilm is dependent on the type of filling restoration. More cariogenic biofilms have been observed on the surface of composite than other filling materials such as amalgam restorations (28). This is mainly due to the lack of or limited antibacterial properties of dental composite restorations. Moreover, it has been reported that the leakage of un-polymerised resin monomer from the composites might raise the growth rate of some cariogenic species (29). Consequently, the composite resins develop secondary caries at higher rates than any other restorative materials (16).

2.4.2. Dietary factors

Low molecular weight monosaccharides such as glucose and fructose are cariogenic because they can be easily metabolised by bacteria (30). More complex high molecular weight carbohydrates such as polysaccharides are less cariogenic (26).

2.4.3. Saliva

Dental caries is affected by saliva secretion level and composition. The buffering capacity of saliva helps to neutralise the acid produced by bacteria. Furthermore, the fluoride and calcium phosphate content of saliva can help in remineralisation activity. Once salivary secretion function is reduced (xerostomia), the risk of dental caries is increased.

2.5. Tooth Structure

Teeth have two anatomical parts: crown and root, the crown is covered with enamel while the root is covered with cementum. Enamel provides the hard outer covering of the crown that allows efficient mastication. Dentine forms the bulk of the tooth. It is located between the pulp and the enamel and joined to the enamel at the dentine-enamel junction. The pulp is a soft tissue containing blood vessels, sensory nerves and cells which form reparative dentine (31, 32). Cementum forms a thin layer covering root dentine; its composition is similar to dentine having 50 wt % inorganic and 50 wt % organic matrix (33). The primary function of cementum is to promote attachment of the tooth to alveolar bone by the periodontal ligament (34).

2.5.1. Enamel

Enamel is the hardest substance in the body; it covers the outer layer of the crown and produced by ameloblasts. Enamel is the most highly calcified tissue in the human body. It contains 95 % by weight inorganic hydroxyapatite crystals, 5 % by weight organic matrix and a small amount of water; therefore, it is less hydrophilic as compared to dentine which has a higher amount of water. The hydroxyapatite crystals in enamel are closely packed rods known as enamel prisms or enamel rods (35). These rods are about 5 μm in diameter near the dentine and 8 μm on the surface (10). The enamel prisms are exposed easily by phosphoric acid etching, commonly used in enamel bonding and when removing dentine smear layers during cavity preparation. Enamel is very brittle with low tensile strength and high modulus of elasticity making it a rigid structure but the dentine below the enamel acts as a cushion to help withstand the masticatory forces.

2.5.2. Dentine

Dentine is a complex hydrated biological composite structure that forms the bulk of the tooth. It is covered by enamel on the crown and cementum on the root, and provides covering for the pulp tissue (36). Without the support of the dentine structure, the enamel could fracture when exposed to mastication forces. Dentine is composed of 70 weight % inorganic hydroxyapatite crystals or 50 % by volume. Dentine has a higher percentage organic content (18 % by weight or 25 % by volume) and water content (12 % by weight or 25 % by volume) as compared to enamel (37). Dentine also contains microscopic channels called dentinal tubules surrounded by highly mineralised peri-tubular dentine embedded in inter-tubular dentine (Figure 2-2) (38).

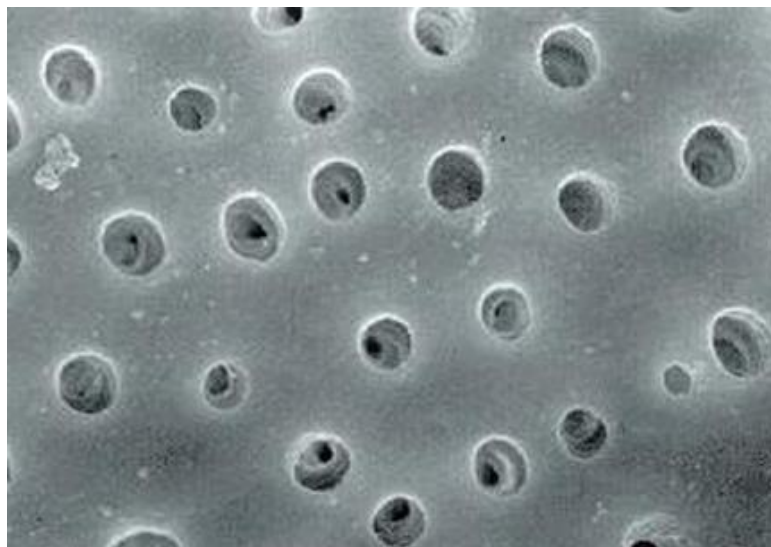


Figure 2-2: SEM images of human dentine tubules (39).

The inter-tubular dentine contains hydroxyapatite embedded in the collagen matrix that forms the bulk of dentine, and peri-tubular dentine lining of the tubular walls (40). The diameter of dentinal tubules gradually increases from 0.9 μm in diameter near the dentino-enamel junction (DEJ) to 2.5 μm in near the pulp chamber. The number of the dentinal tubules increased from 20,000 / nm^2 near the enamel to 45,000 / nm^2 near the pulp chamber (37, 41).

Different forms of dentine include primary, secondary and reparative or tertiary dentine (42). The primary dentine is formed during the tooth development; whereas, secondary dentine is formed slowly throughout the life while the tooth (pulp) is still vital. However, tertiary dentine is formed in response to the protective mechanism of the pulp against pathogenic bacteria or bacterial acid production and trauma or injury. Tertiary dentine is located between secondary dentine and pulpal tissue (35).

2.6. Demineralisation and remineralisation of tooth structure

The processes of demineralisation and remineralisation are dynamic processes affected by both the tooth structure and the oral environment. The mineral composition of the tooth structure (hydroxyapatite) is at equilibrium at pH 6-7 (43). Demineralisation is the process of removing minerals from the tooth structure and occurs as a result of the pathogenic bacteria metabolise the fermentable carbohydrates resulting in the production of organic acid. Moreover, the consumption of acidic food and beverage can lead to a drop of pH below 5.5. This results in the hydroxyapatite dissolving (12, 24). However, demineralisation can be reversed by the buffering or restoring of minerals back in the presence of calcium and phosphate in the oral cavity. When the pH increases to 6-7 the re-precipitation of calcium and phosphate is enhanced within the demineralized tooth structure. This process is called remineralisation (11, 44). Furthermore, saliva and regular teeth brushing provide calcium and phosphate ions diffuse through the tooth surface and increase the rate of tooth remineralisation. The caries process itself cannot be prevented but can be controlled (45).

2.7. Concept of adhesion

The main mechanism of adhesive bonding to enamel and dentine involves an exchange process in which there is substitution of inorganic tooth material by resin monomers. This mechanism can be achieved by two steps. The first step, is to clean the tooth surface and

remove the smear layer by application of acid, most commonly, phosphoric acid (46). Second step, involves infiltration of adhesive monomer which upon polymerisation becomes micromechanically interlocked with the tooth surface (47). This process results in a hybrid-layer, that is a few micrometres deep (48). There may additionally be some chemical (ionic or covalent) bonding between the adhesive and tooth surface (37). The adhesive is subsequently chemically bound to the composite through monomer polymerisation.

2.7.1. Enamel bonding

The mechanism of adhesion of dental composites to enamel is the micromechanical retention from the formation of resin tags into the irregular surface created by acid etching (42). Normally, etching enamel with 30-40 % phosphoric acid for 15 seconds is sufficient for retention. Applying acid etching to enamel is a standard clinical procedure that results in the demineralisation of the superficial enamel layers, and creates a rough surface (49). Normally, acid etching removes about 10µm of the enamel surface and dissolves the rods. The effect of acid etching on enamel surface is dependent on type of acid, acid concentration and the time of etching.

When a resin monomer or adhesive is applied and infiltrated into the surface, and polymerised it becomes mechanically interlocked with the enamel structure (46, 50). Effective adhesion to enamel has been achieved with relative ease and has proven to be reproducible, durable and reliable in routine clinical applications (51).

2.7.2. Dentine bonding

Dentine bonding is far more challenging when compared to enamel bonding. This is largely due to dentine being a more heterogeneous and an intrinsically wet substance which makes it more difficult to be wet by hydrophobic adhesive monomers. Another contributing factor is

the formation of a smear layer that covers the dentine after cavity preparation with rotary instruments (41, 52). This can be defined as any debris such as cut collagen fibres and hydroxyapatite crystals over the tooth surfaces (53). The thickness of the smear layers is about 0.5 to 2 μm , and blocks the dentinal tubules. This leads to decrease in dentine permeability by about 86 % (54). These layers must be removed to increase dentine permeability by applying acid etching to allow contact between resin monomer and dentinal tubules.

Due to the hydrophilic nature of dentine, the combined use of hydrophilic and hydrophobic resin monomer has been suggested to improve adhesion. The hydrophilic functional group enables infiltration of the monomer into the dentinal tubules (collagen matrix), enabling enhanced formation of a hybrid- layer. However, the hydrophobic methacrylate groups enables bonding to the hydrophobic resin monomer of the restoration (55).

2.8. Current restorative materials

Dental restorative materials have been used to restore the function of decayed and injured teeth, improve aesthetics or replace missing tooth structure. Restorative dental materials can be classified according to the principles of application as direct restorative materials and indirect restorative materials. Restorative materials include direct amalgam, resin composite and glass ionomer cements (GIC) and are used directly inside the oral cavity to restore the function of teeth and to increase the aesthetics appearance (56). Whereas, indirect restorative materials such as indirect porcelain or ceramic , gold alloys and indirect resin composites are consumed extra orally to damaged or missing teeth (42, 57).

2.8.1. Amalgam restoration

Previously dental amalgam was one of the most important dental filling materials in dentistry. It has been widely used as a restorative material for decayed posterior teeth during the 20th

century. In the USA about 100 million people have amalgam restorations (58). Dental amalgam is produced by combining liquid mercury with alloy. The alloy is a powder and consists mainly of silver, tin and copper. Zinc and palladium may also be present in small amounts. The set compound has a high durability, high occlusal load resistance due to high strength, high fracture toughness, excellent wear resistance and is also inexpensive (36). Dental amalgam fillings are also known as silver fillings because of their appearance. More recently, the use of amalgam has declined due to increased demand for more aesthetically pleasing restorations. Furthermore, due to lack of chemical adhesion cavity preparations for amalgam fillings require excessive sound tooth structure removal to provide mechanical retention as they do not bond to tooth surface (59).

Many studies have been conducted on the possible health hazard from dental amalgam use (60). These studies have failed to demonstrate a deleterious effect of mercury in dental amalgam on human health (61, 62). The mercury management in dental practice has, however, become an important issue (63, 64). Upon the placement and removal of amalgam filling restorations, small amounts of mercury vapours are released, leading to mercury accumulation in dental staff or discharge to the environmental (65-67).

2.8.2. Glass ionomer cements

In 1970, Wilson and Kent introduced glass ionomer cements (GIC) into dentistry. GICs are typically set by an acid base reaction between an aqueous polyacrylic acid solution and a fluoroaluminosilicate glass powder (68, 69). GICs are widely used as luting agents and mainly for filling materials of abrasion and erosion lesion due to their chemical adhesion to enamel and dentine (70). They can potentially reduce bacterial microleakage by improving adhesion to the hard dental tissue and by releasing fluoride. Furthermore, fluoride ions interact with the tooth surface to form fluoroapatite, which makes tooth less soluble in acids

produced by cariogenic bacteria (71). Moreover, the coefficient of thermal expansion of GICs is close to the tooth structure. Thus, they show more dimensional stability compared to resin composites (72). However, GICs exhibit initial moisture sensitivity, insufficient physical properties to be used in stress bearing areas, and poor aesthetics (73, 74).

2.8.3. Resin modified glass ionomer cements and compomers

To overcome the drawbacks of GICs, many manufacturers have been developing hybrids of dental composites and glass ionomer cements to improve adhesion, fluoride release, aesthetic and mechanical characteristics. These materials can be divided into Resin-modified glass ionomers cements (RMGICs) and polyacid modified composites (compomers) (75).

In the late 1980s, RMGICs were introduced. These are a combination of GICs components (polyacrylic acid and water) and a hydrophilic monomer (e.g. HEMA). RMGICs have superior mechanical strength, a better aesthetic appearance and reduced moisture sensitivity compared to GICs (76). The major disadvantage of HEMA is increased water sorption, which leads to plasticity, potentially excessive expansion and dimensional changes (77, 78).

Compomers contain composite components such as Bis glycidyl ether dimethacrylate (Bis-GMA) with a small amount of acid functional monomers which can attract water and subsequently react with additional inorganic particles that contain fluoride (79). The materials are initially set by light activated polymerisation, which is followed by water sorption (80, 81). Compomers have a greater resistance to occlusal load than GICs (82). However, they release limited amounts of fluoride (83). Furthermore, compomers generally require additional bonding agents and undergo polymerisation shrinkage. Bacterial micro leakage and secondary caries therefore remain a concern (79).

2.8.4. Dental composite

Over the last two decades dental composites have become the most widely used as dental filling materials (84). Recent developments in resin restorative composites has enabled improved aesthetic quality and bonding with the enamel surface properties and greater safety compared to dental amalgam (1, 85). Dental composites are used for many applications such as filling materials, crown restorations, pit and fissure sealants, cavity liners and orthodontic devices (86). Class one and two posterior cavity restorations should have dental composites that show high strength, whilst anterior restorations require more aesthetic appearance. Dental composites contain three essential ingredients: inorganic filler phase, a cross-linkable organic phase containing initiator/ co-initiator, and a coupling agent (36). Manufacturers may also add other ingredients such as stabilisers, catalysts and/or pigments but specific information regarding the composition of these ingredients is often not fully disclosed.

2.8.4.1. Filler phase

The inorganic filler phase of current dental composites consists of silanated quartz particles, fused silica and glass particles such as aluminium silicates, barium, strontium and zirconium glasses (87). The primary purpose of these fillers is to improve mechanical properties (88), reduce polymerisation shrinkage (89), and limit the amount of expansion by water sorption (86). There are different types, sizes, shapes and amounts of filler particles in different dental composites. Dental composites were classified according to the filler particle size by Robertson in 2006 (86). Conventional or macro-fill dental composites have 60-80 wt % filler and average particle size range of between 10 and 50 μm (Figure 2-3) (90). These composites have good flexure strength (110 to 135 MPa), but due to polishing difficulties, have poor aesthetics and are therefore now rarely used (87).

In micro-fill composites the filler particle size was decreased to approximately 40-50 nm. This reduction improves the polishing surface and therefore the aesthetic appearance. However, the micro-fill composites have higher shrinkage and lower strength compared to conventional composites due to the low percentage of filler ~ 35-50 wt % (86).

To overcome the disadvantages of micro-fill composites hybrid composites were developed. These contain more than one filler size in order to increase filler loading and mechanical properties. The particles sizes are typically 10 to 50 μm and 40 nm diameter (87). Further refinements and improved grinding methods resulted in dental composites called mini-fill with an average size of between 0.4 and 1 μm . These hybrid composites are considered more universal since they are applicable on both anterior and posterior teeth (86, 91).

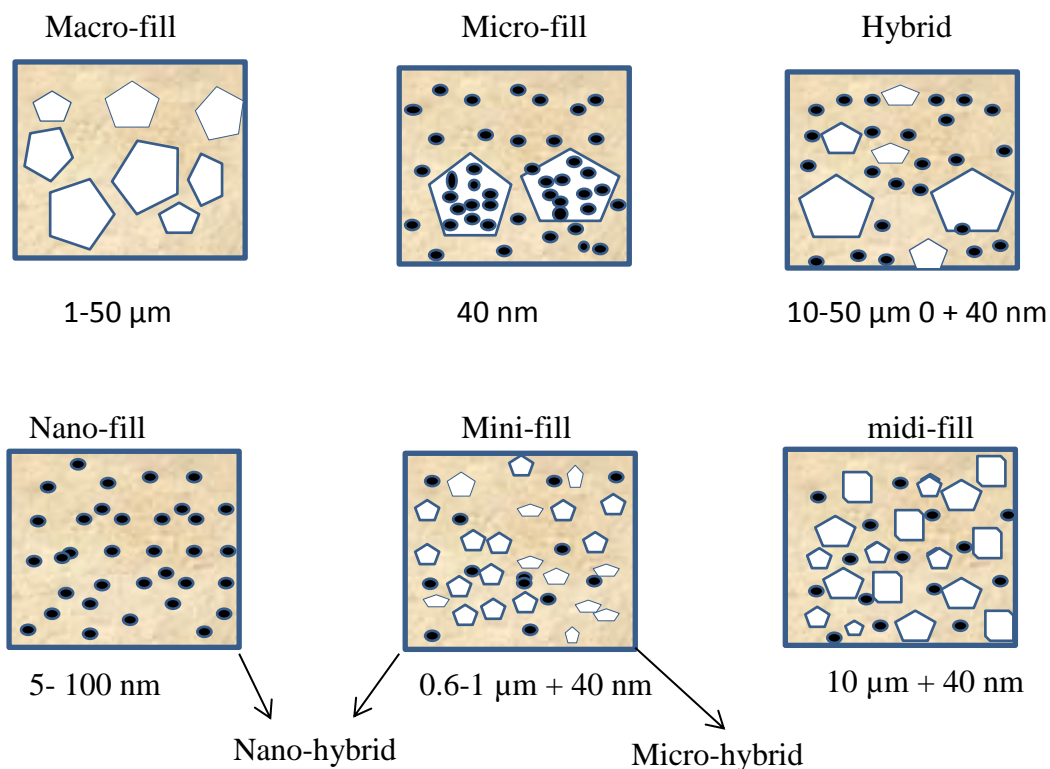


Figure 2-3 : Dental composites based on filler particles size (87).

The nano-fill composites contain a combination of non-agglomerated 20 nm nano silica and aggregated zirconia/silica nano clusters (with primary particle sizes from 5 to 20 nm). These are claimed to provide increased aesthetics, strength and durability. The cluster particle size range is 0.6 to 1.4 μm and filler loading is about 59% by volume (92).

2.8.4.2. Organic resin matrix

The monomer phase in most dental composites contains a mixture of aromatic and aliphatic dimethacrylate monomers, such as Bis-GMA and/or UDMA. The organic matrix additionally contains diluent monomers and an initiator/ co-initiator.

2.8.4.2.1. Base monomer

2.8.4.2.1.1. Bisphenol A-glycidylmethacrylate (Bis-GMA)

Bisphenol a-glycidylmethacrylate (Bis-GMA) or Bowne's resin is one of the most commonly used monomers. It is a viscous monomer with high molecular weight (512 g/mol) (93). It contains two aromatic rings in the structure, and also hydrogen bonding hydroxyl groups (OH) (Figure 2-4) (76, 94). This base monomer creates filling materials with good mechanical properties. Furthermore, its high molecular weight ensures low polymerisation shrinkage (95, 96).

The double aromatic rings make the monomer quite rigid compared to other more flexible dimethacrylates with no aromatic groups. This can lead to low (C=C) monomer conversion, Uncured monomers may leach from the set filling over time, adversely affecting biocompatibility (97). It can also stimulate bacterial growth around the filling restoration (98). Additionally, poor conversion may reduce strength and provide limited crosslinking which is important for wear resistance. Two major concerns with current dental composites are the fracturing of the restorations and inadequate resistance to wear under masticatory

attrition (29). To solve these issues Bis-GMA is used with diluents and other dimethacrylate monomers such as urethane dimethacrylate (UDMA).

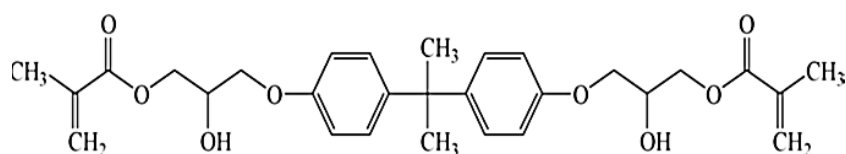


Figure 2-4: Chemical structure of Bis-GMA.

2.8.4.2.1.2. Urethane dimethacrylate (UDMA)

Urethane dimethacrylate (UDMA) (Figure 2-5) is an alternative aliphatic high molecular weight dimethacrylate monomer, compared to Bis-GMA. It has been used alone or in combination with Bis-GMA in dental composites previously (99). The molecular weight of UDMA is 470 g/mol and has a polymerisation shrinkage percentage of 6.5 % (100). It has two amine groups (NH), which can associate with carbonyl groups (C=O) (78, 101). The amine groups in UDMA however, produce weaker hydrogen bonds than the hydroxyl groups in Bis-GMA. This greater rotational freedom is responsible for the much lower viscosity and greater conversion of UDMA compared to Bis-GMA (87). The higher conversion may also reduce water uptake due to greater crosslinking and increased mechanical properties. Moreover, UDMA has been reported as less cytotoxic than Bis-GMA (102).

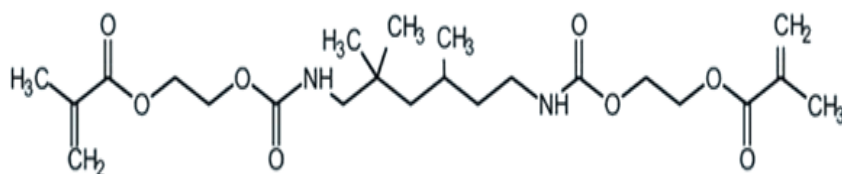


Figure 2-5: Chemical structure of UDMA.

2.8.4.2.2. Diluent monomer

Due to the high viscosity of bulk Bis-GMA and UDMA, monomers they are usually diluted with low viscosity monomers. The most commonly used diluent monomers are triethylene glycol dimethacrylate (TEGDMA) and 2-hydroxyethylmethacrylate (HEMA)

2.8.4.2.2.1. Triethylene glycol dimethacrylate (TEGDMA)

Triethylene glycol dimethacrylate (TEGDMA) is an aliphatic and low molecular weight component (Figure 2-6). The molecular weight of TEGDMA is 286 g /mol (93) and the flexibility of the C-O groups results in lower viscosity, lower glass transition temperature (T_g) and a higher degree of conversion (103). TEGDMA addition can therefore improve the composite paste consistency. Unfortunately this monomer also has high affinity for water due to the presence of ether linkages (C-O-C). This in combination with the low molecular weight of these monomers increases shrinkage and water sorption (104). Despite these limitations, TEGDMA is still used within most current dental composites.

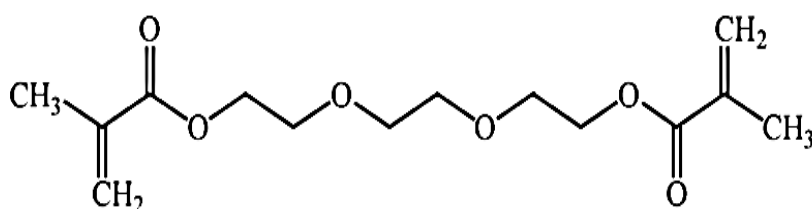


Figure 2-6: Chemical structure of TEGDMA.

2.8.4.2.2.2. Poly (propylene Glycol 425 Dimethacrylate) (PPGDMA)

A new diluent monomer has been used in this thesis polypropylene glycol 425 dimethacrylate (PPGDMA) (Figure 2-7). PPGDMA is a low viscosity dimethacrylate but has three times the molecular weight (660 g / mol) of TEGDMA. It should therefore result in lower

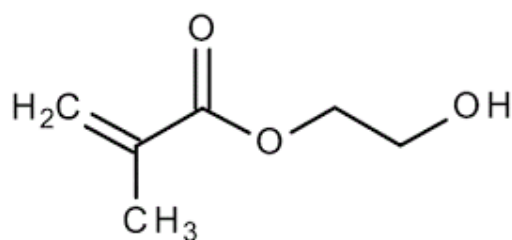


Figure 2-8: Chemical structure of HEMA.

2.8.4.2.3.2. 4-Methacryloxyethyl trimellitic anhydride (4-META)

4-methacryloxyethyl trimellitic anhydride (4-META) (Figure 2.9) is an acidic monomer frequently used as an adhesion promoting monomer (111). 4-META is a crystalline powder. After the addition of water to 4-META powder it is swiftly hydrolysed into 4-MET. The resultant monomer contains two carboxylic groups attached to the aromatic group. These provide the acidic (demineralising) properties, and also enhance wettability.

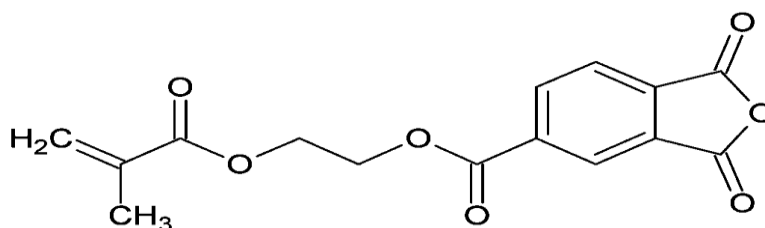


Figure 2-9: Chemical structure of 4-META.

However, the hydrophobic aromatic group of these monomers will moderate the acidity of and hydrophilicity of the carboxyl groups (112). 4-META has been reported to form a chemical bond with calcium in hydroxyapatite which may improve adhesion to tooth structure (76).

2.8.4.2.4. Initiator and co-initiator

Dental composites are normally cured by a free radical polymerisation reaction. Free radicals can be generated either by thermal, chemical or photochemical activation (light cure).

2.8.4.2.4.1. Camphorquinone (CQ)

The initiator used in photo-activated systems is usually camphorquinone (CQ) (Figure 2.10). The amount of initiator added is typically very small (from 0.2 to 1 wt %) and is consumed during the polymerisation reaction. The initiator is combined with a co-initiator containing tertiary amine groups. These don't absorb light but react with the initiator to produce more stable free radicals which provoke the polymerisation (86).

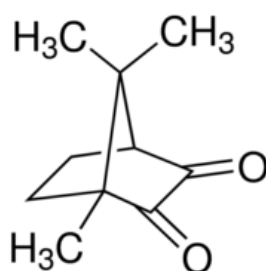


Figure 2-10: Chemical structure of Camphorquinone CQ.

2.8.4.2.4.2. N, N-dimethyl-p-toluidine DMPT

A common co-initiators used in dental composites are n, n-dimethyl-p-toluidine DMPT (Figure 2.11) and dimethylaminoethyl methacrylate (DMAEMA) (113, 114). CQ absorbs blue light at 400-500 nm wavelengths, and then reacts with the co-initiator to produce free radicals (115, 116).

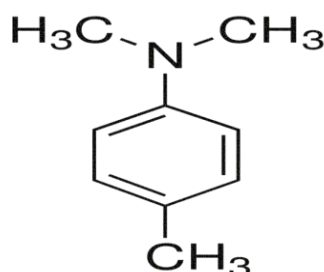


Figure 2-11: Chemical structure of DMPT.

2.8.4.2.4.3. N-tolyglycine Glycidyl Methacrylate (NTG-GMA)

In this study n-tolyglycine glycidyl methacrylate NTG-GMA (Na) (Figure 2.12) was used as an alternative co-initiator to DMPT. NTG-GMA is an adhesion promoting monomer which also functions as a co-initiator due to the presence of a tertiary amine group. It also contains a carboxyl group for calcium binding (117). Binding of the monomer group could result in lower levels of toxicity in the set composite.

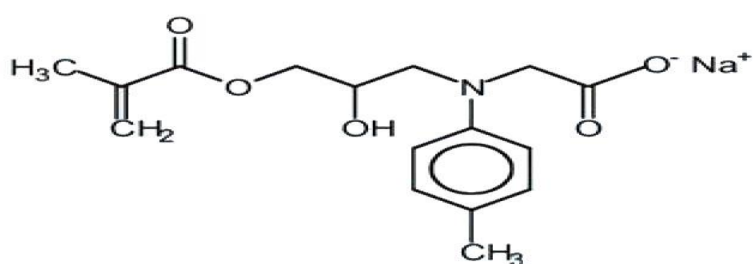
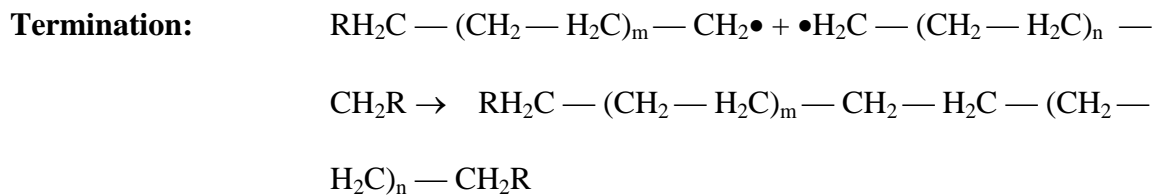
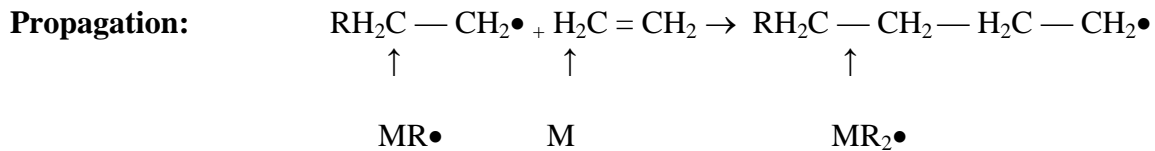
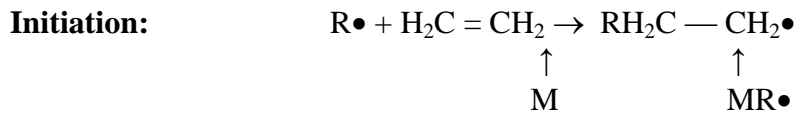


Figure 2-12: Chemical structure of NTGGMA.

2.8.4.3. Polymerisation mechanism

The process of polymerisation consists of three main steps: initiation, propagation/crosslinking and termination. Generally, the polymerisation reaction in dental composites is activated by free radicals ($R\bullet$). As described above the photo-initiator CQ is required to generate the free radical. During the initiation, the free radical ($R\bullet$) reacts with the C=C double bond at the ends of monomer, which opens the double bond and creates an excited monomer ($MR\bullet$). The excited monomer can react with the C=C double bond to bond to other monomers, leading to the formulation of cross-linking or bigger polymer chains and propagation (87). Termination occurs when two growing chain radicals are combine to produce a dead polymer (118). The steps of a polymerisation reaction can be seen in the following:



2.8.4.4. Coupling agent

The primary goal when using coupling agents is to achieve a good bonding between the filler and matrix phases of the dental composites. Silanation improves the resin composites resistance to hydrolytic degradation and enhances mechanical properties. The most widely used coupling agent is 3- methacryloxypropyltrimethoxysilane (MPS). This contains a silane group at one end to bond to OH groups on the glass surfaces and a methacrylate (C=C) on the other end to form covalent bonds with the monomer. This forms a strong interfacial bridge that binds the fillers to the monomer and improves the mechanical properties of the composites (87).

2.8.4.5. Glass fibre

Various different types of fibre have been added to dental composites and bone cements in order to increase the strength and improve the fracture toughness and fatigue properties of dental materials (119-123). Moreover, fibres were used in the reinforcement of denture base resins, bridges, splints, retainers, orthodontic arch wires, fixed prosthodontic appliances and fixed partial dentures (124-127). Different types of fibre have been added in dental materials

ranging from micron-scale quartz, silicate glasses to nano-scale carbon tubes (128). Glass fibre has been preferred for use in dental materials because of their translucency, ease of silane surface treatment, higher fatigue properties, improved toughness and flexural strength (129). Kane et al, has shown that addition of relative small concentrations of fibre improve the fatigue resistance and fracture toughness of acrylic bone cement without drastically affecting the strength and handling properties (130).

2.9. Properties of dental composites

2.9.1. Handling properties

Resin composites are viscoelastic materials by nature. Viscosity and elasticity are important factors in determining the handling properties of dental composites. The handling of composite is determined by the chemical structure of the monomer matrix and filler particle size and level. Placing filling composites in posterior teeth is more challenging compared to placing an amalgam filling. Dental composite should be easy to place in the oral cavity and easy to manipulate, in terms of shaping the restored cavity and being packable. Moreover, composite paste should be adhered to the tooth surface and not stick to instruments (131). The success of composite filling restoration depends heavily on having a good bond to enamel and dentine. In order to place dental composites in an oral cavity, a rubber dam is therefore required because the composite bonding is susceptible to fluid contamination. In molar class two cavity restorations rubber dam should be used to control moisture contamination.

2.9.2. Degree of conversion

The final degree of conversion in dental composites rarely reaches 100 % (132). Instead, typically light cured dental composites exhibit a degree of conversion ranging from 55 % to

75 % (133, 134). Uncured monomers that leach from the filling restoration over time, may stimulate the growth of bacteria or cause allergic reactions in patients (135). Moreover, these monomers are potentially harmful to pulp cells (97).

The monomers used in dental composites play a key factor in determining the final degree of conversion. With Bis-GMA as monomer and TEGDMA as diluent, the degree of conversion has been found to decline when the amount of Bis-GMA is increased (136). The degree of conversion can also be higher when the mixture contains UDMA as bulk monomer and TEGDMA as diluent (136). Some studies have also shown that increasing inorganic filler loading may decrease conversion (137).

There are many techniques available to determine the degree of conversion of resin composites such as Fourier transforms infrared spectroscopy (FTIR), RAMAN spectroscopy, differential scanning calorimetry (DSC) and nuclear magnetic resonance (NMR). FTIR has been widely employed to identify chemical functional groups by their different vibration modes in the molecular structure and for monitoring the kinetics of chemical reactions (64).

2.9.3. Polymerisation shrinkage

Despite major improvements in dental composites since the 1960s, polymerisation shrinkage still remains of considerable concern. Polymerisation shrinkage occurs due to the transformation of monomer molecules (C=C carbon double bond) into a polymer network (C-C single bonds) (138). This is due to a decrease in the distance between groups of atoms and a reduction in the amount of free volume during polymerisation (118). The Bis-GMA and TEGDMA monomers exhibit high polymerisation shrinkage of ~ 5 to 6 % and 12.5 % respectively (139). The high amounts of TEGDMA in the monomer phase increase polymerisation shrinkage, because its low molecular weight increases C=C density. Furthermore it increases fluidity and thereby the final level of monomer reaction (89).

Current commercial dental composites available in the market exhibit volumetric shrinkage between 2.6 to 6 % upon curing (89, 90, 118, 140).

Polymerisation shrinkage depends on the degree of conversion and the molecular weight of the monomers (141), and the amount of inorganic filler used in dental composites. In general, a higher percentage of filler leads to a decrease in polymerisation shrinkage (142).

Polymerisation shrinkage generates contraction stress which may result in the formation of micro cracks within the bulk of the filling (143). The resultant stress can also affect the integrity of bonding, particularly at the dentine restoration interface. Contraction stresses can then disrupt the marginal seal between the composite restoration and tooth structure (7). This allows bacteria and oral fluid to accumulate between restoration and dentine, leading to sensitivity, discoloration of the restoration, secondary caries and a reduced filling lifetime (8).

The polymerisation shrinkage of resin dental composites is proportional to the number of monomers polymerising per unit volume. As a result it decreases with increased filler content, or reduced monomer conversion or increased monomer molecular weight (89). Composites with high filler loading at (~ 60 vol % as in hybrid composites) exhibit low polymerisation shrinkage of 2 to 3.5 %. However, composites with filler contents below 50 vol %, e.g. flow-able composites, exhibit polymerisation shrinkage of more than 5 % (142, 144).

2.9.4. Depth of cure

Increasing the distance between a light source and the sample might lead to a decrease in the light transmitted and in the degree of conversion (145). Decreasing the degree of conversion compromises physical properties and increases the elution of monomers, and thus might lead to the failure of the filling cavity. Dental composites can be placed in incremental layers, recommended by manufactures as 2 mm (146). In deep cavities, sufficient bonding between incremental layers is required (147). Layering is time consuming and involves a risk of

contamination between increments. Manufactures have therefore been developing new types of dental composites called “bulk fill” with maximal increment thickness of 4 mm (147).

There are many techniques to determine the depth of cure. Firstly there are direct methods such as FTIR and Raman spectroscopy (148). Secondly, there are indirect methods such as a scraping ISO 4049 and Vickers hardness. This approach is a simple, inexpensive and suitable technique that researchers can employ when comparing the depth of cure of different dental composites (149). The ISO 4049 standard for dental composites materials should have a minimum depth of cure of 1.5 mm after curing (150, 151).

2.9.5. Water sorption

Dental composites exhibit water sorption upon immersion in water. Water sorption in dental composites is determined mainly by the chemical composition/ hydrophilicity and crosslinking/ conversion of the monomer phase, filler phase and the properties of the interface between the matrix and filler (152, 153). The factors influencing water sorption are immersion time, temperature, surface condition, stress and concentration of water that is ultimately absorbed (154, 155).

Monomers such as Bis-GMA and UDMA produce hydrophobic polymers (153). However, Bis-GMA can exhibit high water sorption. This may be a consequence of lower monomer conversion or because of its hydrophilic hydroxyl groups (135). TEGDMA based polymers absorb more water in comparison to other monomers; this is due to the presence of hydrophilic polyethylene glycol groups (156).

Water sorption can lead to a decrease in mechanical properties. This may be due to the breakdown of the bond between the filler and monomer, or silane and filler particles (157). Moreover, water sorption can also plasticise the polymer phase. It may also enhance the release of uncured monomers which could induce cytotoxic effects. Conversely, one

advantage of water sorption is the potential for expansion, which relieves the stress produced during polymerisation shrinkage (158). This expansion can be between 3 and 6 % (157).

In theory, the water sorption is determined by the diffusion coefficient and boundary conditions at the surface of the sample. The appropriate dimensions of the sample and immersion time in water should be determined in water sorption studies. Water sorption is often governed by Fick's Law with the initial stage of water sorption ($\Delta M_t / \Delta M_{t \rightarrow \infty}$) being given by (159, 160).

$$\frac{\Delta M_t}{\Delta M_{t \rightarrow \infty}} = 2 \sqrt{\frac{Dt}{\pi l^2}} \quad \text{Equation 2-1}$$

M_t and $M_{t \rightarrow \infty}$ are the mass uptake at time t , and at equilibrium, $2l$ is the specimen thickness.

From this equation the diffusion coefficient, D , can be calculated from the gradient of $M_t / M_{t \rightarrow \infty}$ against $t^{1/2}$.

2.9.6. Wear resistance

Wear is defined as the continuous loss of substance resulting from direct opposing surface contact during mechanical interaction between two contacting surface (161). Dental restorative materials are subjected to very specific varying condition such as contact load, mastication force, saliva, pH values and temperature (162).

Wear can be two or three body wear (163). Two body wear occurs in the occlusal or proximal surface of the restoration due to the direct contact of the opposing or adjacent restoration. Care should be taken when placing posterior composites in patients who have bruxism grinding or clenching habits which accelerate wear (164). Two body wear will lead to micro-cracks in or below the surface of the restoration (165). Three body wear usually occurs in the presence of food during mastication or brushing with toothpaste (163).

Wear resistance is dependent on the composition and properties of the filler and monomer phase in the dental composites. Increasing the size of filler particles in dental composites adversely increases the wear resistance as compared with composites which contain smaller filler particles. This is due to exposed filler particles in the surface being plucked out and increasing space between filler particles and thereby increased wear (166). Smaller filler particles size reduce the space between filler and thus reducing the rate of wear resistance (167). A previous study has shown that dental composites containing UDMA and TEGDMA have more resistance to wear as compared to those containing Bis-GMA and TEGDMA (168). Wear may cause loss of the outline form of the restoration and staining due to an increase in the surface roughness. Moreover, the leaching of dental monomer due to low monomer conversion, and inhaled or swallowed composite filler particles might be related to diseases of the liver and respiratory system (169).

2.9.7. Mechanical properties

Currently, dental composites have sufficient mechanical properties to be placed in oral cavity (86). According to ISO 4049 dentistry polymer based filling materials should have flexural strength > 80 MPa for occlusal restorations and > 50 MPa for other indication. Mechanical properties of current composites have been extensively vitro studies (170, 171), It can be seen that the flexural strength and flexural modulus of current dental composites range from 70 to 180 MPa and 3 to 10 GPa respectively. This strength is comparable to amalgam restoration and much better than glass ionomer cements (86).

2.9.8. Bond strength

Despite all the improvements in dental adhesive systems, bonding to enamel and dentine still remains a major drawback of dental composites. Insufficient bonding to tooth structure leads to marginal gap formation, marginal discoloration and loss of filling restorations (172). The

current dental adhesives can initially provide good bonding to exposed enamel and dentine for white filling materials. However, long term durability and stability of bonding on the tooth structure remain unclear (173). Bonding to tooth structure is dependent on the chemical compositions of dental adhesives. Moreover, dentine bonding is also dependent on the demineralised dentine, which helps resin infiltration and produces a hybrid layer. Incomplete dryness or presence of fluid in etched dentine during infiltration might lead to incomplete penetration of dental composites into the hybrid layer (174).

2.10. Dental adhesives

GICs are still considered the only truly self-adhering restorative materials for enamel and dentine (175). This bonding occurs via chemical interactions between carboxyl groups of polyacrylic acid and the calcium of hydroxyapatite (176). The hybrid layer formed between glass ionomers and the tooth structure is thinner than that of resin-based materials with adhesives. This has been attributed to the relatively high molecular weight of the polyacrylic acid which limits the tooth etching as well as the infiltration capability of glass ionomer which effectively influences bond strength (177). Tooth pre-treatment with polyacrylic acid favours adhesion by cleaning the dentine surface before adding the GICs (178).

The primary goal of dental composite adhesives is to improve marginal sealing between the filling materials and enamel and dentine (86). This results in the reduction of bacterial microleakage along the restoration margins and postoperative pain, and reduces the likelihood of restoration failure. The basic mechanism of composite adhesive bonding to tooth structure is by an exchange process involving the replacement of minerals removed during tooth preparation by resin monomers. Upon setting, the resultant polymers become mechanically interlocked in the created porosities (179). Dental adhesives can be classified based on the underlying adhesion strategy as “etch and rinse, or self-etch” (172).

2.10.1. Etch- and rinse application

The “etch-and-rinse” adhesive systems are still considered by many to be the most effective method to achieve efficient and stable bonding to tooth structure, thus it is used in numerous bonding applications. A wide range of conditioning agents has been used including aqueous citric, nitric and phosphoric acid typically at concentrations of 30 to 40 %. The conditioning agent is applied to the tooth structure for 15 to 20 s before being rinsed off with copious amounts of water. This is followed by a priming step and the application of the adhesive resin, resulting in a so called ‘three step application procedure’. In “two step etch-and-rinse” systems the primer and adhesive resin are combined (179, 180). The primers usually contain HEMA, a polyacrylic acid, initiators and solvent (water, acetone and/or ethanol). The adhesive resin often contains Bis-GMA, HEMA, tertiary amines and a photo-initiator (181, 182).

2.10.2. Self-etch adhesive

“Self-etch” adhesives employ non-rinse acidic monomers that simultaneously condition, prime and demineralise the smear layer and underlying dentine (179). These adhesives are preferred by clinicians as their use eliminates the rinsing phase. This not only reduces the clinical application time, but also significantly reduces the technique sensitivity/ application errors (183).

Self-etch can come as two step and one step adhesives. In the two step adhesives, the primer and etchant are in one bottle whilst the adhesive resins are in a separate bottle. In two-step self-etch adhesives, the primer contains acidic monomers such as 10-Methacryloyloxydecyl dihydrogen phosphate (MDP), HEMA, hydrophilic di methacrylates, photo-initiators and water (183). The bonding adhesive may contain MDP, HEMA, Bis-GMA, hydrophobic dimethacrylate, photo-initiators, silanated colloidal silica and, surface-treated NaF. On the

other hand, the one step self-etch adhesive includes all the necessary ingredients: etchant, primer and resin adhesive. The one step self-adhesive such as Ibond contains UDMA, 4-META, glutaraldehyde, acetone, water, photo-initiators, and stabilizers (76).

Self-etch adhesive systems are classified as mild or strong dependent upon their pH (179). Strong self-etch adhesives produce a level of dentine demineralisation comparable with etch-and-rinse systems, due to their very low pH (< 1), while mild self-etch adhesives (pH ~ 2) result in less aggressive demineralisation (183). These mild self-etch adhesives dissolve the dentine surface only partially. Consequently, the demineralisation of dentine occurs simultaneously with primer infiltration. Incomplete penetration of the primer into a demineralised surface might enable microleakage or nano leakage, which could lead to the failure of the adhesive interface (180). The benefit of mild self-etch may be to keep some hydroxyapatite around the collagen which, may protect against hydrolysis and degradation (172).

2.11. Antibacterial and dental composites

Studies on polymerised dental composites have shown no antibacterial activity, which is expected as individual components of resin composites have no antibacterial agents (79). There have been several attempts to develop dental composites with added antibacterial agents to improve the longevity of restorations through combatting secondary caries (184). Several antibacterial agents have been added to the resin to kill bacterial or inhibit biofilms. There are two approaches used to incorporate antibacterial agents into dental composites. The first approach is the addition of a soluble antibacterial agent that can release from a resin composite into the oral environment. The second approach is to immobilise antibacterial agents in the polymerised resin.

2.11.1. Soluble antibacterial agents

2.11.1.1. Chlorhexidine

Chlorhexidine (CHX) is a broad spectrum antibacterial agent that acts against Gram-positive and Gram-negative bacteria. CHX has been frequently used in the treatment of oral infections as a mouthwash. CHX can significantly reduce the bacterial count within dental plaque (185). In one study, washing the cavity preparations with 2 % CHX solution after etching improved the bonding strength for more than 14 months (186). Similarly 2 % of CHX can also preserve the hybrid layer and dentine collagen on the marginal sealing of the dental composites (187, 188).

CHX has been also added into GICs and RMGICs to improve their antibacterial properties (189). The CHX was incorporated at different levels between 1 to 10 %. The effectiveness of these antibacterial materials was reliant on the concentration of CHX (190). However, high percentages of CHX leads to a decrease in the composite strength.

2.11.1.2. Triclosan

Triclosan “2,4,4-trichloro-2-hydroxydiphenylether” is another antibacterial agent which inhibits growth of bacteria by acting on their enzymatic activities. Triclosan has been used in tooth pastes and dental composites to inhibit the growth of oral biofilms (191).

2.11.1.3. Benzalkonium chloride

“Benzalkonium chloride” (BAC) is a antimicrobial agent which causes disruption to the cell membrane. BAC has been used in dental composites at 0.25 % to 2.25 % and shown to be effective at inhibiting bacterial growth. Also its addition, to these composites did not alter mechanical properties (192).

2.11.2. Other antibacterial agents used previously in dental composites

2.11.2.1. Methacryloyloxydodecylpyridinium bromide

Methacryloyloxydodecylpyridinium bromide (MDPB) has also been incorporated into dental composites. This molecule contains both antibacterial quaternary ammonium and methacrylate groups. After polymerisation, the MDPB monomer will copolymerise within the resin composite and be immobilised within the cross-linked resin, stopping it leaching out (191). The antibacterial mechanism occurs as a result of positive charges that disrupt the bacterial cell wall. Dental composites with 0.2 % MDPB exhibited inhibition of bacterial growth. However, the antibacterial MDPB agent has direct action through surface contact only, and has no effect beyond the composite surface (193).

2.11.2.2. Dental composites containing silver

The incorporation of silver in the filler phase of dental composites can inhibit bacteria growth upon the direct contact of silver ions with the bacterial cell membrane. However, the most common disadvantage of silver presence in dental composites is poor color stability (194).

2.12. Remineralising dental composites

In the last two decades, dental composites containing amorphous calcium phosphate (ACP), monocalcium phosphate monohydrate (MCPM), dicalcium phosphate anhydride (DCPA) and tricalcium phosphate (TCP) have been extensively investigated as fillers in an attempt to produce CaP release from dental composites and remineralise the demineralised tooth structure (195-200).

However, these experimental composites containing CaP have lower mechanical properties due to the soluble release of mineral content, and therefore they have not been suitable for bulk filling (196). The CaP has to be more soluble than hydroxyapatite (HA) so that it can be

released from the cured resin and re-precipitate within an affected tooth (201). Generally, a low ratio of calcium to phosphate correlates with a higher aqueous solubility. At a physiological pH the solubility increases in the order of hydroxyapatite, < TCP < DCPA < ACP, < MCPM (202).

2.12.1. Amorphous calcium phosphate

ACP has a calcium (Ca) over phosphate (PO_4) molar ratio of ~ 1.5 (203). Upon placement in water, cured dental composites containing ACP have been observed to release Ca and PO_4 to inhibit demineralisation and promote remineralisation (204). Typically a maximum of 40 wt % ACP was added. The levels of Ca and PO_4 ions released from the ACP composite were considered insufficient to remineralise the affected enamel and dentine structure (196, 205, 206). The low solubility of ACP, however, may hamper calcium phosphate release. Furthermore, poor wetting between the monomers and filler could limit filler loading and reduce strength. The biaxial flexural strength of ACP composites was ~ 50 MPa, which is well below that of good dental composites (201). The ACP composite is recommended to be used as pit and fissure sealants (207). Therefore, there is a need to develop new composites with a combination of CaP to improve mechanical properties, CaP ion release and remineralisation.

2.12.2. Other calcium phosphates used previously in dental composites

In recent experimental dental composites a combination of monocalcium phosphate (MCPM) and tricalcium phosphate (TCP) has been employed (198). When combined with water, MCPM and TCP react via hydrogen ion exchange and re-precipitate as dicalcium phosphate (DCP) or brushite (109, 208). The addition of water-soluble MCPM fillers encourages water sorption into the set resin materials and promotes expansion which may compensate for polymerisation shrinkage. The level of water sorption and expansion was controlled primarily

by the amount of MCPM. In the tooth structure it was anticipated that calcium ions arising from phosphoric acid etching would slowly convert the brushite to more stable and less soluble hydroxyapatite, enabling the tooth structure to be repaired (158, 198).

2.13. Self- adhesive dental composites

Nowadays, significant improvement has been made in the development of self-adhesive dental flowable composites containing adhesive monomers (209). Flowable composites have become an integral part of the restorative process since they were first introduced in the mid 1990's (210). They contain methacrylate monomers as well as acidic adhesive monomers such as 4-META and glycerol-phosphate dimethacrylate (GPDM) (86, 209).

Flowable dental composites have low filler loading and / or higher proportion of diluent monomers in their composition (133). They are designed to be less viscous to offer better marginal adaptation to the cavity wall and easier insertion. Flowability and handling properties allows these composites to be injected thus simplifying the placement procedure. These composites are currently recommended for liners and small cavity preparations (210) or placed underneath a posterior restoration to allow better marginal adaptation and reduce micro-leakage (211, 212).

However, several studies have shown that flowable composites have higher polymerisation shrinkage compared to conventional composites. This is due to these composites having higher monomer contents (211). Moreover, mechanical properties such as flexural strength and wear resistance have been reported to be generally lower compared to those of the conventional composites (210).

2.14. Outline for experimental composites

In this study Urethane dimethacrylate (UDMA) was used as the main bulk monomer and Poly propylene Glycol 425 Dimethacrylate (PPGDMA) as diluent instead of Bis-GMA and

TEGDMA. The organic phase also contains 2-Hydroxyethylmethacrylate (HEMA) or 4-methacryloxyethyl trimellitic anhydride (4-META) as adhesion promoting monomers, and CQ and N-tolyglycine Glycidyl Methacrylate (NTG-GMA) (Na) as polymerisation initiator and activator. The powder phase consisted of calcium phosphate, chlorhexidine and glass fibres mixed with a conventional composite glass.

3. Hypothesis

1. UDMA based composites with PPGDMA diluent and NTGGMA as co-initiator may have improved monomer conversion compared with commercial materials.
2. Addition of chlorhexidine and fibres should have negligible detrimental effects on composite water sorption, mechanical or adhesive properties.
3. Adding adhesive monomer 4-META instead of HEMA in experimental formulations should enable improved chemical bonding with calcium in hydroxyapatite, reduce water sorption and increase strength.
4. Adding soluble calcium and phosphate fillers (MCPM and TCP) in dental composites should encourage water sorption into the set resin materials. This in turn will enhance expansion to compensate polymerisation shrinkage, release of chlorhexidine and bonding particularly to demineralised dentine, but may lead to decrease in the mechanical strength.

4. Aims and objectives

4.1. Aims

The aim of this project is to optimise a unique dental composite with high monomer conversion, low net shrinkage, high strength and ability to bond without complex bonding procedures. The proposed composite should also have the potential to re-mineralise minor defects in tooth structure and provide an anti-cariogenic or anti-demineralising environment with the release to help prevent further tooth decay.

From the recommendations of dentists and dental manufacturers and information from the previous literature review a set of targets has been drawn up:

- The dental composite should have a higher degree of conversion and good depth of cure compared to the current commercial composites in order to reduce toxicity risks.
- The polymerisation shrinkage should be less than or comparable to commercial composites e.g. Z250, Gradia and Ecusphere.
- Polymerisation shrinkage should be compensated by water sorption induced water expansion. This may be enhanced by reactive calcium phosphate addition.
- Enhanced water sorption should enable increased release of CHX to kill bacteria and help reduce risk of secondary caries.
- The cured composite must have long term mechanical properties compared with commercial materials to resist mastication forces.
- The composite should have self-adhesive properties enabling it to stick to the dentine tooth structure under various conditions including wet, dry or acid etched/demineralised. This will be done by adding adhesion promoting monomer and remineralising calcium phosphates. Ideally this would enable composite bonding close to that achieved with use of additional bonding agents.

4.2. Objectives

In the following liquid phases of all experimental composites consisted of UDMA and PPGDMA in a 68:25 weight ratio, and 5 wt % of 4-META or HEMA. CQ/ NTGGMA photo initiator and activator were each added at 1wt % of the total monomer phase. The powder and liquid ratio (PLR) was fixed at 3:1. Commercial dental composites Z250, EcuSphere and Gradia were selected for comparison, as they are highly regarded market leaders. Experimental formulations containing solely glass particles in the filler phase were used as experimental formulation controls. The powder phase of subsequent non-control experimental composites all contained CHX and fibres, which were both added to the powder at 5 wt %. Furthermore, equal masses of CaP (TCP and MCPM) were added at combined levels of 0, 10, 20 or 40 wt % of the filler.

The chemical and physical properties of the experimental and commercial dental composite materials were subjected to the following tests to confirm their potential to be used as composites in the future.

- Chemical composition, monomer conversion and polymerisation shrinkage were determined using FTIR spectroscopy.
- Depth of cure was evaluated using an ISO 4049 method.
- Mass and volume changes upon water immersion were quantified using gravimetric analysis.
- Chlorhexidine antibacterial release was checked using UV spectroscopy.
- The mechanical properties BFS and modulus were evaluated using an Instron universal testing machine.

- Shear bond adhesion and a new push-out adhesion test were employed to quantify the self-adhering experimental formulations and commercial dental composite bonding capability to dry, wet and acid etched ivory dentine.

5. Materials and methods

In the present study, UDMA/ PPGDMA based experimental dental composites containing adhesive monomers 4-META or HEMA and various levels of calcium phosphate (CaP) and fixed levels of chlorhexidine diacetate (CHX) added in the filler phase were formulated and characterised. Commercial dental composites Z250, EcuSphere and Gradia were selected for comparison as they are highly regarded market leaders. Experimental formulations with 4-META or HEMA containing solely glass particles in the filler phase were used as controls. The properties evaluated included the degree of monomer conversion, mass and volume changes, chlorhexidine release, and biaxial flexure strength/Young's modulus. Furthermore, push-out adhesion and shear bond strength tests to ivory dentine were assessed.

5.1. Materials

5.1.1. Commercial dental materials

The commercial dental composites used in this project were Z250 (3M/Espe dental, Seefeld, Germany), Gradia direct posterior composite (GC international, Tokyo, Japan) and EcuSphere (DMG, Hamburg, Germany) as they are highly regarded market leaders (Table 5-1). Ibond total etch dental adhesive and Ibond etch 35 gel for the conditioning of dentine (Heraeus-Kulzer, Hanau, Germany) were also selected for use in this study.

Table 5-1: Details of commercial dental composite investigated in this project. Description, chemical component and shade are provided by the manufacturer.

Product Name	Supplier	Shade	Chemical composition
Filtek Z250	Fitek™	B3	Bis-GMA, Bis-EMA, TEGDMA, UDMA, Zirconia / Silica particles
Gradia Posterior	GC Corporation	A2	UDMA, other methacrylate monomers, fluoro-aluminosilicate glass, Pre-polymerised filler, Pigments
EcuSphere Carat	DMG	A2	Bis-GMA, UDMA, TEGDMA, Glass and SiO ₂
Conditioner	Heraeus Kulzer		Phosphoric acid, Distilled water, Aluminium chloride hydrate, Food additive Blue No.1
Ibond	Heraeus Kulzer		UDMA, 4-META, Glutaraldehyde, Acetone, Water, Photo-initiators, Stabilizers

5.1.2. Experimental composites

5.1.2.1. Monomer phase

The experimental resin monomer was prepared from commercially available materials urethane dimethacrylate (UDMA) (DMG, Hamburg, Germany) and poly (propylene Glycol 425 dimethacrylate) (PPGDMA) (Poly-sciences, Warrington, PA, USA). To this was added either 4-methacryloyloxyethyl trimellitic acid anhydride (4-META) powder (Poly-sciences,

Warrington, PA, USA) or 2-hydroxyethyl methacrylate (HEMA) liquid (DMG, Hamburg, Germany). Camphorquinone (CQ) powder (Sigma Aldrich, UK) and n-tolyglycine glycidyl methacrylate (NTGGMA) powder (Sigma Aldrich, UK) were added. The sources of the monomers used to prepare the experimental composite formulations in this project are shown in Table 5-2 below, with molecular weight.

Table 5-2 : Details of monomers, initiator and activator used throughout this project. Molecular weight information was provided by the manufacturer.

Name	Abbreviation	Supplier	Product code	Molecular weight (g/mol)
Urethane dimethacrylate	UDMA	DMG, Germany	90761	470
Poly (propylene Glycol 425Dimethacrylate)	PPGDMA	Polysciences, UK	04380-250	560
2-Hydroxyethyl methacrylate	HEMA	DMG, Germany	100220	130
4-methacryloyloxyethy trimellitic acid anhydride	4-META	Polysciences, UK	17285	286
N-tolyglycine Glycidyl Methacrylate	NTGGMA	Esstech, Inc.	X 863 0050	307
Camphorquinone	CQ	Sigma-Aldrich, UK	10120023	166

5.1.2.2. Filler phase

The different fillers used in preparation of experimental formulations are provided in Table 5-3. For control formulations the powder phase consisted of only radiopaque silane-coated barium aluminosilicate glass with average diameter of 7 μm (DMG, Hamburg, Germany). For all other formulations this was mixed with chlorhexidine diacetate (CHX) of $\sim 44 \mu\text{m}$ in diameter (Sigma-Aldrich, UK) and silane coated boro silicate glass fibres of \sim width 15 x 300 μm diameters (MO-SCI, UK). Furthermore, equal masses of tricalcium phosphate (TCP)

(P306S, Plasma Biotal) and monocalcium phosphate monohydrate (MCPM) (Himed) of ~ 6 and 53 μm diameters respectively were included.

Table 5-3: Summaries of filler phase materials used throughout this project as provided from the manufacturer.

Name	Abbreviation	Supplier	Product code
Barium- aluminosilicate glass powder	GP	DMG, Germany	680326
Monocalcium phosphate monohydrate	MCPM	Himed	MCP-B26
Tricalcium phosphate	TCP	Plasma Biotal	7793
Chlorhexidine Diacetate salt hydrate	CHX	Sigma-Aldrich, UK	1001075054
Silane coated Borosilicate glass fibres	GF	MO-SCI, UK	0322201-S

5.1.3. Formulation of experimental dental compositions

Experimental formulation pastes were prepared by combining a powder with the above two monomer liquids containing 4-META or HEMA 5 wt % (of the total monomer phase) in a 68:25 weight ratio of UDMA and PPGDMA as in Table 5-4 and 5-5. For controlled experimental composites, the powder phase consisted solely of radiopaque silane-coated barium alumina silicate glass.

For all other experimental composites, chlorhexidine diacetate (CHX) and silane coated Borosilicate glass fibres were both added to this powder at 5 wt %. Furthermore, equal masses of calcium phosphate (TCP and MCPM) were added at combined levels of 0, 10, 20 or 40 wt % of the filler. The powder and liquid ratio (PLR) was 3:1 a summary of variables used are listed in Table 5-4.

Table 5-4 Chemical composition of the powder phases of experimental composites

Powder phase	Composition wt %				
	Control	F1	F2	F3	F4
Glass	100	90	80	70	50
TCP	0	0	5	10	20
MCPM	0	0	5	10	20
CHX	0	5	5	5	5
Glass fibres	0	5	5	5	5

Table 5-5: Chemical composition of the monomer phases

Monomer phase	Composition wt %
UDMA	68
PPGDMA	25
4-META or HEMA	5
CQ	1
NTGGMA (Na)	1

5.1.4. Preparation of experimental formulations

5.1.4.1. Monomer preparation

During the preparation of experimental composites, latex gloves were worn to prevent skin problems (dermatitis) associated with direct contact with the monomer. Moreover, a laboratory coat was worn to prevent the contamination of clothes and skin. The bulk monomer was handled using a metal spatula and glass pipettes were used for diluent monomers. The room temperature was $23\text{ }^{\circ}\text{C} \pm 1$.

Initially, the monomers initiator/ activator NTGGMA, CQ, adhesive monomer 4-META or HEMA and diluent monomer PPGDMA were weighed and mixed together in a dark brown bottle using a stirrer (Stuart. bioCote, UK), and magnetic stirring bar at speed 3/9 for 10 to

15 min at room temperature to pre-dissolve the 4-META or HEMA and NTGGMA. Afterwards, the main bulk monomer UDMA was added and mixed for 45 min at room temperature to ensure complete dissolution of the adhesive monomer 4-META and activator NTGGMA. After this, the stirring bar was removed. The monomer made was labelled and stored in a fridge for up to 1 month.

5.1.4.2. Filler preparation

All fillers and reactive filler (MCPM, TCP) were stored at room temperature in sealed containers to ensure that they were kept dry. Care was taken not to introduce moisture into the bulk containers of the filler materials by decanting small amounts of filler into smaller bottles when required.

5.1.5. Paste preparations

The experimental formulations, filler and the monomer were weighed onto rubber mixing pad (Figure 5-1) using a four figure balance. The powder was added to the liquid and mixed thoroughly at room temperature using a stainless steel spatula, making sure all the powder was incorporated into the liquid and avoiding the introduction of air to the mixed paste.



Figure 5-1: Filler powder and monomer mix on a rubber mixing pad prior to mixing

5.1.5.1. Composite disc preparation

After the filler and monomer were mixed to form a paste, about 0.2 g of paste was subsequently placed in a stainless steel metal ring to enable the production of 10 mm diameter and 1 mm thick discs (Figure 5-2). The top and bottom of the filled composite discs were covered with acetate sheet (to prevent air inhibition of polymerised process) and topped with two glass slides. This glass block was used to remove excess material from the disc by slight pressure. The light gun was placed in direct contact to the acetate sheet to decrease the distance between the sample and light cure. The specimens were photo activated from top and bottom for 40 seconds using a blue light curing unit with an 1100 mW/cm² power output (LED. Demetron I, Kerr, USA). The continuing performance of the curing units was confirmed periodically through assessment of ability to cure materials using FTIR. More exact thickness was confirmed using a digitronic caliper (Moore and wright, Shanghai, China) at three different points in each sample after cure. The set samples were removed from the mould rings and the surfaces and edges of each disc were checked to make sure they were flat and smooth. After that, the sample discs were left at room temperature for 24 h for full cure.



Figure 5-2 : Light cured dental composite disc (10 × 1mm thickness) after removed from metal ring.

The composite discs were divided into dry and wet; discs that were to be tested in their wet condition were stored individually in sterilin tubes containing 10 mL of deionized water for different time periods in an incubator at 37 ± 0.5 °C. The circular discs were prepared for

biaxial flexure strength (BFS) measurements, mass and volume change and chlorhexidine release.

5.2. Methods

5.2.1. Degree of monomer conversion

The mechanical and chemical properties of light cured dental composites are directly influenced by the degree of conversion during polymerisation. The degree of conversion is defined as the extent to which monomers react to form polymers or as the degree of which carbon double bonds (C=C) form (213). The degree of conversion may be affected by factors such as; type of photo-initiator, curing protocol, temperature, chemical composition of sample and the sample thickness

There are many techniques available to determine the degree of conversion of resin composites such as Fourier transforms infrared (FTIR), RAMAN, differential scanning calorimetry (DSC) and nuclear magnetic resonance (NMR). FTIR has been widely employed to identify chemical functional groups by their different vibration modes and for monitoring the kinetics of chemical reactions. Furthermore, FTIR is a convenient, and reliable method for measuring the degree of conversion of methacrylate (64, 214). In this study, FTIR spectroscopy has been used to quantify the degree of monomer conversion in the experimental and commercial dental composites, and calculate polymerization shrinkage of the experimental composites.

5.2.1.1. Fourier transform infrared (FTIR)

FTIR spectroscopy is a chemical analytical technique which provides information about the intensity of infrared light that the materials in solid or liquid phase absorb as function of wavenumber. Infrared spectroscopy (IR) can be classified according to the wave number into

near infrared (12800 to 4000 cm^{-1}), mid infrared (4000 to 200 cm^{-1}) and far infrared (200 to 10 cm^{-1}). The mid IR is the most frequently used to measure the conversion of the methacrylate monomer (64, 69, 215). FTIR allows real time assessment of conversion and the rate at which a polymerisation reaction progresses. The technique of FTIR used in this thesis has been outlined previously by Young et al. (69).

5.2.1.2. Principles of infrared absorption

When a molecule absorbs IR radiation, it gains energy as it undergoes a transition from one energy level (E_{initial}) to another level (E_{final}). According to Planck's law the energy of the transition and frequency of absorbed radiation f (Hz) are related by the equation below

$$E_t = hf \quad \text{Equation 5-1}$$

Where E_t is the energy of transition ($E_{\text{final}} - E_{\text{initial}}$), (h) is Planck's constant,

Since $f = \nu c$, where ν and c are the wavenumber (ν) (cm^{-1}) and the velocity of light ($8 \times 10^8 \text{ m s}^{-1}$).

$$E_t = h\nu c \quad \text{Equation 5-2}$$

The wave length lambda (λ) is correlated with the frequency (f) by the below equation:

$$\lambda = c/f \quad \text{Equation 5-3}$$

Therefore, the equation above can be also given as:

$$E_t = hc/\lambda \quad \text{Equation 5-4}$$

The energy absorbed by a molecule must match exactly that required for a molecular transition. The molecular bonds oscillate and vibrate at specific frequencies, behaving like springs. Upon absorption of energy from IR radiation, the vibrational energy and amplitude of the vibrations are enhanced. There are two types of vibration, one that changes the bond length (stretching) and the other changes the bond angle (bending). In order to observe these

changes in FTIR spectra, the vibrational motion should be accompanied by a change in dipole moment (electron distribution) at both ends of the vibration.

FTIR spectra are generally displayed as a plot of absorbance versus wavenumber (cm^{-1}). The peaks shown in the spectrum correspond with different vibration transitions. The FTIR spectra is usually divided into two parts. The first part has an absorbed frequency of between 4000 and 1300 cm^{-1} and is mostly related to the vibration of specific functional groups. The second part has an absorption of between 1300 and 500 cm^{-1} and is associated with the vibration of the whole molecule and is called fingerprint region.

5.2.1.3. FTIR instrumentation

The FTIR instrument consists of a light source, interferometer, sample, detector and computer (Figure 5-3). The light beam, which includes all frequencies of IR radiation is divided into two optical beams via the beam-splitter. The two light are reflected back at the beam-splitter by two mirrors. The time needed for the light to travel from the mirror to the beam-splitter will be different from both beams and will be dependent on the wavelength. The reflected beams recombine at the beam-splitter and the resultant signal is used to produce an interferogram. The interferogram can be converted to absorbance versus wavenumber through computer software and Fourier transformation.

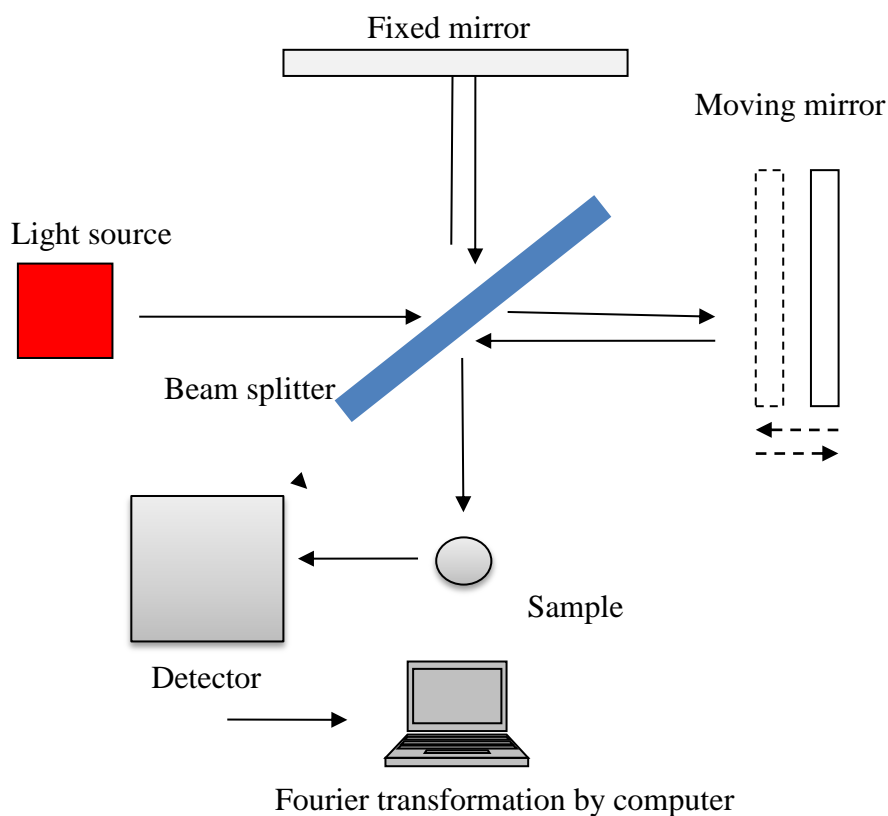


Figure 5-3: Schematic diagram of FTIR

In this project, experimental formulations with 4-META or HEMA and commercial dental composite pastes were prepared as mentioned above, and were immediately moulded at room temperature (23°C) into a brass metal ring (10 mm diameter and 1mm thickness) (n=5) at the center of the ATR diamond top-plate (Specac Ltd, UK) in an FTIR spectrometer (Perkin Elmer series 2000, UK). The top surface of the sample of mixed paste was covered with acetate sheet to prevent oxygen inhibition of the polymerisation. FTIR spectra of the lower surface of the sample in contact with the diamond were recorded with resolution set at 4 cm⁻¹ and wave number range between 400 and 4000 cm⁻¹. The number of scans was fixed at 4 s and the total run time was 20 min for each experimental and commercial composites. After 1 min from start of spectral accumulation, the paste was light cured for 40 s using a blue light curing unit with a 1100 mW/cm² power output (LED. Demetron I, Kerr, USA).

The degree of monomer conversion was calculated through change in the height of the absorbance of the monomer peak at 1320 cm^{-1} (C-O stretch) above the background at 1351 cm^{-1} . The percentage of monomer conversion was calculated using Equation 5-5 which is outlined below:

$$\text{Degree of conversion (\%)} = \frac{100[A_0 - A_t]}{A_0} \quad \text{Equation 5-5}$$

Where A_0 and A_t were taken as peak height of the C–O bond stretch peak at 1320 cm^{-1} before and after polymerisation respectively.

5.2.2. Polymerisation shrinkage

Dental composites still exhibit polymerisation shrinkage after curing and this remains a significant concern in the clinic. Polymerisation shrinkage can be divided into two types; pre-gel and post-gel polymerisation. The pre-gel shrinkage occurs when the composite still flows and the stress within the materials is relieved. In the post-gel phase, however, the viscosity increases and the stress from polymerisation shrinkage cannot be compensated for. Consequently, this post-gel stress will affect the integrity of the bonding to the dentine interface and filling restoration.

Polymerisation shrinkage is proportional to the degree of conversion (216). One mole of polymerising C=C bonds typically give a volumetric shrinkage of $23\text{ cm}^3/\text{mol}$ (217). The total shrinkage due to composite polymerisation can then be estimated using Equation 5-6.

$$\text{vol \%} = 23N * 100 \quad \text{Equation 5-6}$$

Where N is the number of moles reacted per unit volume. N can be estimated using equation below:

$$N = [M]C\rho_{comp} \sum_i \left(\frac{n_i x_i}{w_i} \right) \quad \text{Equation 5-7}$$

Where M is the total monomer mass fraction and C is the final fractional monomer conversion calculated from FTIR. Σ indicates a sum over all the monomers in the monomer

phase. n_i , W_i and x_i present the numbers of C=C bonds per molecule, weight (gmol^{-1}) and mass fraction of monomer respectively.

Total fraction shrinkage φ due to composite polymerisation can then be estimated from FTIR monomer conversion using equation below:

$$\varphi = 23 C \rho \sum_i \frac{n_i x_i}{w_i} \quad \text{Equation 5-8}$$

Where C monomer conversion %, ρ composite density (g/cm^3), n_i number of number carbon double bond per molecular, w_i molecular weight of each monomer and x_i mass fraction of each monomer

Assuming the formulation behaves “ideally”, and is non-porous, composites density ($\rho_{\text{compo}} \text{ gcm}^{-3}$) can be estimated using Equation 5-9 ρ_{monomer} and ρ_{filler} are the densities of the monomer mixture and filler

$$1/\rho_{\text{comp}} = m/\rho_{\text{monomer}} + (1 - m)/\rho_{\text{filler}} \quad \text{Equation 5-9}$$

5.2.3. Depth of cure

The depth of cure of light cure dental composites has been the subject of considerable laboratory research. Increasing the distance between the light source and the sample will lead to a decrease in light levels transmitted and in the degree of conversion. Decreasing the degree of conversion compromises physical properties and increases the elution of the monomer, and thus might lead to failure of the filling cavity.

Resin composites can be placed in incremental layers to reduce shrinkage. The manufacturers recommendation is 2 mm incremental (146). In deep cavities, sufficient bonding between incremental layers is required (147). Moreover, layering is time consuming and involves a risk of contaminations between increments. Thus, researchers and manufacturers of dental composites have been developing new types of dental composites with maximal increment thickness of 4 mm (147).

A technique for defining the maximal incremental layer of dental composites has been introduced by the International Organisation for Standardisation ISO 4049 depth of cure (150). The depth of cure can be measured directly or indirectly. The scraping test is an indirect method to determine the depth of cure. Direct methods such as FTIR and Raman spectroscopy take more time and require expensive equipment (218) . The indirect technique is a simple, inexpensive and suitable technique that researchers can employ when comparing the depth of cure of different dental composites (149).

According to ISO 4049 standard dental composites should have a minimum depth of cure of 1.5 mm after curing, according to the manufacture instructions (151). According to this technique the resin composite to be tested is filled in a stainless steel mould, light cured and pushed out of the mould. The uncured composite is scraped away with a plastic spatula. The remaining length of hard composite specimen is measured and divided by two. The resultant value is recorded as the ISO depth of cure.

This study investigated the ISO 4049 depth of cure of experimental and commercial dental composites. Three samples of each experimental formulation were condensed into 4 mm diameter and 6 mm deep stainless steel moulds. Each specimen was cured from top surface for either 20 or 40 s using a blue light curing unit with a 1100 mW/cm² power output (LED. Demetron I, Kerr, USA). After light activation, the cylindrical samples were gently removed from the stainless moulds and the uncured composite was scraped away using a plastic spatula. The remaining length of the cylindrical cured samples was then measured with a digitronic caliper (Moore &wright, Shanghai, China) at 4 different points in each sample. The average reading length was recorded in millimetres and then divided by two to obtain the ISO standardised depth of cure (150, 151).

5.2.4. Mass and volume change

The mass and volume change is important when characterising the properties of dental composites. Resin composite should be stable and will constantly be interacting with its surrounding environment (219). The water absorption of a material represents the amount of water adsorbed through the exposed surface and into the body of the material (72). Over time, water sorption and dimension change in dental composite is one of the major disadvantages which might lead to the leaching of uncured monomers, decline of mechanical properties and restoration failures (174). This is mainly due to the breakdown of the bond between the silane and filler or of that between the filler and matrix.

The dimensional stability of dental composites is affected by polymerisation shrinkage and thermal contraction and expansion within the oral environment. This dimensional change occurs as the filling materials are continually immersed in an oral environment and water absorption for some materials is inevitable (220).

Conversely, water sorption might also lead to the expansion of composite filling, and increase in weight of the materials. This may lead to micro-cracks and reduced service life of the dental restoration (153). Interestingly, this expansion by water sorption may also help to relieve stress on the tooth and filling materials interface produced during polymerisation shrinkage (158).

In the present study, the mass and volume change of experimental and commercial resin composites were gravimetrically determined using a four-figure balance (Mettler Toledo) with attached density kit (OHAUS Pioneert, UK). The commercial, controlled experimental and experimental formulations containing different levels of calcium phosphate (0, 10, 20 and 40 wt %) and CHX were made. The sample discs (10 mm diameter and 1 mm thick) were prepared as explained above in the composite disc preparation section. Each composite sample was immersed in 10 mL of distilled water in a sterilin tube and incubated at 37 ± 0.5

°C for various time points up to 4 months (1, 2, 4, 6 h, 1, 2, 3 days and 1,2,3 weeks and 1,2,3,4 months (n=3). At each time point, the sample discs were removed from the water and blotted dry on paper tissue (according to ISO 4049 standards to remove excess water). After that the samples were weighed in air for mass change and weighed in water for volume change. Subsequently the samples were placed in new tubes containing fresh distilled water (195, 198). The weights were recorded and percentage volume and mass change at each time point was determined using Archimedes' principle. The sample mass in air and following immersion in water can be combined to calculate the density of a sample via Equation 5-10:

$$\rho = \frac{A}{A-B} (\rho_0 - \rho_L) + \rho_L \quad \text{Equation 5-10}$$

Where ρ is the density of the sample, A and B represent the weight of the sample in air and solution respectively, ρ_0 the density of solution and ρ_L the density of air (0.0012 g / cm³). The percentage mass and volume change of the sample at each time point was determined using Equations 5-11 and 5-12 respectively:

$$\text{Mass change (\%)} = \frac{100 (M_t - M_0)}{M_0} \quad \text{Equation 5-11}$$

$$\text{Volume change (\%)} = \frac{100 (V_t - V_0)}{V_0} \quad \text{Equation 5-12}$$

M_t and V_t represent the mass and volume at time (t) after immersion in water, while M_0 and V_0 are the initial mass and volume respectively.

5.2.5. Ultraviolet-visible Spectroscopy

Ultraviolet spectroscopy has been used for more than 30 years to analyse interaction between electromagnetic radiation and matter. UV spectroscopy is the measurement of the amount of light passing through a sample. UV visible light has a wavelength range of between 200-800 nm. When light passes through any homogenous solution, it can be transmitted through the

solution, scattered, reflected from the surface of the solution and absorbed within the solution. The absorption of light in the UV spectra is dependent on the electronic structure of the absorbing molecules.

Once the sample is exposed to light that matches the energy difference between a possible electronic transition within the molecule, a fraction of light will be absorbed. The excitation might include both bonding and nonbonding electrons. The recorded spectra plotted as absorbance (A) versus wavelength (λ) as shown in Figure 5.4.

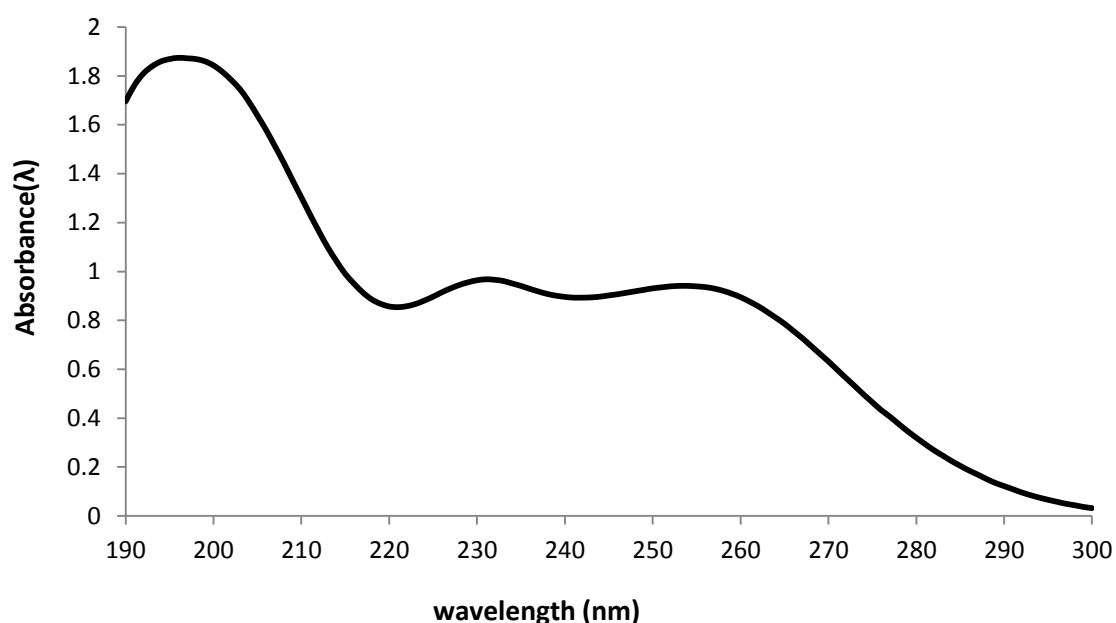


Figure 5-4: Diagram showing UV spectrum of chlorhexidine in water

The relationship between absorbance and intensity of incident light (I_i) and transmitted (I_t) light through homogenous absorbing systems at a given monochromatic wavelength is given by the Beer-Lambert law in Equation 5-13:

$$A = -\text{Log} [I_i/I_t] = kcl \quad \text{Equation 5-13}$$

Where A is the absorbance, while l is the light path length (cm), c is the concentration of absorbing species (mol L^{-1}) in solution (deionised water) and k is the molar absorptivity (L

$\text{mol}^{-1} \text{cm}^{-1}$). At a given wavelength, the molar absorptivity (molar extinction coefficient) for any absorbing species is a constant.

The Ultraviolet-visible spectrometer (Figure 5.5) consists of UV light source (deuterium lamp) for the range of 160-375 nm and visible light source (tungsten lamp) for the range 360-1000 nm. The light beam enters the monochromator through a slit. Subsequently light is reflected via mirrors to a diffraction grating, which can be rotated to allow specific wavelength selection. The monochromatic light then passes through an exit slit into a beam splitter, which splits the light in two. One beam is allowed to pass through the reference cell (quartz cuvette that contains the solvent only) and the second passes through the sample cell (cuvette that contains the sample). The detector measures the difference between the two and provides rate of the absorbance which occurred due to the sample.

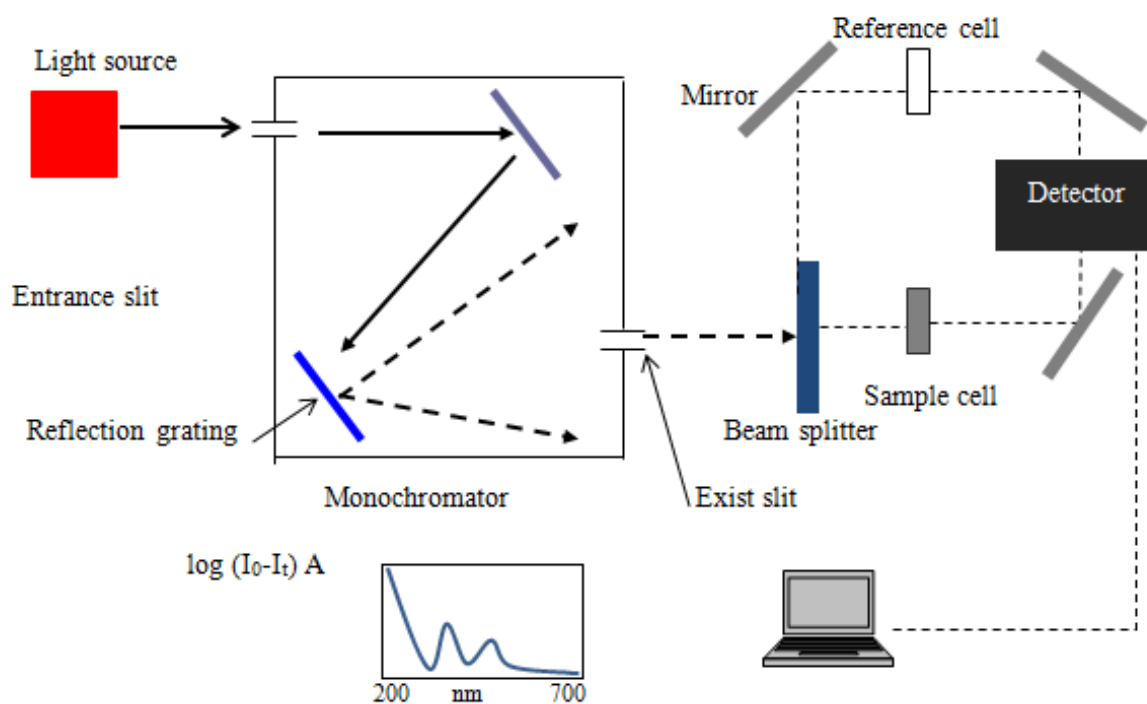


Figure 5-5: Diagram of UV spectrometer.

5.2.5.1. Sample preparation for chlorhexidine release

In this project, UV spectrometry was used to quantify CHX release from experimental composite disc containing adhesive monomer 4-META or HEMA, different levels of CaP (0, 10, 20 and 40 wt %), and 5 wt % chlorhexidine. The sample discs were prepared as mentioned in mass and volume change. Each sample was immersed in 10 ml of distilled/deionized water in sterilin tubes in an incubator at 37 ± 0.5 °C for 1, 2, 4, 6 h, 1, 2 days and 1 to 16 weeks (n=3). At each time point, the samples were removed and placed in new sterilin tube and fresh deionized water. The UV spectra of storage solutions were obtained at each time point between 190 and 300 nm using a UV 500 spectrometer (Thermo-Spectronic[®], UK).

These were compared with calibration graphs created in the same range of solutions of known concentration of CHX to confirm that the CHX was the only component exhibiting absorbance. A calibration curve was prepared using 5 CHX concentrations (1.25, 2.5, 5, 10 and 20 ppm) as shown in Figure 18. The maximum absorption of CHX was found at 231 and 255 nm. By plotting concentration versus absorbance, the calibration curve for CHX was obtained (Figure 5-6) and the gradient calculated through linear regression. The CHX peak at 255 nm was therefore used to calculate the amount of CHX release (R_t in grams) between different time points from each sample using Equation 5-14 below:

$$R_t = \frac{A}{g} V \quad \text{Equation 5-14}$$

Where A is the absorbance at 255 nm, g is the gradient of a calibration curve of absorbance versus CHX concentration and V is the storage solution volume (10 ml).

The percentage cumulative amount of drug release (% R_c) at time (t) was then found using Equation 5-15:

$$\% R_c = \frac{100 [\sum_0^t R_t]}{W_c} \quad \text{Equation 5-15}$$

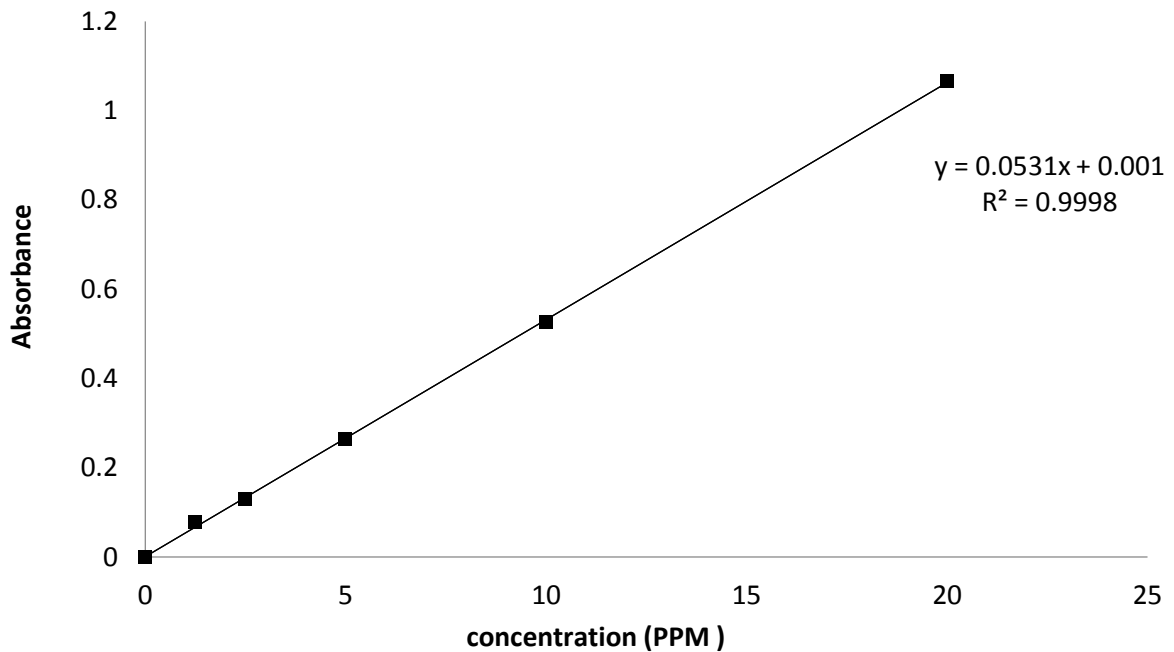


Figure 5-6: Calibration curve of the absorbance of 5 wt % CHX concentrations (absorption at 255 nm)

5.2.6. Biaxial flexural strength test and modulus

There are many tests to evaluate the mechanical properties of dental composites at the failure point, such as compressive strength, tensile strength and flexural strength. A brittle dental material is much weaker in tension than in compression; consequently, when it comes to evaluating brittle materials, tensile strength is a more reliable test (221).

Biaxial flexural strength (BFS) test has been used to evaluate the mechanical behaviour of experimental formulations and commercial dental composites. Dental composites should have sufficient mechanical properties to withstand stresses from masticatory forces or residual internal stresses during curing (222). Moreover, dental composites are exposed to both tensile and compressive stress under flexural strength testing (223).

5.2.6.1. Biaxial flexure test

The most common flexure test methods for characterising maximum tensile stress in a material at failure point are the three and four point bending tests. These tests are recommended in ISO 4049:2009 for determining the flexure strength of polymer based filling materials. Furthermore, three and four point bending tests have been used to determine the flexural strength of cement materials (121, 128, 224). Biaxial flexure strength tests, however, have also been used broadly to determine the mechanical properties of resin dental materials (109, 198, 225-227).

According to the ISO 4049 standards the three and four bending tests require large sample sizes compared to biaxial tests. This means multiple curing with 10 mm diameter light source is required to polymerise the large samples; consequently this may lead inhomogeneous polymerisation and enhanced variability (228). Moreover, extra materials are required to prepare the samples for mechanical properties and are more costly. The main disadvantage doing a test with a large sample is that it is difficult to manufacture and the possibility of edge failures, due to likelihood of unavoidable flaws at specimen edges is hugely increased (153). Biaxial flexure testing however reduces edge effect failures. Moreover, composite discs (10 mm diameter and 1 mm thick) are easier to prepare, can be cured in a single step (225, 227, 229) and can be used for other studies (water sorption, CHX release conversion and polymerisation shrinkage). The BFS test is more reliable for dental materials and more representative of occlusal stress (230). There are several forms of BFS test methods in jig geometries, including ball-on-ring, ball-on-three-ball, piston-on-ring and others (231).

5.2.6.2. Disc Specimen Preparation for BFS and modulus

The BFS and modulus of experimental formulations and commercial dental composites were determined using a “ball-on-ring” biaxial test (Figure 5-7). Composite discs (with 10 mm diameter and 1 mm thick) as in Figure 14 were prepared for each experimental formulation

and commercial composite as mentioned before in sample disc preparation (sample repetition $n=6$). The samples discs of all materials were left to dry for 24 h in order to fully cure. Subsequently, the composite discs were stored either dry at room temperature 23 ± 1 °C or hydrated in sterilin tubes containing 10 mL of distilled water for 24 h, 1 and 4 weeks in an incubator at 37 ± 0.5 °C.



Figure 5-7: BFS jig with ‘ball on ring’ jig.

For testing the sample was placed on a knife edge ring support (4mm) and the BFS was determined using a computer-controlled universal testing machine (Instron 4505, Canton, MA, USA) with a 1 kN load Instron cell as shown in Figure 5-8. The crosshead speed was set as 1 mm/min.

The load and central deflection of the disk were recorded and plotted on a load versus deflection graph (Figure 5-9). From this graph, the maximum load at fracture and the pre-fracture slope were determined to find the BFS and elastic modulus respectively.

The BFS and modulus were determined using Equation 5-16 (232).

$$\sigma = \frac{P}{t^2} \left[(1 + \nu) \left(0.485 \left(\frac{a}{t} \right) + 0.52 \right) + 0.48 \right] \quad \text{Equation 5-16}$$

Where σ is the biaxial flexural strength (MPa), (P) is maximum load at break (kN), (t) is thickness of sample (mm), ν is Poisson's ratio (0.3) and a is support radius (mm). The 95 % confidence interval was calculated assuming 95 % CI = 2SD/ \sqrt{n} where (n) is the number of samples.

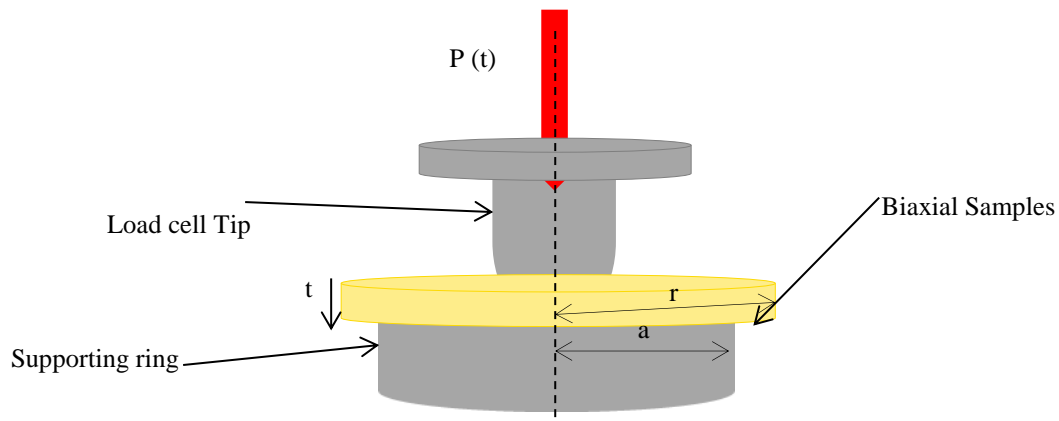


Figure 5-8 Schematic of Biaxial test

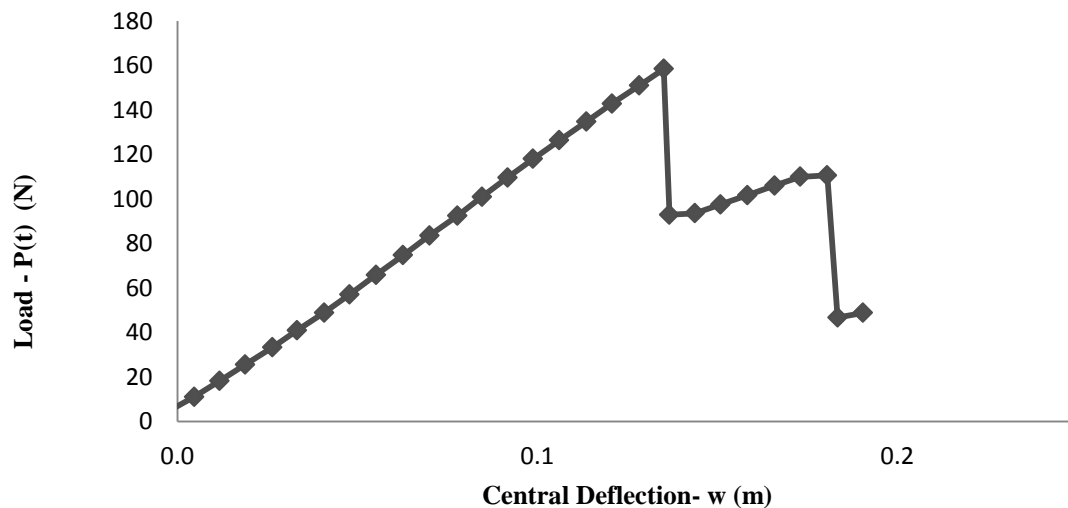


Figure 5-9 : Load vs. central deflection plot generated by the computer connected to the load of the cell.

5.2.6.3. Modulus

The Young's modulus of a composite disc was found from the gradient of the load versus the central deflection plot. The deflection of the centre of the disc specimen during testing is related to the applied load using Equation 5-17 (233).

$$E = 0.502 \frac{df}{dw} \left(\frac{a^2}{h^3} \right) \quad \text{Equation 5-17}$$

Where E is Young's (elastic) modulus (GPa) and df/dw is the slope of the load versus central deflection plot, a is support radius (mm), h is average thickness of the sample (mm).

5.2.7. Adhesion test

5.2.7.1. Push out test

The push-out test has been used in dental research for many years. In 1973 it was used to evaluate the bonding of adhesive to root canal and in 1996 to assess the bonding of bone to orthopaedic implants (234, 235). More recently, the push out test has been used to evaluate the bond strength of filling materials in root canals (236). Push out strength estimates clinical failure better than a shear test because the fracture occurs parallel to the dentine interface (237). Furthermore, this method simultaneously provides information about marginal sealing (238). In addition, push out tests mimic the clinical situation more closely (239) .

In this project, the push out test was carried out using ivory tusks. Ivory tusks consist of an inorganic component hydroxyapatite which gives strength and rigidity and an organic component (collagen) for flexibility, growth and repair. Elephant tusks have a similar physical structure to human teeth: dentine, cementum and enamel, the latter found in the tip of the tusk only (240). Dentine is the main component of the teeth while cementum forms the outer layer surrounding the dentine of the tusk. Ivory cementum is the hardest animal tissue and covers the surface of the tusk which receives the most wear (241, 242).

Ivory dentine has been used to assess adhesion between endodontic posts and adhesives (243). Ivory tusks are suitable as they allow the testing of large numbers of samples in a standardised way. This would not have been possible using human teeth samples.

The ivory tusk used in the following studies was seized under the Convention on International Trade in Endangered Species (CITES) and donated by the UK Border Agency Heathrow. It must be noted that this tusk may only be used for academic research and teaching purposes and must be returned for destruction if not destroyed during testing. The use of ivory can only currently be justified when there is material available that would otherwise be destroyed after seizure. The outer layer (cementum) of tusk was cut longitudinally from all sides with a tile cutter into rectangular blocks of $\sim 30 \text{ mm}^3$ dentine. Using a diamond saw these blocks were then further cut transversely; parallel to the direction of dentinal tubules, to give blocks of 33 x 30 mm in length and 5 mm in depth (Figure 5-10).

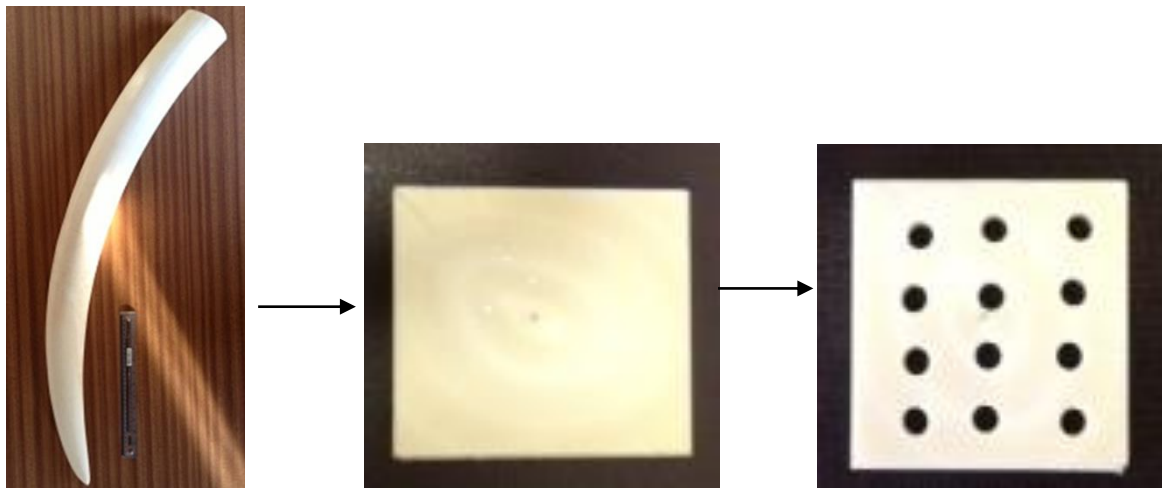


Figure 5-10: Schematic photographs ivory tusk rectangular block and cylindrical holes.

The samples are stored dry at room temperature $23 \text{ }^\circ\text{C} \pm$ or placed in distilled water for 24 h in an incubator at $37 \text{ }^\circ\text{C} \pm$ and then left to dry in the incubator for a further 24 h (control hydration). This resulted in a slightly moist dentine and was found to improve

reproducibility. A 3 mm diameter bur and drill was used to create 5 mm deep cavities entirely through each block and perpendicular to the tubules. The resultant holes were whither etched with 37 % phosphoric acid for either 0 s (i.e. no treatment) or 20 s. The etchant gel was washed with copious amounts of water and dried using a filter paper. Moreover, applying dental adhesive gel I bond Total Etch (Heraeus-Kulzer,Hanau,Germany) for 20 s and then cured for 20 s with same light cure gun. Finally, cavities were fully filled with either the commercial or experimental composite pastes prepared as above in materials section. Each filling cavity was cured top and bottom for 40 s with the blue light curing unit. The samples were then stored in an incubator at 37 ± 0.5 °C for 24 h prior (n=6).

The push out test was performed with a computer-controlled universal testing machine (model 4505, Instron, Canton, MA, USA) with 1 or 50 kN load cell (244). The ivory dentine blocks were placed on an aluminium device, with a central hole to allow the displacement of the filling materials upon application of load (Figure 5-11).

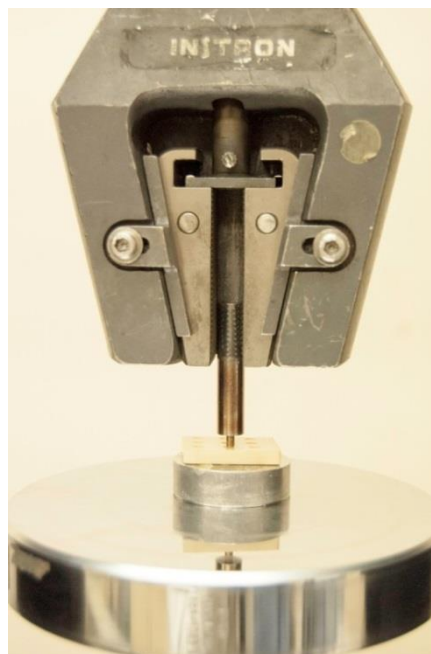


Figure 5-11: Push out test using Instron instrument and ivory dentine filled with composite

The load was applied at a cross head speed of 0.5 mm/min through a plunger positioned on the surface of the composite filling (245). The debonding stress was defined as the maximum load that could be applied before the filling began to be pushed out from the cavity.

5.2.7.2. Shear test

The Shear bond strength test was performed using wet ivory dentine (control hydration) as above in push out test. The ivory was cut into approximately 1 cm³ blocks, by using a diamond saw, and fixed in self-cured acrylic resin as shown in Figure 5-12. The top surface was ground using a polishing machine (Struers, Denmark) with silicon carbide paper (500 grain) to create a standardised smear layer on the exposed ivory surface. The dentine orientation was such that dentinal tubules were perpendicular to the top surface. The ivory dentine was treated as above. The composite pastes were then placed in two incremental layers in stainless steel tubes placed on the surface of the exposed dentine. The tubes had a chamfered edge to reduce dentine contact and were 4 mm in diameter and 6 mm in height. Each incremental layer was light cured for 40 s as above.

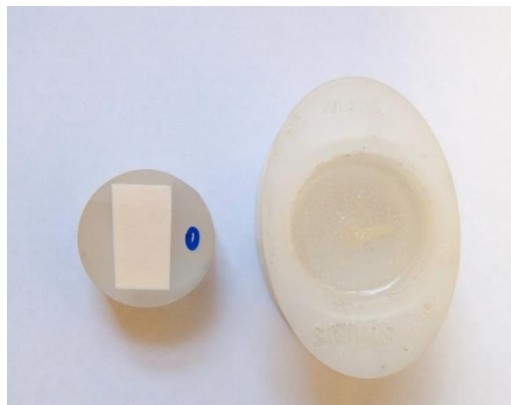


Figure 5-12: Ivory dentine fixed in self-cured acrylic resin

The samples were subsequently stored in an incubator at 37 ± 0.5 °C for 24 h. The shear bond test was performed according to ISO 29022:213 using the Instron machine with a “flat-edge shear fixture jig” as in Figure 5-13 (a & b). The jig consists of a holder that fixes the surface of the dentine directly against a blade. Upon application of a load the blade provides an increasing shear force on the composite containing cylinder. The test was conducted at a cross-head speed of 0.5 mm/min, using a 1 kN load cell. The bond strength was calculated using Equation 5-18:

$$S = \frac{P}{A} \qquad \text{Equation 5-18}$$

Where P is the maximum load at bond breakage and A is the composite surface area in contact with the dentine.

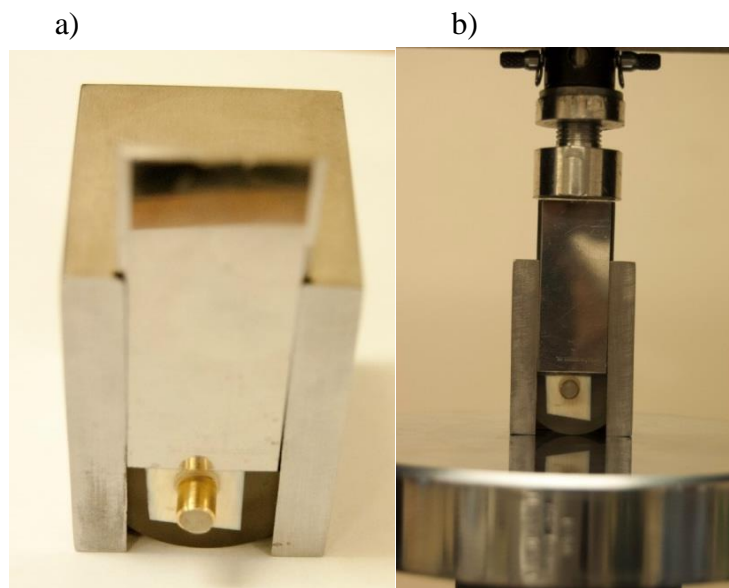


Figure 5-13: a) Ivory sample secured in flat edge shear fixture jig, b) Instron machine with “flat-edge” shear bond testing jig.

5.2.8. Statistical analysis

5.2.8.1. Linest analysis

In this project a Linest functional in Microsoft office excel (Microsoft, 2010) was used to fit straight lines to data. This is an alternative to using the data Analysis package commonly installed in most versions of Microsoft Excel called the Regression Function. The benefit of using a Linest function is the ease of using it multiple times to generate many regressions. The Linest function calculates the statistics for a line by using the "least squares" method to calculate a straight line that best fits the data. Linest can also combine other functions to calculate the statistics for other types of models including, polynomial, logarithmic, exponential, and power series. The equation of a straight line is;

$$Y = MX + B$$

Equation 5-19

Where the dependent (Y) values are a function of the independent (X) values, (M) is the slope or gradient of the line, equal to the change in Y/change in X, and can be positive or negative. (B) is the point where the line crosses Y-axis

The Syntax for linest function is; Linest = (value_ Y's, value_ X's), (const), true

The p value for statistical description can be calculated from the Linest function result by using the function TDIST.

The Syntax for the Linest function is "TDIST" (intercept/standard error, degree of freedom, 2). These outcomes explain if the data is statistically significant or not, when the p value is smaller than 0.05 the data is often considered as statistically significant.

In this project, the functional Linest analysis was used on the experimental formulations as described above. The x-axis represented the calcium phosphate (CaP) levels in most of the results, except in mass and volume changes and chlorhexidine release where the x axis was the square root of time. The y-axis results are shown in Table 5-6.

Table 5-6: Shows the X and Y axis for Linest equation for experimental formulations with 4-META and HEMA.

	X axis	Y axis
Degree of conversion	Cap levels	Degree of conversion (%)
Polymerisation shrinkage	Cap levels	Polymerisation shrinkage (%)
Depth of cure	Cap levels	Depth of cure (mm)
Mass and volume change	Time (SQRT)	Mass and volume change (%)
Chlorhexidine release	Time (SQR)	Chlorhexidine release (%)
Biaxial flexural strength	CaP levels	BFS (MPa)
Adhesion tests	CaP levels	Interfacial stress (MPAa)

5.2.8.2. Statistical analysis

In all studies, the data was statistically analysed with analysis in the first instance of variance (ANOVA) with statistical software SPSS (SPSS 21.0, Chicago, IL, USA). For all technique analysis the differences between groups were identified using post-hoc multiple Bonferroni comparisons test at $P < 0.05$.

In the first study, for the controlled experimental and commercial dental composites ANOVA were used. A Bonferroni post-hoc test was used to determine whether there was a significant difference between the control and commercial dental composites, and between experimental formulations with 4-META and HEMA with different levels of CaP.

Result and Discussion Chapter

6. Control and commercial dental composites

6.1. Introduction

The data provided in appendices 1, 2 and 3 informed the choice of particle source, PLR, monomer types and levels for study in this next chapter. In the experimental composites Bis-GMA was replaced by UDMA due to the toxicity concerns which can rise when low conversion rates result from the relatively high glass transition temperature of this monomer (76, 231, 246). Additionally, TEGDMA was replaced by higher molecular weight diluent monomer PPGDMA. Its large size in combination with a greater degree of conversion, compared to TEGDMA containing composites can further reduce toxicity concerns.

This chapter provides results for control experimental formulations containing UDMA: PPGDMA at 68:25 wt %. Previous work revealed that the addition of filler particles to 70/30 wt % base monomer and diluent lead to a higher value of conversion and mechanical properties (109, 247). To this was added, 4-META or HEMA (5 wt %) fixed at the maximum solubility of 4-META, in the other monomers to enhance bonding. Furthermore, CQ and monomers and CQ and amine accelerator NTGGMA (each 1 wt %) was included instead of traditional amines, as initiator and co-initiator, at the maximum solubility as it is able to bond with both monomers and calcium. Controlled formulations contained solely glass particles in the filler phase. The powder to liquid ratio was 3:1 by weight.

Commercial dental composites Z250, EcuSphere and Gradia were selected for comparison. The properties evaluated included: chemical composition and monomer conversion, the depth of cure and mass and volume changes. The mechanical properties assessed included the biaxial flexure strength (BFS) and Young's modulus. Moreover, push out and shear bond strengths with ivory were assessed.

6.2. FTIR spectra for individual dental monomers

FTIR spectra for monomers used in commercial composites, including Bis-GMA, Bis-EMA, UDMA and TEGDMA are shown in Figure 6-1. The spectra have strong monomer peaks at 1716 cm^{-1} due to a methacrylate C=O stretch. The absorbance of this peak is higher in UDMA and TEGDMA as compared to Bis-GMA and Bis-EMA. Peaks at 1636 and 1400 cm^{-1} are due to C=C stretch and a C-H attached to C=C in uncured methacrylate. Further, peaks were observed at 1612 cm^{-1} due to aromatic C=C in benzene rings of Bis-EMA and Bis-GMA. The peak at 1530 cm^{-1} in the UDMA spectra is due to an N-H deformation. In all monomer spectra, peaks appeared at 1452 cm^{-1} due to aliphatic C-H vibrations, 1296 and 1320 cm^{-1} associated with C-O stretch and 1164 cm^{-1} due to C-O-C asymmetric stretch.

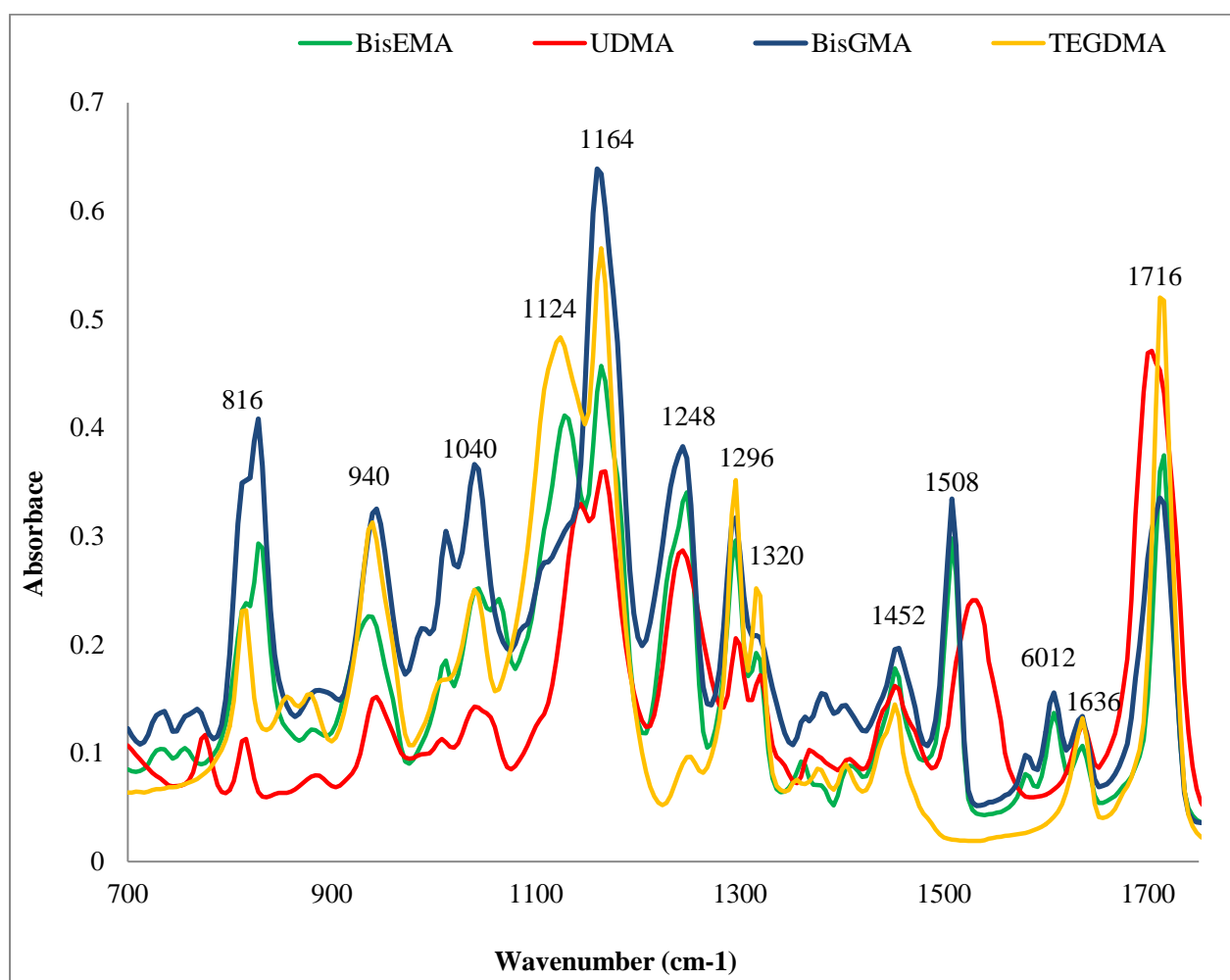


Figure 6-1: FTIR spectra for monomers used in commercial dental composites

6.3. FTIR spectra for commercial composites

6.3.1. Z250

Figure 6-2 shows the FTIR spectra for Z250 dental composite before and after light curing for 40 s. The peaks shown at 1608 cm^{-1} are the result of the carbon double bond in the aromatic benzene ring found in both Bis-EMA and Bis-GMA. A strong monomer peak at 1718 cm^{-1} (C=O stretch) is also observed (248). There was decrease in the intensity of 1298 and 1318 cm^{-1} (C-O stretch) peaks upon polymerisation. The strong peak at 1027 cm^{-1} is due to high filler loading and small particles making better contact with the FTIR diamond than larger particles.

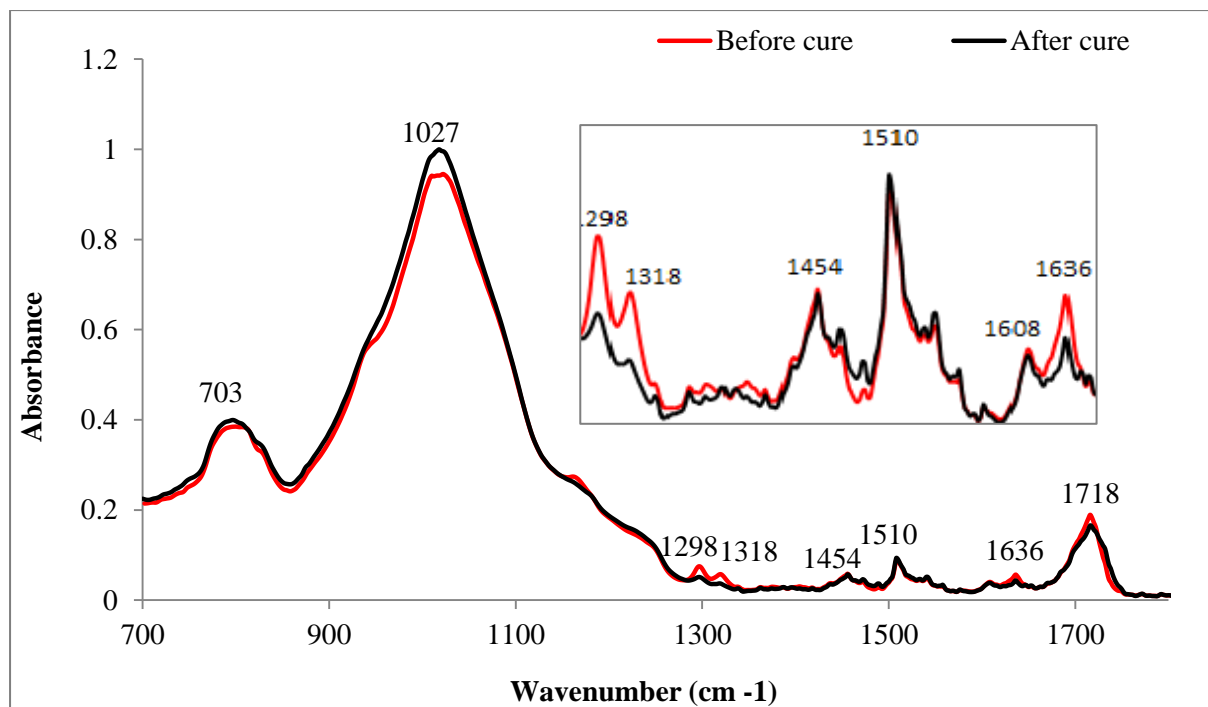


Figure 6-2: FTIR spectra for Z250 dental composite before and after light cure for 40 s

6.3.2. Gradia

The FTIR spectra for the commercial dental composite Gradia before and after 40 s light curing are presented in Figure 6-3. The figure shows the high absorbance peaks associated with UDMA at 1530 and 1716 cm^{-1} . The 1636 cm^{-1} C=C stretch peak decreased after polymerisation as did those at 1320 and 1298 cm^{-1} (C-O stretch). The dominate peak at 981 cm^{-1} is primarily the result of the glass filler phase. This may lower than in Z250 due to glass filler content.

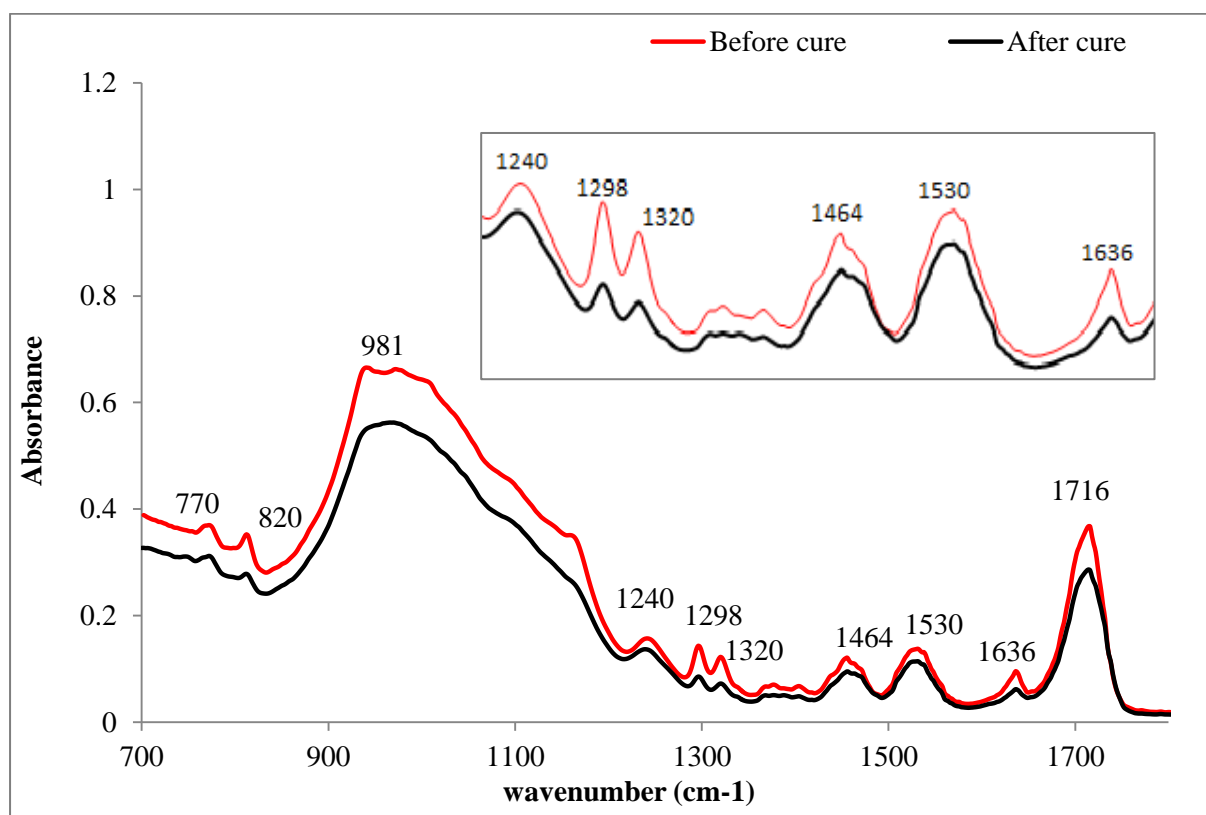


Figure 6-3: FTIR spectra for Gradia dental composite before and after light cure for 40 s.

6.3.3. Ecusphere

FTIR spectra for commercial dental composite Ecusphere before and after curing for 40 s are displayed in Figure 6-4. The peak at 1512 cm^{-1} (C=C stretch) is consistent with the presence of Bis-GMA. The high intensity peaks at 1720 cm^{-1} (C=O stretch) and 1320 cm^{-1} (C=O stretch) may be due to any methacrylate monomer. The intensity of the peak at 996 cm^{-1} due to the glass filler phase may be due to both high filler loading and good contact with the FTIR diamond due to small size

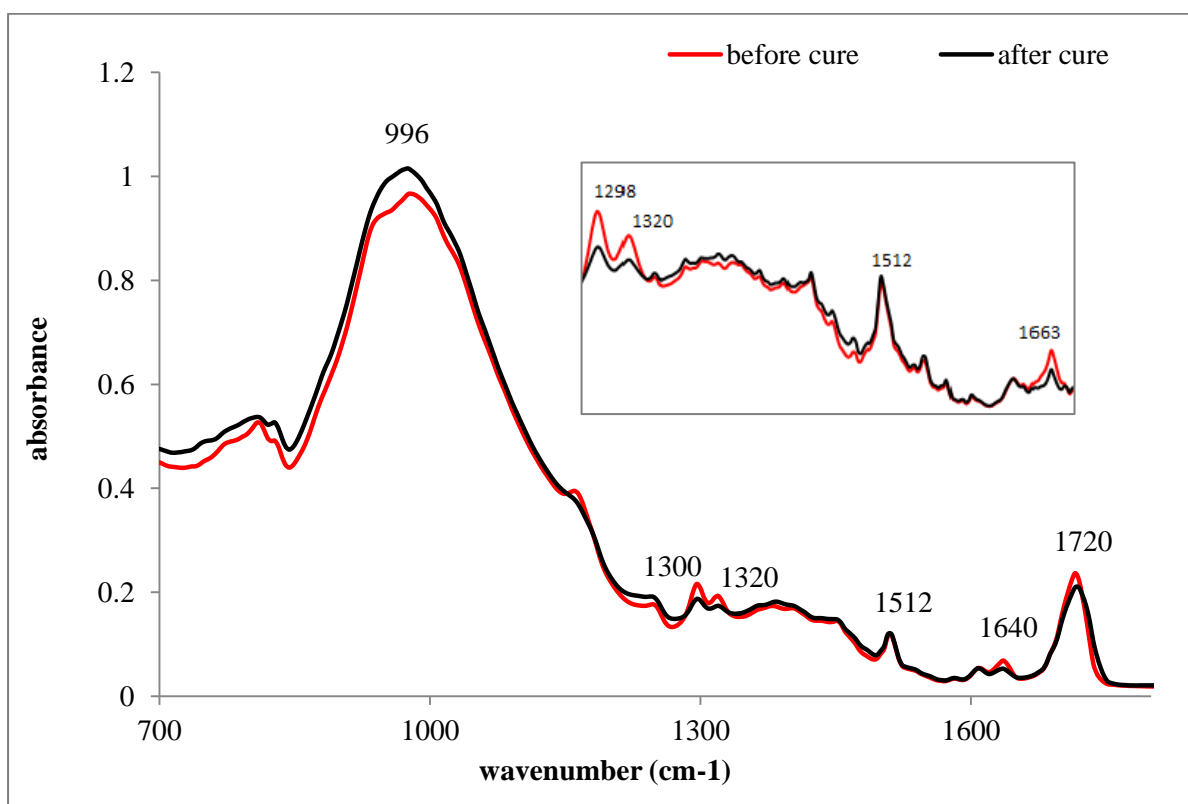


Figure 6-4: FTIR spectra for Ecusphere dental composite before and after light cure for 40 s

6.3.4. FTIR spectra for control experimental

The FTIR spectra for control experimental formulations with 4-META and HEMA before and after curing for 40 s are exhibited in Figure 5-6 (a & b). The peaks at 1716 cm^{-1} (C=O stretch) 1640 cm^{-1} (C=C stretch), 1456 cm^{-1} (C-H scissor) and 1376 cm^{-1} (C-H bend) $1294/1320\text{ cm}^{-1}$ (C-O stretch), 1152 cm^{-1} (C-O-C asymmetric stretch) and changes with light exposure are all consistent with a polymerising UDMA / PPGDMA mixture. The glass peak at 950 cm^{-1} may be low due to lower filler loading and large filler particle size.

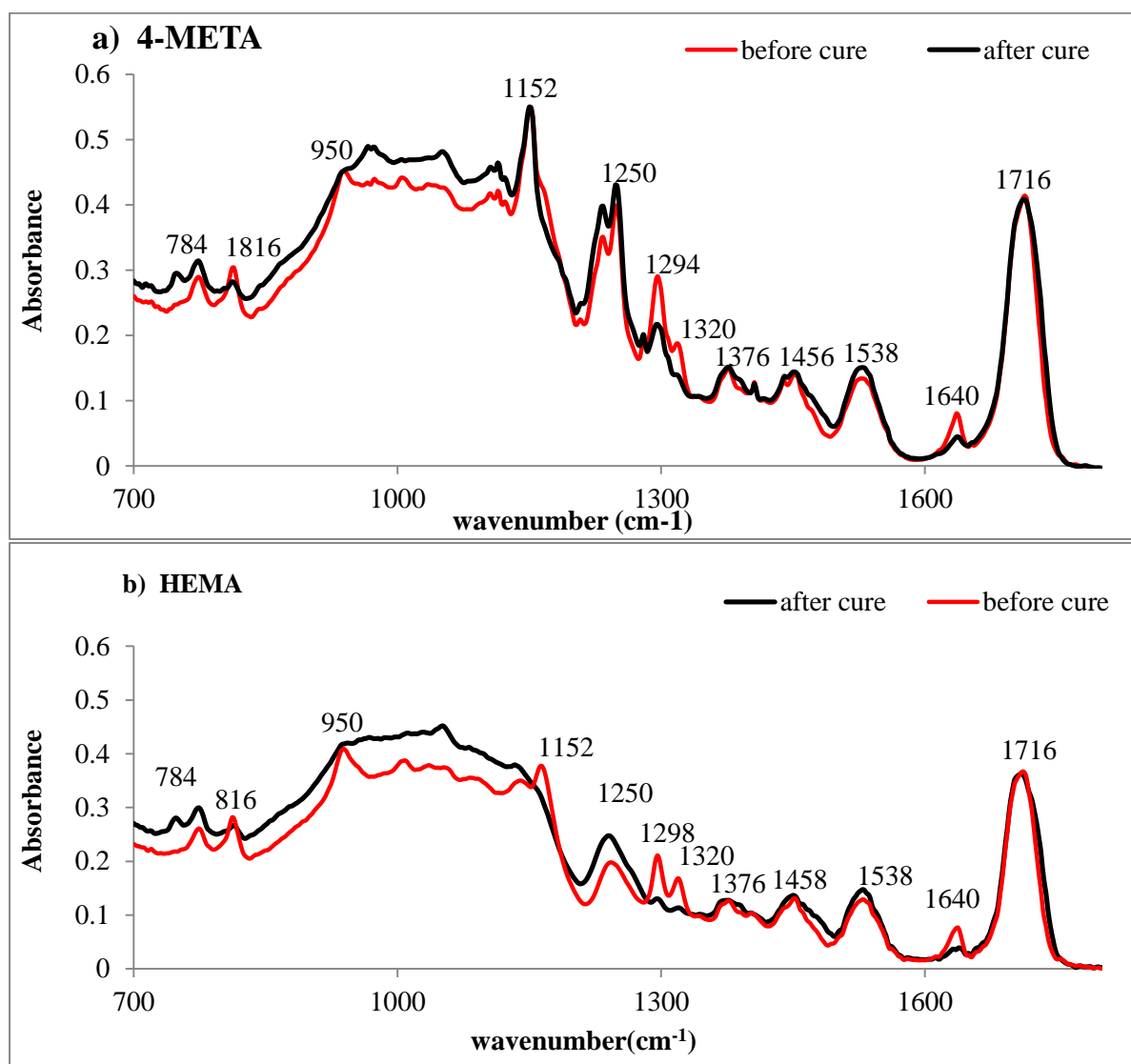


Figure 6-5: FTIR spectra for control experimental formulations with 4-META (a) and HEMA (b) before and after curing for 40 s

6.4. Degree of conversion of control formulations and commercial composites

The degree of conversion for control experimental formulations and commercial dental composites after curing for 40 s is provided in Figure 6.6. The figure reveals that the control experimental formulations with HEMA and 4-META at $80 \% \pm 1.6$ and $77 \% \pm 1.6$ respectively, had the highest level of conversion as compared to commercial composites. The Ecusphere dental composite generally had a higher conversion ($68 \% \pm 1.6$) than Z250 and Gradia, which had only $47 \% \pm 1.5$ and $55 \% \pm 1.4$ conversions respectively.

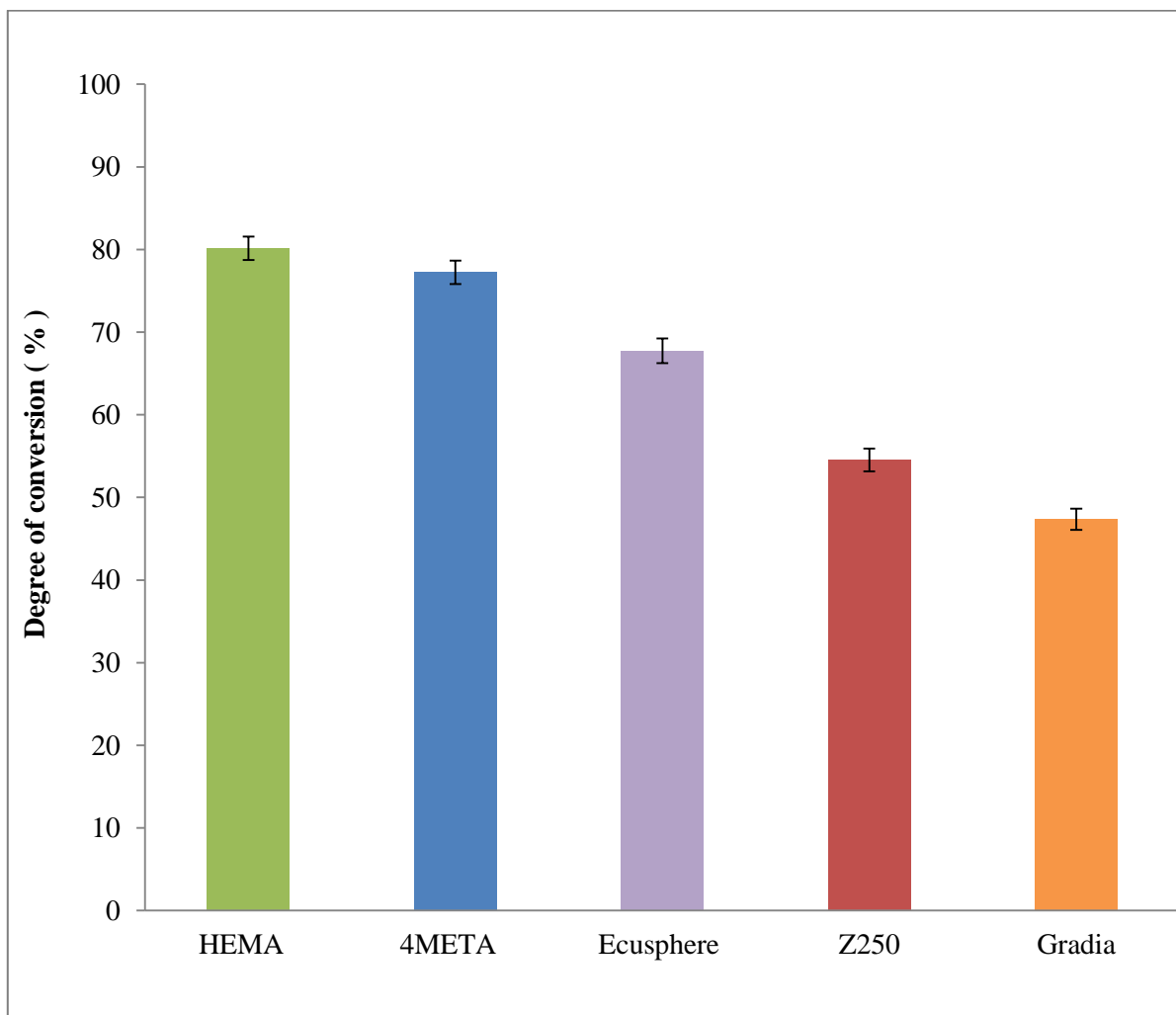


Figure 6-6: Degree of conversion for control experimental and commercial composites after curing for 40 s. The error bars indicate 95 % C.I of the mean (n=5).

The subsequent result from one way analysis of variance (ANOVA) showed that there was sufficient evidence to reject the null hypothesis that the mean conversion in the five dental composites was the same ($P < 0.001$). The post-hoc Bonferroni multiple comparisons showed that there were significant statistical differences between control experimental formulations and commercial composites. Furthermore, all commercial composites were significantly different from each other ($P < 0.001$ in all cases). There were no significant statistical differences, however, between HEMA and 4-META control formulations ($P = 0.085$).

6.5. Depth of cure

The average ISO 4049 depth of cure for control experimental formulations and commercial dental composites after curing for 20 and 40 s is represented in Figure 6-7. The dental composites showed a slightly increased depth of cure measurement at 40 s as compared to 20 s cure. All dental composites after curing for 20 and 40 s, complied with the ISO standard for the depth of cure, which is a minimum 1.5 mm. The analysis of variance (ANOVA) showed that the only variable causing a significant statistical effect on depth of cure was curing time of 20 versus 40 s ($P > 0.001$).

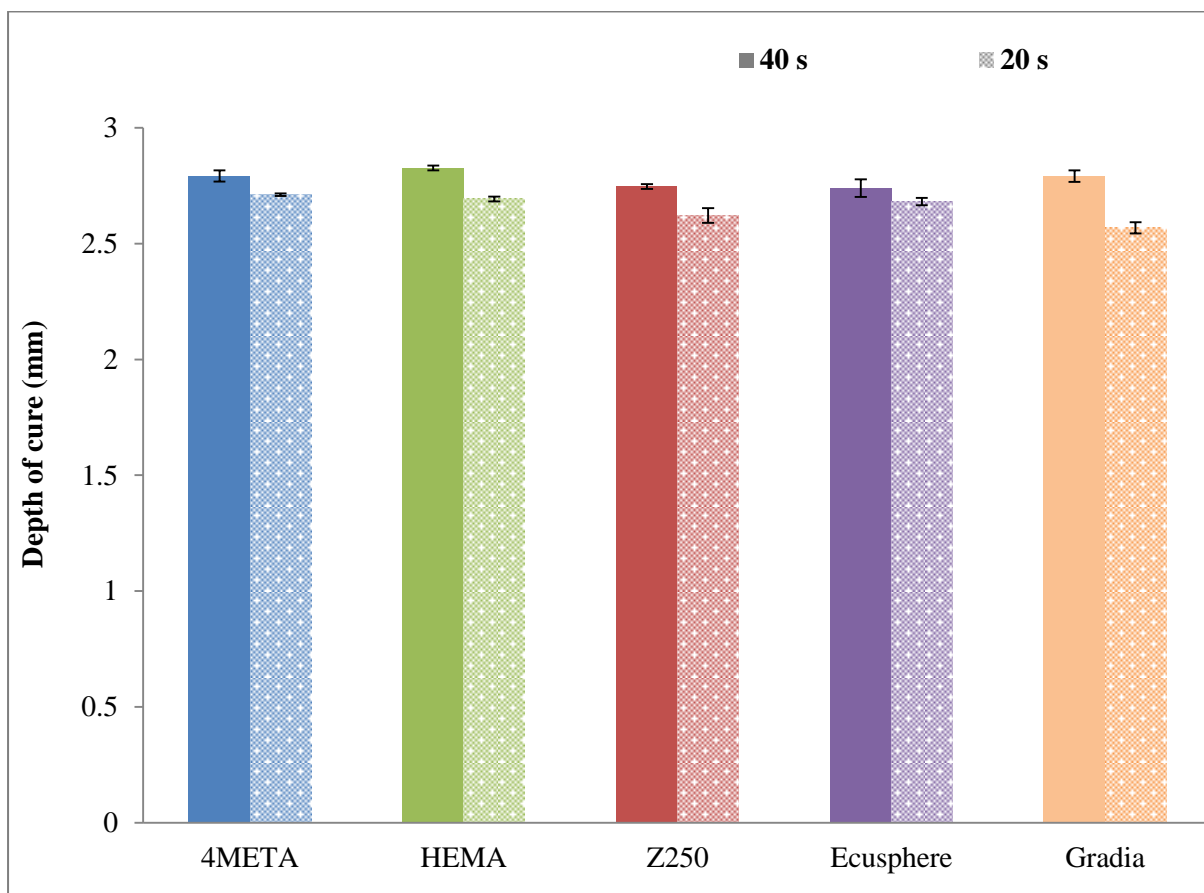
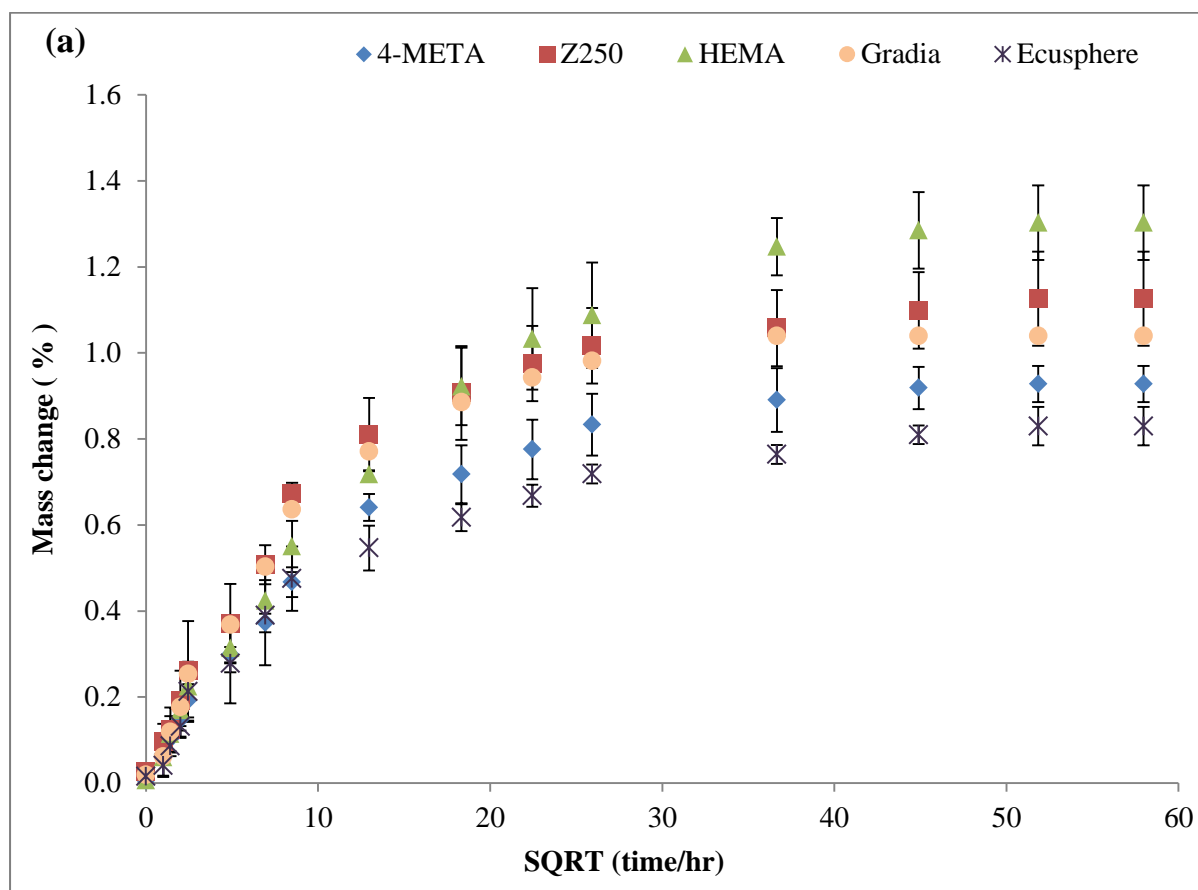


Figure 6-7: Depth of cure for control formulations with 4-META / HEMA and commercial dental composites after curing for 20 and 40 s. The error bars represent the 95 % C.I. (n=3)

6.6. Mass and volume change

Average mass and volume change for control experimental formulations and commercial dental composites over a period of five months plotted versus root square root (SQRT) of time are shown in Figure 6-8 (a & b). In all dental composites the mass and volume increased linearly upon water sorption with the square root (SQRT) of time for the first 24 h. The control experimental formulation with HEMA had the highest final mass and volume change with 1.3 wt % and 1.8 vol % increases respectively. Conversely, control experimental formulation with 4-META had the lowest final volume change of 1.2 vol %. Ecusphere had the lowest final mass change of 0.83 wt %.



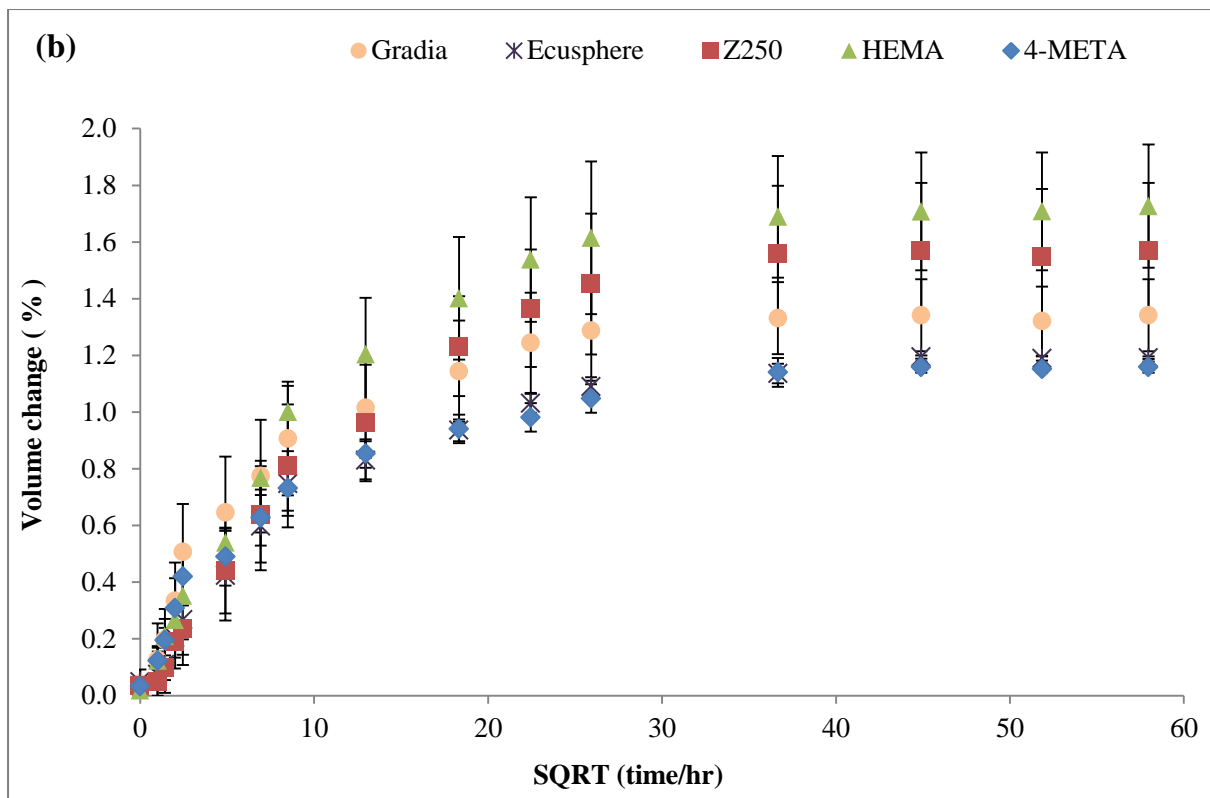


Figure 6-8: Mass and volume change (a and b) in deionised water for control experimental formulations with 4-META/ HEMA and the commercial composites. The error bars represent 95% C.I of the mean (n=3).

The two way analysis of variance (ANOVA) demonstrates that there was sufficient evidence to accept the null hypothesis that the mean initial 24 h mass and volume change in control and commercial composites was not same $P= 0.352 \quad 0.453$ respectively. However, the maximum mass and volume change was the same between the composites ($P < 0.001$). Post-hoc Bonferroni multiple comparisons for maximum mass showed that there was significant statistical difference between 4-META and all other composites ($P < 0.001$) except between 4-META and Ecusphere ($P = 0.235$). There were also no statistical difference between HEMA and Z250 ($P = 0.615$) and Gradia and Z250 ($P= 0.145$). In terms of maximum volume change there were statistical difference between 4-META and HEMA, 4-META and Z250 ($P < 0.05$) and between Ecusphere and HEMA as well as Ecusphere and Z250 Gradia ($P < 0.05$).

6.7. Biaxial flexural strength and Young's modulus

6.7.1. Biaxial flexural strength

The average biaxial flexural strength (BFS) for control experimental formulations and commercial dental composites both dry and hydrated (24 h, 1 day and 28 days immersion in deionised water) are provided in Figure 6-9. It is shown that the initial dry strength for 4-META and Z250 composites had the highest BFS of 170 ± 9 MPa, followed by HEMA and Ecusphere composites with 163 ± 6 and 157 ± 9 MPa respectively. However, Gradia dental composite had the lowest BFS with 96 ± 5 MPa.

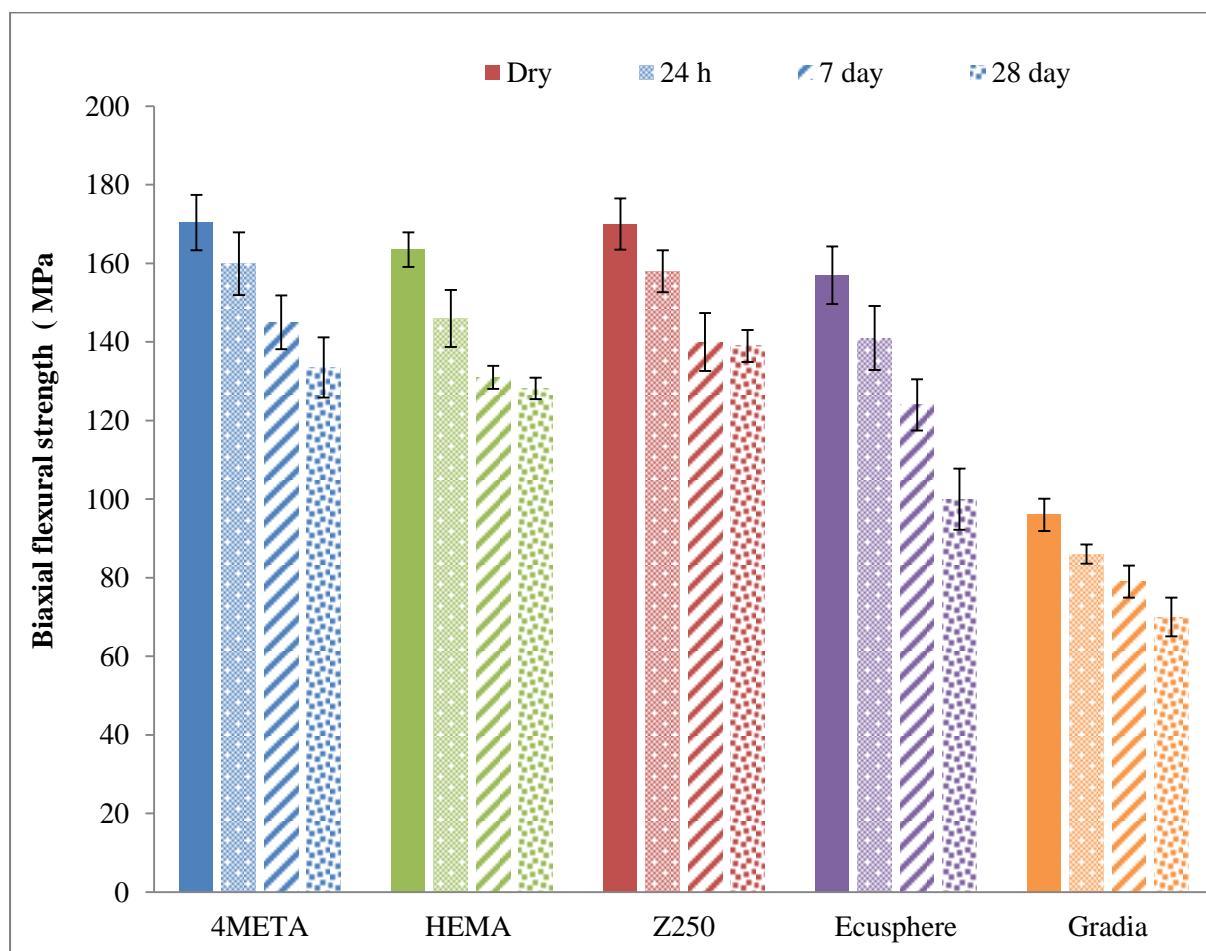


Figure 6-9: BFS for control experimental and commercial dental composites dry and wet (after immersion in water for 24 h, 7 day and 28 days). The error bars represent 95% C.I of the mean. (n=6).

Upon immersion in water for 24 h, all of the control experimental and commercial composites exhibited a decrease in strength. Further decline in strength was shown after 7 days in water. Whilst the control experimental materials and Z250 showed only minor decline after this time that of Ecusphere and Gradia was more evident.

Two way analysis of variance (ANOVA) provided sufficient evidence to reject the null hypothesis that the variances for BFS between the composites were equal at all-time points ($P < 0.001$). Post-hoc multiple Bonferroni comparisons showed that the strength of the 4-META formulation or Z250 was significantly different from Ecusphere and Gradia at all-time points ($P < 0.001$). It was also significantly different from the HEMA formulation after immersion in water ($P = 0.025$). The HEMA formulation was significantly different from Gradia at all times and greater than that of Ecusphere after 28 days ($P < 0.001$).

6.7.2. Young's modulus

The average flexural modulus for control experimental and commercial composites dry or wet for (24 h, 7 day and 28 day immersion in deionised water) are provided in Figure 6-10. The data showed that dry modulus for 4-META and Z250 composites had the highest elastic modulus of 5.4 ± 0.2 and 4.9 ± 0.7 GPa respectively, followed by HEMA and Ecusphere with 4.7 ± 0.6 GPa. However, Gradia dental composite has lowest modulus with 3.3 ± 0.4 GPa.

Upon immersion in water for 24 h all of the control experimental and commercial in modulus has declined, with further decrease observed after 7 days. Whilst the Gradia dental composite showed only minor decline after this time, that of control formulations Z250 and Ecusphere were more evident.

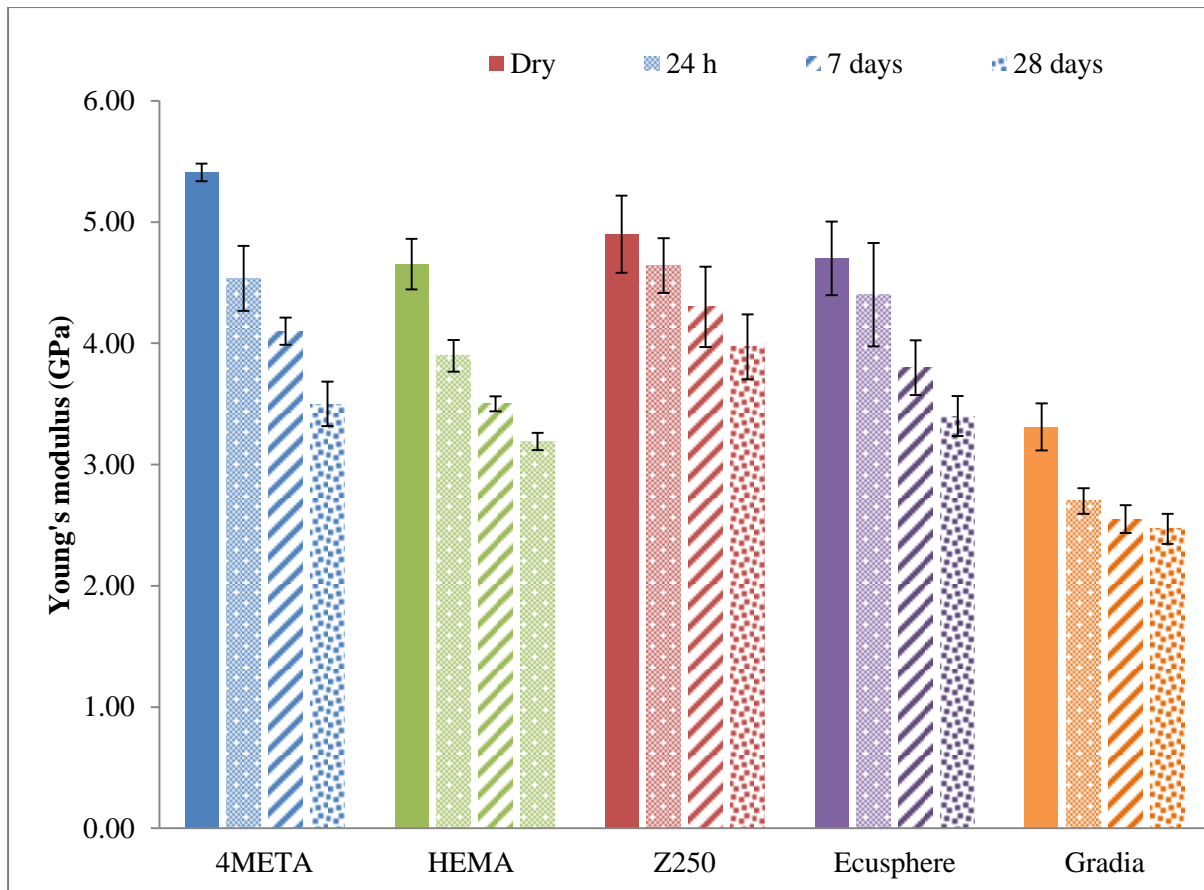


Figure 6-10: Young's modulus for control experimental and commercial dental composites dry and wet (after immersion in deionised water for 24 h, 7 day and 28 days). The error bars indicate 95 % C.I of the mean. (n=6)

A Two way analysis of variance (ANOVA) disclosed that there was sufficient evidence to reject the null hypothesis that the variance for modulus between the composites were equal ($P < 0.001$) at all times. Post-hoc multiple Bonferroni comparisons showed that the modulus of both control formulations with Z250 and Ecusphere were significantly different from Gradia at all-time points ($P < 0.001$). However, there were no significantly different between the 4-META formulation and HEMA, Z250 and Ecusphere at all-time point ($P > 0.05$) except HEMA in dry and 7 day samples ($P < 0.05$). Furthermore, HEMA formulation was not significantly different from Z250 ($P > 0.05$) at all-time point except in 7 days sample.

6.8. Push out adhesion test

6.8.1. Dry ivory dentine

The average push out test results for commercial and control experimental composites from dry ivory dentine are given in Figure 6-11. This data reveals that the debonding stress was on average 46 % higher after acid etching of ivory dentine as compared with non-etched dentine.

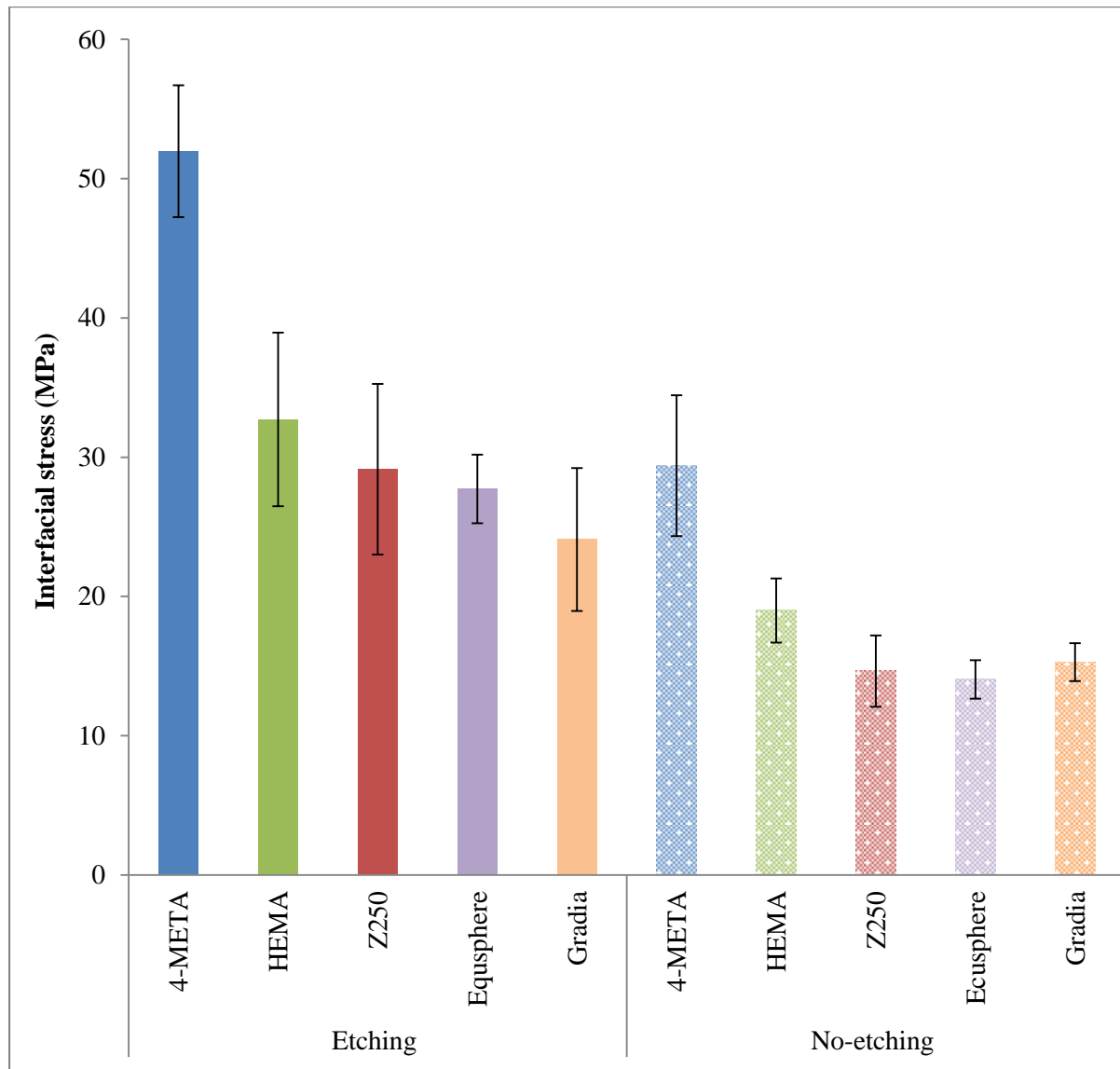


Figure 6-11: Push out stress with dry ivory dentine for control experimental formulation and commercial composites with acid etched dentine for 20 s and no-etched. The errors represent 95 % C.I of the mean. (n=6).

With no acid etching of the ivory dentine, control formulations with 4-META showed the highest push out stress of 29 ± 5 MPa followed by HEMA with a push out stress of 19 ± 4

MPa. The push out stress for all commercial composites with un-etched dentine was ~ 15 MPa.

After acid etching the control formulation with 4-META followed by that with HEMA, had the highest push out stress results of 52 ± 5 and 33 ± 6 MPa respectively. The push out result for commercial composites was also comparable at ~ 27 MPa.

The two way analysis of variance (ANOVA) provided sufficient evidence to reject the null hypothesis that the variance for dry debonding stress between the composites and etching condition were equal ($P < 0.001$). Post-hoc comparisons showed etching had a significant effect on debonding stress for all formulations ($P < 0.001$). Furthermore, the control formulation with 4-META gave a significantly higher debonding stress than all other materials ($P < 0.001$). However, there were no significant differences between all commercial composites with and without acid etching ($p > 0.05$).

6.8.2. Wet (control hydration) ivory dentine

The average debonding stress of commercial and control experimental composites from wet ivory dentine are represented by Figure 6-12. The debonding stress was on average 1.8 times higher after acid etching of the dentine, compared with non-etching dentine. With no acid etching of the ivory dentine, the control formulation with 4-META showed the highest debonding stress (56 ± 5 MPa) in comparison to other control and commercial composites. The results showed that HEMA formulation and Z250 were comparable (37 ± 5 and 35 ± 4 MPa respectively) but both were significantly higher than Ecusphere and Gradia (30 and 22 MPa respectively).

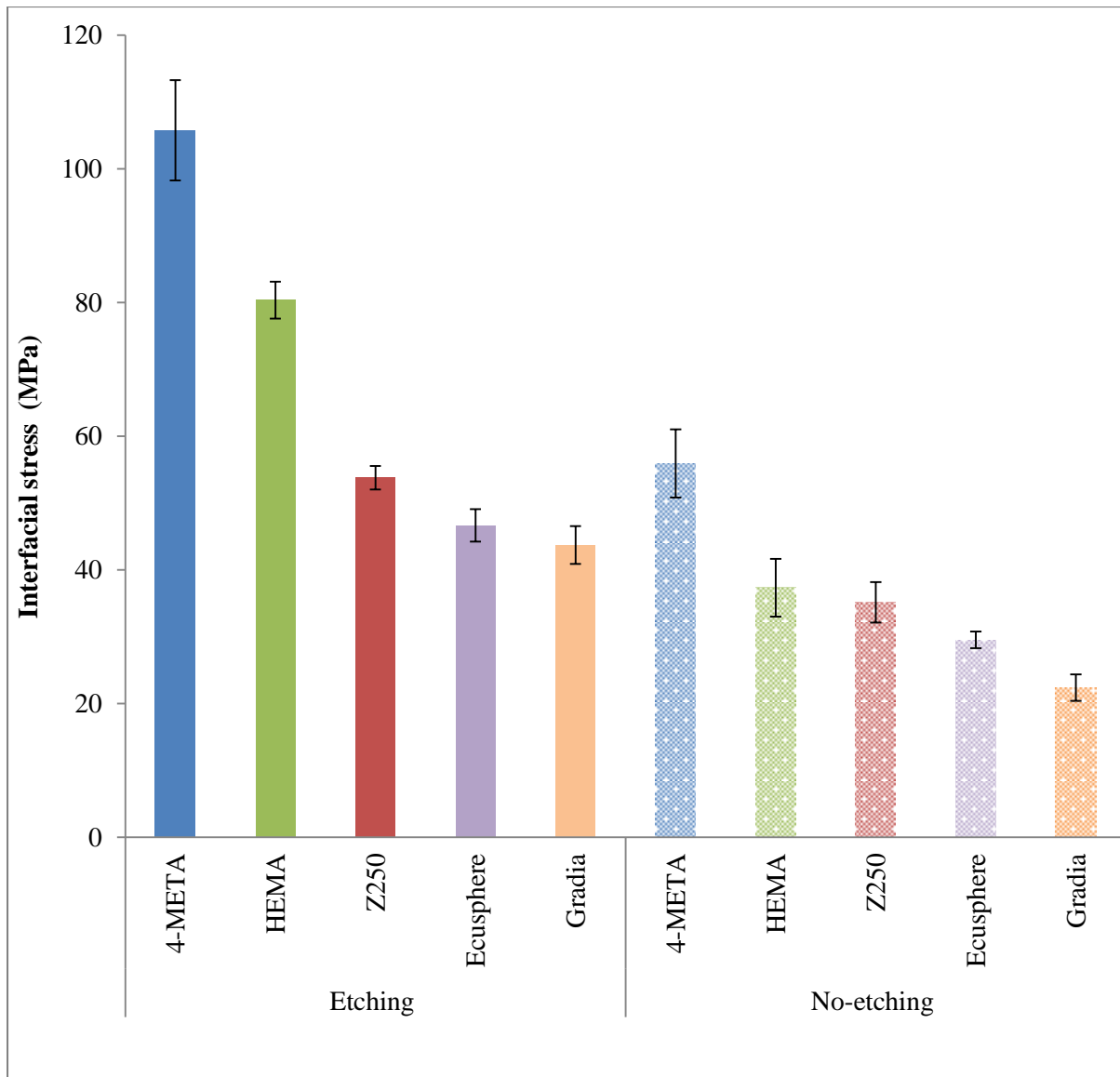


Figure 6-12: Push out stress with wet ivory dentine for control experimental and commercial composites with acid etched dentine for 20 s or no-etched. The error bars represent 95% C.I of the mean. (n=6).

After acid etching the control formulation with 4-META, followed by that with HEMA, had the highest push out stress of 106 ± 9 and 80 ± 4 MPa respectively. The push out stress for commercial composites with Z250 was higher (54 ± 2 MPa) in comparison with other composites ($\sim 45 \pm 3$ MPa).

The two way analysis of variance (ANOVA) presented sufficient evidence to reject the null hypothesis that the variance for hydrated debonding stress between the etched composites and non-etched composites were equal ($P < 0.001$). Post-hoc comparisons showed etching had a significant effect on debonding stress for all formulations ($P < 0.001$). Furthermore, the control formulation with 4-META gave a significantly higher debonding stress than all other materials with and without acid etching ($P < 0.001$). The HEMA formulation was significantly different from Gradia and Ecusphere regardless of acid etching ($P < 0.05$). There were no significant statistical difference found between commercial composites Z250 and Ecusphere with and without acid etching ($P > 0.05$), as well as between Ecusphere and Gradia ($P > 0.05$).

6.8.3. Push out stress with self-adhesive Ibond

The push out stress results for commercial and control composites with a self-adhesive Ibond is given in Figure 6-13. It can be seen that control formulation with 4-META with Ibond showed the highest debonding stress of 207 ± 7 MPa, followed by Ecusphere composite of 196 ± 7 MPa. The push out stress for HEMA formulation was 171 ± 14 MPa; however, Z250 and Gradia composites had the lowest push out stress with ~ 142 MPa.

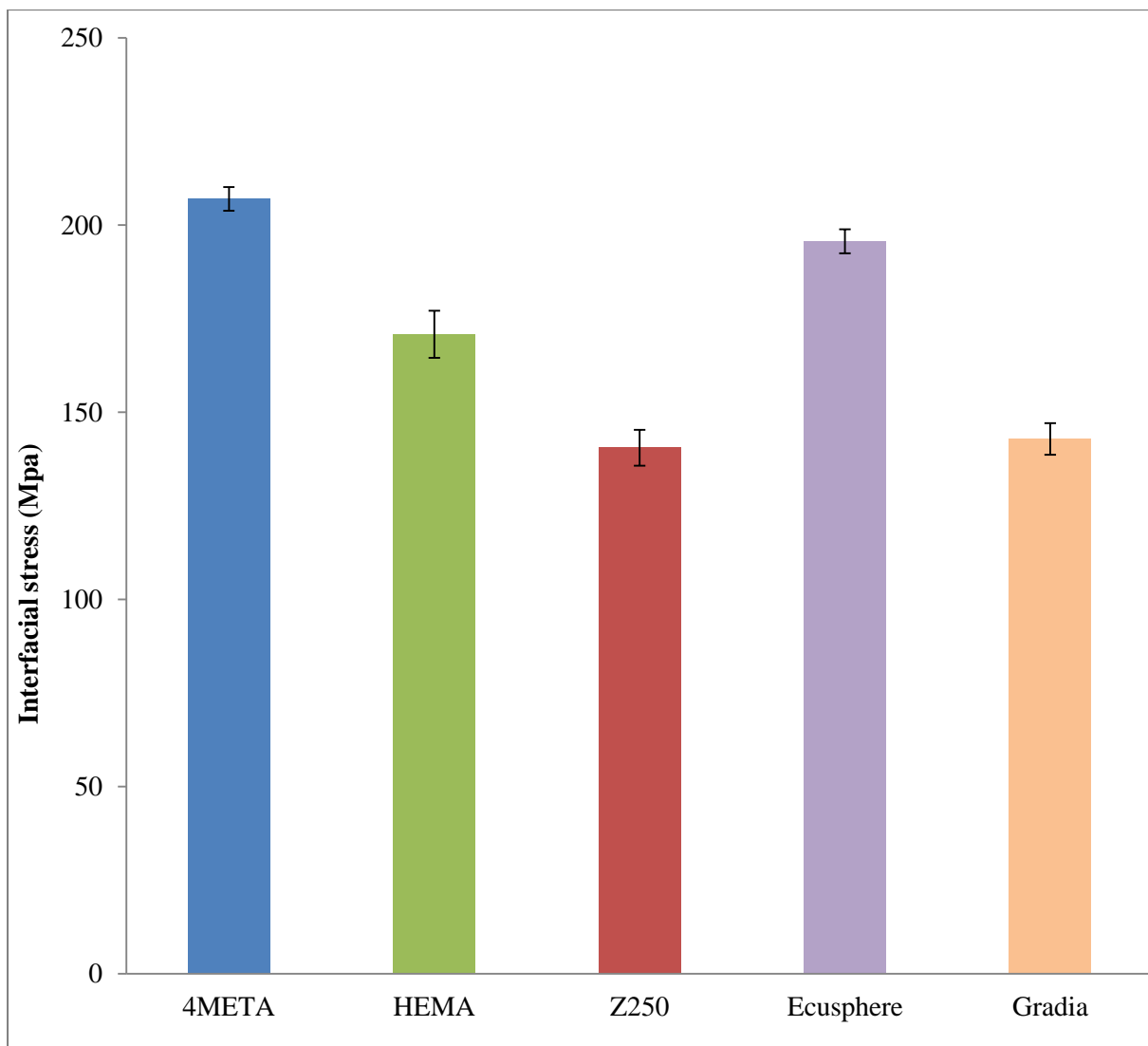


Figure 6-13 : Push out stress with wet ivory dentine for control formulations and commercial composites with self-adhesive Ibond. The error bars represent 95 % C.I of the mean. (n=6).

The analysis of variance (ANOVA) showed that there was sufficient evidence to accept the null hypothesis that the push out stress with a self-adhesive Ibond variance between the composites were not equal (P value = 0.857). Post-hoc Bonferroni comparisons showed that the self-adhesive Ibond had no effect between all composites (P > 0.999).

6.9. Shear test

The average shear bond strength of commercial and control composites from wet ivory dentine is provided in Figure 6-14. It can be seen the shear bond strength was on average 1.8 times higher after the dentine had been etched with phosphoric acid, in comparison to those which had not etching. In term of non-etched dentine, the control formulation with 4-META showed the highest shear bond strength of 11 ± 1.2 MPa followed by HEMA with a shear strength of 8 MPa. The Z250 composite had lowest shear bond strength of 1 MPa as compared to Ecusphere and Gradia ~ 3 MPa

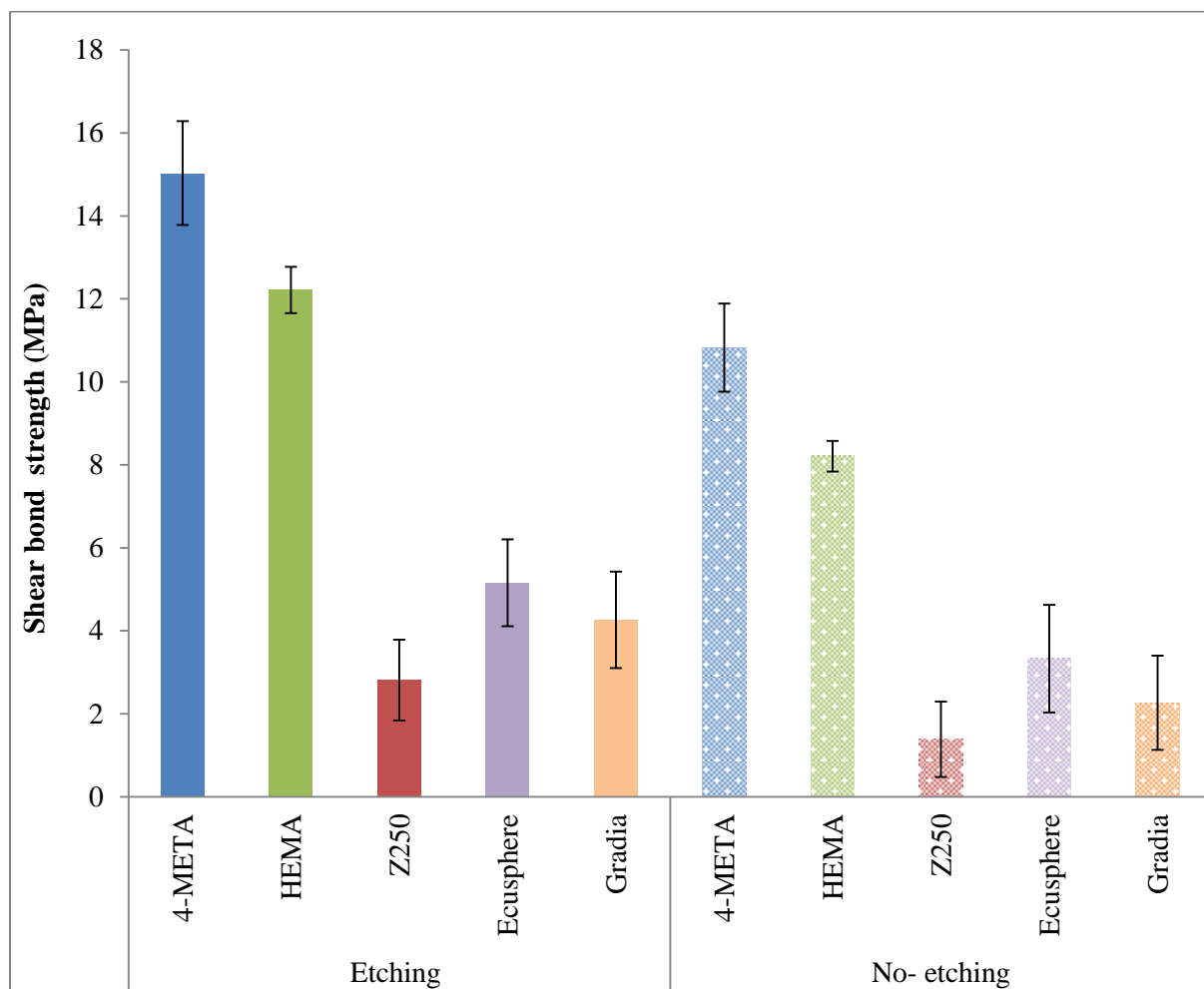


Figure 6-14: Shear bond strength with ivory dentine for control formulations and commercial composites with acid etching dentine for 20 s or no etching. The error bars represent 95% C.I of the mean. (n=6).

After acid etching the control formulation with 4-META followed with HEMA had the highest shear strength of 15 ± 1.4 and 12 ± 0.6 MPa respectively. Once more, the Z250 composite had lowest shear bond strength (3 ± 1 MPa) as compared to Ecusphere and Gradia (~ 5 MPa).

Post-hoc Bonferroni comparisons revealed etching had a significant effect on shear bond strength for control formulations ($P < 0.001$) as compared to other composites. Furthermore, the control formulation with 4-META and HEMA displayed significantly higher bond strength than all other materials, regardless of acid etching ($P < 0.001$). On the other hand, there were no statistical significant differences across shear bond strength and commercial composites ($P > 0.05$) with and without acid etching for 20 s.

6.9.1. Shear bond strength with self-adhesive Ibond

The average shear bond strengths for commercial and control composites with Ibond are provided in Figure 6-15. It can be seen that the control formulation with 4-META showed the highest shear bond strength (50 ± 3 MPa), followed by the formulation with HEMA (40 ± 3 MPa). The shear bond strength for the commercial Z250 composite was (36 ± 2 MPa). However, the lowest shear bond strength was on average $\sim 29 \pm 2$ MPa recorded from both Ecusphere and Gradia composites (30 ± 3 MPa).

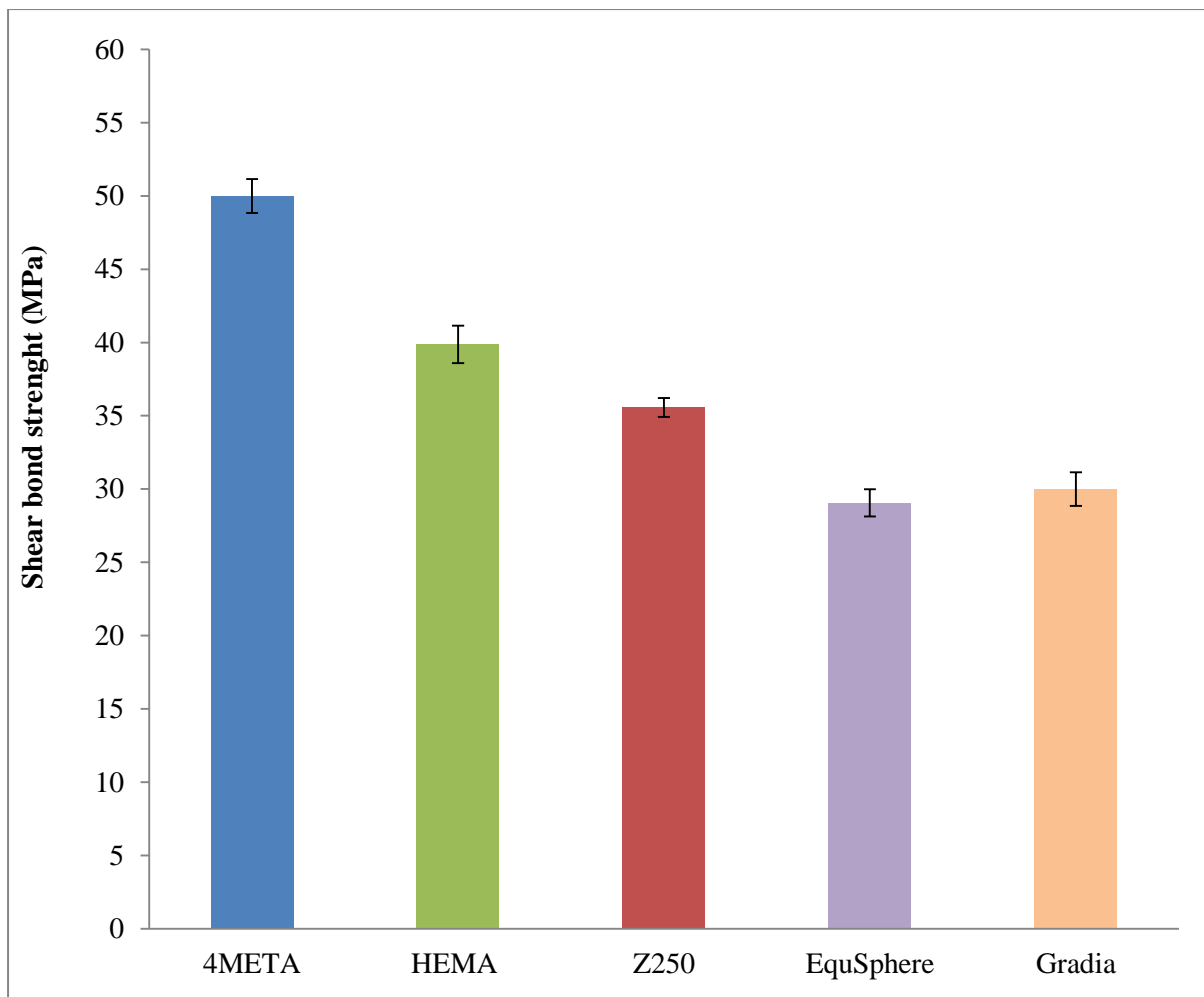


Figure 6-15: Shear bond strength with ivory dentine for control formulations and commercial composites with Ibond. The error bars indicate 95% C.I of the mean. (n=6).

The analysis of variance (ANOVA) showed that there was sufficient evidence to reject the null hypothesis that the shear bond strength and Ibond variance between the composites were equal ($P < 0.0001$). Multiple post- hoc Bonferroni comparisons revealed that the shear bond strength of 4-META formulation displayed a significant statistical difference to all other materials ($P < 0.001$). The HEMA formulation was also significantly different from the commercial composites ($P < 0.001$) except Z250 ($P > 0.05$). There was no significant statistical difference between Ecusphere and Gradia ($P > 0.999$).

6.10. Discussion

6.10.1. Degree of monomer conversion

The first study compared the chemistry and degree of conversion of control experimental composites containing 4-META or HEMA adhesive monomer and solely 100 % glass particles, with three commercial dental composites (Z250, Gradia and Ecusphere) used to provide baseline values. In the above study the degree of conversion at 1 mm depth was assessed as the FTIR method gives conversion on the lower part of the sample.

The FTIR spectra of Z250 and Ecusphere composites both displayed a peak at 1600 cm^{-1} . This is characteristic of with a C=C group present in the Bis-GMA aromatic ring. However, Gradia dental composite exhibited high intensity peaks at 1528 cm^{-1} , confirming the use of UDMA. In addition, there were variations in the peaks at $\sim 1000\text{ cm}^{-1}$ which is a likely consequence of different filler particles size in Z250, Ecusphere and Gradia composites. Smaller particles will make greater contact with the FTIR diamond, which could explain the higher glass peak observed in the Z250 spectra.

Upon light curing, the intensity of 1298 and 1320 cm^{-1} peaks declined due to changes in methacrylate C-O stretching; this was shown for all control and commercial dental composites. In this thesis it was seen that the commercial composites Z250 and Gradia had a lower degree of monomer conversion after 40 s curing, in as comparison to control experimental formulations and Ecusphere dental composites. Commercial dental composites based on Bis-GMA and Bis-EMA generally have a degree of conversion ~ 50 to 60% (249). The literature explains that the, Z250 resin matrix is a combination of Bis-GMA, Bis-EMA, UDMA and TEGDMA monomers (249, 250). It was also previously found to have a degree of conversion of 55% (231), which is in good agreement with the thesis result. Low conversion arises because Bis-GMA has a high glass transition. This is due to the presence of

a rigid aromatic group that causes the material to solidify (and change from rubber to glass) at low conversion (76).

Gradia had a particularly low apparent degree of conversion (~ 47 %) in this thesis. This finding is consistent with values from other researchers, who found it to be ~ 49 % (251, 252). The exact composition of Gradia remains unknown, but from FTIR (Figure 3-6) it can be seen that it contains UDMA but no Bis-GMA. Dental composites based on more flexible monomers with lower glass transition temperature (T_g), such as UDMA, are expected to have greater degree of conversion (253). The glass transition temperature for Bis-GMA (the main monomer in Z250), UDMA (the main monomer in Gradia and Ecusphere) and TEGDMA are -8, -35 and -83 respectively (254, 255). The maximum conversions of these monomers without filler are 35, 72 and 83 % at room temperature (256). The low conversion of Gradia is therefore inconsistent with monomer type, suggesting there is other reason for this issue (257).

Ecusphere dental composite contains a mixture of Bis-GMA, UDMA and TEGDMA monomers with ~ 77 wt % filler phase (171). The high degree of conversion (~ 68 %) observed in this thesis could be a consequence of lower percentage of Bis-GMA compared with Z250. Figure 6-4 displayed a small Bis-GMA peak at 1600 - 1616 cm^{-1} confirming the possibility of incorporating low concentration of Bis-GMA. No previous study could be found which provides the degree of conversion of an Ecusphere composite. The conversion observed in this thesis, however, is consistent with a previous study on degree of conversion of similar composites (~ 65 %) from the same company (258).

The control experimental composite formulations containing HEMA or 4-META showed a high degree of conversion (80 and 77 % respectively after 40 s light cure). This may be due to the use of UDMA in addition to PPGDMA which are both flexible monomers. Increased flexibility and reduced monomer viscosity will decrease the glass transition temperature (T_g)

of the resin monomer and increase the mobility of reactive species respectively, thereby enhancing the degree of conversion (214).

The slightly higher degree of conversion obtained with HEMA formulations may be due to a decrease in monomer viscosity, increased flexibility of the polymer and enhanced wetting of the fillers in the composites (259).

6.10.2. Depth of cure

In the present study, the control experimental formulations and commercial dental composites fulfilled the ISO 4049 requirement of 1.5 mm minimum depth of cure. The average depth of cure of commercial composites cured for 20 and 40 s observed in this thesis of 2.7 and 2.8 mm respectively is comparable with those previously observed for commercial composites (249, 260). The lack of effect observed upon changing HEMA for 4-META is explained by the adhesive monomers present at only low levels (5 wt % of the monomer). A possible explanation for the slightly higher depth of cure for control experimental formulations compared with commercial is the use of flexible UDMA and PPGDMA (253) which enhance conversion and high sample translucency. High light transmission through the sample is important for high conversion at greater depths.

A decrease in light transmission with depth can be caused by light scattering due to a mismatch in refractive indices of the monomer and filler particles (261, 262). The literature asserts that Z250 contains between 80 and 84 wt % zirconium / silicon based oxide filler particles (249, 263-265). Gradia contains 78 wt % filler that is a mixture of fluoro-aluminium-silicate glass and pre-polymerised filler (266). The refractive index of the filler phase in commercial composites, such as those containing strontium, barium and zirconium is about 1.55 which is similar to that for Bis-GMA 1.56 (267). That for aluminosilicate glass, as in Gradia and the experimental materials is ~ 1.46 which matches better that of UDMA (1.48)

and TEGDMA (1.46). As refractive index increases with polymerisation, however, the pre-polymerised filler in Gradia may have contributed to a lack of translucency and increased refractive index mismatch (227). As refractive index of propylene glycol is 1.43 the use of PPGDMA may have helped in matching new composite refractive indices (268). The depth of cure can also be reduced by light absorbance.

In this study different composite colour shades were used, which will have an effect on this property. Usually a curing time of 20 to 30 s will ensure a curing depth of 2 to 2.5 mm with shade (A) composites (269). However, by increasing the curing time to 40 s an adequate conversion of composites of darker shade (B and C) is ensured (270). Light absorbance is also however affected by concentration of photo-initiator (271). With higher concentrations light will penetrate less, although this issue becomes less prominent with time due to photo-initiator bleaching.

6.10.3. Mass and volume change

Dental composite restorations exhibit water sorption upon immersion in water. The water sorption level is controlled by various factors including: the chemical composition of monomers, their level of conversion and crosslinking, the filler phase composition and level, and filler/ matrix bonding (157, 272). Dental composites containing more hydrophilic resin monomer generally have more water sorption compared to composites containing hydrophobic resin monomers. Dental composites with lower filler content and higher monomer phase also generally exhibit higher water sorption (195). Furthermore, crosslinking of the matrix can reduce water sorption. The rate of water sorption into the composite is also dependent upon storage time and sample size.

Water sorption can lead to debonding between the filler and monomer, degradation of the filler phase and expansion of the polymer phase (273). This will result in a decline in

mechanical properties (156, 274). Water sorption may also lead to release of uncured monomer into the oral cavity, which could induce provoke cytotoxic effects. The effects of water sorption, however, are not entirely negative. Expansion caused by water sorption can help to overcome polymerization shrinkage (158).

The mass and volume of both control formulations and commercial composites increased linearly with the square root of time in the initial 6 h, and after that the increase was negligible (Figure 6-8 a and b). Of the commercial composites, Z250 had the highest maximum mass and volume change (1.1 wt % and 1.5 vol % respectively) followed by Gradia (1 wt % and 1.5 vol % respectively) and Ecusphere (0.96 wt % and 1.19 vol % respectively). The control experimental formulations with HEMA had the highest mass and volume change 1.3 wt % and 1.7 vol % respectively. The higher water sorption in this experimental composite may be due to decreased PLR 3:1 and addition of hydrophilic HEMA. The mass and volume change with 4-META was ~ 0.93 wt % and 1.2 vol %. This is most likely because HEMA is more hydrophilic than 4-META (76).

Conventional dental composite water sorption occurs primarily in the monomer phase. Difference in water sorption could be explained by the difference in matrix composition, hydrophilicity level and crosslinking (72).

Water sorption is influenced by the composite's affinity for water which in turn depends on the quantities of hydrophilic monomer. The presence of TEGDMA as a diluent in commercial composites may increase water sorption (275). Hydroxyl groups within the matrix, for example in the Bis-GMA or HEMA and acidic group in 4-META, can also attract and form hydrogen bonds with water (276). Furthermore, water sorption is often correlated to degree of conversion of dental composites (153). Crosslinking associated with high monomer conversion is expected to reduce water sorption. Previous research about water sorption

found that composites based upon UDMA absorbed less water than those with Bis-GMA (156).

If the water only expands the polymer phase then the percentage of volume change should be comparable with the percentage of mass change multiplied by the sample density. Alternatively, if the water occupies pores then the mass increases but the volume remains unchanged. The ratio of maximum volume divided by mass change with control composites was less than commercial composites. This could be due to the lower density in control experimental formulation resulting from lower filler content. Additionally it could be the result of hand mixing experimental composite formulations (monomer with filler phase) and thereby creating pores within the sample. These air bubbles may fill with water, causing an increase in mass but not volume.

6.10.4. Biaxial flexural strength and modulus

Current commercial composites typically have flexural strengths between 100 and 180 MPa (277). Of the commercial dental materials in this thesis study, Z250 had the highest BFS (170 MPa), followed by Ecusphere (157 MPa) and Gradia (93 MPa). The higher strength for Z250 is in agreement with previous work (278-280). The filler phase of dental composites can have a significant effect on the strength of dental composites. The higher levels of inorganic filler and smaller filler particles size in Z250 contribute to the higher strength. Moreover, Z250 high strength could be the result of using a different filler, which in this case is a mixture of zirconium and silicon oxides instead of barium aluminosilicate as in Ecusphere and Gradia. (281).

The filler loading for Gradia is slightly lower than for Z250, while the biaxial flexural strength of Gradia is significantly lower. The particularly low BFS of Gradia is in agreement with previous work (280, 282). The lower strength of Gradia could be due to the addition of

pre-polymerised fillers, which disturbs the stress transfer from resin monomer to filler particles. The lower degree of conversion could have also contributed to the lower strength for Gradia dental composite (87, 266).

All the commercial dental composites exhibited decline in BFS (10 to 17 MPa) upon immersion in water for 24 h. This is presumably due to water sorption leading to polymer plasticisation. The slowing of further decline in mechanical properties after samples were stored for 7 days in water was presumably due to slowing of water sorption. The limited further deterioration in strength between 7 and 28 days of water immersion is likely due to water sorption reaching equilibrium. The present findings are consistent with previous studies (198, 227, 283).

Of the commercial dental materials Z250 had the highest modulus (4.9 GPa) followed by Ecusphere (4.7 GPa) and Gradia (3.3 GPa). These modulus values are comparable to that of dentine (5 to 10 MPa) and in agreement with those reported in previous studies (258, 280). All the commercial dental composites exhibited decline in modulus upon immersion in water for 24 h, and further decline after samples were stored for 7 days, due to expected with polymer plasticisation.

The BFS of control experimental formulations was comparable to that of Z250 and better than Ecusphere and Gradia. The experimental composite containing 4-META had an initial higher BFS (170 MPa) with a modulus of 5.4 GPa as compared with HEMA (163 MPa) and a modulus of 4.7 GPa.

The high BFS of control formulations could be explained by higher degree of conversions. Moreover, relatively low PLR (3:1) in the control experimental materials could improve physical micromechanical interlocking between monomer and filler phase. This will lead to materials with better strength due to improved filler impregnation (wetting) and reduce voids, which may enhance crack initiation at the surface of the filler. Moreover, good bonding

between the filler and matrix in control experimental formulations can increase mechanical properties by stress transfer between monomer and filler (128).

As with the commercial materials, at 24 h and 7days water immersion, the strength deteriorated. This could be due to water sorption leading to the plasticisation of the polymer network and possibly degradation of the bond between monomer and filler. There was no significant difference between the testing periods of 7 and 28 days possibly due to water sorption levels reaching equilibrium. Control experimental formulations with 4-META had the highest modulus (5.4 GPa), compared to HEMA (4.6 GPa) and commercial composites. The modulus decreased upon immersion in water after 24 h. Further decline was observed between 7 and 28 days. Decreasing the modulus enables increased resilience and energy absorption of the composites.

6.10.5. Push out test

6.10.5.1. Dry un-etched ivory

Many factors may affect the bond strength of composites to dentine. These include dentine composition, age, water content, tubule density and level of demineralisation by caries or acid treatment, remineralisation and smear layer removal (284). Unfortunately, the small size, limited availability, ethical issues and variability of human teeth are significant issues that make testing of the large number of variables very challenging (285). Alternative studies have used bovine dentine which partially addresses some of these problems, but again variability can be a concern (243, 286).

The use of a single ivory tusk, however, can help overcome variability and availability. Ivory dentine is similar to that of human dentine in that it contains collagen and hydroxyapatite in addition to tubules. It should be appreciated, however that with ivory dentine the hydroxyapatite content is only ~ 63 % compared with ~ 70 % in human dentine (287).

Additionally, the density of the tubules is lower in the ivory dentine (39). Despite these differences bond strengths of composites to moist ivory and human dentine have been comparable for a wide range of composites, adhesives and dentine pre-treatments (39). Therefore, in this thesis ivory dentine was used as a model substrate in push out and shears bond strength tests.

The average push out stress of commercial composites without acid etching was only ~ 16 MPa, presumably due to a lack of chemical or micromechanical bonding to ivory dentine. Commercial composites contain hydrophobic monomers and high levels of filler that reduce wetting and thereby bonding of composites to dentine.

The control experimental formulation with 4-META had a higher push out stress (29 MPa) as compared to control formulation with HEMA (19 MPa). 4-META has been reported to enable excellent bond strength to many substrates including dentine (288). This is because 4-META reacts with any surrounding water (e.g. from the atmosphere) to produce two carboxylic acid groups. These can demineralize the dentine and provide some micromechanical interlocking (247). 4-META also interacts electrostatically with the amino acid groups in the collagen (289).

6.10.5.2. Dry etched ivory

Upon acid etching of the dry ivory dentine, the above study showed the push out stress increased for the control and commercial composites. The results also showed that control formulations with 4-META displayed better bonding to acid etched ivory dentine than the HEMA control composite and commercial materials. This is due to the 37 % phosphoric acid gel demineralising and dissolving the collagen and exposing the dentinal tubules, thus allowing more penetration of composites into the demineralized dentine surface (46). Etching human dentine with phosphoric acid for 20 s has been shown to demineralise from 2 to 55 μm depth in carious dentine, basically depending on the etching time and concentration of the

acid. However, this depth could be doubled if the dentine has caries (290). Previous studies showed that 20 s etched human and ivory dentine are both good models for caries dentine (39). Acid-etching will also enable enhanced the surface area for greater interaction between dentine and 4-META. It may also leave residual water for enhanced 4-META hydrolysis.

6.10.5.3. Wet ivory dentine

With controlled hydration of ivory samples the bonding stress of commercial composites increased by 1.7 and 1.9 times with and without acid etching respectively. The reason for this is currently unclear but may be a consequence of removal of surface debris and/or some expansion of ivory structure due to water sorption. This result does show, however, how crucial the condition of the dentine is in bond testing. During early studies for this thesis this issue caused considerable complications making study reproducibility initially very hard. This problem was alleviated by use of ivory with controlled hydration and dehydration.

Bond strength also increased by 2.2 and 1.9 times with control experimental formulations with and without acid etching respectively. In this case the enhanced presence of water in wet ivory dentine could increase the 4-META hydrolysis. This is known to provide two carboxylic acid groups attached to the aromatic ring, resulting in a low pH (76). This enables the demineralisation of the dentine to allow some micromechanical interlocking. In addition, it is believed that 4-META might bond with basic amino acid groups in the collagen (ionic bond), and may also interact with calcium in hydroxyapatite (291). Moreover, the hydrophilicity of HEMA improves wetting properties of dental adhesives and the penetration efficacy of the adhesive into water-containing demineralized tooth structure (107, 108).

6.10.5.4. Push out stress with self-adhesive Ibond

Using the self-adhesive Ibond significantly increased the push out stress for all control and commercial composites, compared to etched and non-etched wet and dry ivory dentine

(Figure 6-13). Ibond contains solvent and low viscosity hydrophilic monomers that help adhesive infiltration into collagen and dentinal tubules. Furthermore, it contains 4-META (292, 293) to aid bonding to dentine through the mechanisms discussed above (247).

Z250 had Gradia had the lowest bond strengths with Ibond. The control formulation with 4-META had once again the highest push out stress (207 MPa), followed by Ecusphere and control formulation with HEMA. Lowering the viscosity of controlled experimental formulations by decreasing the PLR 3:1 would have enabled better penetration and bonding than found in commercial composites. The higher polymerisation shrinkage of the experimental formulations, however, clearly was insufficient to negate this benefit. Furthermore, Ibond contains UDMA monomer (292, 293). It may therefore intermix better with experimental formulations and Ecusphere, which contain the same base monomer than with the Bis-GMA based Z250 or Gradia, where some of the monomer is pre-polymerised.

6.10.6. Shear bond strength

Although, there has been much criticism of the reproducibility of the shear bond test, it is still commonly used for dentine adhesion studies (294). The shear strength is calculated by dividing the maximum applied force by the bonded cross-sectional area (295, 296). This measurement provides information about the adhesive behaviour of different types of materials and can be considered as a screening test (239). The shear bond strength can, however, depend on the dimensions of the samples tested along with the speed of stress loading. This can make shear bond strengths resulting from different research groups difficult to compare (297). Moreover, as shown in this thesis, the exact state of the dentine is also crucial and must be carefully controlled.

6.10.6.1. Shear bond test with wet ivory dentine

In this thesis study, the commercial dental composites demonstrated very low bond strength to non-etched and etched ivory dentine, compared to control experimental formulations. These results are similar to, but more pronounced, than those observed with the push out results in this thesis. The particularly high bond strength with experimental materials could in part be a consequence of their higher fluidity, which in turn results from their lower powder content. In contrast to the push out test, this benefit would be counteracted less in the shear bond test by the concomitant increase in shrinkage. These studies are supported by those of Liaquat et al, who reported that the shear bond strength achieved with Z250 and Gradia to both ivory and human dentine was low compared to flowable composites (39). The reported bond strength of 4 MPa, with etched ivory dentine and conventional composites was similar to this study (39).

This thesis found that the control experimental formulation with 4-META significantly increased the ivory dentine bond strength, compared to the control formulation with HEMA. The hydrophilicity of HEMA was also shown to improve the bonding to dentine by increasing the wetting and penetration into the dentine surface. This result was agreement with a previous result (39). An increase in average bond strength upon acid etching was also consistent with previous work (298).

6.10.6.2. Shear bond test with self-adhesive Ibond

Applying the self-adhesive Ibond significantly increased the shear bond strength for control and commercial composites, as expected from the literatures (299). As discussed, Ibond enables greater penetration of composites into dentinal tubules and enhances the mechanical interlock between adhesive agent and dentine (291). In comparison with the push out test, the benefit of 4-META, HEMA and enhanced fluidity arising from lower powder content was

more pronounced with the shear bond method. As discussed above this could be a consequence of the composite shrinkage being less important in the shear test.

7. Experimental formulations with 4-META or HEMA, CHX, glass fibre and different levels of CaP.

7.1. Introduction

In the following chapter, the results for experimental composite formulations containing UDMA: PPGDMA: (4-META or HEMA): CQ: NTGGMA was 68:25:5:1:1 by weight as in the previous chapter are discussed. The choice of TCP particle size and feasible range of CaP were addressed in preliminary studies provided in appendix 1. Calcium phosphate (CaP, MCPM: β -TCP at 1:1 weight ratio) (0, 10, 20 or 40 wt %), chlorhexidine diacetate (CHX 5 wt %) and glass fibre (5 wt %) were added in the filler phase. The powder to liquid ratio was 3:1 by weight.

A range of chemical and mechanical properties of experimental formulations were carried out on 8 experimental formulations (4 CaP levels and 2 adhesive monomers). The properties evaluated are the same as the ones used in the previous chapter in addition to the chlorhexidine release as in the previous chapter. In all figures results the control formulations from the previous chapter are provided to enable clear observation of any effect of adding CHX and glass fibre.

7.2. FTIR spectra for experimental formulations

An example FTIR spectra for experimental formulations containing adhesive monomer (4-META or HEMA), 20 wt % CaP and 5 wt % CHX before and after curing for 40 s are shown in Figure 7-1 (a & b). With all formulations the spectra have strong monomer peaks at 1716 cm^{-1} (C=O stretch). Peaks at 1638 cm^{-1} and 1530 cm^{-1} are due to C=C stretch and N-H deformation. Further peaks are observed at 1458 cm^{-1} due to the aliphatic C-H vibration, 1298 and 1320 cm^{-1} associated with a C-O stretch and 1164 cm^{-1} due to a C-O-C asymmetric stretch. The spectra also exhibit P-O stretch peaks at 1048/940 cm^{-1} due to β -TCP and MCPM respectively. The chlorhexidine level is too low to detect. Upon polymerisation, there was a decrease in the intensity of C=C peak (1638 cm^{-1}) and C-O peaks (1298 and 1320 cm^{-1}). All these changes in the FTIR spectra are representative of methacrylate monomer conversion.

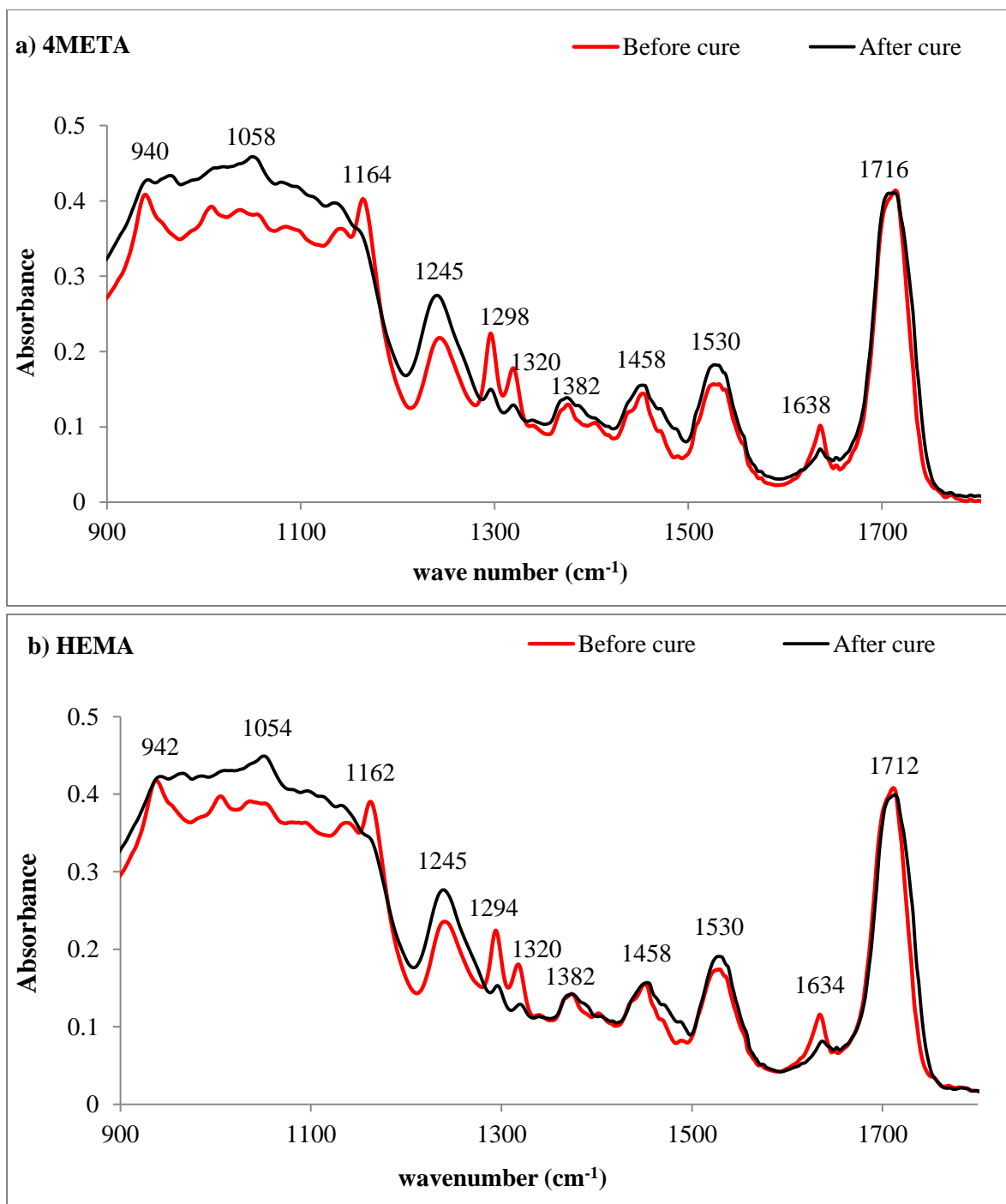


Figure 7-1: Representative FTIR spectra of experimental formulations containing adhesive monomer a) 4-META and b) HEMA before and after curing for 40 s. The specific examples have PLR 3:1, 20 wt % CaP and 5 wt % CHX and fibre.

7.3. Degree of monomer conversion

7.3.1. Experimental formulations with 4-META

The degree of conversion for 4-META experimental formulations and different levels of CaP after curing for 40 s is represented in Figure 7-2. From the figure below it can be seen that the average conversion was 76 % for 4-META formulations. Furthermore, effect of CHX and fibre addition was negligible and there was no systematic trend upon increasing CaP concentration from 0 to 40 wt %.

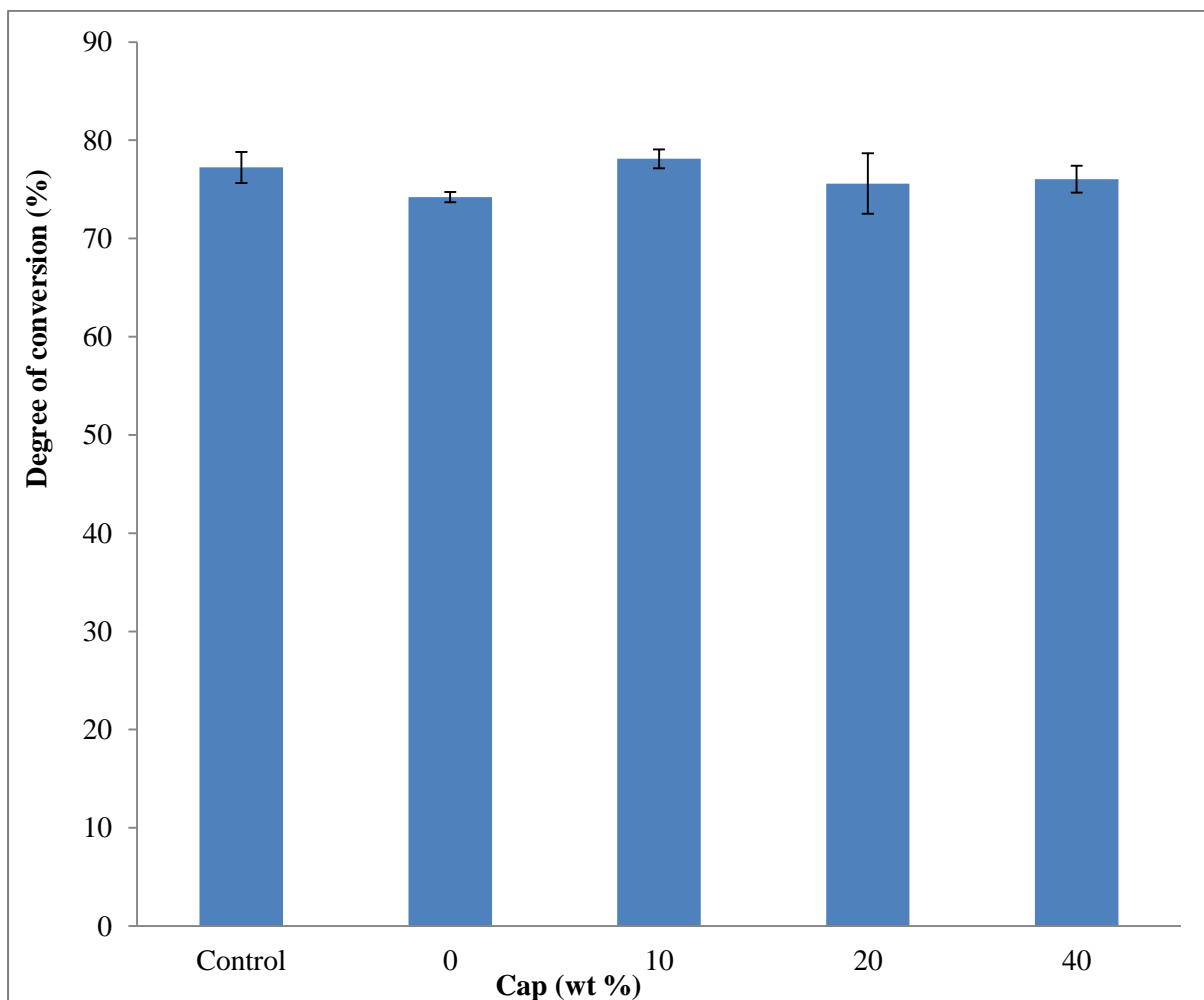


Figure 7-2: Degree of conversion for 4-META formulations with CaP (0, 10, 20 and 40 wt %), 5 wt % CHX and fibre, in addition of control formulation after curing for 40 s. The error bars represent 95% C.I of the mean (n=5).

The analysis of variance (ANOVA) concluded that there was sufficient evidence to reject the null hypothesis that the mean conversion in the 4-META formulations with different levels of CaP was the same ($P < 0.001$). The post-hoc Bonferroni multiple comparisons showed that the only pairs of formulations with a significant difference were those with 0 and 10 wt % CaP ($P < 0.001$).

7.3.2. Experimental formulations with HEMA

The average degree of conversion for HEMA formulations containing control CHX and fibre and different CaP levels was comparable to that for 4-META formulations at 75 % (Figure 7-3).

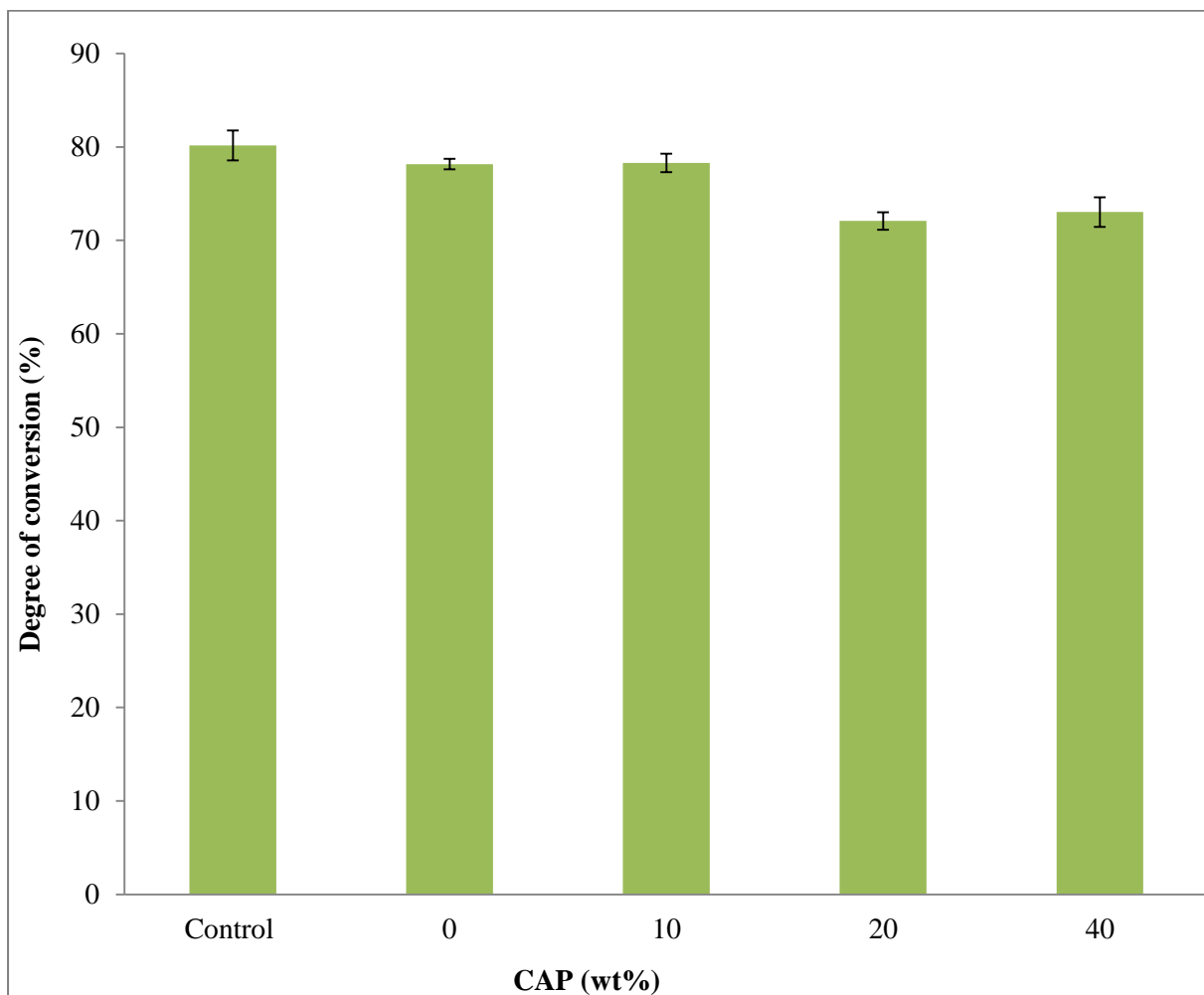


Figure 7-3: Degree of conversion for HEMA formulations with CaP (0, 10, 20 and 40 wt %), 5 wt % CHX and fibre in addition of control formulation after curing for 40 s. The error bars indicate 95 % C.I. of the mean (n=5).

Control formulation, 0 and 10 wt % CaP containing formulations had a higher conversion than formulations with 20 and 40 wt % CaP. Overall, the effect of CaP was too small to fit a trend line. The analysis of variance (ANOVA), however, confirmed that there was sufficient evidence to reject the null hypothesis that the mean degree of conversion for the HEMA formulations with different levels of CaP was the same ($P < 0.0001$). The post-hoc Bonferroni multiple comparisons showed that the only formulations with no significant differences were 0 and 10 wt % ($P > 0.999$) or 20 and 40 wt % CaP ($P > 0.05$). The average result with 10 and 0 wt % CaP was 78 % and was 73% for 20 and 40 wt %.

7.4. Polymerisation shrinkage

7.4.1. Experimental formulations with 4-META

As the shrinkage is directly proportional to the polymerisation level the same statistical analysis applies for each set of data. Figure 7-4 shows that the mean calculated polymerisation shrinkage for 4-META formulations and different levels of CaP (0, 10, 20 and 40 wt %) was 3.4 vol %. The shrinkage of experimental formulations was calculated to be 3.4, 3.6 and 3.5 vol % with an average conversion of 74, 78 and 76 % respectively. The figure shows CHX and fibre addition has negligible effect as compared to control formulation and no consistent trend for polymerisation shrinkage versus increasing CaP concentration.

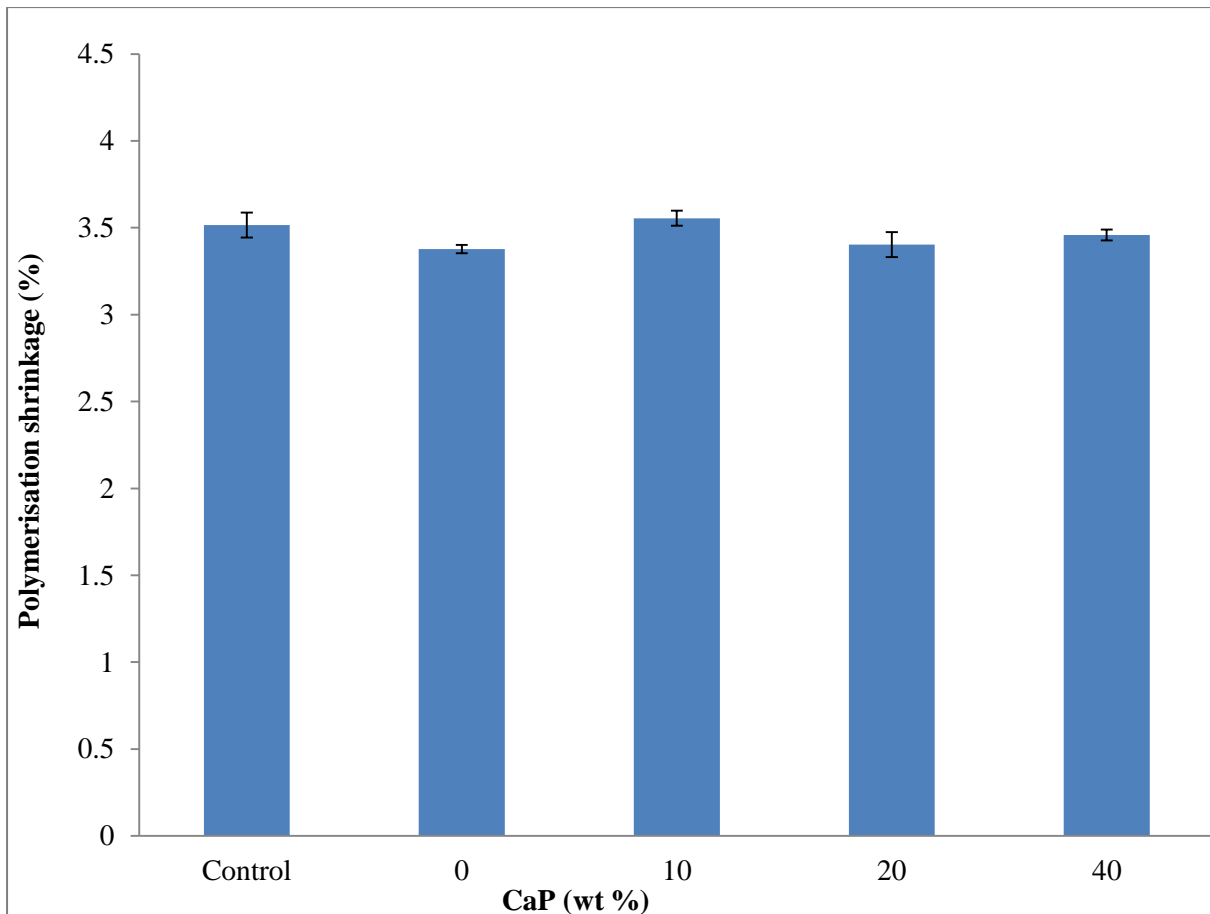


Figure 7-4: Polymerisation shrinkage for 4-META formulations with CaP (0, 10, 20 and 40 wt %), 5 wt % CHX and fibre in addition of control formulation after curing for 40 s. The error bars represent 95 % C.I of the mean (n=5).

7.4.2. Experimental formulations with HEMA

As the shrinkage is directly proportional to the polymerisation level the same statistical analysis applies for each set of data. The average polymerisation shrinkage for experimental composite formulations containing HEMA and different CaP concentration is 3.6 vol % as shown in Figure 7-5. CHX and fibre addition was again negligible. Experimental formulation shrinkage was calculated to be 3.8 and 3.5 vol % with an average conversion of 78 and 73 % observed with the lower and higher levels of CaP respectively.

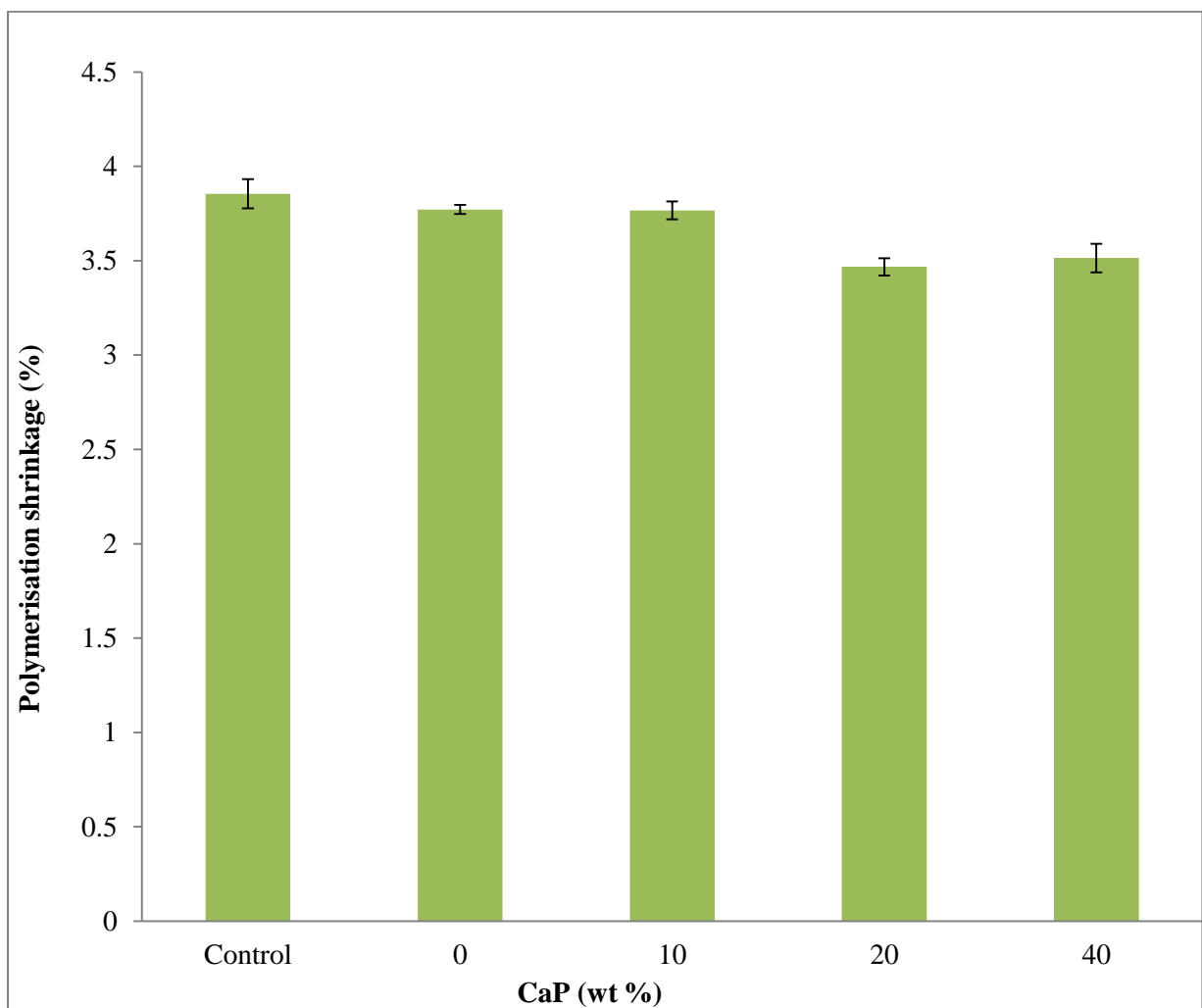


Figure 7-5: Polymerisation shrinkage for HEMA formulations with CaP (0, 10, 20 and 40 wt %), 5 wt % CHX and glass fibre in addition of control formulation after curing for 40 s. The error bars represent 95 % C.I of the mean (n=5).

7.5. Depth of cure

7.5.1. Experimental formulations with 4-META

The average ISO depth of cure for 4-META formulations with different levels of CaP after 20 and 40 s light exposure is provided in Figure 7-6. It can be seen from the figure below that all experimental formulations meet the ISO standard depth of cure of at least 1.5 mm at either cure time. The depth of cure decreased linearly with increasing CaP. Moreover, the depth of cure measurement was higher at 40 s as compared to 20 s cure. The two formulations with 0 wt % CaP and control had comparable average depth of cure of 2.8 mm. The experimental formulations with 40 wt % CaP had lowest depth of cure of 2.1 ± 0.02 and 1.9 ± 0.01 mm after curing for 40 and 20 s respectively.

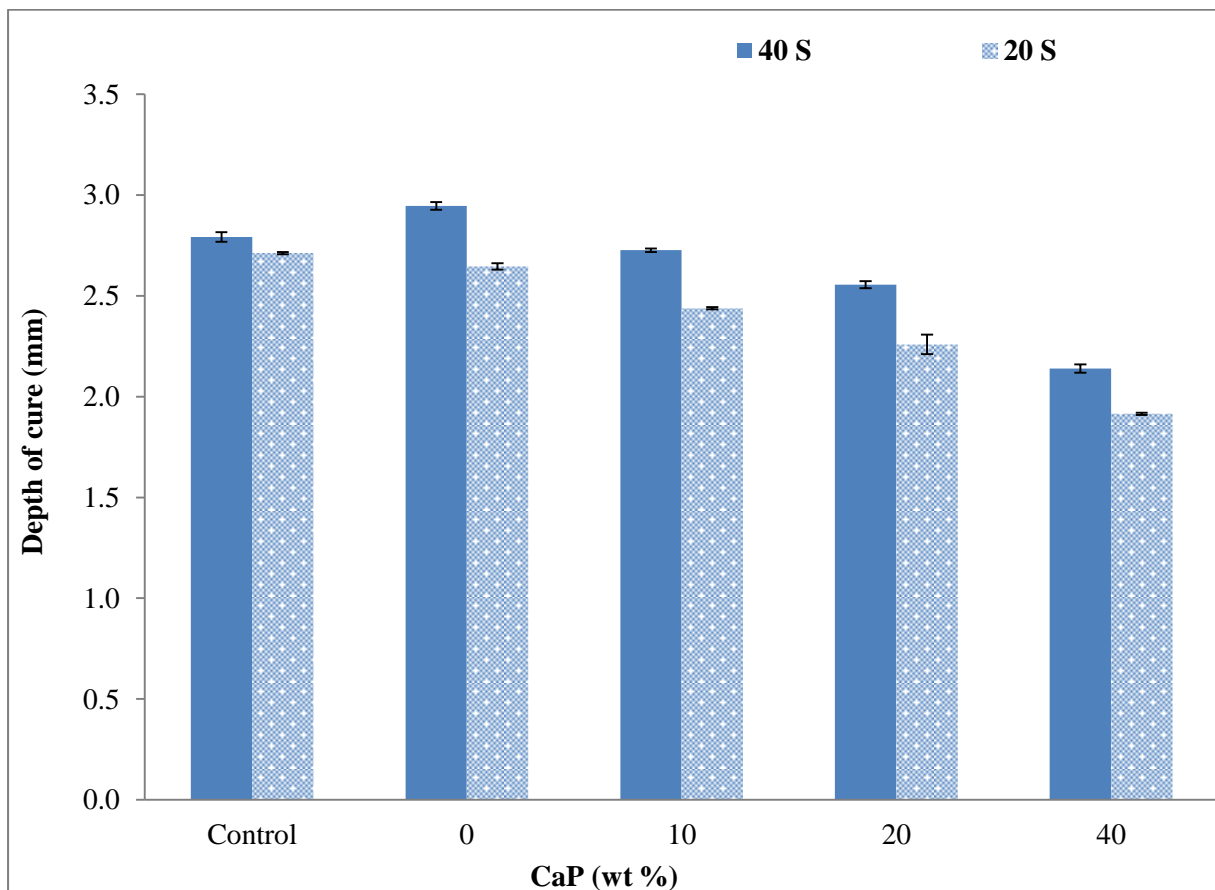


Figure 7-6: Depth of cure for 4-META formulations with CaP (0, 10, 20 and 40 wt %), 5 wt % CHX and fibre in addition of control formulation after curing for 20 and 40 s. The errors indicate 95% C.I of the mean (n=3).

Linear regression analysis of the depth of cure versus CaP was obtained using a Linest analysis; it gave high R^2 values and errors on the gradient and intercepts of ~ 10 and < 1 % respectively (see Table 7-1 below). On average the depth of cure increased by 11 % (0.31/2.9) upon increasing cure time from 20 to 40 s.

Table 7-1 : Depth of cure for 4-META formulations with CaP (0, 10, 20 and 40 wt %) and CHX after curing time of 20 and 40 s from the up surface. The lower section gives linear regression analysis with gradient, intercept and R^2 values for average depth of cure versus Cap wt %.

CaP (wt %)	Depth of cure (mm)	
	Curing for 20 s	Curing for 40 s
0	2.65 \pm 0.02	2.95 \pm 0.02
10	2.44 \pm 0.01	2.73 \pm 0.01
20	2.26 \pm 0.05	2.55 \pm 0.02
40	1.91 \pm 0.01	2.14 \pm 0.02

Linear Regression of Cure depth versus CaP% (n=3)

	Curing for 20 s	Curing for 40 s
Gradient (mm / wt %)	-0.018 \pm 0.001	-0.020 \pm 0.002
Intercept (mm)	2.63 \pm 0.01	2.94 \pm 0.01
R^2	0.99	0.99

An analysis of variance (ANOVA) confirmed that there was sufficient evidence to reject the null hypothesis that the mean depth of cure in 4-META formulations with different levels of CaP after curing for 20 and 40 s were the same ($P < 0.0001$). Multiple post-hoc Bonferroni comparisons showed that there were significant statistical differences between 4-META formulations with all different levels of CaP ($P < 0.05$). The depth of cure was also increased significantly by increasing the time of exposure from 20 to 40 s ($P < 0.0001$).

7.5.2. Experimental formulations with HEMA

Figure 7-7 shows that average depth of cure for HEMA formulations with different levels of CaP (0, 10, 20 and 40 wt %) after 20 and 40 s light exposure. It can be seen that all experimental HEMA containing formulations also meet the ISO standard requirement of a depth of cure of at least 1.5 mm. Addition of CHX and fibre caused a minor decrease in depth of cure as compared to control formulation. Increasing CaP from low to high caused a linear decline in the depth of cure. Furthermore, the depth of cure also increased with 40 s as compared to 20 s cure. The formulation with 0 wt % had 2.7 and 2.4 mm cure depth after curing for 40 and 20 s, respectively. With 40 wt % CaP these declined to 2.1 and 1.9 mm.

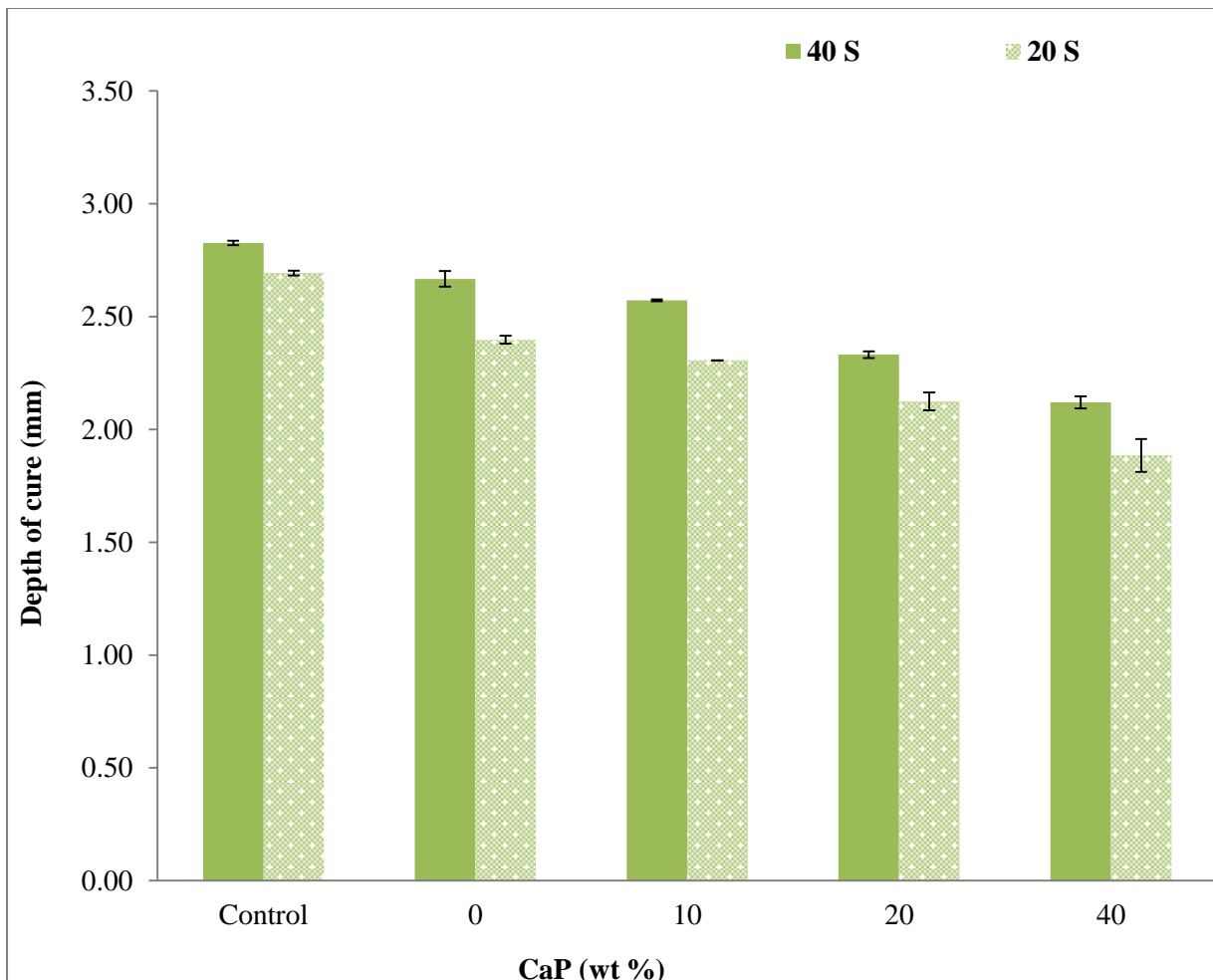


Figure 7-7: Depth of cure for HEMA formulations with CaP (0, 10, 20 and 40 % wt) and CHX and fibre at 5 wt % and control formulation after cured for 20 or 40 s. The error bars indicate 95% C.I of the mean (n=3).

Linest analysis is provided in Table 7-2 below. Data from this table shows that high R^2 values and small errors on the gradient and intercepts of depth of cure versus CaP concentration. Moreover, the depth of cure was increased by 7 % with increasing time of exposure from 20 to 40 s irrespective of the CaP concentrations.

Table 7-2 : Depth of cure for HEMA formulations with CaP (0, 10, 20 and 40 wt %) and CHX after curing time of 20 and 40 s from the up surface. The lower section gives linear regression analysis with gradient, intercept and R^2 values for average depth of cure versus CaP wt %.

CaP (wt %)	Depth of cure (mm)	
	Curing for 20 s	Curing for 40 s
0	2.40 ± 0.02	2.67 ± 0.03
10	2.31 ± 0.00	2.57 ± 0.00
20	2.12 ± 0.04	2.38 ± 0.01
40	1.89 ± 0.07	2.12 ± 0.03

Linear Regression of Cure depth versus CaP% (n=3)		
	Curing for 20 s	Curing for 40 s
Gradient (mm/ wt %)	-0.013 ± 0.001	-0.015 ± 0.004
Intercept (mm)	2.41 ± 0.01	2.68 ± 0.02
R^2	0.99	0.99

An analysis of variance (ANOVA) confirmed that there was sufficient evidence to reject the null hypothesis that the mean depth of cure in HEMA formulations with different levels of CaP after curing for 20 and 40 s were the same ($P < 0.001$). Multiple post- hoc comparisons confirmed significant effects of CaP and time ($P < 0.05$).

7.6. Mass and volume change

7.6.1. Experimental formulations 4-META

The average mass and volume change for all 4-META formulations over a period of 5 months versus the square root (SQRT) of time are shown in Figure 7-8 (a & b). Initially, these plots increased linearly for a time period of up to 6 h with 0 and 10 wt % CaP or 24 h with 20 and 40 wt % CaP ($R^2 > 0.98$). Gradients are provided in Table 7.3. These ranged from 0.003 to 0.6 wt % $\text{hr}^{-0.5}$ for mass changes and from 0.09 to 1.69 vol % $\text{hr}^{-0.5}$ for volume changes.

All formulations had reached a maximum stable change by the time one month. The formulation with 40 wt % CaP had the highest final mass and volume change of 3.8 wt % and 5 vol % increase respectively followed by formulations with 20, 10 and then 0 wt % CaP. The formulation with 0 wt % CaP, CHX and fibres had mass and volume change of 1.2 wt % and 1.5 vol % respectively. This was only slightly higher than observed for the control without CHX and fibres.

Table 7-3 provides a linear regression of the initial gradients and maximum changes in mass and volume change for 4-META formulations. Both increased linearly with CaP level (see Linest analysis in Table 7-3). The early volume change was ~1.5 times (0.0048/0.0032) higher than that for mass, irrespective of CaP content. The maximum volume change was ~1.3 times higher than mass regardless of CaP content. The early change divided by final values was given by equation below:

$$\frac{\Delta M_t}{\Delta M_{t \rightarrow \infty}} = \frac{0.0032}{0.06} \left(\frac{t}{\text{hr}} \right)^{0.5} \quad \text{Equation 7-1}$$

$$\frac{\Delta V_t}{\Delta V_{t \rightarrow \infty}} = \frac{0.0048}{0.08} \left(\frac{t}{\text{hr}} \right)^{0.5} \quad \text{Equation 7-2}$$

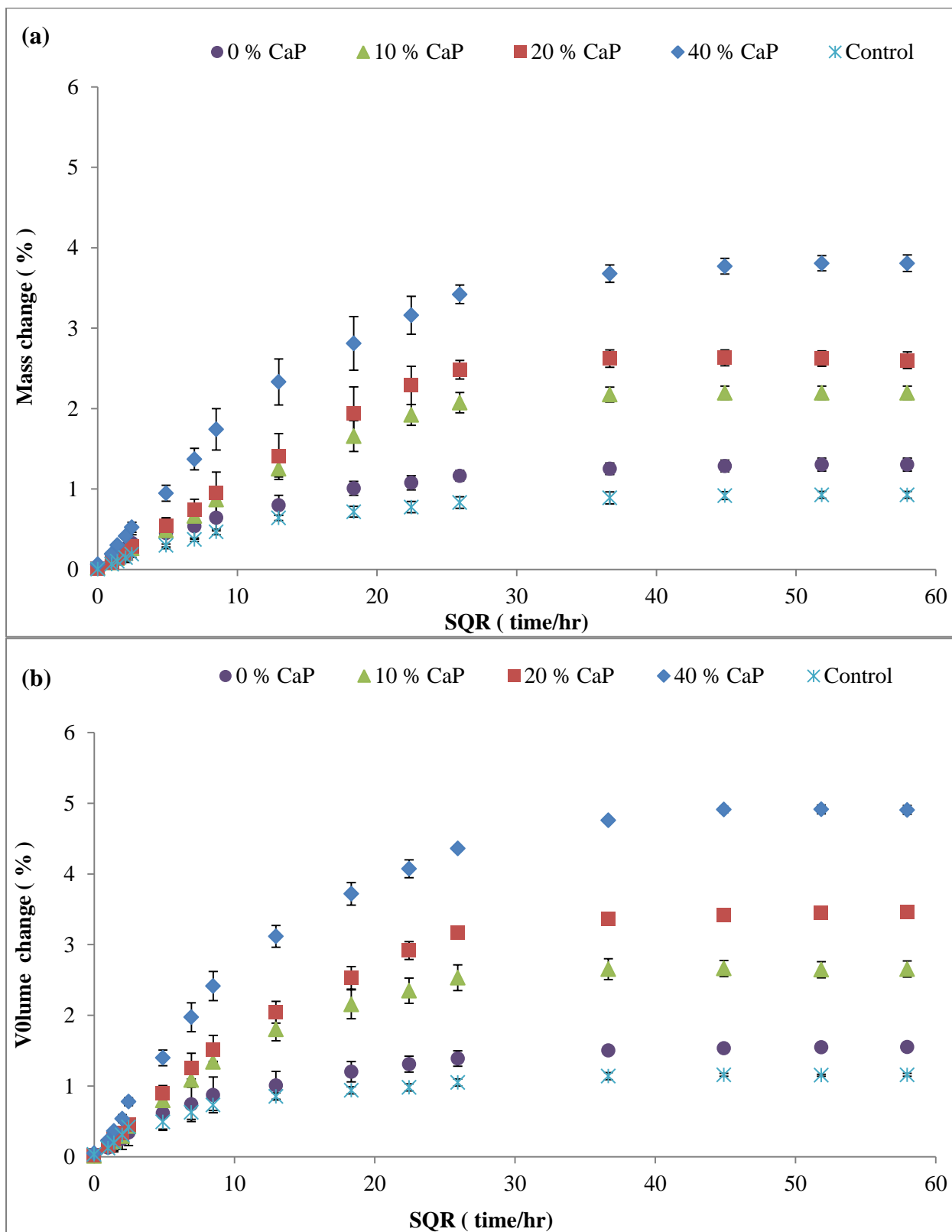


Figure 7-8 (a) and (b): Mass and volume change in deionised water for 4-META formulations with different CaP level (0, 10, 20, and 40 % wt), 5 wt % CHX and control experimental formulation. Error bars give 95 % C.I of the mean (n=3).

Table 7-3: Initial gradient of mass and volume change vs SQRT time and maximum mass & volume increase and linear regression analysis of the results versus CaP wt % for 4-META formulations with CaP (0, 10, 20 and 40 wt %) and CHX.

CaP (wt %)	Initial gradient of mass vs SQRT time (wt % / hr ^{0.5})	Max. mass increase (wt %)	Initial gradient of volume vs SQRT time (vol %/ hr ^{0.5})	Max. volume increase (vol %)
0	0.070 ± 0.01	1.30 ± 0.08	0.08 ± 0.05	1.55 ± 0.03
10	0.09 ± 0.01	2.20 ± 0.08	0.157 ± 0.002	2.65 ± 0.11
20	0.11 ± 0.03	2.61 ± 0.08	0.15 ± 0.03	3.44 ± 0.05
40	0.20 ± 0.03	3.79 ± 0.14	0.28 ± 0.03	4.91 ± 0.10

Linear Regression of mass and volume change versus CaP % (n=3)

Gradient of column vs CaP (column unit / wt % CaP)	0.0032 ± 0.0005	0.060 ± 0.005	0.0048 ± 0.0005	0.082 ± 0.006
Intercept (wt %)	0.063 ± 0.0107	1.42 ± 0.12	0.09 ± 0.01	1.69 ± 0.13
R²	0.96	0.98	0.98	0.99

The analysis of variance (ANOVA) showed that there was sufficient evidence to reject the null hypothesis that the mean 24 h and maximum mass and volume change in experimental composites with 4-META and different CaP levels was the same ($P < 0.001$). Post-hoc multiple comparisons for 24 h mass and volume change showed that there were significant statistical difference between formulations with 40 and 0 wt % CaP and between 40 and 10 wt % CaP ($P < 0.05$). The maximum mass and volume change results showed that there were significant statistical differences between formulations with 0 and 20 wt % CaP and between 0 and 40 wt % CaP as well as between 10 and 40 wt % CaP ($P < 0.05$).

7.6.2. Experimental formulations with HEMA

The average mass and volume change for all HEMA formulations over a period of 5 months versus the square root (SQRT) of time are plotted in Figure 7-9 (a & b). Initially, these plots increased linearly up to 6 h with 0 and 10 wt % CaP or 24 h with 20 and 40 wt % CaP ($R^2 > 0.99$). Gradients are provided in Table 7.3. These ranged from 0.006 to 0.11 wt % hr^{-0.5} for mass changes and from 0.0089 to 1.45 vol % hr^{-0.5} for volume changes.

All HEMA formulations had reached a maximum stable change by one month. The formulation with 40 wt % CaP underwent the greatest mass and volume change of 5.5 wt % and 7.3 vol % increase respectively followed by formulations with 20, 10 and 0 wt % CaP. The control and 0 wt % formulations had the lowest mass and volume change of 1.1 wt % and 1.5 vol % respectively.

Linear regression of the initial gradients and maximum increase in mass and volume for HEMA formulations are provided in Table 7-4. The initial and maximum mass and volume changes increased linearly with increased CaP levels. The early (24 h) volume change was ~ 1.5 times (0.0089/0.006) higher than that for mass, irrespective of CaP levels. Mass and volume change increased linearly with increasing CaP level, giving high R^2 values and small errors on the gradients and intercepts upon linear regression analysis (see Linest analysis in Table 7-4). The maximum volume change was 1.3 times higher than mass regardless of CaP content. The early change divided by final values was given by the equations below:

$$\frac{\Delta M_t}{\Delta M_{t \rightarrow \infty}} = \frac{0.006}{0.11} \left(\frac{t}{hr} \right)^{0.5} \quad \text{Equation 7-3}$$

$$\frac{\Delta V_t}{\Delta V_{t \rightarrow \infty}} = \frac{0.009}{0.15} \left(\frac{t}{hr} \right)^{0.5} \quad \text{Equation 7-4}$$

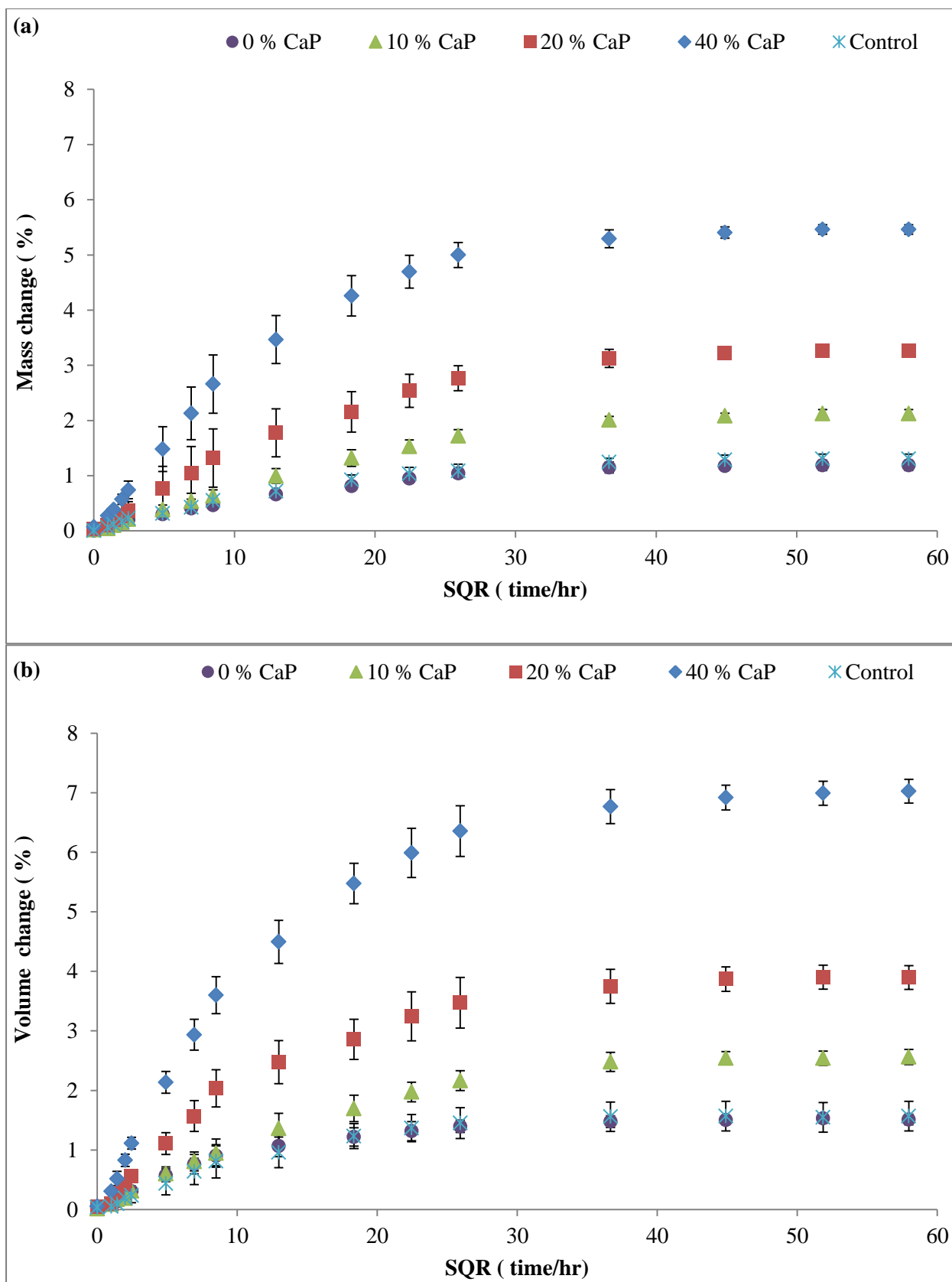


Figure 7-9: (a) and (b): Mass and volume change in deionised water for HEMA formulations with 5 wt % CHX and fibre, CaP (0, 10, 20, and 40 wt %) in addition of control experimental formulation. Error bars indicate 95 % C.I of the mean (n=3).

Table 7-4 : Initial gradient mass and volume change vs SQRT time and maximum mass and volume increase and linear regression analysis of the results versus CaP wt % for HEMA formulations with CaP (0, 10, 20 and 40 wt %) and CHX.

CaP (wt %)	Initial mass gradient vs SQRT time(wt%/ hr ^{0.5})	Max. mass increase (wt %)	Initial volume gradient vs SQRT time(vol %/ hr ^{0.5})	Max. volume increase (vol %)
0	0.069 ± 0.005	1.184 ± 0.068	0.088 ± 0.016	1.51 ± 0.09
10	0.079 ± 0.012	2.12 ± 0.07	0.120 ± 0.021	2.53 ± 0.13
20	0.153 ± 0.077	3.26 ± 0.07	0.227 ± 0.043	3.87 ± 0.25
40	0.295 ± 0.056	5.46 ± 0.12	0.429 ± 0.045	7.25 ± 0.51

Linear Regression of mass and volume change versus CaP % (n=3)

Gradient of column vs CaP (column unit / wt % CaP)	0.006 ± 0.001	0.107 ± 0.002	0.0089 ± 0.0010	0.145 ± 0.011
Intercept	0.045 ± 0.021	1.118 ± 0.057	0.06 ± 0.02	1.24 ± 0.25
R ²	0.95	0.99	0.97	0.98

The analysis of variance (ANOVA) showed that there was sufficient evidence to reject the null hypothesis that the mean initial (24 h) and maximum mass and volume change in experimental composites with HEMA and CaP was the same ($P < 0.0001$). Post-hoc Bonferroni multiple comparisons showed, that for the initial mass and volume change up to 24 h, there was significant statistical difference between formulations with 0 and 40 wt % CaP and between 10 and 40 wt % CaP as well as between 40 and 20 wt % CaP ($P < 0.001$) but not 0 and 10 wt % CaP ($P > 0.05$). The maximum mass and volume change results show that there were significant statistical differences between formulations at all CaP levels ($P = < 0.0001$).

7.7. Chlorhexidine release

7.7.1. Experimental formulations with 4-META

The average chlorhexidine (CHX) release for 4-META formulations with 0, 10, 20, 40 wt % CaP, and 5 wt % CHX over a period of 16 weeks immersion in deionised water versus the square root (SQRT) of time are shown in Figure 7-10. Initially, these plots increased linearly for all formulations. Experimental formulations with 0 and 10 wt % CaP approached their maximum release after 3 and 6 weeks respectively. Those formulations with 20 and 40 wt % CaP continued to release CHX for up to 11 and 15 weeks respectively. The formulation with 40 wt % CaP exhibited highest maximum CHX release of $11 \% \pm 0.69$. Formulations with 20 and 10 wt % CaP had a maximum release of $5 \% \pm 0.18$ and $2.5 \% \pm 0.69 \%$ respectively. The formulation with 0 wt % CaP had the lowest maximum CHX release of $1.1 \% \pm 0.11$.

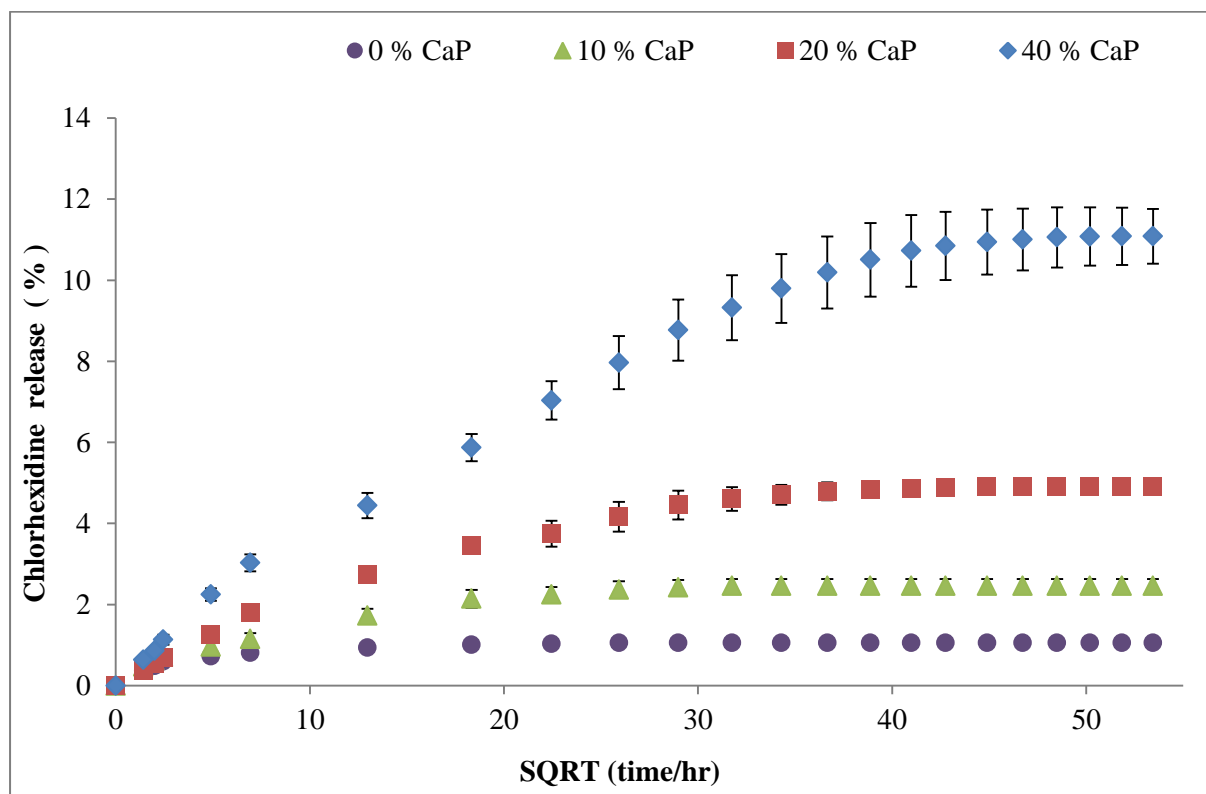


Figure 7-10: Chlorhexidine release into deionised water as a function of square root (SQRT) of time for 4-META formulations with CaP (0, 10, 20 and 40 wt %) and 5 wt % CHX. The error bars indicate 95% C.I of the mean (n=3).

Table 7-5 provides linear regression of the initial gradients and total CHX release for 4-META formulations versus CaP level. The high R^2 values and relatively small errors on gradients and intercepts obtained by linear regression shows that a linear equation describes the data well (see Linest analysis in Table 7-5).

Table 7-5: Initial gradient of CHX release versus SQRT time and total CHX release for 4-META formulations with different level of CaP (0, 10, 20 and 40 wt %) and 5 wt % CHX with linear regression results versus Ca P wt %.

CaP (wt %)	Initial gradient of CHX release vs SQRT time (wt%/hr ^{0.5})	Total CHX release (wt %)
0	0.10 ± 0.01	1.06 ± 0.11
10	0.19 ± 0.01	2.46 ± 0.17
20	0.237 ± 0.004	4.90 ± 0.18
40	0.33 ± 0.02	11.5 ± 0.69

Linear Regression of chlorhexidine release versus CaP% (n=3)

Gradient of column vs CaP (column unit / wt % CaP)	0.0054 ± 0.0006	0.27 ± 0.03
Intercept	0.120 ± 0.014	0.30 ± 0.07
R^2	0.97	0.97

The ANOVA showed that there was sufficient evidence to reject the null hypothesis that the mean of early and maximum CHX release in 4-META composites with different levels of CaP was the same ($P < 0.0001$). Post- hoc Bonferroni multiple comparisons for initial CHX release up to 24 h showed that there was significant statistical difference between 4-META formulations and all different levels of CaP ($P < 0.05$), except formulations with CaP levels of 0 and 10 wt % ($P = 0.249$). For the maximum CHX release, the post-hoc multiple comparisons result revealed that there were significant statistical differences between all different CaP levels ($P = < 0.001$).

7.7.2. Experimental formulations with HEMA

Figure 7-11 provides the average CHX release from HEMA formulations with CaP (0, 10, 20 and 40 wt %) and 5 wt % CHX immersed in deionised water over a period of 16 weeks plotted versus the SQRT of time. Initially, these plots increased linearly with the SQRT of time and formulations with 0 and 10 wt % CaP approached their maximum release after 3 and 7 weeks. Those with 20 and 40 wt % CaP continued to release for 13 and 16 weeks respectively. Formulation with 40 wt % CaP showed highest CHX release of 17 % \pm 0.3 followed by formulations with 20 and 10 wt % CaP with 6 % \pm 0.13 and 2.6 % \pm 0.03 respectively. The formulation with 0 wt % CaP had the lowest maximum CHX release of only 1.5 % \pm 0.03.

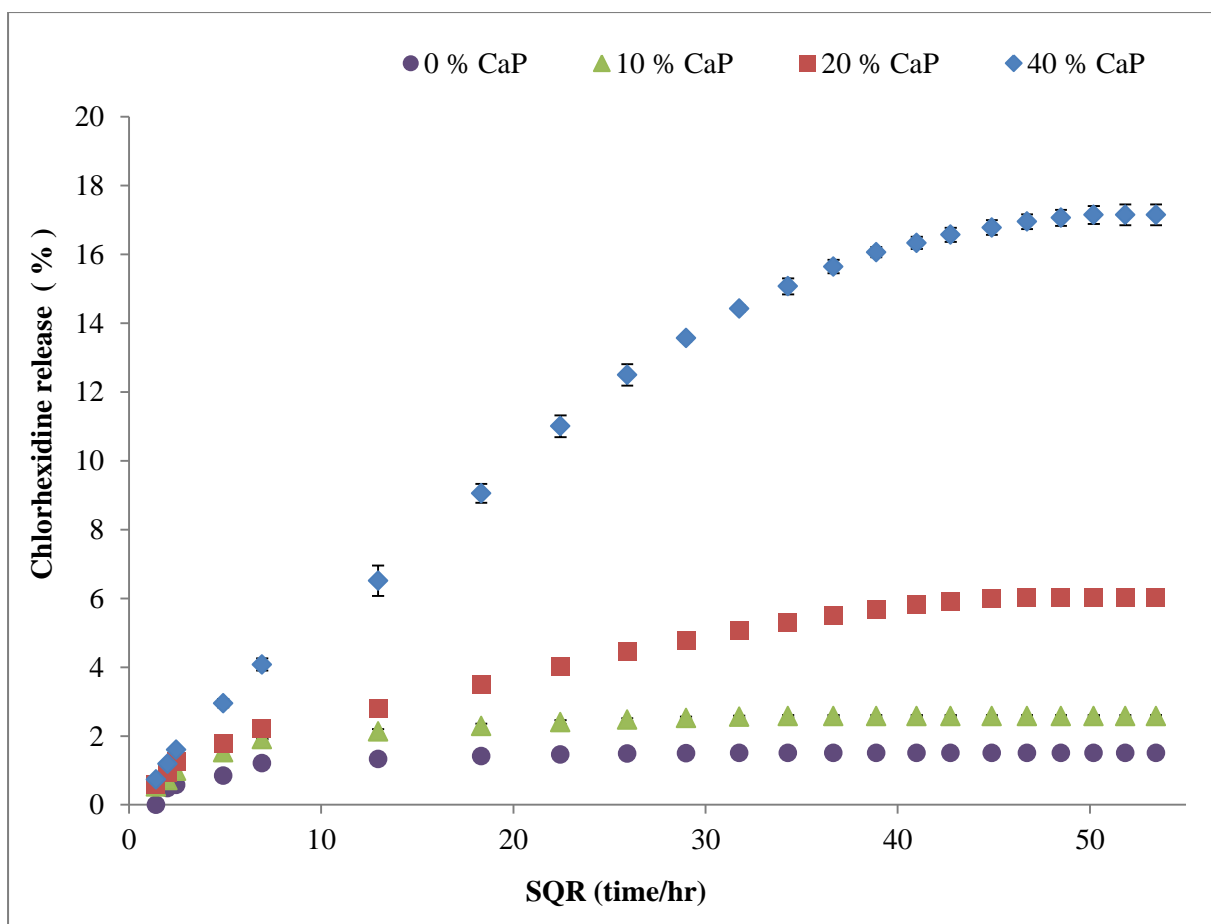


Figure 7-11: Chlorhexidine release into deionised water as a function of square root (SQRT) of time for HEMA formulations with CaP (0, 10, 20 and 40 wt %) and 5 wt % CHX. Error bars indicate 95% C.I of the mean (n=3).

Table 7-6 presents the initial gradients and maximum CHX release. High R^2 values, small errors on gradients and intercepts are observed. In the early CHX release obtained by linear regression shows that these gradients increase linearly with CaP level. The low R^2 values 0.94 and large standard error on intercepts on maximum release obtained by linear regression shows less effect of CaP level on final CHX release for HEMA formulations (see Linest analysis in Table 7-6).

Table 7-6: Initial gradient of CHX release and total CHX release versus SQRT time for HEMA formulations with CaP (0, 10, 20 and 40 wt %) and 5 wt % CHX with linear regression analysis versus CaP wt%.

CaP (wt %)	Initial gradient of CHX release, vs SQRT time (wt%/hr ^{0.5})	Total CHX release (wt %)
0	0.24 ± 0.01	1.50 ± 0.03
10	0.310 ± 0.003	2.58 ± 0.03
20	0.36 ± 0.03	6.03 ± 0.13
40	0.48 ± 0.02	17.15 ± 0.30
Linear Regression of Chlorhexidine release versus CaP% (n=3)		
Gradient of column vs CaP (column unit / wt % CaP)	0.0059 ± 0.0001	0.41 ± 0.07
Intercept	0.25 ± 0.033	-0.29 ± 1.67
R^2	0.99	0.94

The analysis of variance (ANOVA) showed that there was sufficient evidence to reject the null hypothesis that the initial and maximum CHX release in HEMA composites with CaP was the same ($P < 0.0001$). Post-hoc Bonferroni multiple comparisons for initial CHX release up to 24 h showed that there was significant statistical difference between formulation with 40 and 0 wt % CaP, and 40 and 10 wt % CaP, as well as 40 and 20 wt % CaP ($P < 0.001$).

There were no significant difference between formulation with 0 and 10 wt % CaP, and 0 and 20 wt % CaP ($P > 0.05$), as well as between 10 and 20 wt % CaP ($P > 0.999$). For maximum CHX release, the post- hoc multiple comparisons result showed that there were significant statistical differences between HEMA formulations for all CaP levels ($P < 0.0001$).

7.8. Biaxial flexural strength and modulus

7.8.1. BFS for experimental formulation with 4-META

The average biaxial flexural strength (BFS) for 4-META formulations with CaP (0, 10, 20, 40 wt %), 5 wt % CHX and fibre dry and hydrated (24 h, 7 and 28 days immersion in deionised water) are given in Figure 7-12.

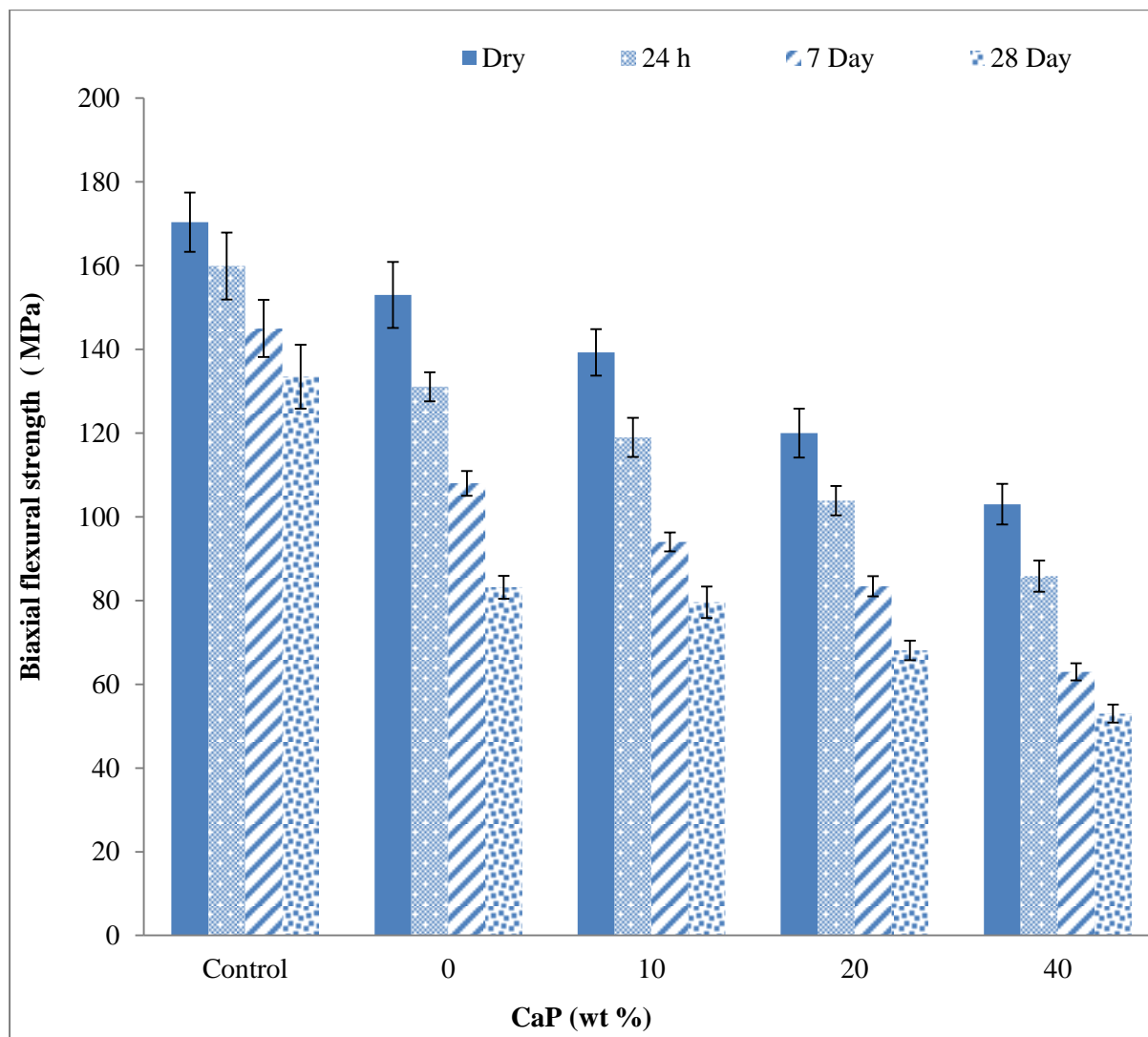


Figure 7-12: Biaxial flexural strength for 4-META formulations with added CHX, Fibres (5 wt %) in addition to CaP (0, 10, 20 and 40 wt %) and control experimental formulation. The error bars give 95% C.I of the mean (n=6).

The addition of the CHX and fibre to the control formulation caused a particularly large decline in strength at 28 days. With CHX and fibre containing formulations, initial dry strengths decreased from 153 ± 9 , 139 ± 6 , 120 ± 9 and 103 ± 6 MPa with, 0, 10, 20, and 40

wt% CaP levels respectively. Upon immersion in water for 24 h, all experimental formulations exhibited decrease in strength and further decline in strength was also seen after 7 and 28 days in water. Experimental formulations with 40 wt % CaP had the lowest BFS at all-time points.

Table 7-7 shows the linear regression of BFS of the experimental composites versus CaP levels at each time point. This Table showed that the BFS decreased linearly with increased CaP concentration at all times. The high R^2 values and small standard error on the gradient and intercept obtained by Linest analysis confirmed that increasing CaP levels from 0 to 40 wt % decreased BFS at all-time points(see linest analysis in table 7-7).

Table 7-7: Biaxial flexural strength for 4-META formulations with CaP (0, 10, 20 and 40 wt %) before and after 24 h, 7 and 28 days immersion in deionised water. Additionally gradient, intercept and R^2 from linear regression analysis versus CaP level is provided in lower section.

CaP (wt %)	BFS (MPa)			
	Dry	24 h	7 days	28 days
0	153 ± 9	131 ± 4	108 ± 4	83 ± 3
10	139 ± 6	119 ± 6	94 ± 3	80 ± 5
20	119 ± 9	104 ± 4	82 ± 4	68 ± 3
40	103 ± 6	85 ± 5	63 ± 3	53 ± 4
Linear Regression of BFS versus CaP% (n=6)				
Gradient (MPa/ CaP wt %)	-1.26 ± 0.15	-1.13 ± 0.09	-1.11 ± 0.05	-0.78 ± 0.08
Intercept (MPa)	151 ± 4	130 ± 2	106 ± 1	85 ± 2
R^2	0.97	0.99	0.99	0.98

The analysis of variance (ANOVA) showed that there was sufficient evidence to reject the null hypothesis that the variance between the 4-META experimental formulations and CaP levels and time were equal ($P < 0.001$) at each time point. The post-hoc multiple comparisons for dry samples showed that there were no significant statistical differences found between formulations with 10 and 20 wt % CaP and 10 and 40 wt % ($P > 0.05$), as well as between 20 and 40 wt % CaP ($P > 0.999$). Upon immersion in water for 24 h and 7 days there were significant statistical differences between formulations with all different levels of CaP ($P < 0.0001$). However, for samples immersed for 28 days, there were no significant statistical differences found between formulations with 0 and 10 wt % CaP ($P = 0.590$) and those with 20 and 40 wt % CaP ($P > 0.999$).

7.8.1.1. Young's modulus for experimental formulations with 4-META

The average Young's modulus for 4-META formulations with different levels of CaP, CHX and fibre dry and hydrated (24 h, 7 day and 28 days immersion in deionised water) are shown in Figure 7-13. Adding CHX and fibre to the control formulation decreased the modulus particularly at later times. With CHX and fibre present the average dry Young's modulus for experimental formulations with 0 wt % CaP had the highest modulus of 5.2 ± 0.15 GPa followed by 10 and 20 wt % CaP with 4.6 ± 0.25 and 4.2 ± 0.31 GPa respectively. The formulation with 40 wt % CaP level had the lowest modulus (4 ± 0.31 GPa). Upon immersion in water for 24 h, all experimental formulations exhibited a decrease in modulus and further decline was also shown after 7 and 28 days in water. Formulations with 40 wt % CaP had the lowest modulus at all times.

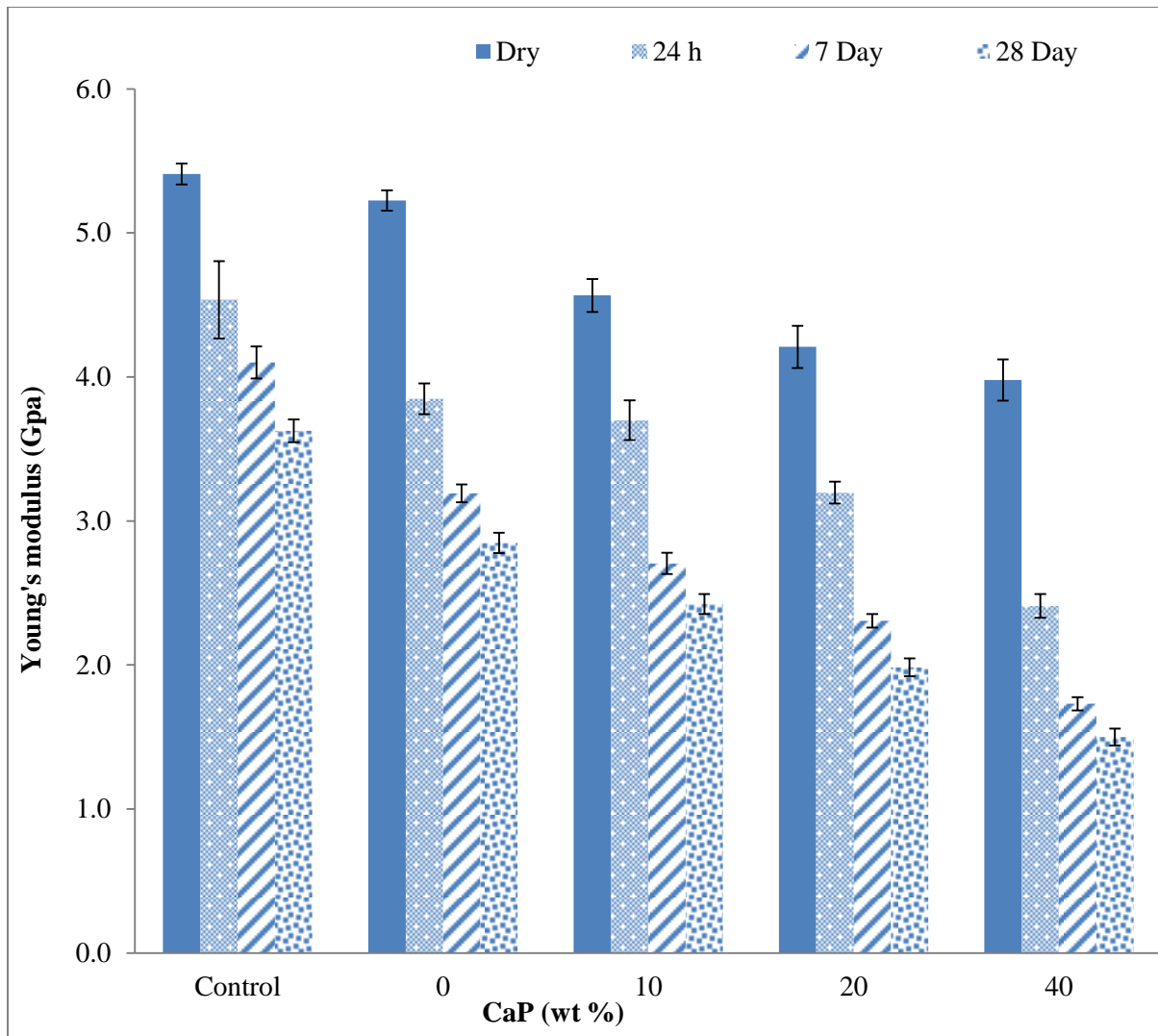


Figure 7-13: Young's modulus for 4-META experimental composites with added CHX, Fibres (5 wt %) in addition to CaP (0, 10, 20 and 40 wt %) and control formulation. The error bars indicate 95% C.I of the mean (n=6).

The gradient and intercept of Young's modulus of the experimental formulations versus CaP levels and are provided in Table 7-8. Linear regression for this Table showed that the Young's modulus decreased linearly with increased CaP levels from 0 to 40 wt % at all times. The high R^2 values and small standard error on the gradient and intercept obtained by the Linest analysis confirmed that linear equations described the data well (see linest analysis in table 7-8 below).

Table 7-8: Young's modulus and gradient, intercept and R^2 from linear regression analysis versus CaP for experimental formulations with 4-META and CaP (0, 10, 20 and 40 wt %) before and after 24 h, 7 and 28 days immersion in deionised water.

CaP (wt %)	Young's modulus (GPa)			
	Dry	24 h	1 day	28 day
0	5.23 ± 0.15	3.85 ± 0.2	3.19 ± 0.13	2.85 ± 0.15
10	4.57 ± 0.25	3.70 ± 0.31	2.7 ± 0.22	2.42 ± 0.14
20	4.21 ± 0.31	3.20 ± 0.16	2.31 ± 0.13	1.98 ± 0.13
40	3.98 ± 0.31	2.41 ± 0.17	1.73 ± 0.11	1.50 ± 0.12

Linear Regression of Young's modulus versus CaP% (n=6)				
Gradient (GPa/wt%)	-0.029 ± 0.008	-0.037 ± 0.004	-0.036 ± 0.003	-0.031 ± 0.004
Intercept (GPa)	5.0 ± 0.2	3.9 ± 0.09	3.1 ± 0.07	2.7 ± 0.1
R^2	0.84	0.98	0.98	0.97

An analysis of variance (ANOVA) showed that there was sufficient evidence to reject the null hypothesis stating that the variance between the 4-META experimental formulations and CaP levels were equal ($P < 0.001$) at all times. The post-hoc multiple comparisons for dry and 24 h in water showed that there were significant statistical differences with time and formulations with different levels of CaP ($P < 0.05$) except between dry formulations with 20 and 40 wt % CaP ($P = 0.361$) and between 0 and 10 wt % CaP ($P > 0.999$) for 24 h samples. All other samples immersed for 7 and 28 days in water showed significant statistical differences between time and levels of CaP ($P < 0.001$).

7.8.2. BFS for experimental formulations with HEMA

The average BFS for all HEMA formulations dry and hydrated (24 h, 7 day and 28 days immersion in deionised water) are provided in Figure 7-14. The results reveal again that addition of CHX and fibre to the control formulation decreases strength. With CHX and fibre added the dry strength decreased from 126 ± 7 , 119 ± 4 , 116 ± 7 and 106 ± 4 MPa with 0, 10, 20 and 40 wt % CaP respectively. Upon immersion in water for 24 h, all experimental formulations exhibited decrease in strength with a further drop seen after 7 days in water. All the formulations showed minor decline after this time point. Formulations with 40 wt % CaP had the lowest BFS at all-time points.

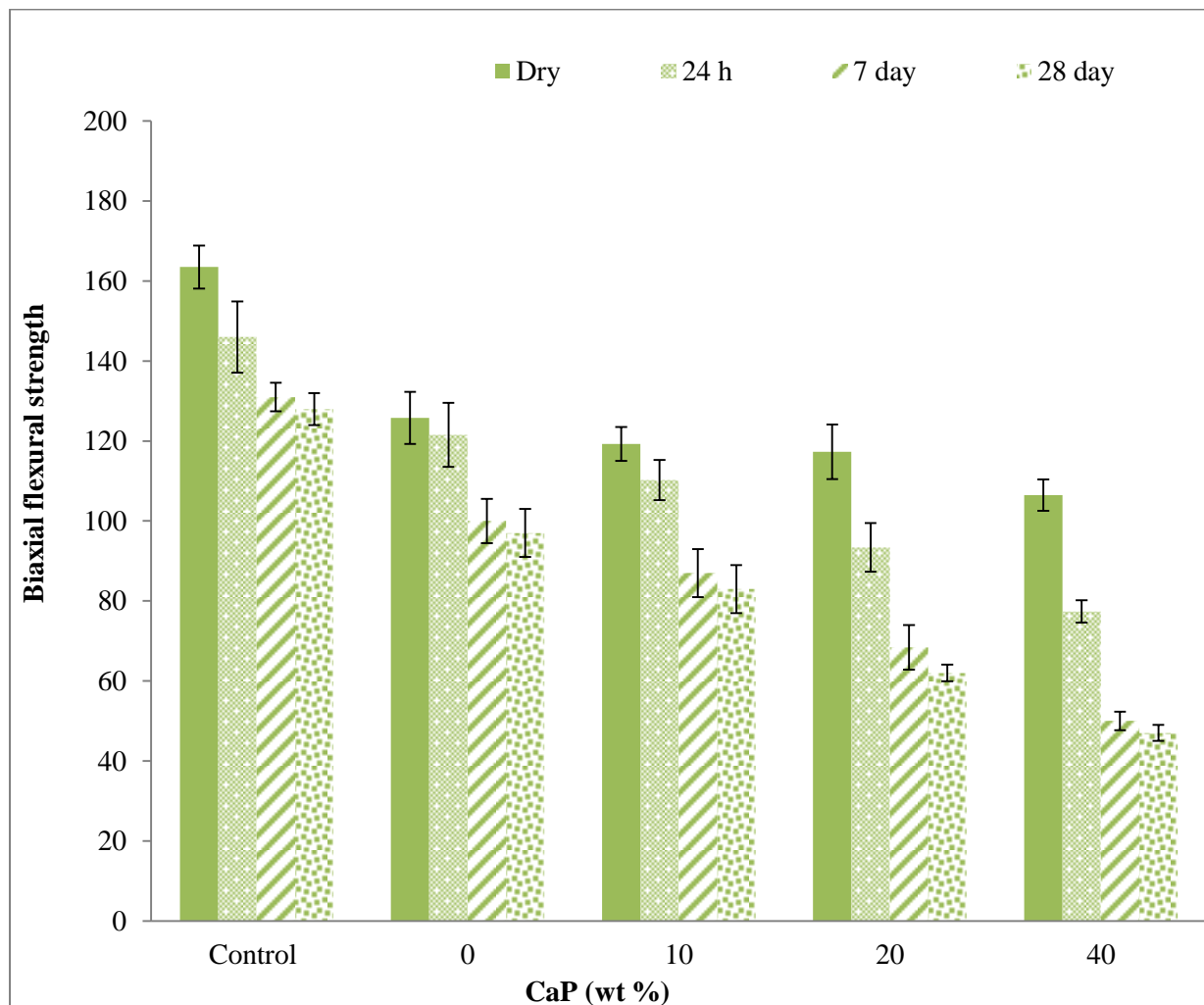


Figure 7-14: Biaxial flexural strength of HEMA experimental composites with added CaP (0, 10, 20 and 40 wt %) in addition to CHX, Fibres (5 wt %) and control formulation. The errors bars give 95% C.I of the mean (n=6).

Table 7-9 provides the gradient of BFS for HEMA formulations versus CaP levels at each time point. This table showed that the BFS decreased linearly with increased CaP levels at each time point. The high R^2 values and small standard error on the gradient and intercept obtained by the Linest analysis confirmed there was significant effect when increasing CaP levels from low to high levels (see linest analysis in table 7-9).

Table 7-9: Biaxial flexural strength of HEMA formulations with CaP (0, 10, 20 and 40 wt %) before and after 24 h, 7 and 28 days immersion in water and linear regression analysis with gradient, intercept and R^2 values from average BFS versus CaP.

CaP (wt %)	BFS (MPa)			
	Dry	24 h	7 day	28 day
0	126 ± 7	122 ± 8	100 ± 6	97 ± 6
10	119 ± 4	110 ± 5	87 ± 6	83 ± 6
20	117 ± 7	93 ± 6	68 ± 6	62 ± 2
40	106 ± 4	77 ± 3	50 ± 2	47 ± 2
Linear Regression of BFS versus CaP % (n=6)				
Gradient (Mpa/ wt %)	-0.46 ± 0.04	-1.11 ± 0.12	-1.26 ± 0.13	-1.27 ± 0.19
Intercept (MPa)	125 ± 1.07	120 ± 3	98 ± 3	94 ± 5
R^2	0.98	0.98	0.98	0.95

Analysis of variance (ANOVA) concluded that there was sufficient evidence to accept the null hypothesis that the variance between HEMA experimental formulations and CaP levels were equal ($P < 0.0001$) at each time point. The post-hoc multiple comparisons for dry samples showed that there were no significant statistical differences between formulations with 0 and 10 wt % CaP, and between 0 and 20 wt % CaP ($P > 0.05$), as well as between 10 and 20 wt % CaP ($P > 0.999$). At 24 h there were significant differences between

experimental formulations with all different levels of CaP ($P < 0.01$), except between formulations with 0 and 10 wt % CaP ($P = 0.110$). However, there were significant statistical differences between formulations and all different levels of CaP ($P < 0.001$) for samples immersed for 7 and 28 days.

7.8.2.1. Young's modulus for HEMA formulations

Figure 7-15 shows the average Young's modulus for HEMA formulations dry and hydrated (24 h, 7 and 28 days immersion in deionised water). In this case, effects of addition of CHX and fibre to the control were small.

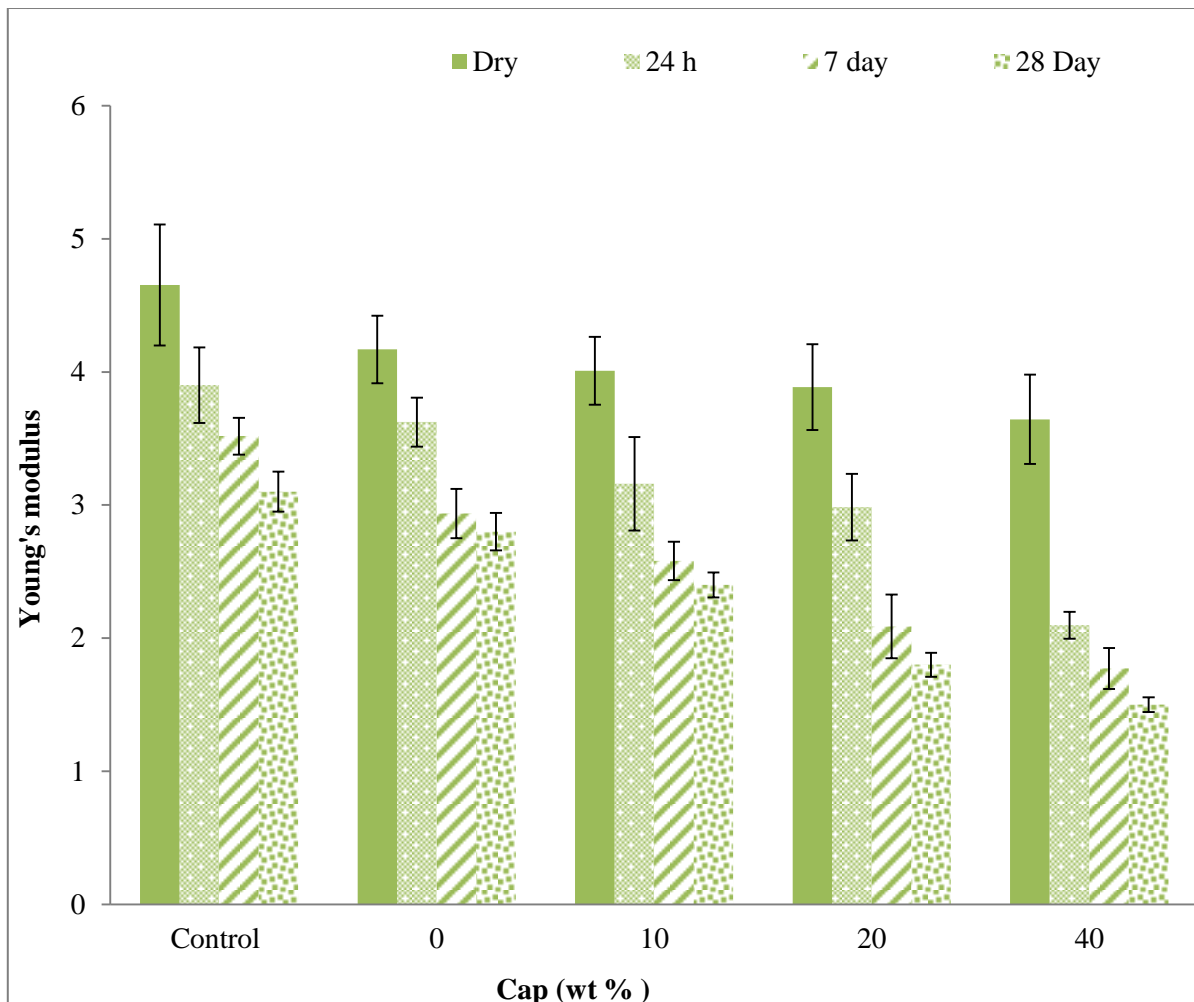


Figure 7-15 : Young's modulus of experimental composites containing HEMA with added CHX, Fibres (5 wt %) in addition to CaP (0, 10, 20 and 40 wt %) and control formulation. Error bars indicate 95% C.I of the mean (n=6).

It can be seen that the initial dry Young's modulus decreased from 4.2 ± 0.25 , 4 ± 0.25 , and 3.9 ± 0.31 to 3.6 ± 0.34 GPa with, 0, 10, 20, and 40 wt % CaP formulations respectively. Upon immersion in water for 24 h, all experimental formulations showed a decrease in modulus; further decline was also shown after 7 and 28 Days in water. Experimental formulations with 40 wt % CaP had the lowest modulus in all time point.

Table 7-10 provides the linear regression of modulus for HEMA formulations versus CaP concentration at each time point. This table showed that the Young's modulus decreased linearly with increased CaP levels. The high R^2 values, small standard error on the gradient and intercept obtained by a Linest analysis confirmed that Young's modulus decrease linearly with CaP concentrations during early times. At later times, R^2 values decreased and errors on gradients and intercepts increased, indicating slightly poorer fit of linear equations (see linest analysis in table 7-10).

Table 7-10: Young's modulus, gradient, intercept and R^2 from linear regression of formulations with HEMA and CaP (0, 10, 20 and 40 wt %) before and after 24 h, 7 and 28 day immersed in deionised water.

CaP (wt %)	Young's modulus (GPa)			
	Dry	24 h	7 day	28 day
0	4.17 ± 0.25	3.62 ± 0.19	2.94 ± 0.19	2.82 ± 0.14
10	4.01 ± 0.25	3.16 ± 0.35	2.58 ± 0.14	2.41 ± 0.09
20	3.89 ± 0.32	2.98 ± 0.25	2.1 ± 0.24	1.83 ± 0.09
40	3.64 ± 0.34	2.10 ± 0.12	1.7 ± 0.2	1.52 ± 0.06
Linear Regression of modulus versus CaP % (n=6)				
Gradient (GPa/wt %)	-0.013 ± 0.001	-0.037 ± 0.003	-0.03 ± 0.01	-0.032 ± 0.007
Intercept (GPa)	4.15 ± 0.01	3.61 ± 0.07	2.85 ± 0.11	2.70 ± 0.16
R^2	0.99	0.98	0.94	0.91

An analysis of dependent variables (ANOVA) for the dry samples showed that there was sufficient evidence to accept the null hypothesis that the variance was ($P = 0.049$). However, analysis of variance (ANOVA) for the remaining samples immersed in 24 h, 7 and 28 days showed that there was sufficient evidence to reject the null hypothesis that the variance between the HEMA formulations and CaP levels were equal ($P < 0.001$).

The post-hoc multiple comparisons for dry samples showed that there were no significant statistical differences between dry sample formulations and all different levels of CaP ($P > 0.05$). Upon immersion in water for 24 h, the results showed that there were significant statistical differences between formulations and all different levels of CaP ($P < 0.001$) except between 10 and 20 wt % CaP ($P = 0.923$).

Moreover, for samples immersed for 7 days, there were no significant statistical differences found between formulations with 0 and 10 wt % CaP ($P = 0.511$) and 20 and 40 wt % CaP ($P = 0.068$). Finally, samples immersed in water for 28 day showed significant statistical differences between formulations and all different CaP levels ($P < 0.001$).

7.9. Push out adhesion test

7.9.1. Experimental formulations with 4-META

7.9.1.1. Bonding to dry ivory dentine

The average push out stress for 4-META formulations with CaP (0, 10, 20 and 40 wt %), CHX and fibre formulations and dry ivory dentine are shown in Figure 7-16. The push out stress was on average 64 % higher after acid etching of dry ivory dentine than with non-etched dentine.

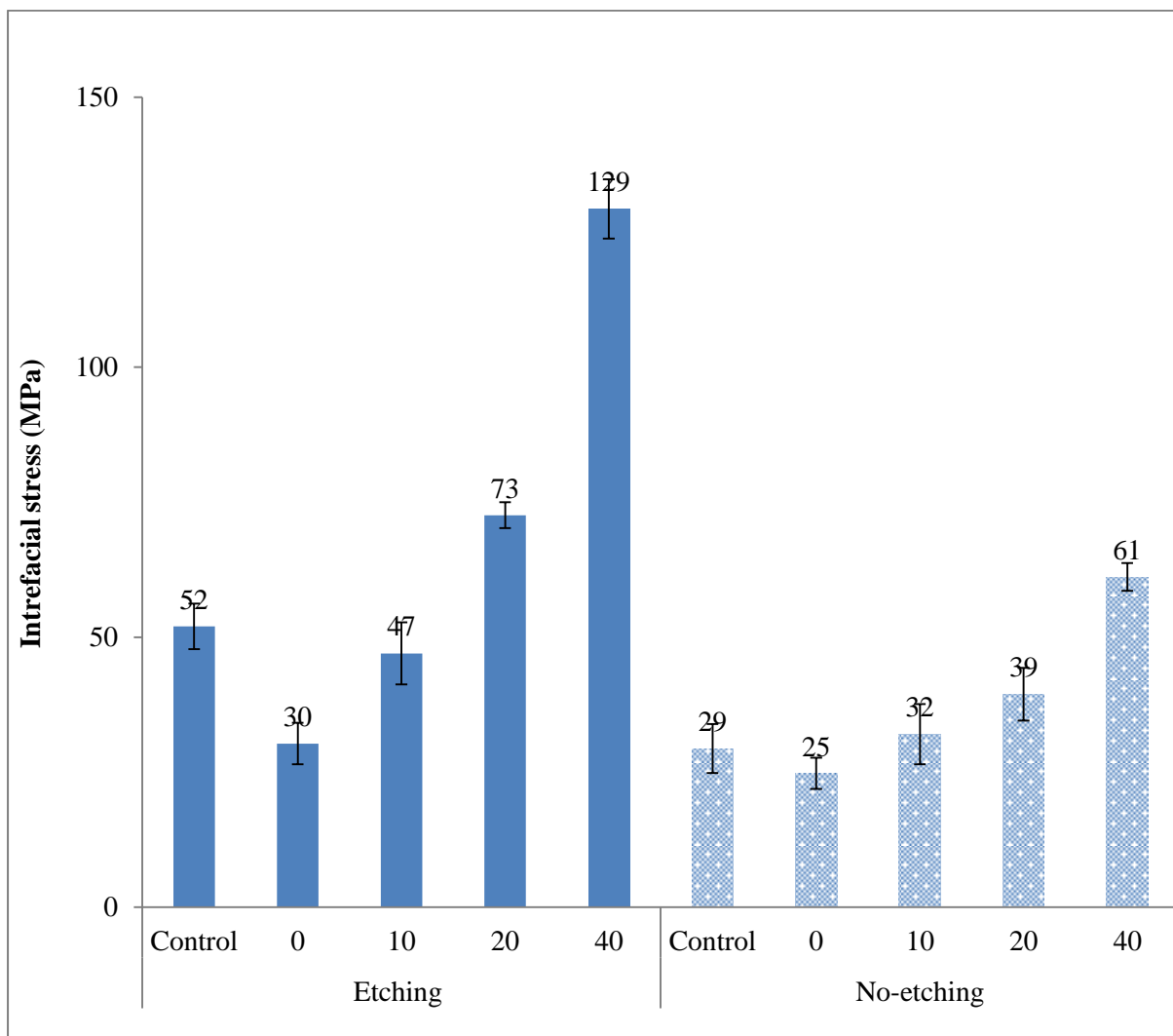


Figure 7-16 : Push out stress for dry ivory dentine with 4-META formulations with added CHX and fibre at 5 wt %, Cap (0, 10, 20 and 40 wt %) in addition of control formulation. Dentine etching with phosphoric acid was for 20s or no-etching. The error bars represent 95 % C.I of the mean. (n=6).

The effects of CaP increase was much greater than that observed with CHX and fibre addition to the control formulation. The formulation with 40 wt % CaP had the highest push out stress with and without acid etching, of 129 ± 5 and 61 ± 3 MPa respectively. The formulation with 0 wt % CaP showed the lowest debonding stress regardless of acid etching of 30 ± 4 and 25 ± 3 MPa respectively, followed by formulations with 10 and 20 wt % CaP. The debonding stress decreased linearly with increasing CaP levels with and without acid etching of dentine.

Table 7-11 shows the linear regression gradient of debonding stress for 4-META formulations versus CaP level. The high R^2 values with the small standard error on the gradient and intercept confirms a linear equation describes the data well. The gradient after etching was 3 times that with no etching whilst intercepts were not very different (see table 7-11 below).

Table 7-11: Push out stress for dry ivory dentine, using etching with phosphoric acid for 20s or non-etching for 4-META formulations with Cap (0, 10, 20 and 40 wt %). Additionally, gradient, intercept and R^2 from linear regression analysis values CaP level is provided.

CaP (wt %)	Push out stress (MPa)	
	Etching	No-etching
40	129 ± 5	61 ± 3
20	73 ± 3	39 ± 5
10	47 ± 6	32 ± 6
0	30 ± 4	25 ± 3
Linear Regression of push out stress versus CaP % (n=6)		
Gradient (MPa/wt %)	2.5 ± 0.2	0.9 ± 0.1
Intercept (MPa)	26 ± 4	23 ± 2
R^2	0.98	0.98

The analysis of variance (ANOVA) showed that there was sufficient evidence to reject the null hypothesis that the variance between 4-META formulations, different levels of CaP and etching and non-etching were equal ($P < 0.001$). With acid etching, post-hoc Bonferroni multiple comparisons showed that there were significant statistical differences between formulations and all different levels of CaP ($P < 0.001$). With no acid etching, there were no significant statistical differences between formulations with 10 and 0 wt % CaP ($P = 0.420$) and between 10 and 20 wt % CaP ($P = 0.490$).

7.9.1.2. Bonding to controlled hydration ivory dentine

The debonding stress for all 4-META formulations and ivory with controlled hydration is shown in Figure 7-17. It can be seen that the push out stress was on average 52 % higher after acid etching of wet ivory dentine. Again the effect of CaP increase was much greater than that observed with CHX and fibre addition to the control formulation. The formulation with 40 wt % CaP had the highest push out stress with and without acid etching of 221 ± 8 and 145 ± 5 MPa respectively. Decreasing the CaP levels from 40 to 0 wt % decreased debonding stress linearly, with and without acid etching. The formulation with 0 wt % CaP had the lowest debonding stress regardless of acid etched, followed by formulations with 10 and 20 wt % CaP.

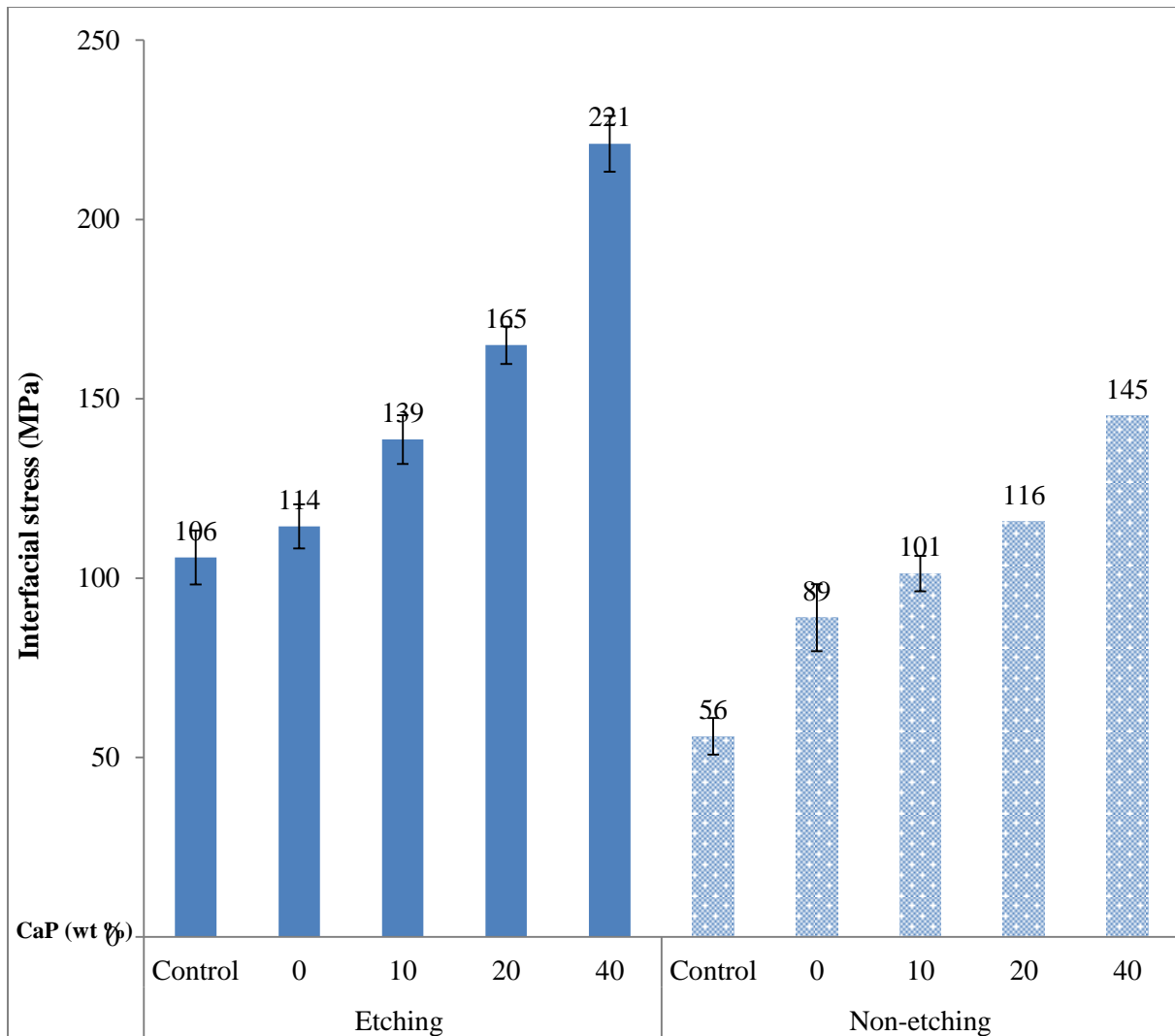


Figure 7-17: Push out stress for wet ivory dentine (control hydration) sample with 4-META formulation with added CHX and fibre at 5 wt % and Cap (0, 10, 20 and 40 wt %), in addition of control formulation. Dentine was etching with phosphoric acid for 20s or no-etching. The errors bars indicate 95% C.I of the mean (n=6).

The linear regression gradient of debonding stress of 4-META formulations versus CaP levels are provided in Table 7-12. This table showed that, on average, increasing CaP levels from 0 to 40 % caused a linear increase in debonding stress. The high R^2 and small standard errors confirm that a linear expression was suitable for described well how debonding stress varied with CaP percentage both with and without acid etching of the dentine. The gradient after acid etching was double that with no acid etching whilst the intercept was 22 % higher.

Table 7-12: Push out stress for wet ivory (control hydration) gradient, intercept and R² from linear regression for 4-META formulations with and Cap (0, 10, 20 and 40 wt %) and etching with phosphoric acid for 20s or no-etching.

CaP (wt %)	Push out stress (MPa)	
	Etching	No-etching
40	221 ± 8	145 ± 5
20	165 ± 6	116 ± 5
10	139 ± 7	101 ± 4
0	114 ± 6	89 ± 9

Linear Regression of Cure depth versus CaP% (n=6)		
Gradient (MPa/wt %)	2.9 ± 0.1	1.41 ± 0.03
Intercept (MPa)	112.8 ± 1.4	88 ± 1
R ²	0.99	0.99

An analysis of variance (ANOVA) provided sufficient evidence to reject the null hypothesis that the variance between formulations, CaP levels and etching and non-etching were equal ($P < 0.001$). With acid etching the post-hoc multiple comparisons result showed that there were significant statistical differences between formulations and different CaP levels ($P < 0.0001$). With no acid etching there were no significant statistical differences, it was only observed between formulations with 10 and 0 wt % CaP ($P = 0.68$).

7.9.1.3. 4-META formulations with self-adhesive Ibond

The push out stress for all 4-META formulations and applying self-adhesive agent (Ibond) to wet ivory dentine surface is given in Figure 7-18. Addition of CHX and fibre caused a minor decrease in push out stress as compared to control formulation. It can also be seen that the formulation containing 40 wt % had the highest push out stress (443 ± 9 MPa) followed by the formulation with 20 wt % CaP (314 ± 18 MPa). Decreasing the CaP level from 40 to 0 wt % caused a linear decrease in debonding stress. The formulation with 0 wt % CaP had the lowest debonding stress (186 ± 13 MPa), followed by the formulation with 10 wt % (253 ± 21 MPa).

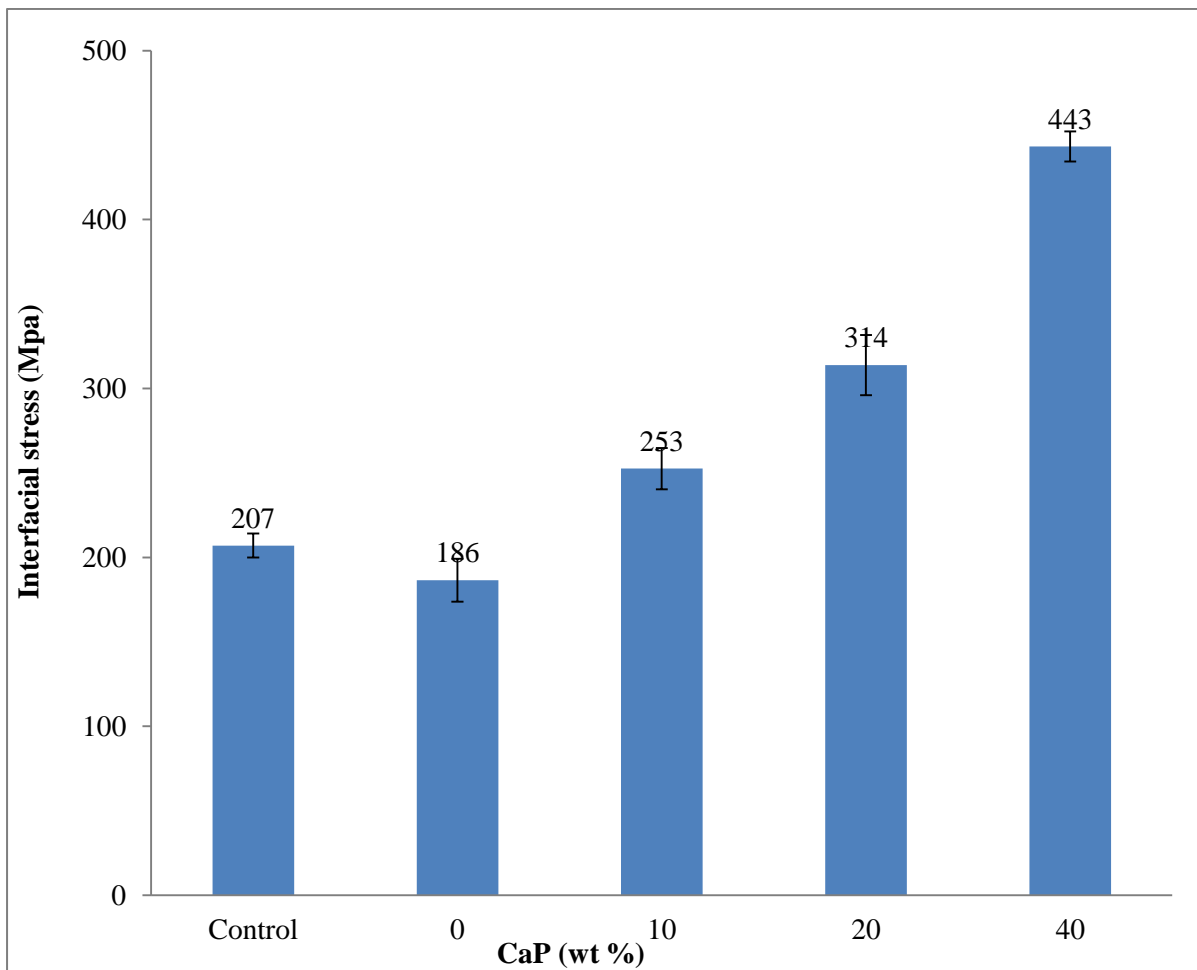


Figure 7-18 : Push out stress for 4-META formulation with Cap (0, 10, 20 and 40 wt %) and 5 wt % CHX and fibre in addition of control formulation with self-adhesive Ibond. The errors bars give 95% C.I of the mean. (n=6).

Table 7-13 shows the linear regression analysis of push out stress for 4-META formulations with the self-adhesive agent Ibond. The high R^2 values obtained by a Linest analysis confirmed a linear relationship between CaP with push out stress with the use of self-adhesive agent Ibond. The gradient after applying Ibond was more than double that with dry and wet ivory dentine, as seen in Table 7-12.

Table 7-13: push out stress gradient, intercept and R^2 from linear regression analysis versus CaP for 4-META formulations with Cap (0, 10, 20 and 40% wt) and self-adhesive agent Ibond.

CaP (wt %)	push out test with Ibond (MPa)
40	443± 9
20	314 ± 18
10	253 ± 21
0	186 ± 13
Linear Regression of push out test versus CaP wt % (n=6)	
Gradient (MPa/wt %)	6.4± 0.05
Intercept (MPa)	187 ± 1
R^2	0.99

The analysis of variance (ANOVA) showed that there was sufficient evidence to reject the null hypothesis that the variance between the 4-META experimental formulations with adhesive agent Ibond was equal ($P < 0.001$). Post-hoc multiple comparisons showed that there were significant statistical differences between formulations and all different CaP levels ($P < 0.001$).

7.9.2. Experimental formulations with HEMA

7.9.2.1. Bonding to dry ivory dentine

The debonding stress for the experimental formulations containing HEMA, with control formulation, different levels of CaP, 5 wt % CHX and fibre with dry ivory dentine is shown in Figure 7-19. The push out stress was on average 42 % higher with acid etching of dry ivory dentine.

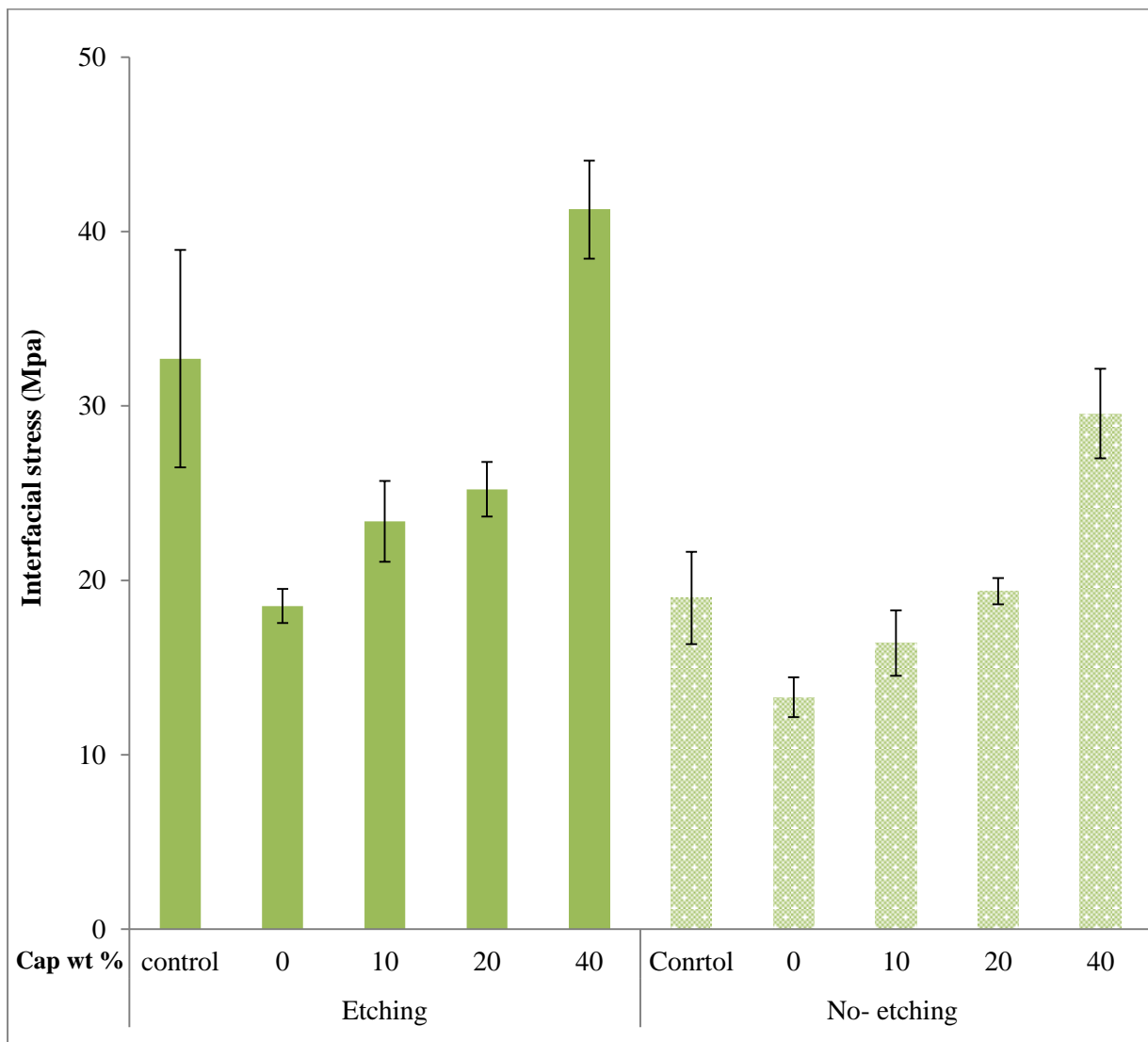


Figure 7-19: Push out stress for dry ivory sample with HEMA formulation with Cap (0, 10, 20 and 40 wt %), 5 wt % CHX and fibre and control formulation after etching with phosphoric acid for 20 s or 0 s of dentine. The error bars give 95 % C.I of the mean (n= 6).

The figure shows CHX and fibre addition caused decrease in push out stress as compared to control formulation with and without acid etching. The HEMA formulation and high CaP levels (40 % wt) showed the highest push out stress with both etched and non-etched ivory dentine: 41 ± 3 and 30 ± 3 MPa respectively. The formulation with 0 wt % CaP showed the lowest debonding stress with and without acid etching: 19 ± 1 and 13 ± 1 MPa respectively. Decreasing the CaP caused a linear decrease in the debonding stress, regardless of acid etching.

Table 7- 14 shows the linear regression gradient of debonding stress of HEMA formulations versus CaP levels. High R^2 and small error on the gradient and intercept confirmed that debonding stress increased with increased CaP concentrations. The gradient after acid etching was ~ 1.8 ($0.71/.4$) times higher than the non-etching dentine (see Table 7-14).

Table 7-14: Push out stress for wet ivory (controlled hydration) gradient, intercept and R^2 from linear regression analysis of formulation with HEMA, Cap (0, 10, 20 and 40 wt %), etching with phosphoric acid for 20s or no-etching.

CaP (wt %)	Push out stress (MPa)	
	Etching	No-etching
40	41 ± 3	30 ± 3
20	25 ± 2	19 ± 1
10	23 ± 2	16 ± 2
0	19 ± 1	13 ± 1
Linear Regression of push out test versus CaP wt % (n=6)		
Gradient (MPa/wt)	0.71 ± 0.09	0.40 ± 0.04
Intercept (MPa)	17 ± 2	12 ± 0.9
R^2	0.95	0.98

The analysis of variance (ANOVA) showed that there was sufficient evidence to reject the null hypothesis that the variance between the formulations and with etching and non-etching were equal ($P < 0.001$). With acid etching, the post-hoc multiple comparisons result showed that there were only no significant statistical differences between formulations with 10 and 20 wt % CaP ($P > 0.999$). Without acid etching, there were significant statistical differences between the formulation with 40 wt % CaP and all other CaP levels ($P < 0.001$) and between 0 and 20 CaP wt % ($P < 0.05$), but not between other formulations ($P > 0.05$).

7.9.2.2. Bonding to controlled hydrated Ivory dentine

The debonding stress for HEMA formulations with control formulation and different levels CaP and wet ivory after controlled hydration are shown in Figure 7-20. The push out stress was on average 52 % higher when the wet ivory dentine had been etched with phosphoric acid. The figure shows CHX and fibre addition has higher push out stress 105 MPa as compared with control 80 MPa with acid etching, however, the effect was negligible with no acid etching dentine. The formulation with high CaP levels (40 wt %) had the highest push out stress with both etched and non-etched dentine: 150 ± 9 and 86 ± 9 MPa respectively. Decreasing the CaP level decreased the debonding stress with and without acid treatment. The formulation with 0 % CaP had the lowest debonding stress, regardless of acid etched, followed by formulations with 10 and 20 % CaP.

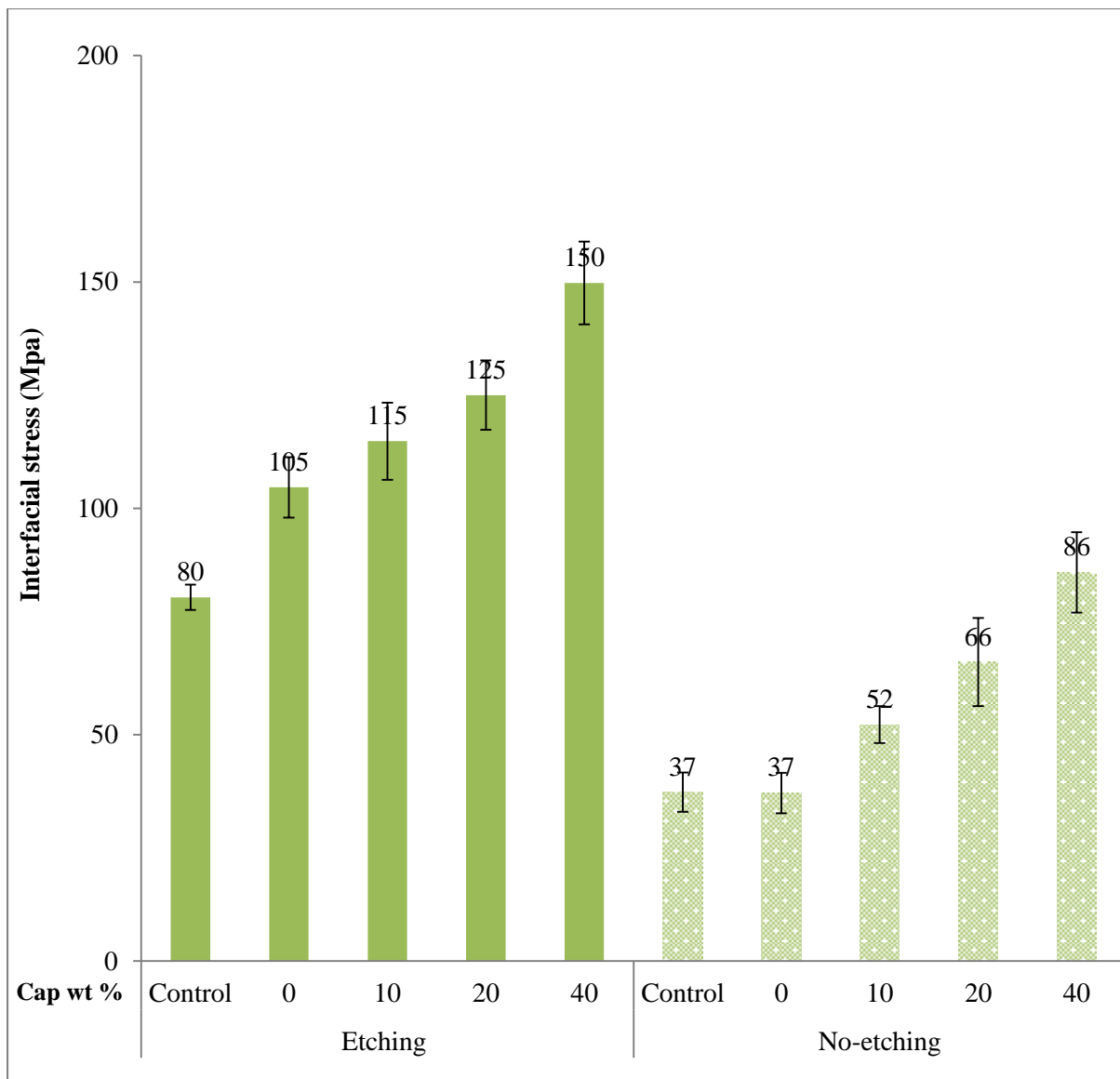


Figure 7-20: Push out stress for wet ivory dentine for formulations with HEMA, CaP (0, 10, 20 and 40 wt %) and etching with phosphoric acid for 20s or no-etching. Errors bars indicate 95% C.I of the mean. (n=6).

The linear regression gradient of push out stress versus CaP using wet ivory dentine is provided in Figure 7-15. The high R^2 value and small error on the gradient and intercept confirmed that debonding increased linearly with increasing CaP concentrations. The gradients after acid etching was double that with no acid etching whilst the intercept was 30% higher, as seen in Table 7-12.

Table 7-15: Push out stress using wet ivory (control hydration) for HEMA formulations with CaP (0, 10, 20 and 40 wt %) after etching the dentine with phosphoric acid for 20 s or no-etching. Lower section gives linear regression analysis with gradient, intercept and R² for average data versus CaP wt %.

CaP (wt %)	Push out stress (MPa)	
	Etching 20 s	Non-etching
40	150 ± 9	86 ± 9
20	125 ± 8	66 ± 10
10	115 ± 8	52 ± 4
0	105 ± 7	37 ± 4
Linear Regression of push out stress versus CaP% (n=6)		
Gradient (N/wt %)	1.13 ± 0.04	1.21 ± 0.09
Intercept (N)	103 ± 1	39 ± 2
R²	0.99	0.98

The analysis of variance (ANOVA) revealed sufficient evidence to reject the null hypothesis that the variance between the experimental formulations with etching and no etching were equal ($P < 0.001$). With acid etching, the post-hoc multiple comparisons result showed that there were significant statistical differences between formulations with 40 wt % CaP and all other CaP levels ($P < 0.0001$), and between 0 and 20 wt % CaP ($P < 0.01$). There were no significant statistical differences between formulations with 0 and 10 wt % ($P = 0.476$) and between 10 and 20 wt % CaP ($P = 0.561$). With no acid etching, the statistical analysis was fairly similar.

7.9.2.3. HEMA formulations with self-adhesive Ibond

The push out stress results for all HEMA formulations and applying the self-adhesive agent (Ibond) to wet ivory dentine surface is given in Figure 7-21. Addition of CHX and fibre caused a minor decrease in push out stress as compared to control formulation. It can be seen that the formulation containing 40 wt % had the highest push out stress (288 ± 9 MPa) followed by the formulation with 20 wt % CaP (227 ± 14 MPa). The formulation with 0 wt % CaP had the lowest debonding stress (125 ± 9 MPa), followed by the formulation with 10 wt % (174 ± 10 MPa).

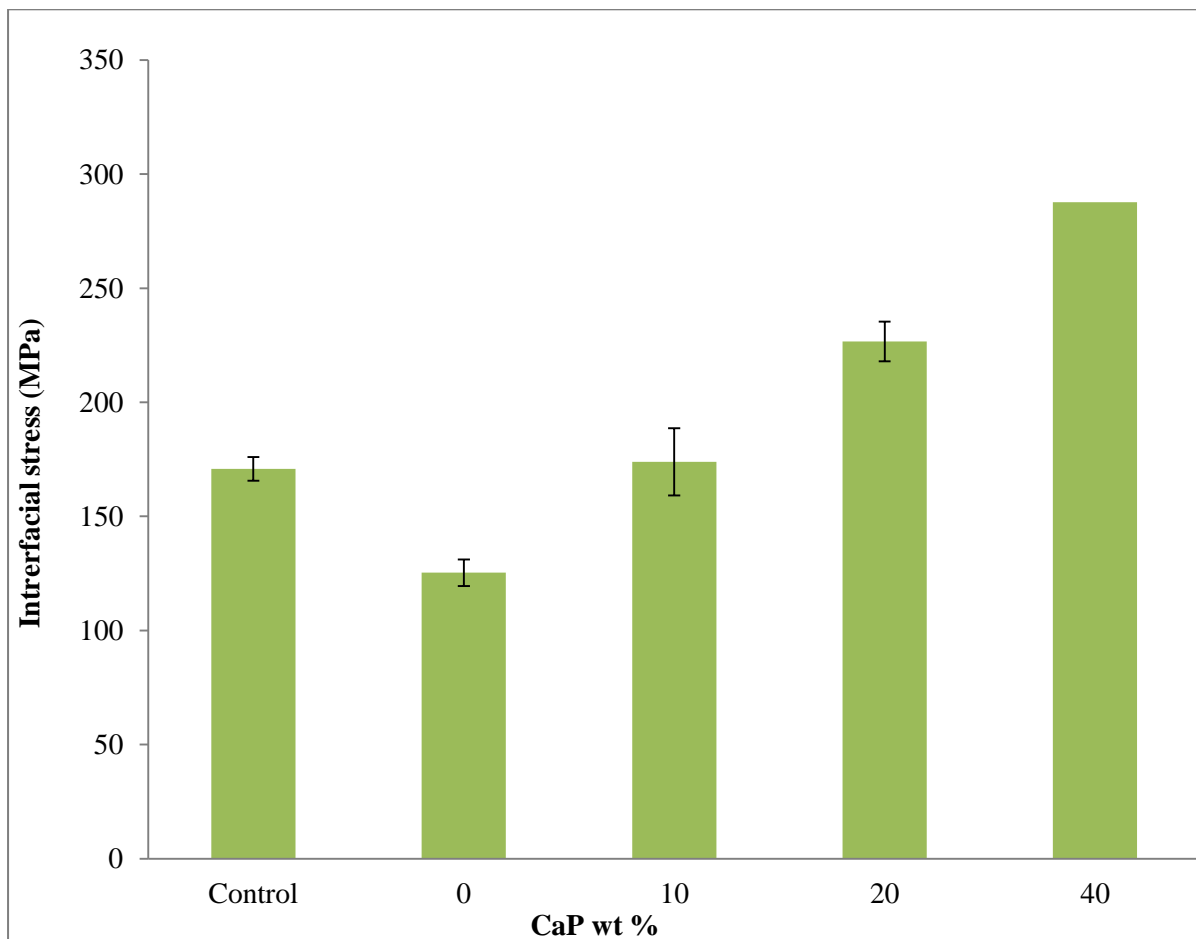


Figure 7-21 : Push out stress for wet ivory dentine (control hydration) sample with HEMA formulations with Cap (0, 10, 20 and 40 wt %) after etching of dentine with phosphoric acid for 20s or no-etching. The errors bars represent 95% C.I of the mean. (n=6).

Decreasing the CaP level from 40 to 0 wt % caused a linear decline in debonding stress. The linear regression analysis results of push out stress for formulations with different CaP levels and the self-adhesive agent Ibond are provided in Table 7-16. The high R^2 values confirm linear equations describe the data well.

Table 7-16: Push out stress for experimental formulation with HEMA, Cap (40, 20, 10 and 0% wt) and self-adhesive agent Ibond. Lower section gives linear regression analysis with gradient, intercept and R^2 for average data versus CaP wt %.

CaP (wt %)	Shear bond strength with Ibond (MPa)
40	288± 9
20	227 ± 14
10	174 ± 10
0	125 ± 9
Linear Regression of push out stress versus CaP % and adhesive agent (n=6)	
Gradient (MPa/wt %)	4.0± 0.39
Intercept (MPa)	132 ± 9
R^2	0.98

An analysis of variance (ANOVA) showed that there was sufficient evidence to reject the null hypothesis that the variance between the HEMA formulations, CaP and the adhesive agent Ibond was equal ($P < 0.001$). The post-hoc multiple comparisons result showed that there were significant statistical differences between formulations and all different CaP levels ($P < 0.001$).

7.10. Shear test

7.10.1. Experimental formulations with 4-META

The shear bond strength for 4-META formulations with control formulation and added CaP (0, 10 20 and 40 wt %), 5 wt % CHX and fibre and hydrated ivory dentine are represented in Figure 7-22.

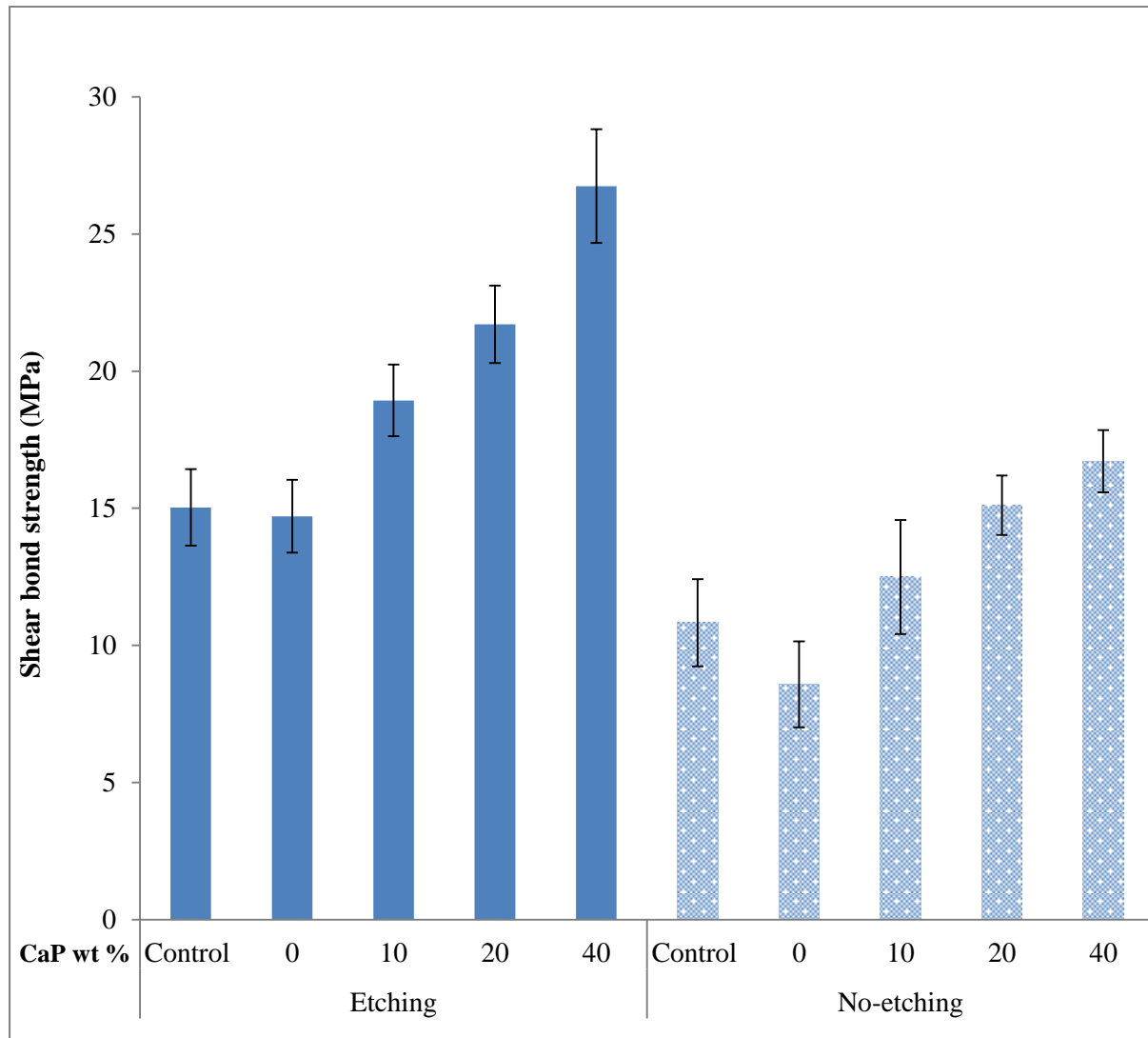


Figure 7-22: Shear bond strength for wet ivory dentine for 4-META formulation with Cap (0, 10, 20 and 40 wt %), 5 wt % CHX and fibre in addition of control formulation after etching with phosphoric acid for 20 s 0 s. The error bars represent 95% C.I of the mean (n=6).

The figure shows CHX and fibre addition has negligible effect as compared to control formulation with and without acid etching. The shear bond strength was on average 36 % higher with acid etching. The formulation with high CaP (40 % wt) had the highest shear strength with etched and non-etched dentine of 27 ± 2.1 and 17 ± 1.1 MPa respectively. Decreasing the CaP level decreased the shear bond strength linearly with and without acid etching. The formulation with 0 wt % CaP had the lowest shear bond strength with and without acid etching of 15 ± 1.3 and 9 ± 1.6 MPa respectively, followed by formulations with 10 and 20 wt % CaP.

Table 7-17 shows the linear regression gradient of shear bond strength versus CaP wt % with wet dentine (control hydration). The high R^2 values are obtained by a Linest analysis with, but not without acid etching. The gradient after acid etching was 1.6 times that with no acid etching.

Table 7-17: shear bond strength gradient, intercept and R^2 from linear regression analysis versus CaP for 4-META formulation with Cap (0, 10, 20 and 40 wt %) after etching with phosphoric acid for 20s or no-etching.

Cap (wt %)	Shear bond strength (MPa)	
	Etching 20 s	Non-etching
40	27 ± 2.1	17 ± 1.1
20	22 ± 1.4	15 ± 1.1
10	19 ± 1.3	12 ± 2.1
0	15 ± 1.3	9 ± 1.6
Linear Regression of Cure depth versus CaP% (n=3)		
Gradient (MPa/wt %)	0.28 ± 0.025	0.18 ± 0.05
Intercept (MPa)	15 ± 0.6	10 ± 1.2
R^2	0.98	0.87

The analysis of variance (ANOVA) showed that there was sufficient evidence to reject the null hypothesis that the variance between the experimental formulations with etching and no etching were equal ($P < 0.001$). With acid etching, the post-hoc multiple comparisons showed that there were significant statistical differences between formulations and all CaP levels ($P < 0.001$) except the formulation with 10 and 20 wt % CaP ($P = 0.138$). With no acid etching, the result showed that there no were significant statistical differences between formulations with 40 and 20 wt % CaP ($P > 0.999$) and between those with 20 and 10 wt % CaP ($P = 0.69$), as well as 0 and 10 wt % Cap ($P = 0.053$). However there was a significant difference between 40, 10 wt % and 40 and 0 wt % ($P < 0.05$).

7.10.1.1. 4-META formulations with CaP and self- adhesive Ibond

The shear bond strength results for all 4-META formulations and application of self-adhesive (Ibond) to wet ivory dentine is given in Figure7-23. The figure shows on average the control formulation has higher shear bond strength (50 MPa) as compared to CHX and fibre formulation (34 MPa) and different levels of CaP. It can be seen that formulation with 40 wt % CaP had shear bond strength of 45 ± 1.8 MPa, followed by formulation with 20 wt % CaP of 41 ± 2.1 MPa. The shear bond strength of formulations with 0 and 10 wt % CaP were comparable (~ 34 MPa).

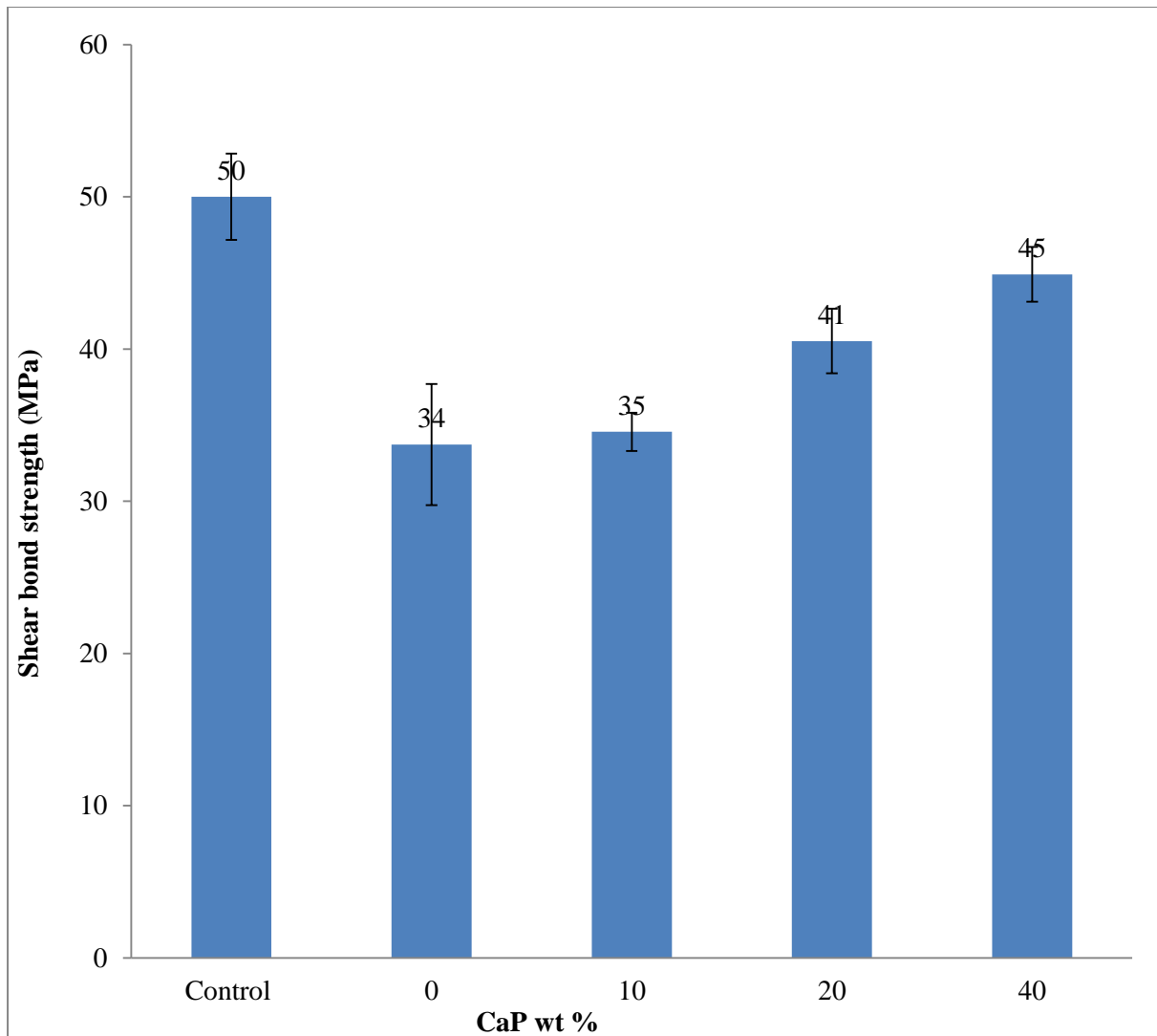


Figure 7-23: Shear bond strength for 4-META formulation with Cap (40, 20, 10 and 0% wt), CHX and glass fibre at (5 wt %) in addition of control formulation and self-adhesive Ibond. The error bars indicate 95% C.I of the mean

Table 7- 18 displays the linear regression analysis of the shear bond strength for 4-META formulations with using the self-adhesive Ibond versus CaP wt %. This shows an increase in the shear bond strength with increasing CaP level. Whilst the error on the intercept is small, the R^2 value is < 0.95 and error on the gradient is high.

Table 7-18: shear bond strength gradient, intercept and R² from linear regression of formulation with 4-META, Cap (0, 10, 20 and 40 wt %) and self-adhesive Ibond.

CaP (wt %)	Shear bond strength with Ibond (MPa)
40	45± 1.8
20	41 ± 2.1
10	35 ± 1.3
0	34 ± 4
Linear Regression of Cure depth versus CaP% (Standard errors (n=3))	
Gradient (MPa/wt %)	0.30± 0.05
Intercept (MPa)	33 ± 1.2
R²	0.94

An analysis of variance (ANOVA) showed that there was sufficient evidence to reject the null hypothesis that the variance between the 4-META experimental formulations with the adhesive agent Ibond was equal ($P < 0.001$). The post-hoc multiple comparisons showed that there were no significant statistical differences between formulations with CaP 0 and 10 wt % CaP ($P > 0.999$) and between 40 and 20 wt % CaP ($P = 0.083$). There was significant statistical difference between 40 wt % and all levels of CaP ($P < 0.05$) and between formulations with 20 and 10 wt % CaP ($P < 0.05$), as well as between 20 and 0 wt % ($P < 0.05$).

7.10.2. Experimental formulations with HEMA

The shear bond strength for HEMA formulations with control formulation and different levels of CaP, 5 wt % CHX, fibre and wet ivory dentine (control hydration) are shown in Figure 7-24. The shear bond strength was increased on average by 10 % after the acid etching of wet ivory dentine. Addition of CHX and fibre caused a minor decrease in shear bond strength as compared to control formulation with and without acid etching. The formulation with high CaP (40 wt %) had the highest shear strength with etched and non-etched dentine with 14 ± 1.4 and 11 ± 0.9 MPa respectively.

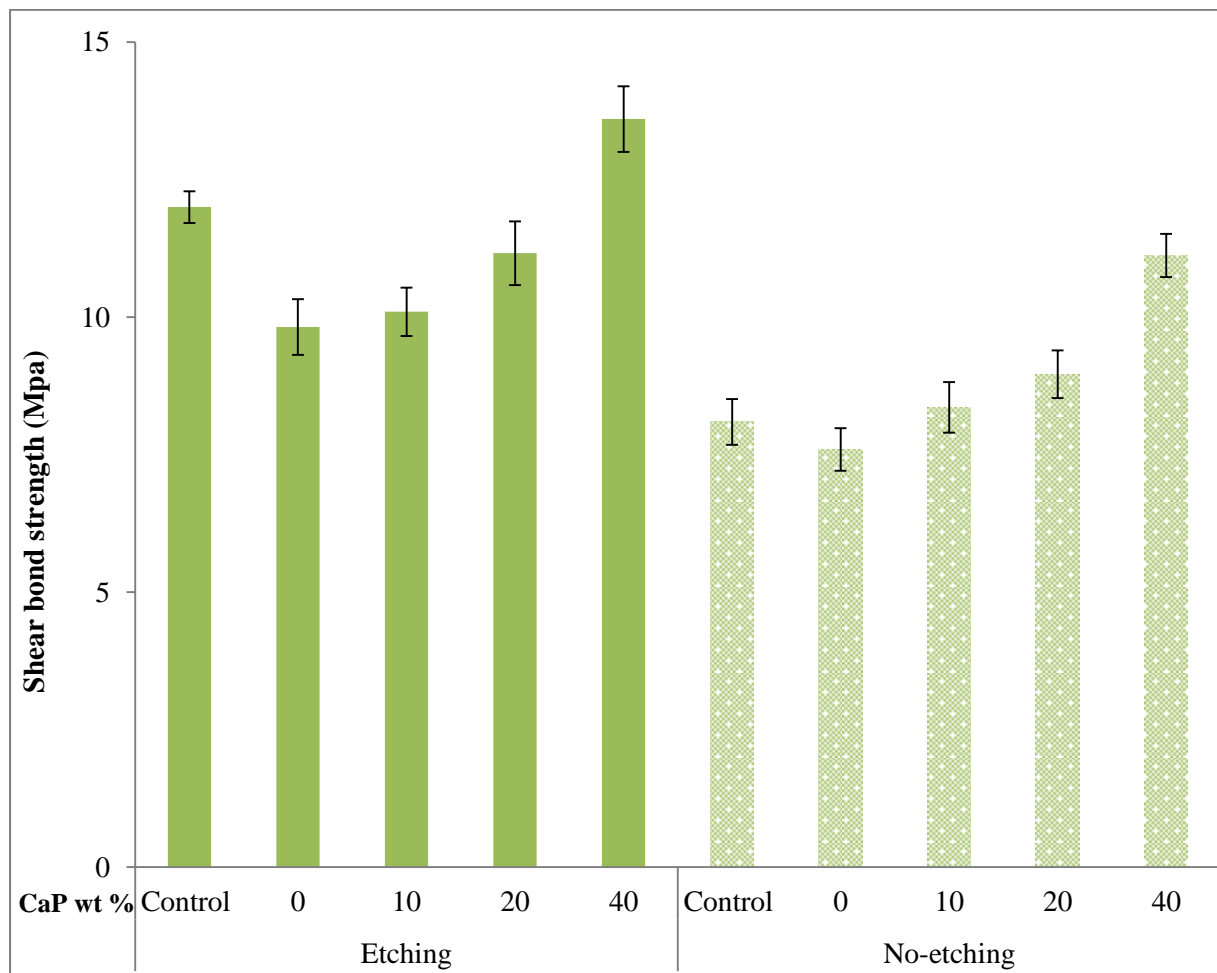


Figure 7-24: Shear bond strength for wet ivory dentine for HEMA formulations with Cap (0, 10, 20 and 40 wt %), CHX and glass fibre at 5 wt % in addition of control formulation after etching with phosphoric acid for 20 s or 0 s. The error bars represent 95% C.I of the mean (n=6).

A linear regression analysis of shear bond strength for HEMA formulations versus CaP wt % showed that increased CaP levels increased the shear bond strength both with and without acid etching. The high R^2 values, the relatively small errors on gradients and intercepts showed that linear equations described the data well (see Linest analysis in Table 7-19).

Table 7-19: Linear regression analysis of shear bond strength versus CaP for HEMA formulations with CaP (0, 10, 20 and 40 wt %) upon dentine etching with phosphoric acid for 20s and no etching.

Cap %	Shear bond strength (MPa)	
	Etching for 20 s	Non-etching
40	13.6 ± 1.3	11.1 ± 0.9
20	11.2 ± 1.3	9.0 ± 0.9
10	10 ± 1	8 ± 1
0	9.3 ± 1.1	7.5 ± 0.8
Linear Regression of shear bond strength versus CaP% (n=6)		
Gradient (MPa/wt %)	0.098 ± 0.014	0.088 ± 0.007
Intercept (MPa)	9.4 ± 0.3	7.4 ± 0.17
R²	0.96	0.98

The analysis of variance (ANOVA) showed that there was sufficient evidence to reject the null hypothesis that the variance between the HEMA formulations with and without acid etching were equal (P value < 0.001). The post-hoc multiple comparisons for etched and non-etched ivory dentine showed that there were significant statistical differences between formulations with 40 wt % CaP and all other CaP levels (P < 0.001).

7.10.2.1. HEMA formulations with CaP and self-adhesive Ibond

The shear bond strength results for all HEMA experimental and self-adhesive Ibond to wet ivory dentine is given in Figure 7-25. The figure shows CHX and fibre addition has negligible effect as compared to control formulation. It can be seen that the formulation with 40 wt % had the highest shear bond strength (45 MPa). The shear bond strength of formulations with 0, 10 and 20 wt % CaP were comparable (~ 36 MPa). There was no consistent effect evident on shear bond strength from increasing CaP concentration from 0 to 40 wt % with self-adhesive Ibond.

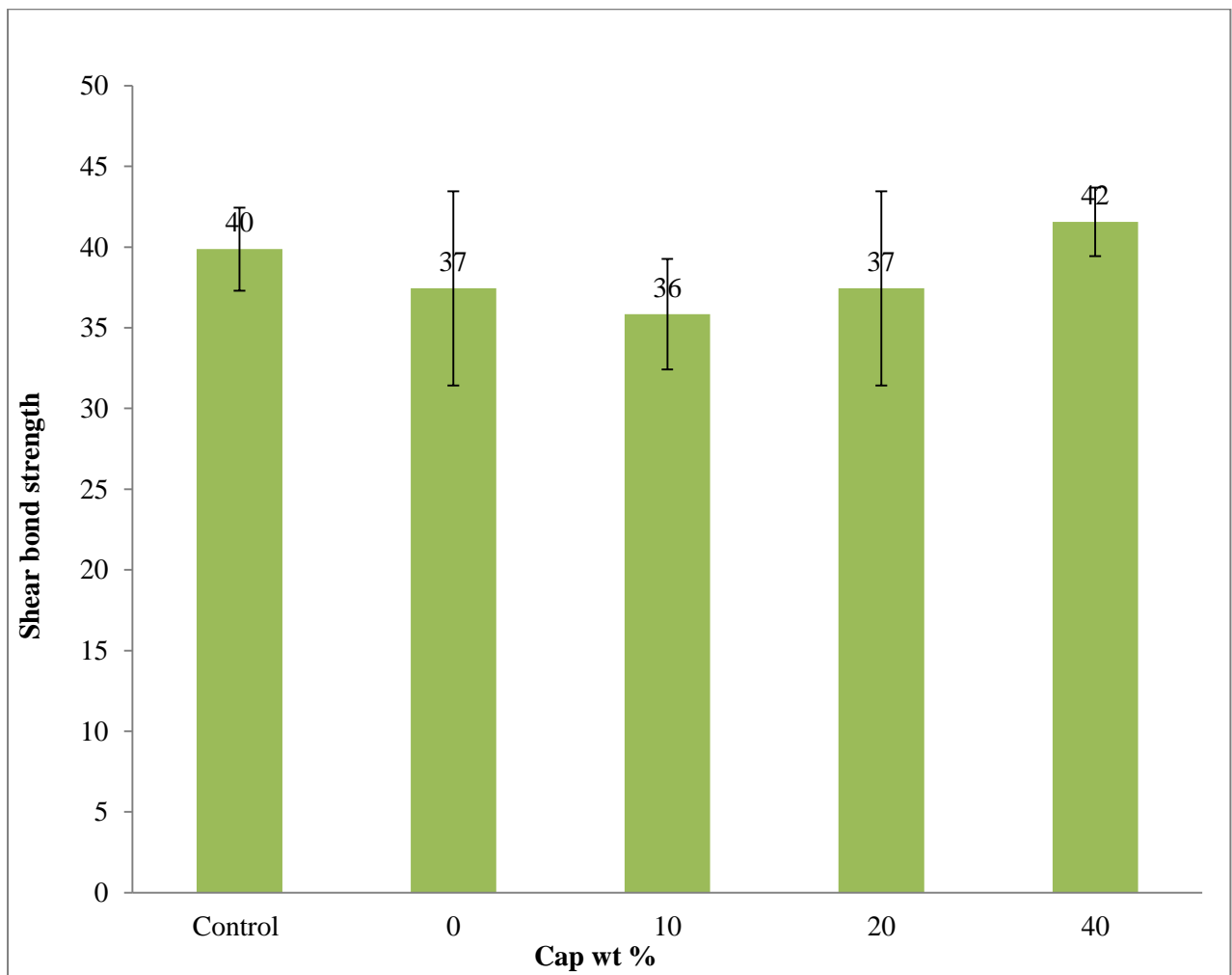


Figure 7-25 : Shear bond strength for wet ivory dentine for HEMA formulation with Cap (0, 10, 20 and 40 wt %), 5 wt % CHX and glass fibre in addition of control formulation and Ibond. The error bars represent 95% C.I of the mean (n=3).

The analysis of variance (ANOVA) showed that differences between HEMA formulations with different levels of CaP and self- adhesive agent Ibond were not significant ($P > 0.05$).

7.11. Discussion

The aim of this thesis was to develop composites with good handling properties, high monomer conversion and depth of cure, low shrinkage, water sorption induced expansion to compensate for shrinkage, CHX release, high strength and ability to bond to dentine without application of an adhesive.

The same monomers used in the control formulations in the previous chapter were used here for the reasons previously discussed. The PLR of the experimental composites was fixed at 3:1 for all formulations, as pastes with 20 or 40 wt % CaP and higher PLR were too dry.

7.11.1. Degree of conversion

The degree of conversion of experimental composites with CHX 0 wt % reactive CaP was on average ~ 76 %, which was slightly lower than control experimental formulations (~ 78 %). This is contrary to a previous study which showed that adding 5 wt % CHX in dental composites can improve degree of conversion (300). The formulations with HEMA again had slightly better conversion than the formulation containing adhesive monomer 4-META (Figure 7-2 and 7-3). This could be explained by HEMA improving the wetting of the filler phase and thereby reducing air incorporation and oxygen inhibition.

The results with HEMA but not 4-META indicate that CaP can reduce conversion. A possible explanation is that CaP reduces wetting, but 4-META aids in the dispersion of the CaP, thus counteracting, this problem. Despite the remineralising filler reducing conversion in the HEMA formulations, the overall degree of conversion of experimental composites with differing levels of CaP, however, was always significantly higher than commercial dental composites.

7.11.2. Polymerisation shrinkage

In the literature, conventional commercial composites were shown experimentally to have between 2 to 3.5 % shrinkage following polymerisation (89, 122). Previous studies showed that the polymerisation shrinkage of Z250 was 2.4 %. Another study found that the polymerisation shrinkage of Z250 was ~ 2 % (277, 301, 302). This particularly low shrinkage is the result of the high molecular weight monomer, high filler content and low conversion.

The Gradia dental composite has been reported to have slightly higher polymerisation shrinkage of about 2.7 %. This could be due to higher monomer volume fractions. It was reported in the literature that dental composites using pre-polymerised filler reduce the

shrinkage (257). This may not be true however if their use means higher monomer volume fractions are required (280).

One mole of polymerising C=C bonds usually gives a volumetric shrinkage of 23 cm³/ mol. Polymerisation shrinkage therefore increases proportionally with the amount of C=C present and the percentage conversion (204). Employing this concept, the polymerisation shrinkage of the control experimental formulations with HEMA or 4-META was calculated to be 3.8 % and 3.6 % respectively with conversion of 80 and 77 % respectively. The lower powder to monomer ratio 3:1 (required to enable high calcium phosphate addition in the next chapter) and higher monomer conversion are the primary reasons for these high calculated shrinkage. Wiliest Z250 contains ~ 18 wt % (~ 40 vol %) monomer, and the experimental materials contain 25 wt % (~ 45 vol %).

It is also known that replacing the high molecular weight bulk monomer Bis-GMA with a base monomer such as UDMA with enhanced molecular flexibility can lead to increased polymerisation shrinkage, due to an increase in the monomer conversion (255). PPGDMA, being of a higher molecular weight than TEGDMA, could potentially have decreased control experimental composite shrinkage. The higher conversion with PPGDMA, however, increases it.

The polymerisation shrinkage of experimental composites with 4-META or HEMA and different levels of reactive CaP (0, 10, 20, 40 wt %) were on average between 3.4 and 3.7 % respectively. This is higher than that of the commercial composites both in chapter 6 and the literature (89, 122). As discussed previously, this could be due to the higher conversion of the experimental formulations and could be attributed to lower filler loading. In general the experimental formulations with HEMA had slightly higher shrinkage than those with 4-META. This was due to HEMA giving a slightly higher degree of conversion. It should be noted that conversions provided are the polymerisation at 1 mm depth. Theoretically

polymerisation shrinkage is directly related to conversion, which is often reduced at greater depth. Placement of composite restorations in thick layers might reduce shrinkage in the lower part of the restoration as a result of lower conversion. Too low a conversion however, could cause cytotoxicity. Conversely if the top surface has a higher degree of conversion, surface properties such as hardness and wear resistance could be improved.

7.11.3. Depth of cure

The depth of cure is an important factor because it determines the number of steps clinicians must use when placing the restoration. Low depth of cure may lead to the elution of the monomer near the pulp cavity if the composite is placed in a thick layer. Factors affecting depth of cure include: the curing time distance between light tip and sample and composite colour shade (151). Increasing the distance between light tip and composite filling by more than 1 mm can decrease the intensity of light reaching the sample. Thus, increasing the curing time to more than 20 s in some filling restorations, such as class two inter proximal cavity, has been advised to ensure optimum polymerisation of the composites (270, 303). Additionally, dental composite manufactures recommend that the curing time should be increased to 40 and 60 s for bulk fill composites placed up to 5 mm in depth (304).

Experimental formulations with high levels of reactive fillers and 4-META had a higher depth of cure (~ 8 %) than those with HEMA formulations- except formulations with 40 wt % CaP which were similar. A possible explanation therefore is that 4-META interacts with the CHX thus reducing aggregation of the CHX particles and thereby reducing light scattering (261, 262). Furthermore, the formulation with HEMA and 0 % CaP had lower conversion than the HEMA control. Dental composites with small particles size (or less aggregation) reduce scattering of light and lead to higher depth of cure (36, 270).

The depth of cure of all experimental composites formulations containing different levels of CaP (0, 10, 20 and 40 wt %) and CHX all fulfilled the ISO 4049 requirement of 1.5 mm minimum depth of cure with 20 or 40 s light exposure. This was despite the depth of cure decreasing linearly with CaP increase from 0 to 40 wt % ($R^2 = 0.99$) (Table 7-1 and 7-2). The light transmission can be reduced as a result of light scattering, in turn caused by a mismatch in the refractive index of the monomer and filler phase (305) and this being further enhanced by particle aggregation. The refractive index of the powder components are 1.48, 1.52, 1.63 and 1.66 for glass, MCPM, TCP and CHX respectively (306). In the experimental formulations the glass and monomer are well matched, as mentioned in the previous chapter. The addition of increasing levels of TCP with CHX, however, is expected to enhance scattering. This explains the reduction in depth of cure with formulations with high CaP wt % in this study. Moreover, in all experimental formulations there was a significant increase in the depth of cure when the light exposure increased from 20 s to 40 s ($P < 0.05$) (Figure 7-6 and 7-7). This is in agreement with previous results (307, 308). Clinically inadequate degree of conversion and depth of cure are more likely in class two and deep class one cavities, where longer cure time is advised (309, 310).

7.11.4. Mass and volume change

The effect of fibre and chlorhexidine release will have limited effect on mass and volume changes because it's both are hydrophobic in nature and CHX percentage mass is relatively low and it is likely to be replaced in the bulk of the material by water of similar density.

The mass and volume change (water sorption) was enhanced by increasing CaP (MCPM and TCP) for HEMA or 4-META formulations. This is presumably due to the presence of highly soluble MCPM. Previous studies showed that adding combinations of MCPM and TCP increased mass and volume changes in resin composites (109, 198). Other studies, with added

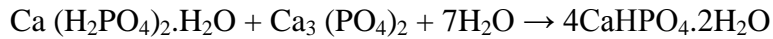
amorphous calcium phosphate (ACP), also exhibited increased water sorption (311). As expected, the experimental formulations with HEMA had higher water sorption levels than 4-META formulations. This was due to HEMA being more hydrophilic than 4-META (76).

The water sorption reached a maximum; after 3 months the increase continues at a slower rate. The experimental formulations with HEMA or 4-META with 10 and 20 wt % CaP were increased and reach maximum change at 2 months after which increase continues at a slower rate. This is probably due to the amount of CaP (MCPM) available in the sample, which encourage water sorption, having decreased. The highest observed mass and volume change in both formulations with higher CaP (40 wt % CaP) was probably due to having replaced silane treated glass with CaP. This may lead to poor wetting between polymer matrix and filler phase (312).

If water is expanding the polymer matrix phase, the percentage volume change should be comparable to the percentage mass change multiplied by the sample density. Alternatively, if water fills pores within the sample or air bubbles are generated, for example due to hand mixing or poor wetting of non-silane treated CHX and CaP, mass will increase but volume will remain unchanged. With experimental composites the ratio of volume divided by mass was less than the density for all formulations. This suggests some expansion, but also some pores filling.

A further complication affecting the mass and volume changes of reactive filler composite is that new products in the material bulk may have differing densities from reactants, causing porosities and reaction with or bind of water in new structures. Furthermore, water may replace fillers of higher density, causing a decrease in mass but negligible change in volume. The maximum water sorption was proportion to the CaP percentage. A Previous study has shown that water enables a MCPM reaction with TCP to form brushite (109).

The chemical reaction for brushite formulation is shown below:



This shows that each gram of MCPM requires 0.5 g of water to enable the formation of brushite in the composite (208). For the experimental composites this would correspond to a 1 wt % of CaP requiring 0.2 wt % increase in mass for full MCPM reaction. From gradients of maximum change in mass versus CaP in Table 7-3 and 7-4, ~ 30 to 60 % of the water required to provoke the transformation for all MCPM into brushite is therefore absorbed irrespectively of CaP concentration. The unreacted MCPM might be released to enhance remineralisation. Previous studies confirmed that dental composites containing CaP need adequate water sorption to release the Ca and PO₄ ions for remineralisation (109, 198).

According to Fick's law of diffusion:

$$\frac{\Delta M_t}{\Delta M_{t \rightarrow \infty}} = 2 \sqrt{\frac{Dt}{\pi l^2}} \quad \text{Equation 7-5}$$

D is the diffusion coefficient of water into the composite (cm² s⁻¹), t is time (s), l is sample thickness (cm). Combining this with equation 7-6 and 7-7 gives:

$$\frac{0.006}{0.11} (hr)^{0.05} = 2 \sqrt{\frac{D}{\pi l^2}} \quad \text{Equation 7-6}$$

$$\frac{0.0032}{0.06} (hr)^{0.05} = 2 \sqrt{\frac{D}{\pi l^2}} \quad \text{Equation 7-7}$$

After correcting the use of h instead of seconds and as the sample has a thickness of 0.1 cm, this gives D= 6.5 × 10⁻⁹ cm² s⁻¹ for formulations with HEMA and 6.2 × 10⁻⁹ cm² s⁻¹ for 4-META formulations. This is in the range expected, based on a previous study of water sorption of resin composite (214). The data above indicates that this diffusion coefficient is

independent of CaP content. This suggests the structure of the monomer phase is crucial in determining the early rate of water sorption, whilst the level of CaP determines the final amount.

The formulations with HEMA and 4-META with 10 and 20 wt % CaP expand by 2.5 and 3.9 vol % and 2.6 and 3.4 vol % respectively upon maximum water sorption. This expansion compensates for the 3.7 and 3.5 % polymerisation shrinkage which occur after curing in HEMA and 4-META formulations respectively. However, the expansion of these formulations with 40 wt % CaP was higher than the average polymerisation shrinkage (3.5 %), which could potentially crack the tooth. Excessive water sorption can also lead to the deterioration of composite's mechanical properties (313).

7.11.5. Chlorhexidine release

The lack of antibacterial activity in the current dental composites can enable bacterial growth at margins of tooth restorations, secondary caries and decreased restoration longevity (36). There have been several attempts to develop dental composites with added antibacterial agents to combat these problems (184). Chlorhexidine (CHX) has previously been incorporated into dental filling materials, such as GIC and RMGIC to improve their antibacterial properties (184, 189, 199, 314, 315). Previous studies also showed that even a low release of CHX from filling materials significantly reduce acidogenic bacteria such as *Streptococcus. mutans*, biofilms formation, and lactic acid production (184).

For this thesis, the initial CHX release for experimental formulations with CaP was proportional to the square root (SQRT) of time, as expected for diffusion controlled processes (Figure 7-10 and 7-11). Increasing the CaP levels substantially increased the release of CHX in both HEMA and 4-META formulations, which agrees with a previous study (198). This might be due to higher water sorption upon increasing the CaP levels. According to several

other studies, water sorption encourages CHX to be released more readily from composites (315, 316). The absorbed water dissolves the solid CHX, enabling its release into the surrounding environment. Water sorption could also, however, make the polymer more flexible allowing the release of more CHX.

With high CaP, CHX release continued for several months despite water sorption reaching equilibrium within 1 month. Release from experimental formulations with 0 and 10 wt % CaP continued until 1 and 2 months respectively, whilst release from formulations with 20 and 40 wt % CaP continued to 3 and 4 months respectively. The reduction of CHX release over time might be due to the decreased water sorption abilities of these formulations. The initial release of CHX is particularly important for elimination of unremoved acidogenic bacteria during the restoration procedure (317). Longer term CHX release from composites may help decrease occurrences of secondary caries. Moreover, CHX release for a prolonged time might also protect the smear layer from collagen degrading enzymes (318).

For a diffusion controlled process the mass of drug released would be expected to be given by:

$$\frac{R_t}{R_{t \rightarrow \infty}} = 2 \sqrt{\frac{Dt}{\pi l^2}} \quad \text{Equation 7-8}$$

Where R_t is initial gradient of drug release and $R_{t \rightarrow \infty}$ is final release. D is the diffusion coefficient of drug from the composite ($\text{cm}^2 \text{s}^{-1}$), t is time (s), l is sample thickness (cm)

From Table 7-5 and 7-6

$$\frac{0.0054}{0.27} (hr)^{-0.5} = 2 \sqrt{\frac{D}{\pi l^2}} \quad \text{Equation 7-9}$$

$$\frac{0.0059}{0.41} (hr)^{-0.5} = 2 \sqrt{\frac{D}{\pi l^2}} \quad \text{Equation 7-10}$$

The diffusion coefficients D for CHX release were therefore $8.7 \times 10^{-10} \text{ cm}^2 \text{ s}^{-1}$ for formulations with HEMA and $4.6 \times 10^{-10} \text{ cm}^2 \text{ s}^{-1}$ for 4-META formulations. The difference

may be caused by the more hydrophilic nature of HEMA compared to hydrophobic 4-META (214, 319). The present findings are consistent with previous research which found that adding CHX in dental composite with increased HEMA lead to an increase in CHX release (198).

7.11.6. Biaxial flexure strength and modulus

The experimental formulations with added glass fibre and CHX each at 5 wt % had BFS decreased by ~ 30 MPa compared to control formulations. As the fibres are silane treated they are unlikely to have been the main cause of this reduction. Factors such as chemistry, fibre dimensions and concentration of fibre may all play an important role in the mechanical properties (121, 122, 128). Some studies showed that fibre incorporated at low levels improves mechanical properties (224, 320). Conversely, other studies found that fibre may cause stress points or crack initiation sites resulting in decreased mechanical properties (129). Previous studies however, have found that 5 % CHX decreased mechanical properties (321).

Further replacement of silane coated glass with increasing CaP (MCPM and TCP) (10, 20 and 40 wt %) caused further decline in dry flexure strength. The reduction observed with dry formulations is presumably due to the lack of coupling agent between the CaP filler and matrix. Having no chemical bond between the filler and resin is a key factor responsible for decreasing the mechanical properties of dental composites (9, 198). All the experimental formulations showed a much greater decline in BFS and modulus after 24 h and 7 days of immersion in water. The decline in mechanical properties upon addition of CaP is most likely due to the solubility of MCPM encouraging further water sorption. The water can penetrate into polymer network; consequently, the swollen and plasticized polymer network and reduce mechanical properties (158, 174). Furthermore, it is well known that silane coating glass filler

enhances mechanical properties (322, 323); they provide both a chemical bond between matrix and filler and enhancing wetting of filler particles to prevent air entrapment. More air bubbles were seen in formulations with 20 and 40 wt % CaP than with lower levels. The level of porosity has been previously shown to correlate with the mechanical properties (324). Moreover, this result was in agreement with previous studies where it was found storing dental composites in water for 24 h resulted in decreased strength (198, 325).

Hand mixing of experimental composites is also thought to be a major source of porosity and variability in porosity. In commercial materials this can be overcome partially via machine centrifugal mixing and/or vacuum mixing. Reducing PLR can help with particle wetting. This is why, in preliminary studies, better strength was observed with PLR of 3 rather than 4 and why the former was chosen for the experimental materials

Generally, the greatest rate of decline in strength upon water immersion was observed in the first 24 h. This is due to the greater water sorption and faster component release over this period. Upon immersion in water, formulations with CHX but no CaP declined in strength less with HEMA than with 4-META formulations. This might be attributed to water sorption negating the benefit of 4-META interaction with CHX. CHX release can lead to the formation of holes upon drug release (214). The level of release, however without CaP is small in this thesis study.

The factors which control the decline in strengths upon water immersion with the reactive fillers are more complex. It is known that MCPM readily dissolves in water, which can contribute to the deterioration in strength of the composite (109). In addition to greater water sorption, MCPM and CHX release increase upon increasing CaP addition, however, the reaction between MCPM and TCP to form brushite may bind water. This could reduce the amount of water infiltrating into the polymer network. Additionally, greater volumes of

brushite could enable filling of holes caused by component release. This could reduce the negative effects of water sorption and component release on strength.

The modulus of dental composites is dependent on the modulus and volume fraction of each phase (326). Moreover, the level of porosity is also correlated with the modulus (324). A strong proportional co-relation has been found between the inorganic weight percent in the resin composite and modulus of the materials, which could explain the higher modulus of the experimental composites than commercial composites. It has been also shown that the modulus of materials increases with increase the monomer conversion of dental composites (327).

Furthermore, the manufacture composition is difference between the same resin composite such as particles size and shape of inorganic filler and kind monomer might influence the mechanical properties of formulations (328).

In the above thesis there was a strong correlation between modulus and strength. This is due to factors such as pores and water sorption, which reduce strength and having a similar effect on modulus. High strength is important to reduce fracture and low modulus can increase resilience and energy absorption.

7.11.7. Push out test

Good bond strength between composite restoration and tooth structure is important for increasing the longevity of the filling restorations (76). With current materials there is evidence of insufficient marginal sealing between the composite and tooth structure (86). This study was therefore carried out to assess if experimental composites containing adhesive monomer 4-META or HEMA and CaP might overcome these issues. The push out test simulates the clinical condition more closely than in shear tests because it constraint the curing composite and the associated polymerisation stress (72).

7.11.7.1. Dry ivory

The push out stress of experimental formulation containing 0 wt % CaP (CHX and glass fibre at 5 wt %) showed the lowest push out stress with and without acid etching. This could be attributed to the lack of adhesion promoting components in this formulation. Upon adding CaP, an increase in the push out stress was showed. The push out stress of experimental formulations with adhesive monomers 4-META or HEMA containing 40 wt % CaP showed the highest push out stress to acid etched ivory dentine. This is due the dentine being acid etched, which exposes dentinal tubules and allowing greater penetration of experimental composites into the demineralised dentine surface (46), and enhance interlocking between composites and dentine.

From Tables 7-11 and 7-12 the intercept of dry ivory dentine showed that experimental formulations with 4-META had 1.5 times higher of bonding to ivory dentine when the surface was etched with phosphoric acid for 20 s and 1.9 time higher bonding for non-etched, when compared to HEMA formulations. This is due to is 4-META being hydrolysed to provide two carboxylic acid group attached to the aromatic ring, resulting lower pH (76). This is considered sufficient for satisfactory etching potential; it also demineralises the dentine to allow the composite to infiltrate into dentinal tubules and offers some micromechanical interlocking. On the other hand, the gradient also showed that 4-META formulations had 3 times higher debonding stress versus CaP levels.

7.11.7.2. Wet ivory dentine

With controlled hydration ivory dentine, the push out stress bond strength increased significantly for both experimental formulations, compared to dry ivory dentine. In 2000 Van Dijken demonstrated that the degree of composite penetration is improved by keeping dentine wet to ensure optimal resin permeability. Formulations with 0 wt % CaP showed the lowest bond stress to acid etched wet ivory dentine and slightly higher than control

formulations. With increasing the CaP level a significant increase in the push out stress was experienced. This could be due to the CaP's ability to remineralise the hydrated ivory dentine and help bind with collagen. On average the results also showed that experimental formulations with 4-META had better bonding to ivory dentine when the surface was etched with phosphoric acid for 20 s (160 MPa) in comparison to HEMA formulations (124 MPa). With no acid etching the push out strength for 4-META formulations was 55 % higher than HEMA formulations. It is believed that anhydride group in the 4-META formulations is hydrolysed to provide two carboxylic acid groups. It is proposed that these may partially demineralise the dentine to allow some micromechanical interlocking, but in addition enable a chemical bond with calcium in the remaining hydroxyapatite. Furthermore, it may bond with basic amino acid groups in the collagen (291).

7.11.7.3. Experimental formulations using self-adhesive Ibond

Using the self-adhesive agent Ibond significantly increases the push out stress by 40 % for the 4-META formulation and 22 % for HEMA formulation when compared to wet ivory dentine. Replacing HEMA with 4-META increased the push out stress by ~ 30 %. A possible explanation is that the 4-META in the composite and adhesive binds to the CaP phases enabling greater interactions between the different interfaces. The increased hydrophilicity of the composite might also enable greater interaction and wetting of the adhesive layer.

This was the result of the carboxylic acid group in 4-META forming within Ibond in the presence of water. These groups could potentially further demineralise the ivory dentine to allow further penetration of composites, more mechanical interlocking and chemical bond with calcium in the remaining hydroxyapatite (329). The solvent evaporates after air drying and adhesive curing which additionally provides chemical bonds with the monomer in dental composites. Moreover, the low viscosity of the adhesive agent allows deep penetration into the dentinal tubules (330). The push out stress for 4-META formulations with high level of

CaP (40 wt %) was exceeded the 3000 N and caused the ivory dentine sample to break instead of pushing the composite.

7.11.8. Shear bond strength

The addition of CHX (0 wt % CaP) had negligible effect on shear bond strength. The shear bond strength of 4-META or HEMA formulations with different levels of CaP and a fixed percent of CHX increase, compared to control and commercial composites.

The formulation containing 4-META and CaP displays a significant increase in shear bond strength with and without acid etching (65 and 51 % increase respectively): more than formulations with HEMA and different level of CaP. The bond strength was increased linearly with an increase in CaP levels for both formulations. The experimental formulations with HEMA and 4-META and high level of CaP (40 wt %) had the highest bond strength across the formulations. Generally the shear bond strength was similar to the push out results. Using the self-adhesive agent Ibond significantly improved the shear bond strength for all experimental formulations. The shear bond strength for experimental formulations HEMA and 4-META, and the effect of CaP 0, 10, 20 and 40 wt % was similar to the push out stress.

8. Conclusion

The goal of this research study was to develop a self-adhesive dental composite that is easier to place and has the potential to reduce bacterial microleakage to prevent recurrent caries compared to current composite filling material available in the market. The results of experimental and commercial dental composites allow for a better understanding of the behaviour of these materials in terms of conversion, shrinkage, water sorption, CHX release, mechanical properties and adhesion to ivory dentine.

The literature review of dental composites in the first chapter indicated that the current dental materials have a low conversion and that the uncured monomers that leach can from the filling restoration over time contain levels of residual monomer. In addition, high polymerisation shrinkage leads to gap formation and secondary caries, which is believed to be the main reason for current composite filling restoration failure. The problem is enhanced by lack of antibacterial and remineralising properties.

8.1. Commercial and control composites

The commercial composites Z250, Ecusphere and Gradia were first compared with control experimental composites containing solely glass particles as control.

The result of the first study showed that control experimental composites with UDMA as the main monomer and PPGDMA as diluent gave higher monomer conversion than the commercial composites. The polymerisation shrinkage however, determined by degree of conversion and composition was slightly higher than observed experimentally in the literature. Commercial Z250 and HEMA control composites had higher mass and volume change, followed by Gradia. The control formulation with 4-META and Ecusphere had the

lowest levels of water sorption. Expansion due to water sorption was insufficient to balance polymerisation shrinkage entirely.

Commercial Z250 and control 4-META composites provided the highest BFS and modulus both dry and after immersion in water for up to 28 days. These were followed by HEMA and Ecusphere composites. Gradia posterior had lower BFS and modulus.

Applying phosphoric acid gel for 20s increased adhesion ability of control experimental and commercial composites to dry and wet ivory dentine. Replacing HEMA with the acidic adhesive monomer 4-META gave formulations higher dentine bonding with and without acid etching than commercial dental composites based on mixed dimethacrylate monomer. Using wet dentine or the self-adhesive Ibond significantly increased the dentine bond strength of control and commercial composites.

8.2. Experimental formulations with CaP and CHX

In the second study, experimental composite formulations containing the same monomer, but in addition partial replacement of the glass filler particles by calcium phosphate (MCPM and TCP) (0, 10, 20 or 40 wt %), chlorhexidine diacetate (CHX 5 wt %) and glass fibre (5 wt %) were evaluated. High monomer conversion (76 %) was achieved with almost negligible effect of both CHX and CaP being observed. Calculated polymerisation shrinkage for experimental formulations was ~ 3.6 %. This was comparable to that obtained experimentally for current flowable dental composites but more than for conventional composites.

The experimental composites formulations with CaP (0, 10, 20 and 40 wt %) and CHX exceeded the required ISO 44049 depth of cure after 20 and 40 s curing. Increasing the CaP from 0 to 40 wt % for both experimental formulations decreased the depth of cure linearly after curing for 20 or 40 s.

Incorporating CaP (MCPM and TCP) with CHX enhance water sorption and enabled greater antimicrobial CHX release into deionised water. The experimental formulations with HEMA had higher CHX release and water sorption. Water sorption induced expansion of experimental composites, which can compensate for polymerisation shrinkage. Increased CaP caused a detrimental linear decline in BFS with dry and wet samples. Decreased strength however correlated with a decline in modulus which would raise resilience.

One of the more significant findings to emerge from this study is that adding 4-META at 5 wt % improved bonding to ivory both with and without acid treatment, compared to HEMA. Replacing HEMA with the acidic adhesive monomer 4-META significantly increased the dentine bonding both with and without acid etching. Increasing the CaP from low to high levels could work synergistically with 4-META, further increasing the bonding to ivory dentine. Applying Phosphoric acid for 20 s also significantly increases adhesion to dry and wet ivory dentine, more so than non-etching. Moreover, the bonding to ivory dentine was doubled with controlled hydration ivory dentine samples. Using the self-adhesive Ibond also significantly increased the dentine bonding for all formulations.

In summary, this thesis has shown that experimental composite formulations with 4-META or HEMA could be an excellent alternative to current dental composites available in the market. These experimental composites might overcome the concerns surrounding polymerisation shrinkage, microleakage, and secondary caries as well as promote antibacterial action and remineralisation of the dentine. The mechanical and adhesion test was carried out by and confirmed by the industrial company DMG which concluded with a similar result as this thesis.

9. Future work

This study investigates degree of conversion, polymerisation shrinkage, and depth of cure, water sorption, antibacterial CHX release, mechanical properties and adhesion to ivory dentine. There are other properties should be investigated.

1. Biocompatibility and stability

Dental composites should be not toxic to the oral tissue. The biocompatibility of experimental composite formulations should be investigated. Uncured monomers that leach from resin composite over time may cause cytotoxicity. This leaching from set composite samples soaked in water could be measured by High Performance Liquid Chromatography (HPLC). This would give some idea of the species leached after polymerisation. Cell studies would then be required to assess levels of these components that are toxic.

2. Polymerisation shrinkage

Polymerization shrinkage for experimental formulations was calculated in this project but was not measured. Shrinkage has been found via a density bottle method use of a balance and density kit or computer controlled mercury dilatometer method. The measurement of shrinkage by one of these methods should be performed to fully evaluate the shrinkage calculation method.

3. Change in calcium and phosphate chemistry

The remineralisation properties of experimental composites described in this thesis should be investigated by the chemical change of calcium phosphate species on set material surfaces upon simulated body fluid immersion assessed using Raman spectroscopy or X-ray diffraction (XRD). Furthermore, calcium and phosphate release into water could be assessed using ion chromatography. Raman and SEM could also be

used to understand the effect of acid treatment on ivory and to check any change in hydroxyapatite content.

4. Antibacterial effect

The antibacterial activity of the experimental composite formulations developed in this thesis should be evaluated in addition to drug release kinetics. For example, the effect of samples on the growth of oral biofilms or bacteria penetration under the restoration could be monitored using in vitro models. Moreover, antibacterial characteristics could be assessed using agar diffusion tests and a biofilm forming constant depth film fermentor (CDFF).

5. Mechanical properties

The experimental formulations being developed in this project require further assessment of mechanical properties for more prolonged time. In addition, other mechanical properties such as compressive strength and surface hardness should also be evaluated.

6. Adhesion

The adhesion properties shear and push out test of experimental formulations should be evaluated using human teeth, sound and carious enamel and dentine, and compared with the results found with ivory dentine. Cyclic loading of the adhesive bond and the ability to self-repair due to remineralisation also requires study.

10. List of presentations and publication

- Ben Nuba H, Young A. Assessment of Self-adhesive and re-mineralising dental composites proceeding of Biomaterials and Tissue Engineering Division UCL 17 - July 2013.
- Ben Nuba H, Bozec L, Ashley P, Young A. Self-adhesive, low shrinkage, re-mineralising and high strength dental composites. Proceedings of UAE International Dental Conference & Arab Dental Exhibition AEEDC, Dubai, United Arab Emirates 4-Feb- 2014.
- Ben Nuba H, Bozec L, Ashley P, Young A. Development of self-bonding, re-mineralising antibacterial dental composites. Proceeding of IDAAR general session, Cape Town, South Africa 28-Jun- 2014.
- Liaqat S, Aljabo A, Khan M, Ben Nuba H, Ashley P, Bozec L, Young A (2015). Characterization of Dentine to Assess Bond Strength of Dental Composites. *Materials*, 8(5), 2110-2126.
- Ben Nuba H, Liaqat S, Ashley P, Bozec L, Young A. High strength, Self-adhesive Dental Composites with Reactive Calcium Phosphate and Calcium binding Monomer in preparation.

11. Appendices

11.1. Appendix 1 (Preliminary work)

11.1.1. Biaxial flexural strength test

- **Series one formulations**

The first series contained UDMA, PPGDMA and 4-META or PMDM monomers in fixed ratio 68:25:5 by weight percent. CQ and NTGGMA were both at 1 wt % of the monomer phase. The filler contained equal weight % of CHX and glass fibre fixed at 5 wt %. Equal weights of TCP (306S) and MCPM were also incorporated in the filler. Their combined level was 40 or 10 wt % of the filler phase. The glass particle filler used was IF2019 glass from Sci Pharm. This made up the remainder of the glass particles and was therefore added at a level of 50 or 80 wt % in all powders. The powder liquid ratio (PLR, w/w) was 4:1 or 3:1. The variables used in series one formulations are given in Table 11-1.

Figure 11-1: Variables for series one formulations.

Variables	High (+1)	Low (-1)
PLR	4:1	3:1
Adhesive monomer	4-META	PMDM
CaP wt %(TCP+MCPM)	40	10

- **Series two formulations**

Series two formulations were identical to series one in except:

- 1) BAG glass of 7 μm (DMG) replaced IF2019 (Sci Pharm) glass. These 2 glasses are similar in chemical composition and particle size but from different manufacturers.

- 2) Two types of TCP were used; TCP 306S with average particle size 4.3 μm and TCP 292S with particle size 16 μm .
- 3) The powder liquid ratio (PLR) was fixed at 3:1.
- 4) HEMA replaced PMDM.

Table 11-1: Variables for series two formulations.

Variables	High (+1)	Low (-1)
TCP particle size	292S	306S
Adhesive monomer	4-META	HEMA
CaP wt % (TCP+MCPM)	40	10

11.1.2. Formulations for push out adhesion test

- **Series three formulations**

Series three formulations were identical to series two except the TCP was fixed as 306S. The first variable was instead etching versus non etching of ivory. Variables are summarised in Table 11-3. In this table etching indicates 20 s application of 37 % phosphoric acid gel, rinsing and drying of ivory prior to cavity restoration. The powder liquid ratio was fixed at 3:1 and BAG glass employed.

Table 11-2: Variables factors for series three formulations (etching with 37 % phosphoric acid or no etching).

Variables	High (+1)	Low (-1)
Etching	20 s	0
Adhesive monomer	4-META	HEMA
CaP wt % (TCP+MCPM)	40	10

- **Series four formulations**

Series four formulations were identical to series three except the HEMA was replaced by PMDM and the phosphoric acid gel etching was applied for 20 s or 120 s. Variables are summarised in Table 11-4.

Table 11-3: Variables factors of series four push out test (etching of ivory dentine for 20s or 120 s with 37% phosphoric acid).

Variables	High (+1)	Low (-1)
Treatment	120 s	20 s
Adhesive	4-META	PMDM
TCP+MCPM	40	10

11.2. Factorial analysis

In order to investigate the effect of more than one independent variable simultaneously, this study used a factorial experimental design. This type of Factorial analysis is frequently used in dental research (331-333). The advantage of multiple variables design is that it can provide some unique and relevant information about how variables interact or combine in the effect they have on the dependent variable. In addition, it allows demonstration of the effect of increasing each variable from a low to a high value whilst minimizing the number of samples for the experiment. In the full factorial design, formulations with every possible combination of variables are investigated with three variables at 2 level there are then 8 samples to be tested. For each variable, 4 of the samples will have low variable values and the other 4 high variable values as in (Table 7). C1 to C4 all have F for the first variable equal to +1 but two each of +1 and -1 for variable 2 and 3. The effect of variable 1 can therefore be obtained by comparing the average outcome for sample C1 to C4 with that for C5 to C8. Similarly, comparing the average outcome for samples C3, C4, C7 and C8 with that of C1, C2, C5 and

C6 gives the effect of variable 2, and so on. Interaction between variable 1 and 2 is obtained from the average of C3, C4, C5 and C6 compared with that of C1, C2, C7 and C8.

Figure 11-2: Variable combinations for a two level factorial experimental design involving three variables. +1 and -1 refer to high and low values of the variable respectively.

Sample	Variable 1 F ₁	Variable 2 F ₂	Variable 3 F ₃	Interaction F ₁ F ₂	Interaction F ₁ F ₃	Interaction F ₂ F ₃	Interaction F ₁ F ₂ F ₃
C1	+ 1	+1	+1	+1	+1	+1	+1
C2	+ 1	+1	- 1	+1	-1	-1	-1
C3	+ 1	-1	+1	-1	+1	-1	-1
C4	+ 1	-1	-1	-1	-1	+1	+1
C5	- 1	+1	+1	-1	-1	+1	-1
C6	- 1	+1	-1	-1	+1	-1	+1
C7	- 1	-1	+1	+1	-1	-1	+1
C8	- 1	-1	-1	+1	+1	+1	-1

The results are mathematically analysed using the following equation below

$$P = \langle P \rangle + S_1 a_1 + S_2 a_2 + S_3 a_3 + S_1 S_2 a_{12} + S_1 S_3 a_{13} + S_2 S_3 a_{23} + S_1 S_2 S_3 a_{123}$$

Equation Figure 11-3: Simple factorial expressions for 3 variables at 2 levels

S₁, S₂ and S₃ take values of +1 or -1. a₁, a₂ and a₃ indicate the magnitude of the effect of 3 variables. The other “a” terms indicate levels of variable interaction.

$\langle P \rangle$ is the arithmetic mean result for all 8 possible formulations. a_i quantifies the average effect of changing variable ‘I’ and a_{i,j} and a_{i,j,k} are two and three variable interaction terms.

These were calculated using:

$$2a_i = \langle P \rangle_{F=+1} - \langle P \rangle_{F=-1}$$

$$2a_{ij} = \langle P \rangle_{F_i F_j = +1} - \langle P \rangle_{F_i F_j = -1}$$

$$2a_{ijk} = \langle P \rangle_{F_i F_j F_k = +1} - \langle P \rangle_{F_i F_j F_k = -1}$$

$\langle P \rangle_{F=+1}$ and $\langle P \rangle_{F=-1}$ are the arithmetic mean values of P for all four samples with F_i equal to +1 and -1 respectively. 95 % confidence interval error bars for 2a parameters were calculated assuming $C.I = 1.96 \times S.D/\sqrt{n}$. n is the number of repetitions of the full set of 8 samples in the experiment design. If these error bars cross zero, the variable 'i' has no significant effect on the property.

11.3. Results

11.3.1.1. Biaxial flexural strength Results

- Series one formulations

The average series one BFS for 4-META and PMDM formulations with 10 and 40 wt % CaP are given in Figure 11-1(a). Factorial analysis in Figure 11-1 (b) indicated no significant effect upon replacing 4-META by PMDM as the error bar for "a1" crossed zero. Furthermore, interaction effects between variables were not experimentally significant. It can be seen however that increasing CaP to 40 wt % decreased the BFS on average by 33 MPa (equal to a2) compared to 10 wt % CaP formulation. PLR 4:1 decreased the BFS by ~ 11 MPa (equal to a3) as compared to 3:1.

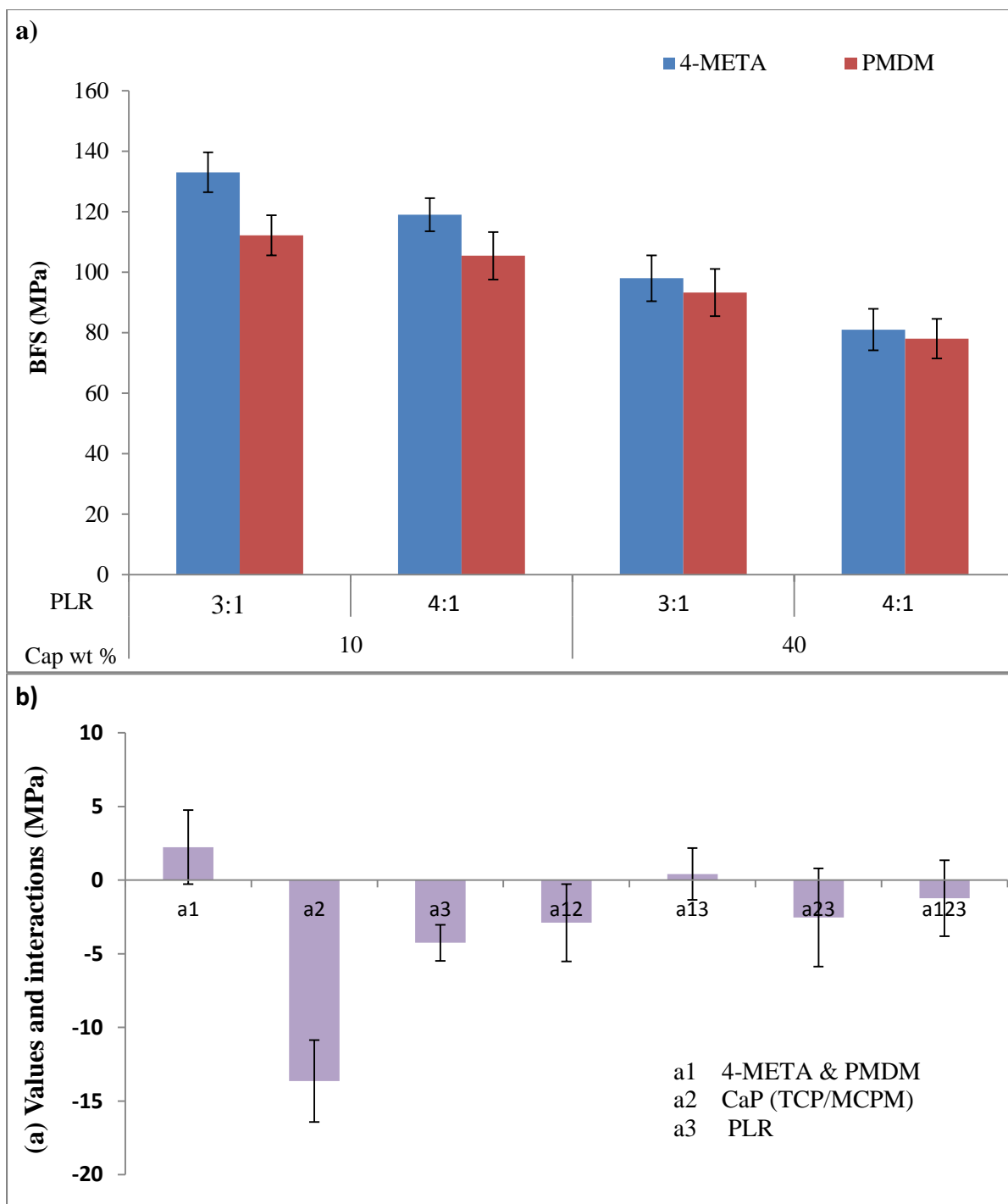


Figure 11-4: a) Biaxial flexure strength of series one formulation with variables 4-META/PMDM, TCP/MCPM and PLR. The errors represent 95% C.I of the mean (n=6). b) Factorial analysis of series one formulations. a1 is 4-META / PMDM, a2 CaP (MCPM / TCP,40 or 10 wt %) and a3 is PLR.

- **Series two formulations**

The average series one BFS for 4-META and HEMA formulations with 10 and 40 wt % CaP and different TCP particles size are given in Figure 11-2 (a). Data from this figure showed that the strength decreased on average by ~ 29 MPa on raising CaP wt %. The factorial analysis indicates the effect of the TCP particle size (a2) is small and 4-META versus HEMA (a3) is negligible. Furthermore, there were clearly no experimentally significant interaction effects between any of the variables (Figure 11-2 b).

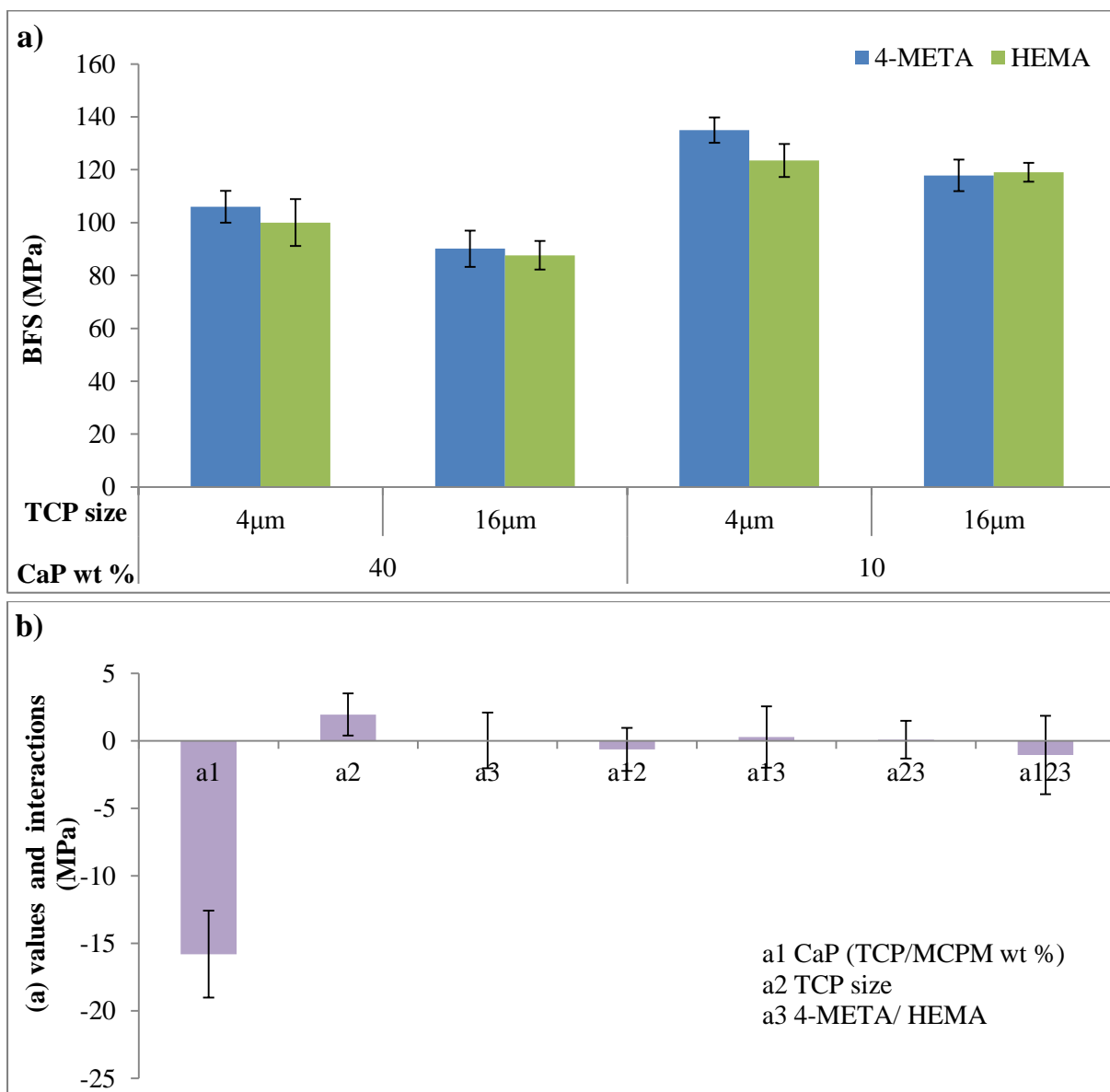


Figure 11-5: a) Biaxial flexure strength of series two formulation with variables 4META/ HEMA, CaP (TCP/MCPM) and TCP particles size. b) Factorial analysis of series two formulations. a1 is CaP (MCPM / TCP,40 or 10 wt %), a2 TCP size and a3 4-META / HEMA is PLR. The errors represent 95% C.I of the mean (n=6).

11.3.1.2. Push out Adhesion test

- **Series three formulations**

The push out test for series three results are provided in Figure 11-3 a. it can be seen that the formulations with 4-META shows better adhesion as compared to HEMA formulations. High level of CaP 40 wt % increases the debonding stress by ~ 61 MPa as compared to low level CaP 10 wt %. The most significant result was the effect of acid etching with 37 % phosphoric acid for 20 s. Factorial analysis (Figure 11-3 b) indicated significant effects for all three variables.

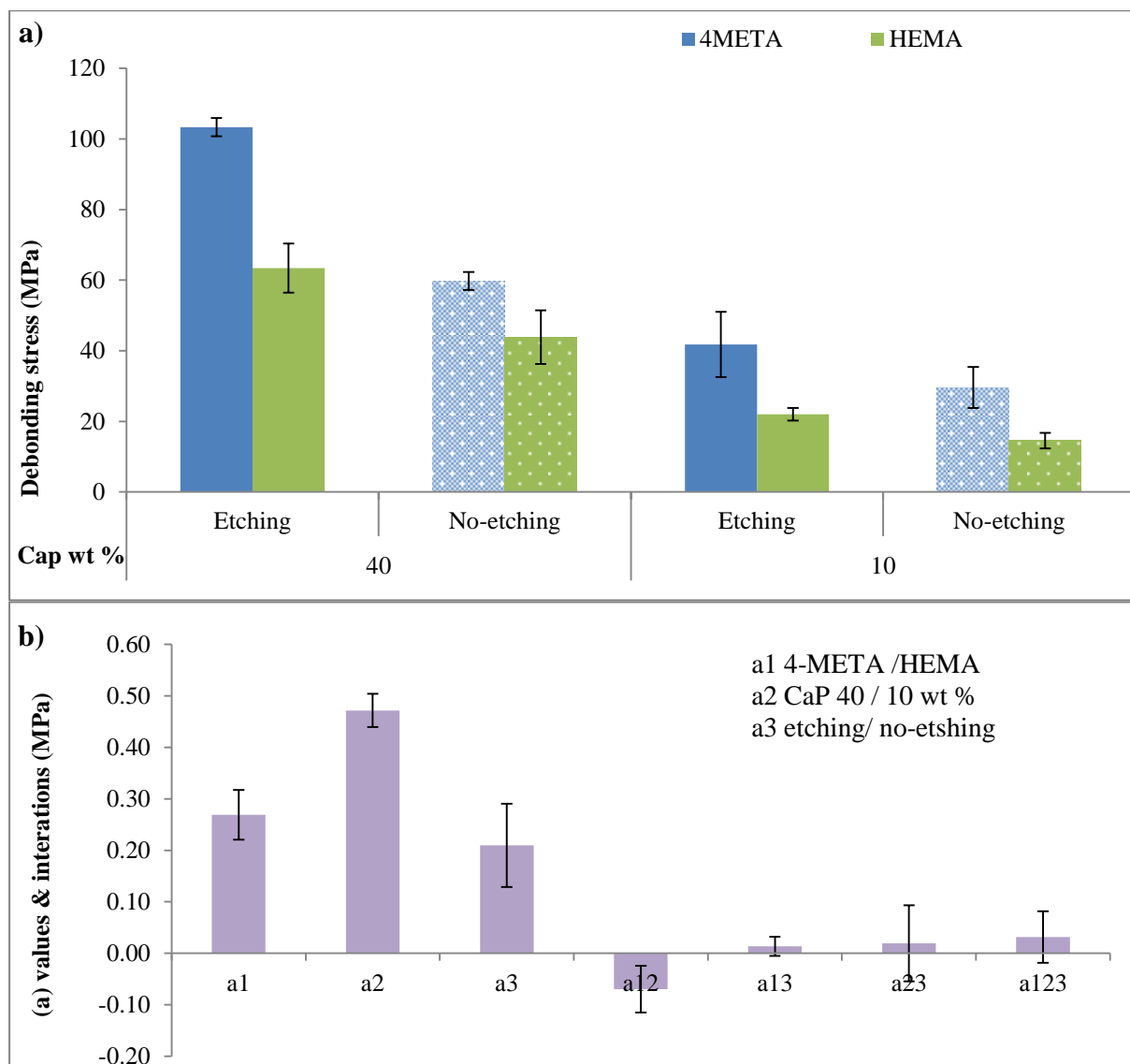


Figure 11-6: a) Push out stress for series three formulations with variables 4-META/ HEMA, CaP (40 and 10 wt %) and etching and non-etchingfor 20 s. b) factorial analysis for series three formulations a1 is 4-META / HEMA, a2 is CaP MCPM / TCP (40 or 10 wt %) and a3 is etching / non-etching phosphoric acid . The error bars showing 95 % confidence interval (n=3).

- **Series four formulations**

The push out test results for series four in Figure 11-4 a shows that the formulations with high CaP have higher bond strengths to ivory dentine as compared to formulations with low CaP. The factorial analysis in Figure 11-4 b indicated significant effect for 4-META versus PMDM (a1) and CaP levels as the error bar dose not cross zero. However, the effects of etching time for 20 and 120 s (a3) was smaller than the 95 % C.I error bar. Furthermore, there were clearly no experimentally significant interaction effects between any of the variables.

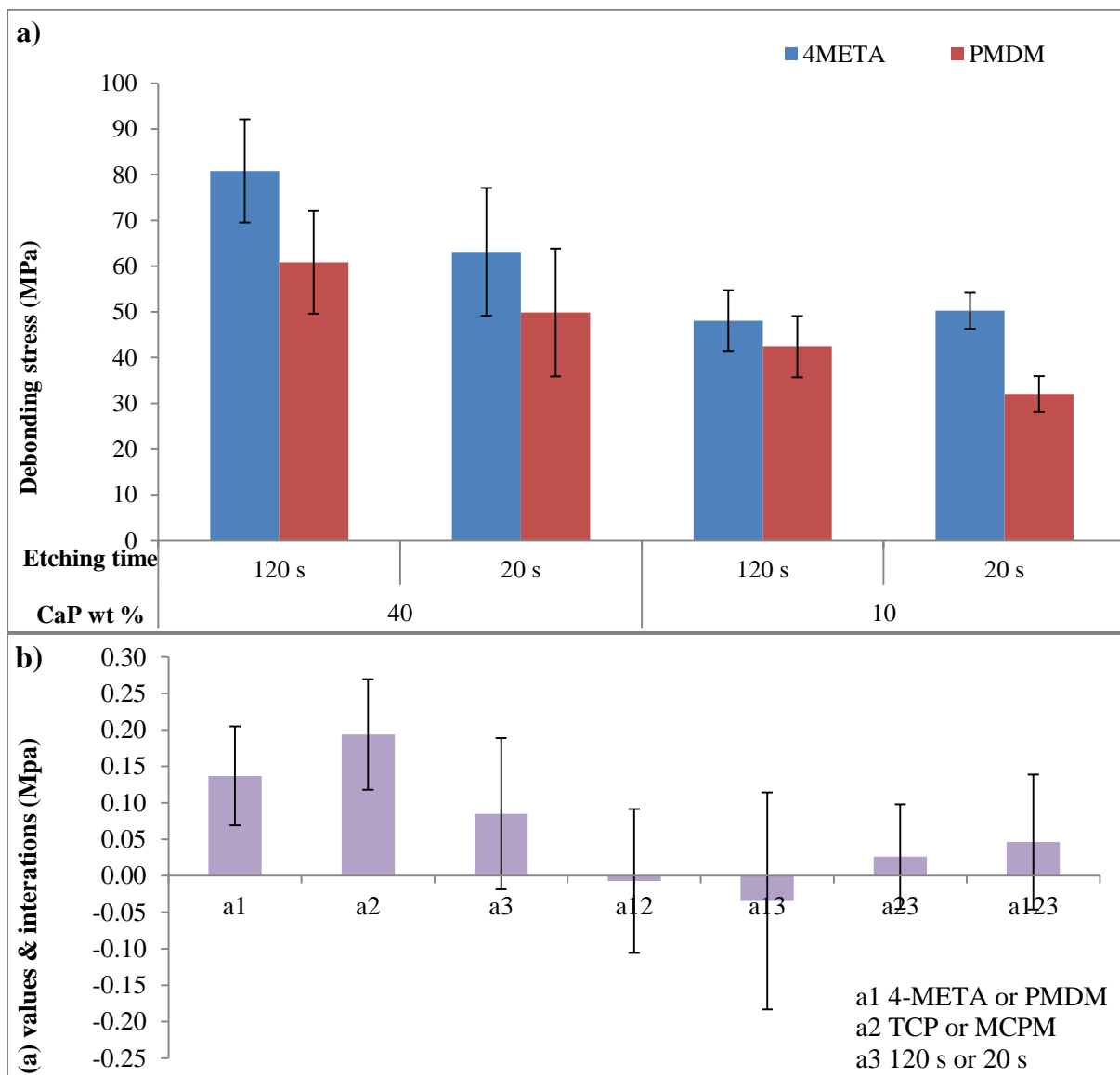


Figure 11-7: Push out stress for four formulations with 4META/ PMDM, CaP (40 or 10 wt %) and etching with 37 % phosphoric acid for 20 s and 120s. b) Factorial analysis of series four formulations a1 4-META/PMDM, a2 CaP wt % and a3 etching with 37 % phosphoric acid for 20 s and 120s. The errors represent 95% C.I of the mean (n=3).

11.2. Appendix 2

Effect of PLR (3:1 or 4:1) on push out test for control formulation with 4-META

11.2.1.1. Methods

The 4-META control experimental formulations contain the same monomer as in the main thesis above and contained solely glass particles in the filler phase. The powder to liquid ratio was 3:1 or 4:1 by weight.

11.2.1.2. Result

The average push out stress for 4-META control formulation with PLR 3:1 or 4:1 and dry ivory dentine are shown in Figure 7-5. The push out stress was on average 42 % higher than with formulation with PLR 3:1 compared to 4:1.

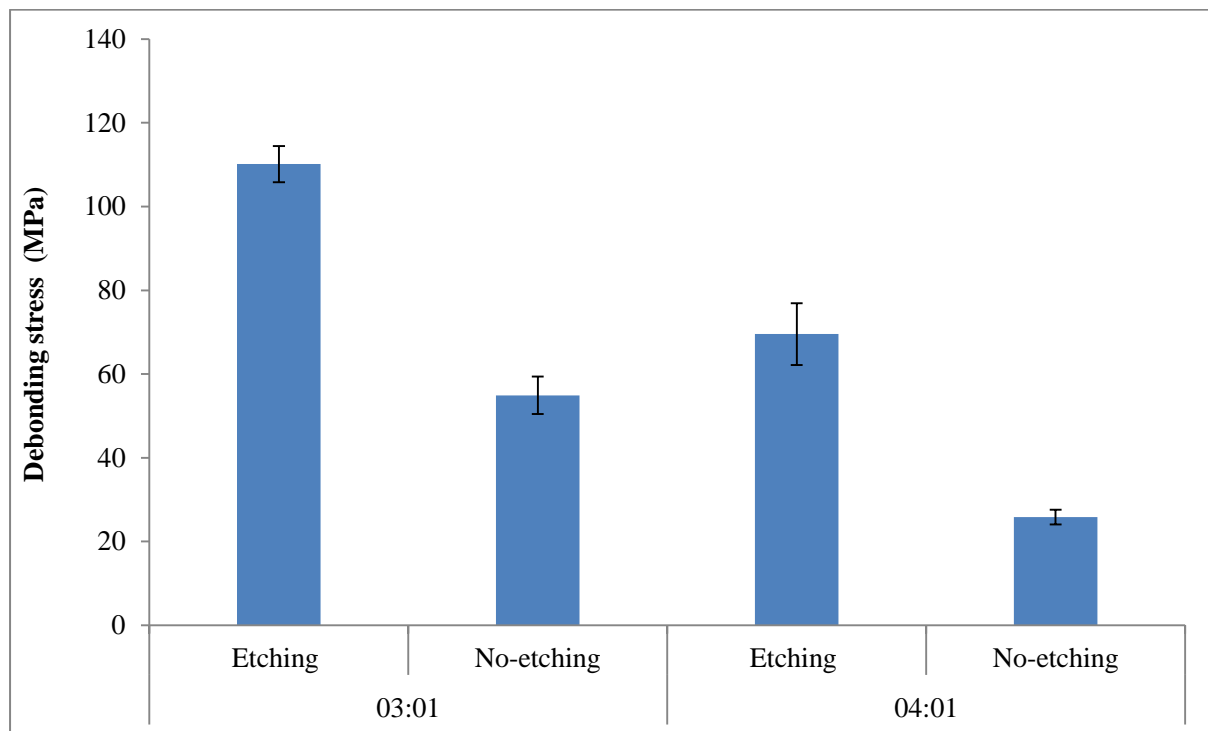


Figure 11-8: push out stress for control formulation with 4-META, PLR 3:1 or 4:1 and etching with phosphoric acid for 20s or no-etching. The errors represent 95 % C.I of the mean. (n=3).

11.3. Appendix 3

Effect of different diluent and co-initiators on push out test

11.3.1.1. Methods

The control experimental formulations containing UDMA: PPGDMA or TEGDMA 68: 25 by weight were assessed. To this was added, 4-META (5 wt %) monomers and CQ and NTGGMA or DMPT (each 1 wt %) as initiator and co-initiator. Control formulations contained solely glass particles in the filler phase. The powder to liquid ratio was 3:1 by weight. The sample was prepared as mentioned in material and methods chapter.

11.3.1.2. Result

The average push out stress for 4-META control formulation with PPGDMA or TEGDMA and NTGGMA or DMPT dry ivory dentine are shown in Figure 7-6. The push out stress for formulation with PPGDMA and NTGGMA was on average 40 and 33 % higher than with formulation with TEGDMA and DMPT with and without acid etching respectively. of dry ivory dentine. The formulation with PPGDMA and NTGGMA had the highest push out stress with and without acid etching of 49 and 33 MPa respectively.

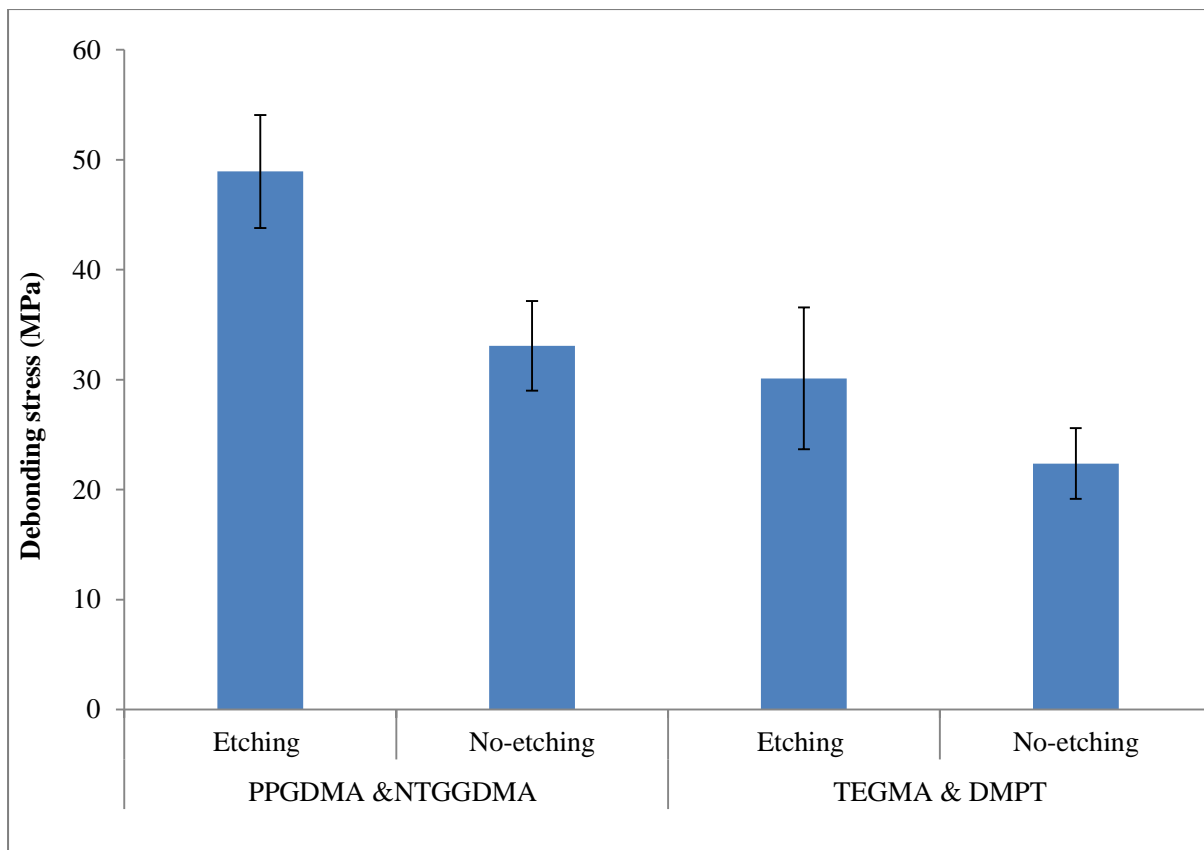
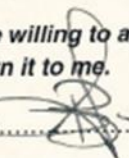


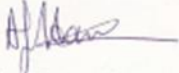
Figure 11-9: push out stress for control formulation with 4-META, PPGDMA or TEGDMA, NTGGMA or DMPT and etching with phosphoric acid for 20s or no-etching. The errors represent 95 % C.I of the mean. (n=3).

11.4. Appendix 4

 Home Office UK Border Agency	Queens Warehouse Custom House Nettleton Road Heathrow Airport Middlesex TW6 2LA
Dr Laurent Bozec UCL Eastman Dental Institute University College London 256 Gray's Inn Road London WC1X 8LD	Tel +44 (0)203-014-5722 Fax +44 (0)203-014-5811 Email afia.hameed@hmrc.gsi.gov.uk Web www.ukba.homeoffice.gov.uk
Date: 10 th July 2012	
Ref: 08/2012	
Dear Dr Bozec,	
<u>Derivative Items made from endangered species seized by UK Border Agency</u>	
In response to your request we are prepared to loan to you, as part of those museums, conversation groups, scientific and educational bodies approved by U.K Border Agency, specimens of seized goods, under the Convention on International Trade in Endangered Species (CITES), the items listed overleaf.	
<i>There are a number of conditions:</i> (a) The articles may only be used for research, experimentation, educational or identification training purposes and in exhibitions publicizing the requirements of CITES controls; (b) It is desirable that the goods are labeled as seizures by U.K Border Agency; (c) The articles must be kept securely; (d) The articles are accepted on the understanding that the Department has no responsibility for any Health and Safety matters relating to them; (e) The articles must not be disposed of without the agreement of this Department and/or returned to the Department upon request.	
<i>If you are willing to agree to the above conditions please sign the enclosed copy letter and return it to me.</i>	
Signature..... 	Company..... University College London
Print Name..... Dr Bozec	Date..... 10/07/2012

A list of the articles you have requested and we are able to supply is attached. Please sign the copy as a receipt and return it to me when you have received the items.

Yours sincerely



Afia Hameed.

Officer

ARTICLES LOANED

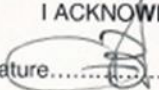
By U.K Border Agency

These articles have been primarily donated for the purposes

..... **Research**

Our Reference	Description	Seal Number
E2734121	1 x Elephant Ivory Tusk . Approx 7kg	AB0125182
E2734121	1x Elephant Ivory Tusk . Approx 7.5kg	AB0125183

I ACKNOWLEDGE RECEIPT OF THE ARTICLES LISTED ABOVE

Signature  Company University College London

Print Name A. Bort Date 10/07/12

12. References

1. Mjor IA, Dahl JE, Moorhead JE. Age of restorations at replacement in permanent teeth in general dental practice. *Acta Odontologica*. 2000; 58(3):97-101.
2. Soncini JA, Maserejian NN, Trachtenberg F, Tavares M, Hayes C. The longevity of amalgam versus compomer/composite restorations in posterior primary and permanent teeth. *The Journal of the American Dental Association*. 2007; 138: 763-72.
3. Bernardo M, Luis H, Martin MD, Leroux BG, Rue T, Leitão J, et al. Survival and reasons for failure of amalgam versus composite posterior restorations placed in a randomized clinical trial. *The Journal of the American Dental Association*. 2007;138(6):775-83.
4. Opdam N, Bronkhorst E, Loomans B, Huysmans MC. 12-year survival of composite vs. amalgam restorations. *Journal of Dental Research*. 2010; 89(10):1063-7.
5. Corbin SB, Kohn WG. The benefits and risks of dental amalgam: current findings reviewed. *The Journal of the American Dental Association*. 1994;125(4):381-8.
6. Berry TG, Nicholson J, Troendle K. Almost two centuries with amalgam: Where are we today. *The Journal of the American Dental Association*. 1994; 125(4):392-9.
7. Goldman M. Polymerization shrinkage of resin-based restorative materials. *Australian Dental Journal*. 2009; 28(3):156-61.
8. Bürgers R, Eidt A, Frankenberger R, Rosentritt M, Schweikl H, Handel G, et al. The anti-adherence activity and bactericidal effect of microparticulate silver additives in composite resin materials. *Archives of Oral Biology*. 2009; 54(6):595-601.
9. Matalon S, Slutzky H, Weiss EI. Surface antibacterial properties of packable resin composites: part I. *Quintessence International-English Edition*. 2004; 35(3):189-93.
10. Fejerskov O, Kidd EAM. *Dental caries: the disease and its clinical management*. John Wiley & Sons; 2009 Mar 16
11. Selwitz RH, Ismail AI, Pitts NB. Dental caries. *The Lancet*. 2007; 369(9555):51-9.
12. Featherstone J. The continuum of dental caries—evidence for a dynamic disease process. *Journal of Dental Research*. 2004; 83(suppl 1):C39-C42.
13. Fontana M, Young DA, Wolff MS, Pitts NB, Longbottom C. Defining dental caries for 2010 and beyond. *Dental Clinics of North America*. 2010; 54(3):423-40.
14. Mjor IA. Clinical diagnosis of recurrent caries. *The Journal of the American Dental Association*. 2005; 136(10):1426-33.

15. Goršeta K. Fissure Sealing in Occlusal Caries Prevention. 2015.
16. Bagramian RA, Garcia-Godoy F, Volpe AR. The global increase in dental caries. A pending public health crisis. *The Journal of the American Dental Association*. 2009; 22(1):3-8.
17. Vos T, Flaxman AD, Naghavi M, Lozano R, Michaud C, Ezzati M, et al. Years lived with disability (YLDs) for 1160 sequelae of 289 diseases and injuries 1990–2010: a systematic analysis for the Global Burden of Disease Study 2010. *The Lancet*. 2013; 380(9859):2163-96.
18. Beltran-Aguilar ED, Barker LK, Canto MT, Dye BA, Gooch BF, Griffin SF, et al. Surveillance for dental caries, dental sealants, tooth retention, edentulism, and enamel fluorosis United States, 1988-1994 and 1999-2002. *Morbidity and Mortality Weekly Report*. 2005; 54(SS3, Suppl. S):1-43.
19. BASCD. NHS Dental Epidemiology Programme for England. England: BASCD; 2009. p. 1-8.
20. Angker L, Nockolds C, Swain MV, Kilpatrick N. Quantitative analysis of the mineral content of sound and carious primary dentine using BSE imaging. *Archives of Oral Biology*. 2004; 49(2):99-107.
21. Cury JA, Tenuta LMA. Enamel remineralization: controlling the caries disease or treating early caries lesions? *Brazilian Oral Research*. 2009; 23:23-30.
22. Kidd E, Fejerskov O. What constitutes dental caries? Histopathology of carious enamel and dentin related to the action of cariogenic biofilms. *Journal of Dental Research*. 2004; 83(suppl 1):C35-C8.
23. Marsh PD, Martin MV, Lewis MA, Williams D. *Oral microbiology*: Elsevier Health Sciences; 2009 Apr 30..
24. Featherstone J. Dental caries: a dynamic disease process. *Australian Dental Journal*. 2008; 53(3):286-91.
25. Melo MA, Guedes SF, Xu HH, Rodrigues LK. Nanotechnology-based restorative materials for dental caries management. *Trends in Biotechnology*. 2013; 31(8):459-67.
26. Marsh PD, Moter A, Devine DA. Dental plaque biofilms: communities, conflict and control. *Periodontology 2000*. 2011; 55(1):16-35.
27. Rosan B, Lamont RJ. Dental plaque formation. *Microbes and Infection*. 2000; 2(13):1599-607.
28. Mjor IA, Toffenetti F. Secondary caries: a literature review with case reports. *Quintessence International English Edition*. 2000; 31(3):165-80.
29. Goldberg M. In vitro and in vivo studies on the toxicity of dental resin components: a review. *Clinical Oral Investigations*. 2008; 12(1):1-8.

30. Barker P, Black M, Arthur J, Farrell DJ. Effects of fluoride, dietary phosphate, wholemeal and white flour on the incidence of dental caries in growing rats. *Proceedings of the Nutrition Society of Australia Annual Conference*. 1981; 6:103.
31. Nanci A. *Ten Cate's Oral Histology-Pageburst on VitalSource: Development, Structure, and Function*: Elsevier Health Sciences; 2007 Sep 26.
32. Yu C, Abbott P. An overview of the dental pulp: its functions and responses to injury. *Australian Dental Journal*. 2007;52(s1):S4-S6.
33. Nanci A, Bosshardt DD. Structure of periodontal tissues in health and disease. *Periodontology 2000*. 2006;40(1):11-28.
34. Diekwisch TGH. The developmental biology of cementum. *International Journal of Developmental Biology*. 2001;45(5/6):695-706.
35. Summitt JB, dos Santos J. *Fundamentals of operative dentistry: a contemporary approach*: Quintessence Publishing.; 2006.
36. Sakaguchi RL, Powers JM. *Craig's restorative dental materials*: Elsevier Health Sciences; 2012.
37. Summitt JB, Robbins JW, Schwartz RS, dos Santos J. *Fundamentals of operative dentistry: a contemporary approach*: *Fundamentals of Operative Dentistry: a contemporary approach.*; 2006.
38. Bohl KS, Shon J, Rutherford B, Mooney DJ. Role of synthetic extracellular matrix in development of engineered dental pulp. *Journal of Biomaterials Science, Polymer Edition*. 1998; 9(7):749-64.
39. Liaqat S, Aljabo A, Khan MA, Nuba HB, Bozec L, Ashley P, et al. Characterization of Dentine to Assess Bond Strength of Dental Composites. *Materials*. 2015;8(5):2110-26.
40. Tjäderhane L, Larjava H, Sorsa T, Uitto V-J, Larmas M, Salo T. The activation and function of host matrix metalloproteinases in dentin matrix breakdown in caries lesions. *Journal of Dental Research*. 1998;77(8):1622-9.
41. Marshall Jr GW, Marshall SJ, Kinney JH, Balooch M. The dentin substrate: structure and properties related to bonding. *Journal of Dentistry*. 1997;25(6):441-58.
42. Powers JM, Sakaguchi RL. *Craig's Restorative Dental Materials*, 13/e: Elsevier India; 2006.
43. Aoba T. Solubility properties of human tooth mineral and pathogenesis of dental caries. *Oral Diseases*. 2004; 10(5):249-57.
44. Poggio C, Lombardini M, Vigorelli P, Ceci M. Analysis of dentin/enamel remineralization by a CPP-ACP paste: AFM and SEM study. *Scanning*. 2013; 35(6):366-74.

45. Fejerskov O. Strategies in the design of preventive programs. *Advances in Dental Research*. 1995;9(2):82-8.
46. Breschi L, Mazzoni A, Ruggeri A, Cadenaro M, Di Lenarda R, De Stefano Dorigo E. Dental adhesion review: aging and stability of the bonded interface. *Dental Materials*. 2008; 24(1):90-101.
47. Van Meerbeek B DMJ, Yoshida Y, Inoue S, Vargas M, Vijay P, et al. Adhesion to enamel and dentin: current status and future challenges. *Operative Dentistry*. 2003; 28:215-35.
48. Nakabayashi N, Kojima K, Masuhara E. The promotion of adhesion by the infiltration of monomers into tooth substrates. *Journal of Biomedical Materials Research*. 1982;16(3):265-73.
49. Garcia-Godoy F, Dodge WW, Donohue M, O'Quinn JA. Effect of a fluoridated etchant on the shear bond strength of a composite resin to enamel. *International Journal of Paediatric Dentistry*. 1992;2(1):25-30.
50. Hilton TJ. Can modern restorative procedures and materials reliably seal cavities? In vitro investigations. Part 2. *American Journal of Dentistry*. 2002;15(4):279-89.
51. Van Meerbeek B, Vargas M, Inoue S, Yoshida Y, Peumans M, Lambreehts P, et al. Adhesives and cements to promote preservation dentistry. 2001: 119-144.
52. Swift EJ, Perdigano J, Wilder AD, Heymann HO, Sturdevant JR, Bayne SC. Clinical evaluation of two one-bottle dentin adhesives at three years. *The Journal of the American Dental Association*. 2001;132(8):1117-23.
53. Ishioka S, Caputo A. Interaction between the dentinal smear layer and composite bond strength. *The Journal of Prosthetic Dentistry*. 1989;61(2):180-5.
54. Pashley D, Horner J, Brewer P. Interactions of conditioners on the dentin surface. *Operative Dentistry*. 1991:137-50.
55. Nakabayashi N, Nakamura M, Yasuda N. Hybrid Layer as a Dentin-Bonding Mechanism. *Journal of Esthetic and Restorative Dentistry*. 1991;3(4):133-8.
56. Matinlinna JP. *Handbook of Oral Biomaterials*: CRC Press; 2014 May 16.
57. Anusavice KJ. *Phillips' science of dental materials*. 11th ed. St. Louis: Elsevier. 2003.
58. Cenci MS, Piva E, Potrich F, Formolo E, Demarco FF, Powers JM. Microleakage in bonded amalgam restorations using different adhesive materials. *Brazilian Dental Journal*. 2004;15(1):13-8.
59. Leisteuvo J, Leisteuvo T, Helenius H, Pyy L, Österblad M, Huovinen P, et al. Dental amalgam fillings and the amount of organic mercury in human saliva. *Caries Research*. 2001;35(3):163-6.

60. Osborne JW, Swift EJ. Safety of dental amalgam. *Journal of Esthetic and Restorative Dentistry*. 2004;16(6):377-88.
61. Kanerva L, Komulainen M, Estlander T, Jolanki R. Occupational allergic contact dermatitis from mercury. *Contact Dermatitis*. 1993;28(1):26-8.
62. Wiltshire WA, Ferreira MR, Ligthelm AJ. Allergies to dental materials. *Quintessence international* (Berlin, Germany: 1985). 1996;27(8):513-20.
63. Baracco B, Perdigão J, Cabrera E, Giráldez I, Ceballos L. Clinical evaluation of a low-shrinkage composite in posterior restorations: one-year results. *Operative Dentistry*. 2012;37(2):117-29.
64. Barszczewska-Rybarek IM. Quantitative determination of degree of conversion in photocured poly (urethane-dimethacrylate) s by Fourier transform infrared spectroscopy. *Journal of Applied Polymer Science*. 2012;123(3):1604-11.
65. Whitters C, Strang R, Brown D, Clarke R, Curtis R, Hatton P, et al. Dental materials: 1997 literature review. *Journal of Dentistry*. 1999;27(6):401-35.
66. Abu-Hanna A, Gordan V, Mjor I. The effect of variation in etching times on dentin bonding. *General Dentistry*. 2004;52(1):28-33.
67. Richardson GM. Mercury exposure and risks from dental amalgam in Canada: the Canadian health measures survey 2007–2009. *Human and Ecological Risk Assessment: An International Journal*. 2014;20(2):433-47.
68. Wilson A, Kent B. The glass-ionomer cement, a new translucent dental filling material. *Journal of Applied Chemistry and Biotechnology*. 1971;21(11):313-.
69. Young A, Rafeeka S, Howlett J. FTIR investigation of monomer polymerisation and polyacid neutralisation kinetics and mechanisms in various aesthetic dental restorative materials. *Biomaterials*. 2004;25(5):823-33.
70. Young A. FTIR investigation of polymerisation and polyacid neutralisation kinetics in resin-modified glass-ionomer dental cements. *Biomaterials*. 2002;23(15):3289-95.
71. Ten Cate J, Featherstone J. Physicochemical aspects of fluoride-enamel interactions. *Fluoride in Dentistry* Copenhagen, Munksgaard. 1996:252-72.
72. Greig V. Craig's restorative dental materials. *British Dental Journal*. 2012;213(2):90-.
73. Ana ID, Matsuya S, Ohta M, Ishikawa K. Effects of added bioactive glass on the setting and mechanical properties of resin-modified glass ionomer cement. *Biomaterials*. 2003;24(18):3061-7.
74. McCabe JF, Walls A, editors. *Applied dental materials*. John Wiley & Sons; 2013 May 7.

75. Nicholson JW. Polyacid-modified composite resins (“compomers”) and their use in clinical dentistry. *Dental Materials*. 2007;23(5):615-22.
76. Van Landuyt KL, Snauwaert J, De Munck J, Peumans M, Yoshida Y, Poitevin A, et al. Systematic review of the chemical composition of contemporary dental adhesives. *Biomaterials*. 2007;28(26):3757-85.
77. Verbeeck RMH, De Maeyer EAP, Marks LAM, De Moor RJG, De Witte A, Trimpeneers LM. Fluoride release process of (resin-modified) glass-ionomer cements versus (polyacid-modified) composite resins. *Biomaterials*. 1998;19(6):509-19.
78. Van Landuyt KL, Snauwaert J, De Munck J, Peurnans M, Yoshida Y, Poitevin A, et al. Systematic review of the chemical composition of contemporary dental adhesives. *Biomaterials*. 2007;28(26):3757-85.
79. Wiegand A, Buchalla W, Attin T. Review on fluoride-releasing restorative materials—Fluoride release and uptake characteristics, antibacterial activity and influence on caries formation. *Dental Materials*. 2007;23(3):343-62.
80. Mitra SC. Photocurable ionomer cement systems. EP Patent 0,323,120; 1994.
81. Huang C, Tay F, Cheung G, Kei L, Wei S, Pashley D. Hygroscopic expansion of a compomer and a composite on artificial gap reduction. *Journal of Dentistry*. 2002;30(1):11-9.
82. Uno S, Finger WJ, Fritz U. Long-term mechanical characteristics of resin-modified glass ionomer restorative materials. *Dental Materials*. 1996;12(1):64-9.
83. Xu X, Burgess JO. Compressive strength, fluoride release and recharge of fluoride-releasing materials. *Biomaterials*. 2003;24(14):2451-61.
84. Lavigne C, Zhu X. Recent advances in the development of dental composite resins. *Royal Society of Chemistry*. 2012;2(1):59-63.
85. Klapdohr S, Moszner N. New inorganic components for dental filling composites. *Monatshefte für Chemie/Chemical Monthly*. 2005;136(1):21-45.
86. Ferracane JL. Resin composite—state of the art. *Dental Materials*. 2011;27(1):29-38.
87. Anusavice KJ, Phillips RW, Shen C, Rawls HR. *Phillips' science of dental materials: Elsevier Health Sciences*; 2012.
88. Schulz H, Schimmoeller B, Pratsinis SE, Salz U, Bock T. Radiopaque dental adhesives: dispersion of flame-made Ta₂O₅/SiO₂ nanoparticles in methacrylic matrices. *Journal of Dentistry*. 2008;36(8):579-87.
89. Gonçalves F, Azevedo CLN, Ferracane JL, Braga RR. BisGMA/TEGDMA ratio and filler content effects on shrinkage stress. *Dental Materials*. 2011;27(6):520-6.

90. Ferracane JL. Developing a more complete understanding of stresses produced in dental composites during polymerization. *Dental Materials*. 2005;21(1):36-42.
91. Powers JM, Wataha JC. *Dental Materials-E-Book: Properties and Manipulation*: Mosby; 2007.
92. Yap A, Soh M. Post-gel polymerization contraction of " low shrinkage" composite restoratives. *Operative Dentistry –University of Washington*. 2004;29(2):182-7.
93. Goncalves F, Kawano Y, Pfeifer C, Stansbury JW, Braga RR. Influence of BisGMA, TEGDMA, and BisEMA contents on viscosity, conversion, and flexural strength of experimental resins and composites. *European Journal of Oral Sciences*. 2009;117(4):442-6.
94. Takahashi Y, Imazato S, Kaneshiro AV, Ebisu S, Frencken JE, Tay FR. Antibacterial effects and physical properties of glass-ionomer cements containing chlorhexidine for the ART approach. *Dental Materials*. 2006; 31;22(7):647-52..
95. Peutzfeldt A. Resin composites in dentistry: the monomer systems. *European Journal of Oral Sciences*. 2007;105(2):97-116.
96. Lohbauer U, Zinelis S, Rahiotis C, Petschelt A, Eliades G. The effect of resin composite pre-heating on monomer conversion and polymerization shrinkage. *Dental Materials*. 2009;25(4):514-9.
97. Poplawski T, Loba K, Pawlowska E, Szczepanska J, Blasiak J. Genotoxicity of urethane dimethacrylate, a tooth restoration component. *Toxicology in Vitro*. 2010;24(3):854-62.
98. Hansel C, Leyhausen G, Mai U, Geurtsen W. Effects of various resin composite (co) monomers and extracts on two caries-associated micro-organisms in vitro. *Journal of Dental Research*. 1998;77(1):60-7.
99. Darvell BW. *Materials science for dentistry*: Woodhead Publishing; 2009.
100. Moszner N, Fischer UK, Angermann J, Rheinberger V. A partially aromatic urethane dimethacrylate as a new substitute for Bis-GMA in restorative composites. *Dental Materials*. 2008;24(5):694-9.
101. Hoszek A, Struzycka I, Jozefowicz A, Wojcieszek D, Wierzbicka M, Wretling K, et al. Chlorhexidine-containing glass ionomer cement. A clinical investigation on the fissure caries inhibiting effect in first permanent molars. *Swedish Dental Journal*. 2005;29(3):89.
102. Vermeersch G, Leloup G, Delmee M, Vreven J. Antibacterial activity of glass-ionomer cements, compomers and resin composites: relationship between acidity and material setting phase. *Journal of Oral Rehabilitation*. 2005;32(5):368-74.
103. Calheiros FC, Daronch M, Rueggeberg FA, Braga RR. Degree of conversion and mechanical properties of a BisGMA: TEGDMA composite as a function of the applied

radiant exposure. *Journal of Biomedical Materials Research Part B: Applied Biomaterials*. 2008;84(2):503-9.

104. Sideridou I, Tserki V, Papanastasiou G. Effect of chemical structure on degree of conversion in light-cured dimethacrylate-based dental resins. *Biomaterials*. 2002;23(8):1819-29.

105. Van Landuyt K, De Munck J, Snauwaert J, Coutinho E, Poitevin A, Yoshida Y, et al. Monomer-solvent phase separation in one-step self-etch adhesives. *Journal of Dental Research*. 2005;84(2):183-8.

106. Moszner N, Salz U, Zimmermann J. Chemical aspects of self-etching enamel-dentin adhesives: a systematic review. *Dental Materials*. 2005;21(10):895-910.

107. Nakabayashi N, Kojima K, Masuhara E. The promotion of adhesion by the infiltration of monomers into tooth substrates. *Journal of Biomedical Materials Research*. 2004;16(3):265-73.

108. Toledano M, Osorio R, Moreira M, Cabrerizo-Vilchez M, Gea P, Tay F, et al. Effect of the hydration status of the smear layer on the wettability and bond strength of a self-etching primer to dentin. *American Journal of Dentistry*. 2004;17(5):310.

109. Mehdawi I, Neel EAA, Valappil SP, Palmer G, Salih V, Pratten J, et al. Development of remineralizing, antibacterial dental materials. *Acta Biomaterialia*. 2009;5(7):2525-39.

110. Nakaoki Y, Nikaido T, Pereira P, Inokoshi S, Tagami J. Dimensional changes of demineralized dentin treated with HEMA primers. *Dental Materials*. 2000;16(6):441-6.

111. Nakabayashi N, Hiranuma K. Effect of etchant variation on wet and dry dentin bonding primed with 4-META/acetone. *Dental Materials*. 2000;16(4):274-9.

112. Unemori M, Matsuya Y, Matsuya S, Akashi A, Akamine A. Water absorption of poly(methyl methacrylate) containing 4-methacryloxyethyl trimellitic anhydride. *Biomaterials*. 2003;24(8):1381-7.

113. Odian G. *Principles of polymerization*: Wiley-Interscience; 2004.

114. Kwon TY, Bagheri R, Kim YK, Kim KH, Burrow MF. Cure mechanisms in materials for use in esthetic dentistry. *Journal of Investigative and Clinical Dentistry*. 2012;3(1):3-16.

115. de Araújo CS, Schein M, Zanchi CH, Rodrigues Jr SA, Demarco FF. Composite resin microhardness: the influence of light curing method, composite shade, and depth of cure. *The Journal of Contemporary Dental Practice*. 2008;9(4):43.

116. Asmussen SV, Schroeder WF, Vallo CI. Photopolymerization of methacrylate monomers using polyhedral silsesquioxanes bearing side-chain amines as photoinitiator. *European Polymer Journal*. 2011.

117. Lapp CA, Schuster GS. Effects of DMAEMA and 4-methoxyphenol on gingival fibroblast growth, metabolism, and response to interleukin-1. *Journal of Biomedical Materials Research*. 2002;60(1):30-5.
118. Schneider LFJ, Cavalcante LM, Silikas N. Shrinkage stresses generated during resin-composite applications: a review. *Journal of Dental Biomechanics*. 2010;1(1):131630.
119. Kotha S, Li C, McGinn P, Schmid S, Mason J. Improved mechanical properties of acrylic bone cement with short titanium fibre reinforcement. *Journal of Materials Science: Materials in Medicine*. 2006;17(12):1403-9.
120. Callister WD, Rethwisch DG. *Fundamentals of materials science and engineering: an integrated approach*: John Wiley & Sons; 2012 May 22.
121. Xu H, Eichmiller F, Antonucci JM, Schumacher GE, Ives L. Dental resin composites containing ceramic whiskers and precured glass ionomer particles. *Dental Materials*. 2000;16(5):356-63.
122. Chen L, Yu Q, Wang Y, Li H. BisGMA/TEGDMA dental composite containing high aspect-ratio hydroxyapatite nanofibres. *Dental Materials*. 2011;27(11):1187-95.
123. Ormsby R, McNally T, Mitchell C, Dunne N. Incorporation of multiwalled carbon nanotubes to acrylic based bone cements: Effects on mechanical and thermal properties. *Journal of the Mechanical Behavior of Biomedical Materials*. 2010;3(2):136-45.
124. Malquarti G, Berruet R, Bois D. Prosthetic use of carbon fibre-reinforced epoxy resin for esthetic crowns and fixed partial dentures. *The Journal of Prosthetic Dentistry*. 1990;63(3):251-7.
125. Goldberg A, Burstone C. The use of continuous fibre reinforcement in dentistry. *Dental Materials*. 1992;8(3):197-202.
126. Patel AP, Jon Goldberg A, Burstone CJ. The effect of thermoforming on the properties of fibre-reinforced composite wires. *Journal of Applied Biomaterials*. 1992;3(3):177-82.
127. Vallittu PK, Lassila VP, Lappalainen R. Transverse strength and fatigue of denture acrylic-glass fibre composite. *Dental Materials*. 1994;10(2):116-21.
128. Zhang H, Zhang M. Effect of surface treatment of hydroxyapatite whiskers on the mechanical properties of bis-GMA-based composites. *Biomedical Materials*. 2010;5(5):054106.
129. Tacir I, Kama J, Zortuk M, Eskimez S. Flexural properties of glass fibre reinforced acrylic resin polymers. *Australian Dental Journal*. 2006;51(1):52-6.

130. Kane RJ, Yue W, Mason JJ, Roeder RK. Improved fatigue life of acrylic bone cements reinforced with zirconia fibers. *Journal of the Mechanical Behavior of Biomedical Materials*. 2010;3(7):504-11.
131. Lee J-H, Um C-M, Lee I-b. Rheological properties of resin composites according to variations in monomer and filler composition. *Dental Materials*. 2006;22(6):515-26.
132. McCabe JF, Walls A. *Applied dental materials*: John Wiley & Sons; 2013.
133. Baroudi K, Saleh AM, Silikas N, Watts DC. Shrinkage behaviour of flowable resin-composites related to conversion and filler-fraction. *Journal of Dentistry*. 2007;35(8):651-5.
134. Galvão M, Costa S, Victorino K, Ribeiro A, Menezes F, Rastelli ANdS, et al. Influence of light guide tip used in the photo-activation on degree of conversion and hardness of one nanofilled dental composite. *Laser physics*. 2010;20(12):2050-5.
135. Sideridou I, Tserki V, Papanastasiou G. Study of water sorption, solubility and modulus of elasticity of light-cured dimethacrylate-based dental resins. *Biomaterials*. 2003;24(4):655-65.
136. Emami N, Söderholm K. Young's modulus and degree of conversion of different combination of light-cure dental resins. *The Open Dentistry Journal*. 2009;3:202.
137. Halvorson RH, Erickson RL, Davidson CL. The effect of filler and silane content on conversion of resin-based composite. *Dental Materials*. 2003;19(4):327-33.
138. Peutzfeldt A. Resin composites in dentistry: the monomer systems. *European Journal of Oral Sciences*. 1997;105(2):97-116.
139. Patel M, Braden M, Davy K. Polymerization shrinkage of methacrylate esters. *Biomaterials*. 1987;8(1):53-6.
140. Heintze S, Zimmerli B. Relevance of in vitro tests of adhesive and composite dental materials, a review in 3 parts. Part 1: Approval requirements and standardized testing of composite materials according to ISO specifications. *Rivista mensile svizzera di odontologia e stomatologia/SSO*. 2011;121(9):804.
141. Cobb DS, MacGregor KM, VARGAS MA, Denehy GE. The physical properties of packable and conventional posterior resin-based composites: a comparison. *The Journal of the American Dental Association*. 2000;131(11):1610-5.
142. Puckett AD, Fitchie JG, Kirk PC, Gamblin J. Direct composite restorative materials. *Dental Clinics of North America*. 2007;51(3):659-75.
143. Ferracane J, Mitchem J. Relationship between composite contraction stress and leakage in Class V cavities. *American Journal of Dentistry*. 2003;16(4):239-43.
144. Weinmann W, Thalacker C, Guggenberger R. Siloranes in dental composites. *Dental Materials*. 2005;21(1):68-74.

145. Dos Santos G, Alto R, da Silva E, Fellows C. Light transmission on dental resin composites. *Dental Materials*. 2008;24(5):571-6.
146. Rueggeberg FA, Ergle JW, Mettenburg DJ. Polymerization Depths of Contemporary Light-Curing Units Using Microhardness. *Journal of Esthetic and Restorative Dentistry*. 2000;12(6):340-9.
147. Fleming GJ, Awan M, Cooper PR, Sloan AJ. The potential of a resin-composite to be cured to a 4mm depth. *Dental Materials*. 2008;24(4):522-9.
148. Shin W, Li X, Schwartz B, Wunder S, Baran G. Determination of the degree of cure of dental resins using Raman and FT-Raman spectroscopy. *Dental Materials*. 1993;9(5):317-24.
149. Koupis NS, Vercruyse CW, Marks LA, Martens LC, Verbeeck RM. Curing depth of (polyacid-modified) composite resins determined by scraping and a penetrometer. *Dental Materials*. 2004;20(10):908-14.
150. Moore B, Platt J, Borges G, Chu TG, Katsilieri I. Depth of cure of dental resin composites: ISO 4049 depth and microhardness of types of materials and shades. *Operative Dentistry*. 2008;33(4):408-12.
151. Flury S, Hayoz S, Peutzfeldt A, Hüsler J, Lussi A. Depth of cure of resin composites: is the ISO 4049 method suitable for bulk fill materials? *Dental Materials*. 2012;28(5):521-8.
152. Braden M, Clarke R. Water absorption characteristics of dental microfine composite filling materials: I. Proprietary materials. *Biomaterials*. 1984;5(6):369-72.
153. Ferracane JL. Hygroscopic and hydrolytic effects in dental polymer networks. *Dental Materials*. 2006;22(3):211-22.
154. Oysaed H, Ruyter I. Composites for use in posterior teeth: mechanical properties tested under dry and wet conditions. *Journal of Biomedical Materials Research*. 1986;20(2):261-71.
155. Oysæd H, Ruyter I. Water sorption and filler characteristics of composites for use in posterior teeth. *Journal of Dental Research*. 1986;65(11):1315-8.
156. Rüttermann S, Dluzhevskaya I, Großsteinbeck C, Raab WH-M, Janda R. Impact of replacing Bis-GMA and TEGDMA by other commercially available monomers on the properties of resin-based composites. *Dental Materials*. 2010;26(4):353-9.
157. Sideridou ID, Karabela MM, Vouvoudi EC. Volumetric dimensional changes of dental light-cured dimethacrylate resins after sorption of water or ethanol. *Dental Materials*. 2008;24(8):1131-6.
158. McCabe JF, Rusby S. Water absorption, dimensional change and radial pressure in resin matrix dental restorative materials. *Biomaterials*. 2004;25(18):4001-7.

159. Sideridou I, Achilias DS, Spyroudi C, Karabela M. Water sorption characteristics of light-cured dental resins and composites based on Bis-EMA/PCDMA. *Biomaterials*. 2004;25(2):367-76.
160. Kanchanasavita W, Anstice H, Pearson GJ. Water sorption characteristics of resin-modified glass-ionomer cements. *Biomaterials*. 1997;18(4):343-9.
161. Sagsoz O, Ilday NO, Sagsoz NP, Bayindir YZ, Alsaran A. Investigation of Hardness and Wear Behavior of Dental Composite Resins. *International Journal of Composite Materials*. 2014;4(4):179-84.
162. Antunes PV, Ramalho A. Study of abrasive resistance of composites for dental restoration by ball-cratering. *Wear*. 2003;255(7):990-8.
163. McCabe J, Molyvda S, Rolland S, Rusby S, Carrick T. Two-and three-body wear of dental restorative materials. *International Dental Journal*. 2002;52(S5):406-16.
164. Manhart J, Chen H, Hamm G, Hickel R. Review of the clinical survival of direct and indirect restorations in posterior teeth of the permanent dentition. *Operative Dentistry University of Washington*. 2004;29:481-508.
165. Turssi CP, de Moraes Purquerio B, Serra MC. Wear of dental resin composites: insights into underlying processes and assessment methods—a review. *Journal of Biomedical Materials Research Part B: Applied Biomaterials*. 2003;65(2):280-5.
166. Ferracane J. Current trends in dental composites. *Critical Reviews in Oral Biology & Medicine*. 1995;6(4):302-18.
167. Turssi C, Ferracane J, Vogel K. Filler features and their effects on wear and degree of conversion of particulate dental resin composites. *Biomaterials*. 2005;26(24):4932-7.
168. Söderholm KJM, Lambrechts P, Sarrett D, Abe Y, Yang MC, Labella R, et al. Clinical wear performance of eight experimental dental composites over three years determined by two measuring methods. *European Journal of Oral Sciences*. 2001;109(4):273-81.
169. Gatti AM. Biocompatibility of micro-and nano-particles in the colon. Part II. *Biomaterials*. 2004;25(3):385-92.
170. Ilie N, Hickel R. Macro-, micro-and nano-mechanical investigations on silorane and methacrylate-based composites. *Dental Materials*. 2009;25(6):810-9.
171. Ilie N, Hickel R. Investigations on mechanical behaviour of dental composites. *Clinical Oral Investigations*. 2009;13(4):427-38.
172. Van Meerbeek B, De Munck J, Yoshida Y, Inoue S, Vargas M, Vijay P, et al. Adhesion to enamel and dentin: current status and future challenges. *Operative Dentistry University of Washington*. 2003;28(3):215-35.

173. Irie M, Suzuki K, Watts D. Marginal gap formation of light-activated restorative materials: effects of immediate setting shrinkage and bond strength. *Dental Materials*. 2002;18(3):203-10.
174. Ito S, Hashimoto M, Wadgaonkar B, Svizero N, Carvalho RM, Yiu C, et al. Effects of resin hydrophilicity on water sorption and changes in modulus of elasticity. *Biomaterials*. 2005;26(33):6449-59.
175. Yoshida Y, Van Meerbeek B, Nakayama Y, Snauwaert J, Hellemans L, Lambrechts P, et al. Evidence of chemical bonding at biomaterial-hard tissue interfaces. *Journal of Dental Research*. 2000;79(2):709-14.
176. Berg JH. Glass ionomer cements. *Pediatric Dentistry*. 2002;24(5):430.
177. Inoue S, Van Meerbeek B, Abe Y, Yoshida Y, Lambrechts P, Vanherle G, et al. Effect of remaining dentin thickness and the use of conditioner on micro-tensile bond strength of a glass-ionomer adhesive. *Dental Materials*. 2001;17(5):445-55.
178. De Munck J, Van Meerbeek B, Yoshida Y, Inoue S, Suzuki K, Lambrechts P. Four-year water degradation of a resin-modified glass-ionomer adhesive bonded to dentin. *European Journal of Oral Sciences*. 2004;112(1):73-83.
179. De Munck J, Van Landuyt K, Peumans M, Poitevin A, Lambrechts P, Braem M, et al. A critical review of the durability of adhesion to tooth tissue: methods and results. *Journal of Dental Research*. 2005;84(2):118-32.
180. Silva e Souza Junior MH, Carneiro KGK, Lobato MF, Silva e Souza PdAR, Góes MFd. Adhesive systems: important aspects related to their composition and clinical use. *Journal of Applied Oral Science*. 2010;18:207-14.
181. Van Meerbeek B DMJ, Yoshida Y, Inoue S, Vargas M, Vijay P, et al. Adhesion to enamel and dentin: current status and future challenges. *Operative Dentistry*. 2003;28:215-35.
182. Wang Y, Spencer P, Walker MP. Chemical profile of adhesive/caries-affected dentin interfaces using Raman microspectroscopy. *Journal of Biomedical Materials Research Part A*. 2006;81(2):279-86.
183. Van Meerbeek B, Yoshihara K, Yoshida Y, Mine A. State of the art of self-etch adhesives. *Dental Materials*. 2011;27(1):17-28.
184. Cheng L, Weir MD, Xu HH, Antonucci JM, Kraigsley AM, Lin NJ, et al. Antibacterial amorphous calcium phosphate nanocomposites with a quaternary ammonium dimethacrylate and silver nanoparticles. *Dental Materials*. 2012;28(5):561-72.
185. Slot D, Vaandrager N, Van Loveren C, Van Palenstein Helderma W, Van der Weijden G. The effect of chlorhexidine varnish on root caries: a systematic review. *Caries Research*. 2011;45(2):162.

186. Carrilho M, Geraldeli S, Tay F, De Goes M, Carvalho R, Tjäderhane L, et al. In vivo preservation of the hybrid layer by chlorhexidine. *Journal of Dental Research*. 2007;86(6):529-33.
187. Brackett W, Tay F, Brackett M, Dib A, Sword R, Pashley D. The effect of chlorhexidine on dentin hybrid layers in vivo. *Operative Dentistry*. 2007;32(2):107-11.
188. Brackett M, Tay F, Brackett W, Dib A, Dipp F, Mai S, et al. In vivo chlorhexidine stabilization of hybrid layers of an acetone-based dentin adhesive. *Operative Dentistry*. 2009;34(4):379-83.
189. Palmer G, Jones F, Billington R, Pearson G. Chlorhexidine release from an experimental glass ionomer cement. *Biomaterials*. 2004;25(23):5423-31.
190. Breschi L, Mazzoni A, Nato F, Carrilho M, Visintini E, Tjäderhane L, et al. Chlorhexidine stabilizes the adhesive interface: a 2-year in vitro study. *Dental Materials*. 2010;26(4):320-5.
191. Imazato S, Torii M, Tsuchitani Y. Antibacterial effect of composite incorporating Triclosan against *Streptococcus mutans*. *The Journal of Osaka University Dental School*. 1995;35:5-11.
192. Othman HF, Wu CD, Evans CA, Drummond JL, Matasa CG. Evaluation of antimicrobial properties of orthodontic composite resins combined with benzalkonium chloride. *American journal of orthodontics and Dentofacial Orthopedics*. 2002;122(3):288-94.
193. Imazato S, Torii M, Tsuchitani Y, McCabe J, Russell R. Incorporation of bacterial inhibitor into resin composite. *Journal of Dental Research*. 1994;73(8):1437-43.
194. Imazato S. Antibacterial properties of resin composites and dentin bonding systems. *Dental Materials*. 2003;19(6):449-57.
195. Santos C, Clarke R, Braden M, Guitian F, Davy K. Water absorption characteristics of dental composites incorporating hydroxyapatite filler. *Biomaterials*. 2002;23(8):1897-904.
196. Langhorst S, O'Donnell J, Skrtic D. In vitro remineralization of enamel by polymeric amorphous calcium phosphate composite: Quantitative microradiographic study. *Dental Materials*. 2009;25(7):884-91.
197. Han B, Ma P-W, Zhang L-L, Yin Y-J, Yao K-D, Zhang F-J, et al. β -TCP/MCPM-based premixed calcium phosphate cements. *Acta Biomaterialia*. 2009;5(8):3165-77.
198. Mehdawi IM, Pratten J, Spratt DA, Knowles JC, Young AM. High strength remineralizing, antibacterial dental composites with reactive calcium phosphates. *Dental Materials*. 2013;29(4):473-84.

199. Xia W, Razi MM, Ashley P, Neel EA, Hofmann M, Young A. Quantifying effects of interactions between polyacrylic acid and chlorhexidine in dicalcium phosphate-forming cements. *Journal of Materials Chemistry B*. 2014;2(12):1673-80.
200. Wu J, Weir MD, Melo MAS, Xu HH. Development of novel self-healing and antibacterial dental composite containing calcium phosphate nanoparticles. *Journal of Dentistry*. 2015;43(3):317-26.
201. Skrtic D, Antonucci J. Dental composites based on amorphous calcium phosphate—resin composition/physicochemical properties study. *Journal of Biomaterials Applications*. 2007;21(4):375-93.
202. Lewis A. *Drug Device Combination Products: Delivery Technologies and Applications*: CRC Press/LLC; 2010.
203. Bohner M. Calcium orthophosphates in medicine: from ceramics to calcium phosphate cements. *Injury*. 2000;31:D37-D47.
204. Regnault W, Icenogle T, Antonucci J, Skrtic D. Amorphous calcium phosphate/urethane methacrylate resin composites. I. Physicochemical characterization. *Journal of Materials Science: Materials in Medicine*. 2008;19(2):507-15.
205. O'donnell J, Skrtic D, Antonucci J. Amorphous Calcium Phosphate Composites with Improved Mechanical Properties¹. *Journal of Bioactive and Compatible Polymers*. 2006;21(3):169-84.
206. Reynolds E, Cai F, Cochrane N, Shen P, Walker G, Morgan M, et al. Fluoride and casein phosphopeptide-amorphous calcium phosphate. *Journal of Dental Research*. 2008;87(4):344-8.
207. Skrtic D, Antonucci JM, Eanes ED, Eichmiller FC, Schumacher GE. Physicochemical evaluation of bioactive polymeric composites based on hybrid amorphous calcium phosphates. *Journal of Biomedical Materials Research*. 2000;53(4):381-91.
208. Hofmann MP, Young AM, Gbureck U, Nazhat SN, Barralet JE. FTIR-monitoring of a fast setting brushite bone cement: effect of intermediate phases. *Journal of Materials Chemistry*. 2006;16(31):3199-206.
209. Arregui M, Giner L, Ferrari M, Mercadé M, editors. *Colour Stability of Self-Adhesive Flowable Composites before and after Storage in Water*. *Key Engineering Materials*. 2015; 6 (631): 143-150.
210. Ikeda I, Otsuki M, Sadr A, Nomura T, Kishikawa R, Tagami J. Effect of filler content of flowable composites on resin-cavity interface. *Dental materials journal*. 2009;28(6):679.
211. Braga RR, Hilton TJ, Ferracane JL. Contraction stress of flowable composite materials and their efficacy as stress-relieving layers. *The Journal of the American Dental Association*. 2003;134(6):721-8.

212. Awliya W, El-Sahn A. Leakage pathway of Class V cavities restored with different flowable resin composite restorations. *Operative Dentistry*. 2008;33(1):31-6.
213. Yoshida K, Greener E. Effects of two amine reducing agents on the degree of conversion and physical properties of an unfilled light-cured resin. *Dental Materials*. 1993;9(4):246-51.
214. Leung D, Spratt DA, Pratten J, Gulabivala K, Mordan NJ, Young AM. Chlorhexidine-releasing methacrylate dental composite materials. *Biomaterials*. 2005;26(34):7145-53.
215. Ho S-M, Young AM. Synthesis, polymerisation and degradation of poly (lactide-co-propylene glycol) dimethacrylate adhesives. *European Polymer Journal*. 2006;42(8):1775-85.
216. Li J, Li H, Fok AS, Watts DC. Multiple correlations of material parameters of light-cured dental composites. *Dental Materials*. 2009;25(7):829-36.
217. Rueggeberg F, Tamareselvy K. Resin cure determination by polymerization shrinkage. *Dental Materials*. 1995;11(4):265-8.
218. Soh M, Yap A, Siow K. The effectiveness of cure of LED and halogen curing lights at varying cavity depths. *Operative Dentistry*. 2002;28(6):707-15.
219. Floyd CJ, Dickens SH. Network structure of Bis-GMA-and UDMA-based resin systems. *Dental Materials*. 2006;22(12):1143-9.
220. Keyf F, Yalcin F. The weight change of various light-cured restorative materials stored in water. *The Journal of Contemporary Dental Practice*. 2005;6(2):72-9.
221. Ikejima I, Nomoto R, McCabe JF. Shear punch strength and flexural strength of model composites with varying filler volume fraction, particle size and silanation. *Dental Materials*. 2003;19(3):206-11.
222. Hirose H, Kawamoto Y, Kojima T, Sakaguchi S, Kimura K, Saitoh M, et al. Density, polymerization shrinkage, filler content and coefficient of thermal expansion of composite resins for crown and bridge. *The Japanese Society for Dental Materials and Devices*. 2006;25(1):62.
223. Karmaker A, Prasad A, Sarkar N. Characterization of adsorbed silane on fillers used in dental composite restoratives and its effect on composite properties. *Journal of Materials Science: Materials in Medicine*. 2007;18(6):1157-62.
224. Petersen R. Discontinuous fiber-reinforced composites above critical length. *Journal of Dental Research*. 2005;84(4):365-70.
225. Palin WM, Fleming GJP, Trevor Burke F, Marquis PM, Randall RC. The reliability in flexural strength testing of a novel dental composite. *Journal of Dentistry*. 2003;31(8):549-57.

226. Chung S, Yap A, Chandra S, Lim C. Flexural strength of dental composite restoratives: Comparison of biaxial and three point bending test. *Journal of Biomedical Materials Research Part B: Applied Biomaterials*. 2004;71(2):278-83.
227. Calheiros FC, S. Costa Pfeifer C, Brandao LL, Agra CM, Ballester RY. Flexural properties of resin composites: Influence of specimen dimensions and storage conditions. *Dental Materials Journal*. 2013;32(2):228-32.
228. Yamazaki PCV, Bedran-Russo AKB, Pereira PNR. Importance of the hybrid layer on the bond strength of restorations subjected to cyclic loading. *Journal of Biomedical Materials Research Part B: Applied Biomaterials*. 2008;84(1):291-7.
229. Jivraj SA, Kim TH, Donovan TE. Selection of Luting Agents, Part. *Journal of the California Dental Association*. 2006;34(2).
230. Palin W, Fleming G, Marquis P. The reliability of standardized flexure strength testing procedures for a light-activated resin-based composite. *Dental Materials*. 2005;21(10):911-9.
231. Palin WM, Fleming GJ, Trevor Burke F, Marquis PM, Randall RC. Monomer conversion versus flexure strength of a novel dental composite. *Journal of Dentistry*. 2003;31(5):341-51.
232. Timoshenko S, Woinowsky-Krieger S, Woinowsky S. *Theory of plates and shells*: McGraw-hill New York; 1959 Dec.
233. Higgs W, Lucksanasombool P, Higgs R, Swain M. A simple method of determining the modulus of orthopedic bone cement. *Journal of Biomedical Materials Research*. 2001;58(2):188-95.
234. Nilles J, Coletti J, Wilson C. Biomechanical evaluation of bone-porous material interfaces. *Journal of Biomedical Materials Research*. 1973;7(2):231-51.
235. Patierno J, Rueggeberg F, Anderson R, Weller R, Pashley D. Push-out strength and SEM evaluation of resin composite bonded to internal cervical dentin. *Dental Traumatology*. 1996;12(5):227-36.
236. Gesi A, Raffaelli O, Goracci C, Pashley DH, Tay FR, Ferrari M. Interfacial strength of Resilon and gutta-percha to intraradicular dentin. *Journal of Endodontics*. 2005;31(11):809-13.
237. Drummond J, Sakaguchi R, Racean D, Wozny J, Steinberg A. Testing mode and surface treatment effects on dentin bonding. *Journal of Biomedical Materials Research*. 1996;32(4):533-41.
238. Frankenberger R, Sindel J, Krämer N, Petschelt A. Dentin bond strength and marginal adaptation: Direct composite resins vs ceramic inlays. *Operative Dentistry*. 1998;24(3):147-55.

239. Sudsangiam S, van Noort R. Do dentin bond strength tests serve a useful purpose? *The Journal of Adhesive Dentistry*. 1998;1(1):57-67.
240. Locke M. Structure of ivory. *Journal of Morphology*. 2008;269(4):423-50.
241. Lafrenz KA. Tracing the source of the elephant and hippopotamus ivory from the 14th century bc uluburun shipwreck: The archaeological, historical, and isotopic evidence: University of South Florida; 2004.
242. Raubenheimer E, Brown J, Rama D, Dreyer M, Smith P, Dauth J. Geographic variations in the composition of ivory of: the African elephant (*Loxodonta africana*). *Archives of Oral Biology*. 1998;43(8):641-7.
243. Thanjal NT. Optimisation of interfacial bond strength of glass fibre endodontic post systems. 2011.
244. Jainaen A, Palamara JEA, Messer HH. Push-out bond strengths of the dentine–sealer interface with and without a main cone. *International Endodontic Journal*. 2007;40(11):882-90.
245. Luethi B, Reber R, Mayer J, Wintermantel E, Janczak-Rusch J, Rohr L. An energy-based analytical push-out model applied to characterise the interfacial properties of knitted glass fibre reinforced PET. *Composites Part A: Applied Science and Manufacturing*. 1998;29(12):1553-62.
246. Lempel E, Czibulya Z, Kunsági-Máté S, Szalma J, Sümegi B, Böddi K. Quantification of Conversion Degree and Monomer Elution from Dental Composite Using HPLC and Micro-Raman Spectroscopy. *Chromatographia*. 2014:1-8.
247. Nicolae LC, Shelton RM, Cooper PR, Martin RA, Palin WM, editors. *The Effect of UDMA/TEGDMA Mixtures and Bioglass Incorporation on the Mechanical and Physical Properties of Resin and Resin-Based Composite Materials*. Conference Papers in Science; 2014: Hindawi Publishing Corporation.
248. Hędzelek W, Marcinkowska A, Domka L, Wachowiak R. Infrared Spectroscopic Identification, of Chosen Dental Materials, and Natural Teeth. *Acta Physica Polonica A*. 2008;114(2):471-84.
249. Kanehira M, Araki Y, Finger WJ, Wada T, Utterodt A, Komatsu M. Curing Depth of Light-activated Nanofiller containing Resin Composites. *World*. 2012;3(2):119-25.
250. Ilie N, Hickel R, Valceanu AS, Huth KC. Fracture toughness of dental restorative materials. *Clinical Oral Investigations*. 2012;16(2):489-98.
251. Bracho-Troconis C, Rudoloh S, Boulden J, Wong N. Conversion vs. shrinkage of N'Durance, dimer acid based nanohybrid composite. *Journal of Dental Research*. 2008;87.

252. Ferrante M, Petrini M, Trentini P, Spoto G. Evaluation of composites light-curing at different times and distances of irradiation. *Journal of Thermal Analysis and Calorimetry*. 2012;107(2):757-61.
253. David JR, Gomes OM, Gomes JC, Loguercio AD, Reis A. Effect of exposure time on curing efficiency of polymerizing units equipped with light-emitting diodes. *Journal of Oral Science*. 2007;49(1):19-24.
254. Sideridou ID, Achilias DS. Elution study of unreacted Bis-GMA, TEGDMA, UDMA, and Bis-EMA from light cured dental resins and resin composites using HPLC. *Journal of Biomedical Materials Research Part B: Applied Biomaterials*. 2005;74(1):617-26.
255. Charton C, Falk V, Marchal P, Pla F, Colon P. Influence of T_g, viscosity and chemical structure of monomers on shrinkage stress in light-cured dimethacrylate-based dental resins. *Dental Materials*. 2007;23(11):1447-59.
256. Gajewski VE, Pfeifer CS, Fróes-Salgado NR, Boaro LC, Braga RR. Monomers used in resin composites: degree of conversion, mechanical properties and water sorption/solubility. *Brazilian Dental Journal*. 2012;23(5):508-14.
257. Naoum SJ, Ellakwa A, Morgan L, White K, Martin FE, Lee IB. Polymerization profile analysis of resin composite dental restorative materials in real time. *Journal of Dentistry*. 2012;40(1):64-70.
258. Czasch P, Ilie N. 2.2 „In-vitro comparison of mechanical properties and degree of cure of a self-adhesive and four novel flowable composites. *Clinical Oral Investigations* 17.1 (2013): 227-235.
259. Morra M. Acid-base properties of adhesive dental polymers. *Dental Materials*. 1993;9(6):375-8.
260. Ceballos L, Fuentes MV, Tafalla H, Martínez Á, Flores J, Rodríguez J. Curing effectiveness of resin composites at different exposure times using LED and halogen units. *Medicina Oral, Patología Oral y Cirugía Bucal*. 2009;14(1):E51-6.
261. Fujita K, Nishiyama N, Nemoto K, Okada T, Ikemi T. Effect of base monomer's refractive index on curing depth and polymerization conversion of photo-cured resin composites. *Dental Materials Journal*. 2005;24(3):403-8.
262. Shortall A, Palin W, Burtscher P. Refractive index mismatch and monomer reactivity influence composite curing depth. *Journal of Dental Research*. 2008;87(1):84-8.
263. Lu H, Roeder LB, Lei L, Powers JM. Effect of surface roughness on stain resistance of dental resin composites. *Journal of Esthetic and Restorative Dentistry*. 2005;17(2):102-8.
264. Koottathape N, Takahashi H, Iwasaki N, Kanehira M, Finger WJ. Two-and three-body wear of composite resins. *Dental Materials*. 2012;28(12):1261-70.

265. Sarabi N, Tajji H, Jalayer J, Ghaffari N, Forghani M. Fracture Resistance and Failure Mode of Endodontically Treated Premolars Restored with Different Adhesive Restorations. *Journal of Dental Materials and Techniques*. 2015;4(1):13-20.
266. Lempel E, Tóth Á, Fábíán T, Krajczár K, Szalma J. Retrospective evaluation of posterior direct composite restorations: 10-Year findings. *Dental Materials*. 2014.
267. Khatri CA, Stansbury JW, Schultheisz CR, Antonucci JM. Synthesis, characterization and evaluation of urethane derivatives of Bis-GMA. *Dental Materials*. 2003;19(7):584-8.
268. Ziming Sun J, Erickson MC, Parr JW. Refractive index matching and clear emulsions. *International Journal of Cosmetic Science*. 2005;27(6):355-6.
269. Kraemer N, Lohbauer U, García-Godoy F, Frankenberger R. Light curing of resin-based composites in the LED era. *The American Journal of Dentistry*. 2008;21(3):135-42.
270. García AH, Lozano MAM, Vila JC, Escribano AB, Galve PF. Composite resins. A review of the materials and clinical indications. *Medicina Oral Patologia Oral Cirugia Bucal*. 2006;11(2):E215-20.
271. Mills R, Jandt K, Ashworth S. Restorative Dentistry: Dental composite depth of cure with halogen and blue light emitting diode technology. *British Dental Journal*. 1999;186(8):388-91.
272. Ferracane J, Berge H, Condon J. In vitro aging of dental composites in water—effect of degree of conversion, filler volume, and filler/matrix coupling. *Journal of Biomedical Materials Research*. 1998;42(3):465-72.
273. Örtengren U, Wellendorf H, Karlsson S, Ruyter I. Water sorption and solubility of dental composites and identification of monomers released in an aqueous environment. *Journal of Oral Rehabilitation*. 2001;28(12):1106-15.
274. Martin N, Jedyakiewicz N. Measurement of water sorption in dental composites. *Biomaterials*. 1998;19(1-3):77-83.
275. Anttila EJ, Krintilä OH, Laurila TK, Lassila LV, Vallittu PK, Hernberg RG. Evaluation of polymerization shrinkage and hygroscopic expansion of fiber-reinforced biocomposites using optical fiber Bragg grating sensors. *Dental Materials*. 2008;24(12):1720-7.
276. Yiu CKY, King NM, Pashley DH, Suh BI, Carvalho RM, Carrilho MRO, et al. Effect of resin hydrophilicity and water storage on resin strength. *Biomaterials*. 2004;25(26):5789-96.
277. Boaro LC, Gonçalves F, Guimarães TC, Ferracane JL, Pfeifer CS, Braga RR. Sorption, solubility, shrinkage and mechanical properties of “low-shrinkage” commercial resin composites. *Dental Materials*. 2013;29(4):398-404.

278. Ersoy M, Civelek A, L'Hotelier E, Say EC, Soyman M. Physical properties of different composites. *Dental Materials Journal*. 2004;23(3):278.
279. Obici AC, Sinhoreti MAC, Correr-Sobrinho L, Góes MFd, Consani S. Evaluation of mechanical properties of Z250 composite resin light-cured by different methods. *Journal of Applied Oral Science*. 2005;13(4):393-8.
280. Blackham J, Vandewalle K, Lien W. Properties of hybrid resin composite systems containing prepolymerized filler particles. *Operative Dentistry*. 2009;34(6):697-702.
281. Wei Y-J, Silikas N, Zhang Z-T, Watts DC. Hygroscopic dimensional changes of self-adhering and new resin-matrix composites during water sorption/desorption cycles. *Dental Materials*. 2011;27(3):259-66.
282. Niewczas AM, Pieniak D, Ogrodnik P. Reliability analysis of strength of dental composites subjected to different photopolymerization procedures. *Eksploatacja I Niezawodnosc Maintenance and Reliability*. 2012(3):249-55.
283. Yap A, Chandra S, Chungo S, Lim C. Changes in flexural properties of composite restoratives after aging in water. *Operative Dentistry*. 2002;27(5):468-74.
284. Lopes GC, Ballarin A, Baratieri LN. Bond strength and fracture analysis between resin cements and root canal dentin. *Australian Endodontic Journal*. 2012;38(1):14-20.
285. Almeida KGB, Scheibe KGBA, Oliveira AEF, Alves CMC, Costa JF. Influence of human and bovine substrate on the microleakage of two adhesive systems. *Journal of Applied Oral Science*. 2009;17:92-6.
286. Torii Y, Ito K, Nishitani Y, Ishikawa K, Suzuki K. Effect of phosphoric acid etching prior to self-etching primer application on adhesion of resin composite to enamel and dentin. *American Journal of Dentistry*. 2002;15(5):305.
287. Jakubinek MB, Samarasekera CJ, White MA. Elephant ivory: A low thermal conductivity, high strength nanocomposite. *Journal of Materials Research*. 2006;21(1):287-92.
288. Kwon TY, Hong SH, Kim YK, Kim KH. Antibacterial effects of 40-META/MMA-TBB resin containing chlorhexidine. *Journal of Biomedical Materials Research Part B: Applied Biomaterials*. 2010;92(2):561-7.
289. Fukegawa D, Hayakawa S, Yoshida Y, Suzuki K, Osaka A, Van Meerbeek B. Chemical interaction of phosphoric acid ester with hydroxyapatite. *Journal of Dental Research*. 2006;85(10):941-4.
290. Wang Y, Spencer P, Walker MP. Chemical profile of adhesive/caries affected dentin interfaces using Raman microspectroscopy. *Journal of Biomedical Materials Research Part A*. 2007;81(2):279-86.

291. Oliveira SS, Pugach MK, Hilton JF, Watanabe LG, Marshall SJ, Marshall Jr GW. The influence of the dentin smear layer on adhesion: a self-etching primer vs. a total-etch system. *Dental Materials*. 2003;19(8):758-67.
292. Faria-e-Silva AL, Fabião MM, Sfalcin RA, de Souza Meneses M, Santos-Filho PCF, Soares PV, et al. Bond strength of one-step adhesives under different substrate moisture conditions. *European Journal of dentistry*. 2009;3(4):290.
293. Al Qahtani MQ, Al Shethri SE. Shear bond strength of one-step self-etch adhesives with different co-solvent ingredients to dry or moist dentin. *The Saudi Dental Journal*. 2010;22(4):171-5.
294. Burke F, Hussain A, Nolan L, Fleming G. Methods used in dentine bonding tests: an analysis of 102 investigations on bond strength. *The European Journal of Prosthodontics and Restorative Dentistry*. 2008;16(4):158-65.
295. Versluis A, Tantbirojn D, Douglas W. Why do shear bond tests pull out dentin? *Journal of Dental Research*. 1997;76(6):1298-307.
296. Tantbirojn D, Cheng Y-S, Versluis A, Hodges J, Douglas W. Nominal shear or fracture mechanics in the assessment of composite-dentin adhesion? *Journal of Dental Research*. 2000;79(1):41-8.
297. Van Meerbeek B, Peumans M, Poitevin A, Mine A, Van Ende A, Neves A, et al. Relationship between bond-strength tests and clinical outcomes. *Dental Materials*. 2010;26(2):e100-e21.
298. Watanabe T, Tsubota K, Takamizawa T, Kurokawa H, Rikuta A, Ando S, et al. Effect of prior acid etching on bonding durability of single-step adhesives. *Operative Dentistry*. 2008;33(4):426-33.
299. Tezvergil A, Lassila L, Vallittu P. Composite-composite repair bond strength: effect of different adhesion primers. *Journal of Dentistry*. 2003;31(8):521-5.
300. Cadenaro M, Pashley D, Marchesi G, Carrilho M, Antonioli F, Mazzoni A, et al. Influence of chlorhexidine on the degree of conversion and E-modulus of experimental adhesive blends. *Dental Materials*. 2009;25(10):1269-74.
301. Kleverlaan CJ, Feilzer AJ. Polymerization shrinkage and contraction stress of dental resin composites. *Dental Materials*. 2005;21(12):1150-7.
302. Nagem Filho H, Nagem HD, Francisconi PAS, Franco EB, Mondelli RFL, Coutinho KQ. Volumetric polymerization shrinkage of contemporary composite resins. *Journal of Applied Oral Science*. 2007;15(5):448-52.
303. Albers HF. *Tooth-colored restoratives: principles and techniques*: People's Medical Publishing House-USA; 2002.

304. Zorzin J, Maier E, Harre S, Fey T, Belli R, Lohbauer U, et al. Bulk-fill resin composites: Polymerization properties and extended light curing. *Dental Materials*. 2015;31(3):293-301.
305. Asmusen S, Arenas G, Cook WD, Vallo C. Photobleaching of camphorquinone during polymerization of dimethacrylate-based resins. *Dental Materials*. 2009;25(12):1603-11.
306. Sun L, Chow LC, Frukhtbeyn SA, Bonevich JE. Preparation and properties of nanoparticles of calcium phosphates with various Ca/P ratios. *Journal of Research of the National Institute of Standards and Technology*. 2010;115(4):243.
307. Bennett AW, Watts DC. Performance of two blue light-emitting-diode dental light curing units with distance and irradiation-time. *Dental Materials*. 2004;20(1):72-9.
308. Rueggeberg FA, Cole MA, Looney SW, Vickers A, Swift EJ. Comparison of Manufacturer-Recommended Exposure Durations with Those Determined Using Biaxial Flexure Strength and Scraped Composite Thickness Among a Variety of Light Curing Units. *Journal of Esthetic and Restorative Dentistry*. 2009;21(1):43-61.
309. Sobrinho LC, De Lima A, Consani S, Sinhoreti M, Knowles J. Influence of curing tip distance on composite Knoop hardness values. *Brazilian Dental Journal*. 2000;11(1):11-7.
310. Aguiar FHB, Lazzari CR, Lima DANL, Ambrosano GMB, Lovadino JR. Effect of light curing tip distance and resin shade on microhardness of a hybrid resin composite. *Brazilian Oral Research*. 2005;19(4):302-6.
311. Skrtic D, Antonucci J, Eanes E. Amorphous Calcium Phosphate-Based Bioactive Polymeric Composites for Mineralised Tissue Regeneration. *Journal of Research of the National Institute of Standards and Technology*. 2003;108(3):167-82.
312. Mohsen N, Craig R. Hydrolytic stability of silanated zirconia-silica-urethane dimethacrylate composites. *Journal of Oral Rehabilitation*. 1995;22(3):213-20.
313. Drummond JL. Degradation, fatigue, and failure of resin dental composite materials. *Journal of Dental Research*. 2008;87(8):710-9.
314. Botelho MG. Inhibitory effects on selected oral bacteria of antibacterial agents incorporated in a glass ionomer cement. *Caries Research*. 2003;37(2):108-14.
315. Anusavice K, Zhang N-Z, Shen C. Controlled release of chlorhexidine from UDMA-TEGDMA resin. *Journal of Dental Research*. 2006;85(10):950-4.
316. Riggs PD, Braden M, Patel M. Chlorhexidine release from room temperature polymerising methacrylate systems. *Biomaterials*. 2000;21(4):345-51.
317. Lahdenperä MS, Puska MA, Alander PM, Waltimo T, Vallittu PK. Release of chlorhexidine digluconate and flexural properties of glass fibre reinforced provisional fixed

partial denture polymer. *Journal of Materials Science: Materials in Medicine*. 2004;15(12):1349-53.

318. Ribeiro LGM, Hashizume LN, Maltz M. The effect of different formulations of chlorhexidine in reducing levels of mutans streptococci in the oral cavity: A systematic review of the literature. *Journal of Dentistry*. 2007;35(5):359-70.

319. Hiraishi N, Yiu C, King N, Tay F, Pashley D. Chlorhexidine release and water sorption characteristics of chlorhexidine-incorporated hydrophobic/hydrophilic resins. *Dental Materials*. 2008;24(10):1391-9.

320. Garoushi S, Vallittu PK, Lassila LV. Short glass fiber reinforced restorative composite resin with semi-inter penetrating polymer network matrix. *Dental Materials*. 2007;23(11):1356-62.

321. Jedrychowski JR, Caputo AA, Kerper S. Antibacterial and mechanical properties of restorative materials combined with chlorhexidines. *Journal of Oral Rehabilitation*. 1983;10(5):373-81.

322. Debnath S, Wunder SL, McCool JI, Baran GR. Silane treatment effects on glass/resin interfacial shear strengths. *Dental Materials*. 2003;19(5):441-8.

323. Oral O, Lassila LV, Kumbuloglu O, Vallittu PK. Bioactive glass particulate filler composite: Effect of coupling of fillers and filler loading on some physical properties. *Dental Materials*. 2014;30(5):570-7.

324. Boger A, Bisig A, Bohner M, Heini P, Schneider E. Variation of the mechanical properties of PMMA to suit osteoporotic cancellous bone. *Journal of Biomaterials Science, Polymer Edition*. 2008;19(9):1125-42.

325. Xu H, Weir M, Sun L, Moreau J, Takagi S, Chow L, et al. Strong nanocomposites with Ca, PO₄, and F release for caries inhibition. *Journal of Dental Research*. 2010;89(1):19-28.

326. Sakaguchi R, Wiltbank B, Murchison C. Prediction of composite elastic modulus and polymerization shrinkage by computational micromechanics. *Dental Materials*. 2004;20(4):397-401.

327. Hofmann N, Hugo B, Schubert K, Klaiber B. Comparison between a plasma arc light source and conventional halogen curing units regarding flexural strength, modulus, and hardness of photoactivated resin composites. *Clinical Oral Investigations*. 2000;4(3):140-7.

328. Junior R, Adalberto S, Zanchi CH, Carvalho RVd, Demarco FF. Flexural strength and modulus of elasticity of different types of resin-based composites. *Brazilian Oral Research*. 2007;21(1):16-21.

329. Yoshida Y, Nagakane K, Fukuda R, Nakayama Y, Okazaki M, Shintani H, et al. Comparative study on adhesive performance of functional monomers. *Journal of Dental Research*. 2004;83(6):454-8.
330. Aguiar T, Andre C, Arrais C, Bedran-Russo A, Giannini M. Micromorphology of resin–dentin interfaces using self-adhesive and conventional resin cements: A confocal laser and scanning electron microscope analysis. *International Journal of Adhesion and Adhesives*. 2012;38:69-74.
331. Cavalcanti AN, Mitsui FHO, Ambrosano GMB, Marchi GM. Influence of adhesive systems and flowable composite lining on bond strength of class II restorations submitted to thermal and mechanical stresses. *Journal of Biomedical Materials Research Part B: Applied Biomaterials*. 2007;80(1):52-8.
332. Lopes MB, Sinhoreti MAC, Correr Sobrinho L, Consani S. Comparative study of the dental substrate used in shear bond strength tests. *Pesquisa Odontológica Brasileira*. 2003;17(2):171-5.
333. Mitsui F, Peris A, Cavalcanti A, Marchi G, Pimenta L. Influence of thermal and mechanical load cycling on microtensile bond strengths of total and self-etching adhesive systems. *Operative Dentistry*. 2006;31(2):240-7.